Philodendron Schott (Araceae): Systematics and evolution of a mega-diverse genus from the New World

Inaugural-Dissertation
to obtain the academic degree
Doctor rerum naturalium (Dr. rer. nat.)

submitted to the Department of Biology, Chemistry and Pharmacy
of Freie Universität Berlin

by
Dubán Canal Gallego

2018

1st reviewer: Prof. Dr. Thomas Borsch

2nd reviewer: Prof. Dr. Julien Bachelier

Date of disputation: Wednesday, 13th February 2019

"Somewhere, something incredible is waiting to be known"

Carl Sagan (1934 -1996)

Acknowledgements

First of all, I am honored to have worked under the supervision of Prof. Dr. Thomas Borsch who provided me the opportunity of conducting this investigation at the Botanischer Garten und Botanisches Museum Berlin - BGBM. Prof. Borsch helped me to design my project and guided me through my studies. I thank Prof. Dr. Julien Bachelier for taking over the role as second reviewer.

I am deeply grateful to Dr. Nils Köster, who shared his endless passion for aroids and encouraged me during my studies. Nils joined me during field work in Colombia, gathered a large part of the samples used in this study, introduced me into the Araceae collections at BGBM and discussed various taxonomic issues with me to ensure the correct identification of the respective plants. I further deeply acknowledge the support of Dr. Katy E. Jones during the elaboration of my all analyses. Her discipline, respect and positive attitude inspired me. Katy made me think that science can be surprisingly easy. I especially thank Dr. Nadja Korotkova for her careful revision of my manuscripts and for supporting me all the way up to the submission of my thesis. Thanks further go to Dr. Robert Lücking for his advice when I could only see difficulties and obstacles.

I thank Dr. Tom Croat for providing material from the living collection of the Missouri Botanical Garden. As one of the world's experts on the taxonomy of the Araceae, my sincere thanks for letting me benefit from his knowledge on the morphology and ecology of *Philodendron*. Thanks go to Carla Kostelac and Alba Luz Arbeláez at the Missouri Botanical Garden for their dedicated support during my visit to St. Louis.

During my studies at the BGBM Berlin I attended the Plant Evolution Seminar and the Journal Club offered by my supervisor Prof. Dr. Thomas Borsch and coordinated previously by Dr. Ludo Müller and Dr. Lars Nauheimer and lately by Dr. Katja Reichel and Dr. Michael Grünstäudl, respectively. My investigation benefited from exchanging ideas and sharing concepts with other students, postdoctoral researchers and visitors. These activities contributed significantly to the improvement of my knowledge on plant systematics.

This study would not have been possible without the living collections of *Philodendron* at the BGBM Berlin and the Botanical Gardens of the Universities of Bonn, Göttingen, München, Potsdam, and Wien; the Palmengarten Frankfurt; the Royal Botanic Gardens, Kew, the Missouri Botanical Garden, and the Jardín Botánico José Celestino Mutis in Bogotá. I am

therefore deeply grateful to those people whose hands have maintained these collections since many years.

The molecular work has been carried out in the molecular laboratory of the BGBM Berlin. I would like to thank the many people who assisted with the laboratory work, in particular Kim Govers, Julia Dietrich, Bettina Giesicke, and Jana Bansemer.

Many thanks go to the researchers who I met at the BGBM and who further contributed to an inspiring atmosphere for study, in particular to Dr. Lars Nauheimer, Dr. Katja Reichel, Dr. Grischa Brokamp, Dr. Eckhard von Raab-Straube, Dr. Norbert Kilian, Dr. Tilo Henning, Dr. Susy Fuentes, Dr. Regine Jahn, Gabriele Dröge, and Dr. Brigitte Zimmer. I further thank Dr. Jeannine Marquardt for the German version of the Summary.

I am especially grateful to Dr. Rocío Cortés and Dr. Bibiana Moncada from Universidad Distrital Francisco José de Caldas in Bogotá, Dr. Leonardo Palacios curator of the Herbario de la Universidad Tecnológica del Chocó – CHOCO, Dr. Felipe Cardona curator of the Herbario de la Universidad de Antioquia – HUA, Dr. Alejandro Zuluaga from Unversidad del Valle for his support during the field work, and Dr. María Cristina Martínez and Dr. Marcela Celis from Universidad del Norte, for their support during my fieldwork in Colombia. Thanks to all the previous and current staff at the Jardín Botánico José Celestino Mutis for establishing the basis of the scientific cooperation with the BGBM Berlin, in particular Luisz Olmedo Martínez, Dr. Ruth Gutiérrez and Dr. Mauricio Díaz-Granados, and for processing the collections carried out in Colombia and the cooperation in exchanging herbarium material, in particular to César Marín, Ángela Rodríguez y Diana Medellín.

I am indebted to the Verein der Freunde des Botanischen Gartens und Botanischen Museums Berlin-Dahlem e.V. for providing financial support for the field work in Colombia. The Bundesministerium für Bildung und Forschung (BMBF) is especially acknowledged for funding a pilot project to facilitate the scientific cooperation between Germany and Colombia (01DN13030). I am deeply grateful to the Deutscher Akademischer Austauschdienst (DAAD) and Colciencias-Colfuturo convocatory 6171 for the financial support.

Thanks to all my friends in Colombia and Germany. In Colombia, I am in debt with my dearest Fabio Ávila, Ángela Guzmán, Sandra Ramírez, Javier Garzón, Marcela Castellanos, Mauricio Vargas and Carolina Molano. Your presence in my life has helped me in all senses. In Germany thanks go to my dearest Nana Silakadze, Elmira Maharramova, Demet Töre, Sarah Bollendorf, Ludo Müller, Julie Piérart, Valentina Guissi, Kristýna Šemberová, Jonathan Pahl, Teresa Ortuño, Astrid de Mestier, Mariasole Calbi, Elham Hatami, Arsen Gasparyan and Phnong Thao Nguyen.

Mil gracias a mis queridos amigos latinoamericanos por haber enriquecido mi vida con tantas experiencias durante mi estadía en Berlín. Martín de León McMannis, Junia Fatorelli, Luciano Tepper, Emmanuel Reyna, Francisco Robles, Rose Álvarez, Vastiane Tamayo, Gerardo Brand, Helena Hernández, Alejandra Baltazares, Rodolfo Paniagua, Nazario López y Nélida Abarca.

Mi eterna gratitud a mi familia por ser la razón de todo lo que hago. A mis padres, Inés y Guillermo, gracias siempre.

Finally, thanks Gregory d'Hoop for bringing music to my noisy mind.

Summary

This investigation presents phylogenetic analyses of the genus *Philodendron*, the second largest genus of the "aroid family" and one of the most conspicuous components of Neotropical rainforests. The evolutionary relationships among *Philodendron* and the closely related genera *Adelonema* and *Homalomena* have remained ambiguous based on previous phylogenetic studies that analyzed plastid and nuclear DNA markers for a limited species coverage. Likewise, the evolutionary relationships among the three subgenera proposed within *Philodendron* (*Meconostigma*, *Philodendron* and *Pteromischum*) remained unclear. Subgenus *Meconostigma* comprises 21 mostly terrestrial, arborescent species distributed in Amazonia, the Cerrado, and the Mata Atlântica. Subgenus *Pteromischum* includes 82 appressed-climbing vine species distributed mostly in Central America, the Chocó ecoregion and Amazonia. Subgenus *Philodendron* accounts for ~85% of the species diversity of the genus, mainly distributed in Central America, the Chocó ecoregion, the Andes and Amazonia. The extraordinary rich species diversity of subgenus *Philodendron* is currently organized in 10 sections, 12 subsections, and 11 series.

The aim of the present study is to elucidate the phylogenetic relationships of *Philodendron* and its evolutionary history in the Neotropics. Therefore, a molecular dataset of three non-coding plastid DNA regions (*petD*, *rpl16* and *trnK/matK*) was generated for 173 taxa (221 accessions) across the entire genus *Philodendron.* Subsequently, the phylogenetic relationships and monophyly of the subgenera were investigated by tree inferences using parsimony-based, maximum likelihood, and Bayesian-based approaches. In order to determine evolutionary time points of the origin of the most recent ancestor and the species diversification process of *Philodendron*, the well resolved and robustly supported phylogenetic tree was calibrated. Furthermore, analyses on diversification rate shifts through time and inferences of the geographic range evolution were conducted. In addition, the impact of the Andean orogeny on speciation, extinction and dispersal rates of *Philodendron* was assessed using geographic state-speciation and extinction model analysis. Finally, five morphological characters were analyzed across the phylogenetic tree to infer the ancestral character states.

The results indicate that *Philodendron* and its three subgenera *Meconostigma*, *Philodendron* and *Pteromischum* are monophyletic. However, the relationships among the three subgenera remain moderately supported. The 12 clades recovered within subgenus

Philodendron do not correspond to the current infrageneric classification. In contrast, clades recovered within subgenus *Pteromischum* correspond to the sections proposed. Divergence-time estimates revealed that *Philodendron* originated in the Oligocene, and diversified more recently from the middle Miocene onwards. Time-dependent diversification rate shift analyses revealed that the diversification process of *Philodendron* combines elements of the two models used to explain the origin of the extraordinary species diversity in the Neotropics: the "cradle" model, which postulates a more recent and faster diversification process (suggested for subgenus *Philodendron*), and the "museum" model, which assumes an older and more constant diversification process (suggested for subgenera *Meconostigma* and *Pteromischum*). Therefore, the present study indicates that the diversification process of *Philodendron* is more in line with a model of global episodic species turnover. *Philodendron* originated ~29 mya in the pan-Amazonian region. The three subgenera of *Philodendron* originated ~24 mya. Overall, the current geographic distribution of *Philodendron* is the result of multiple geographic range expansions: since the middle Miocene onwards from Amazonia to northwest South America and southeast Brazil; and more recently during the Miocene-Pliocene transition from the Chocó ecoregion to Central America, and from South America to the Caribbean islands. The fast species radiation of subgenus *Philodendron* is associated with the colonization of the Andes. Furthermore, this study demonstrates the indirect impact of the rise of the Andes from the middle Miocene onwards on the diversification process of plant lineages distributed in the adjacent lowland rainforests of the northern Andes (the Chocó ecoregion and western Amazonia). Inferences of the ancestral character-state indicate that the most recent common ancestor of *Philodendron* were climbing plants without cataphylls, with cordate blades, few locules per ovary and many ovules per locule.

Overall, the present study represents a significant advance for a better understanding of the diversification process of the genus *Philodendron* in time and space and provides the comparative basis to gain insights into the evolution of plant lineages that are highly diverse in the Neotropical rainforest – one of the most endangered biomes on Earth.

Zusammenfassung

Diese wissenschaftliche Arbeit präsentiert phylogenetische Analysen der Gattung *Philodendron*, die zweitgrößte Gattung der Familie der Aronstabgewächse und eine der auffälligsten Pflanzenarten tropischer Regenwälder in der Neotropics. Vorherige Stammbaumanalysen mit einer begrenzten Auswahl an inkludierten Arten und basierend auf DNA-Plastiden- und Kernmarkern konnten die evolutionären Verwandtschaftsbeziehungen zwischen *Philodendron* und den nah-verwandten Gattungen *Adelonema* und *Homalomena* nicht eindeutig klären. Gleichermaßen sind die evolutionären Verwandtschaftsbeziehungen zwischen den diskutierten Untergattungen innerhalb *Philodendrons* (*Meconostigma*, *Philodendron* und *Pteromischum*) weiterhin unscharf. Die Untergattung *Meconostigma* umfasst 21 überwiegend terrestrische sowie baumartige Arten, welche von Amazonien, den Savannen Zentral-Brasiliens ("Cerrado") bis zu dem atlantischen Regenwaldgebiet ("Mata Atlântica") verbreitet sind. Die Untergattung *Pteromischum* umfasst 82 dicht-andrückend kletternde Lianenarten, die überwiegend in Zentralamerika, der Chocó Ökoregion und Amazonien vorkommen. Die Untergattung *Philodendron* macht etwa ~85% der Artenvielfalt der Gattung aus und sie sind größtenteils in Zentralamerika, der Chocó Ökoregion, in den Anden und dem Amazonasgebiet verbreitet. Die außergewöhnlich reiche Artenvielfalt der Untergattung *Philodendron* wird aktuell in 10 Sektionen, 12 Untersektionen und 11 Serien eingeordnet.

Das Ziel dieser Studie ist es, die phylogenetischen Verwandtschaftsverhältnisse von *Philodendron* sowie dessen Evolutionsgeschichte in der Neotropics zu untersuchen. Dafür wurde ein molekularer Datensatz von drei nicht-kodierenden DNA-Plastidenregionen (*petD*, *rpl16* und *trnK/matK*) für 173 Taxa (von 221 Akzessionen) erstellt, die die gesamte Gattung *Philodendron* abdecken. Anschließend wurden die Verwandtschaft und Monophylien der Untergattungen mittels Stammbaumanalysen basierend auf dem Parsimonieprinzip, Maximum Likelihood und Bayesianischer Statistik untersucht. Um den zeitlichen Ursprung des frühesten gemeinsamen Vorfahren von *Philodendron* zu bestimmen und die Diversifikationsprozesse zeitlich einzuordnen, wurde der best-aufgelöste und unterstützte phylogenetische Baum mittels sekundärer Kalibrierung und Fossilien kalibriert. Des Weiteren wurden Verschiebungen in den Diversifikationsraten und Evolutionsmodelle geografischer Ausbreitungen berechnet. Außerdem wurde der Einfluss der Anden-Orogenese auf die Artentstehung, -auslöschung und Ausbreitungsraten von *Philodendron* mittels geographischer

Zustands-Speziations-und-Extinktions-Modelle untersucht. Abschließend wurden fünf morphologische Merkmale entlang des phylogenetischen Baums analysiert, um den anzestralen Zustand vorherzusagen.

Die Ergebnisse der Analysen unterstützen die Monophylie der Gattung *Philodendron* sowie deren drei Untergattungen *Meconostigma, Philodendron* und *Pteromischum*. Allerdings erhielten die postulierten Verwandtschaftsbeziehungen zwischen den drei Untergattungen nur moderate Unterstützung. Die 12 erhaltenen Kladen innerhalb der Untergattung *Philodendron* sind nicht deckungsgleich mit der aktuell akzeptierten Klassifikation auf Gattungsebene. Hingegen entsprechen die Kladen, welche genetisch innerhalb der Untergattung *Pteromischum* identifiziert wurden, den vorgeschlagenen taxonomischen Sektionen. Molekulare Datierungen der Verzweigungen im Baum haben ergeben, dass die Gattung *Philodendron* im Oligozän entstanden ist und die überwiegende Artenvielfalt frühestens auf das Miozän zurückgeht bzw. sich seit dem diversifiziert hat. Zeitabhängige Analysen der Diversifikationsraten und deren Verschiebungen haben eine parallele Kombination zweier möglicher Modelle für die Evolutionsprozesse innerhalb *Philodendrons* ergeben. Beide Modelle werden angewendet, um den Artenreichtum in der Neotropics zu erklären: das „cradle“ Modell, welches von einem jüngeren und schnelleren Diversifikationsprozess ausgeht (gezeigt für die Untergattung *Philodendron*), und das „museum“ Modell, welches von einem älteren und stetigeren Diversifikationsprozess ausgeht (gezeigt für die Untergattungen *Meconostigma* und *Pteromischum*). Folglich wurde in dieser Studie gezeigt, dass der Diversifikationsprozess von *Philodendron* eine größere Übereinstimmung mit globalen, episodischen Änderungen in der Artzusammensetzung zeigt. *Philodendron* hat seinen Ursprung vor ~29 Millionen Jahren in der Pan-Amazonas Region. Die drei Untergattungen von *Philodendron* entstanden vor ~24 Millionen Jahren. Insgesamt ist das aktuelle geografische Vorkommen von *Philodendron* das Ergebnis mehrerer geografischer Ausbreitungsphasen: zuerst seit des mittleren Miozäns vom Amazonasgebiet nach NW-Südamerika und SO-Brasilien; und in jüngerer Zeit zwischen dem Miozän und Pliozän von der Chocó Ökoregion nach Zentralamerika, und von Südamerika zu den Karibischen Inseln. Die rasche Radiation der Untergattung *Philodendron* steht im engeren Zusammenhang mit der Eroberung der Anden. Des Weiteren verdeutlicht diese Studie den indirekten Einfluss der Hebung der Anden seit dem mittleren Miozän auf die Diversifikation von Pflanzenlinien mit einer Verbreitung in den angrenzenden Flachland-Regenwäldern der nördlichen Anden (der Chocó Ökoregion und des westlichen Amazonasgebietes). Berechnungen der anzestralen, morphologischen Merkmalszustände der Gattung *Philodendron* haben gezeigt, dass die

Vorfahren kletternde Pflanzen waren, die sich durch fehlende Niederblätter, cordate Blattspreiten, und wenige Loculi je Fruchtknoten mit vielen Samenanlagen je Loculus kennzeichneten.

Zusammenfassend bedeutet die vorliegende wissenschaftliche Arbeit einen wesentlichen Fortschritt, um Diversifikationsprozesse der Gattung *Philodendron* in Zeit und Raum besser zu verstehen und liefert somit eine Grundlage für weiterführende Analysen, um die Evolution von Pflanzenlinien in den biodiversitätsreichen Regenwäldern der Neotropics, eines der am meisten bedrohten Biome der Welt, zu ergründen.

Contents

Chapter 1. General introduction

1.1. The Neotropics and their plant diversity

The tropics of the Americas or Neotropics harbor about 37% of the plant extant species diversity on Earth (Antonelli and Sanmartín, 2011). With ~90,000-110,000 angiosperms, the Neotropics accumulated more plant species than the whole Palaeotropics (tropical Africa, Asia and Oceania; Antonelli and Sanmartín, 2011). As currently defined, the Neotropical region includes southern Mexico, southern Florida, Central America, South America, and the West Indies (Morrone, 2014). The tropics of the Americas are distributed across three tectonic plates: the North American, the Caribbean and the South American (Antonelli and Sanmartín, 2011).

Ranging from the sea level to ~4,800 m the Neotropics comprise different biomes (global biotic units of similar vegetation physiognomy; Olson et al., 2001; Moncrieff et al., 2015) including lowland tropical rainforests, seasonally dry tropical forests (SDTFs), savannas, and high-elevation grasslands (Antonelli et al., 2018). Lowland tropical rainforest, the largest biome in the Neotropics, is characterized by annual precipitation above 2,000 mm and mean monthly temperatures of 18°C as lower boundaries, and the absence of a pronounced dry season (Hughes et al., 2013; Eiserhardt et al., 2017). Neotropical lowland rainforest encompasses several soil and vegetation types but is primarily defined by the closed, multi-layered, angiosperm-dominated canopy with an abundance of vines and epiphytes (Hughes et al., 2013). In contrast, other Neotropical lowlands with a marked dry season varying among 4-6 months of less than 100 mm correspond to savannas and SDTFs (Pennington et al., 2006b). Savannas tend to occur in relatively poor soils and in contrast to the SDTFs which are deciduous or semideciduous in the dry season and often rich in cacti and other succulents, savannas are defined by an evergreen, fire-tolerant grass layer (Pennington et al., 2009; Pennington et al., 2010). High-elevation biomes such as páramo, puna and jalca, occur above 3,000 m in the Andes and are mainly occupied by grasses (Pennington et al., 2010; Hughes et al., 2013). Compared to the lowland biomes, high-elevation biomes originated more recently from the Pliocene-Pleistocene onwards (Pennington et al., 2010; Hughes et al., 2013).

Phylogenetic data have significantly contributed to a better understanding of the origin and diversification of the Neotropical flora, in conjunction with other disciplines such as palaeontology and ecology. Based on phylogenetic evidence, scientists have attributed the origin of the Neotropical species diversity either to a recent and rapid diversification facilitated by high speciation rates ("cradle model"), or to a gradual accumulation over longer periods facilitated by low extinction rates ("museum model") (e.g., Stebbins, 1974; Richardson et al., 2001; Mckenna and Farrell, 2006; Couvreur and Baker, 2011; Hughes et al., 2013; Koenen et al., 2015; Eiserhardt et al., 2017; Schneider and Zizka, 2017). For example, dated phylogenies of the families Annonaceae (102-110 million years ago - mya; Couvreur et al., 2011), Arecaceae (92-108 mya; Couvreur and Baker, 2011), Menispermaceae (102-115 mya; Wang et al., 2012), the subfamily Quiinoideae (58-84 mya; Schneider and Zizka, 2017), and the Brownea clade (Leguminosae; Schley et al., 2018) have favored the "museum model". In contrast, dated phylogenies of the genera *Costus* L. subgenus *Costus* (1-7 mya; Kay et al., 2005), *Guarea* F. Allam. ex L. and *Trichilia* P. Browne (18-24 mya, and 20-29 mya, respectively; Koenen et al., 2015), *Guatteria* Ruiz & Pav. (~11 mya; Erkens et al., 2007), *Inga* Mill. (~6 mya; Richardson et al., 2001), and *Renealmia* L. f. (3-16 mya; Särkinen et al., 2007) have supported the "cradle model". More recently, analyses of shifts in diversification rates (speciation rate minus extinction rate over time) reveal that the evolutionary process in the Neotropics might combine elements of both the museum and cradle models and that the species diversity is more likely to have experienced episodic increases interchanged with episodic reductions (Mckenna and Farrell, 2006; Koenen et al., 2015; Pennington et al., 2015). In line with this hypothesis, palaeontological evidence confirms episodic species turnovers during the last 65 million years (Ma) in the Neotropics (Jaramillo et al., 2006).

There is evidence that diversification patterns are associated to different abiotic and biotic factors in the Neotropics (Antonelli and Sanmartín, 2011). For example, Neotropical species-richness through time is associated with global climatic changes from the Cenozoic onwards (Jaramillo et al., 2006). The gradual rise in global temperatures from the early Paleocene to the early Eocene coincided with an increase of species diversity (Jaramillo et al., 2006). The subsequent drop in global temperatures during the middle Eocene until the early Oligocene coincided with a decline in species diversity (Jaramillo et al., 2006; Hughes et al., 2013). A second increase of species diversity co-occurred with the increase of global temperatures from the middle Miocene onwards (Jaramillo et al., 2006; Hoorn et al., 2010).

In addition to these global climate shifts, major geological events such as the formation of the Andes, the closure of the Isthmus of Panama and the emergence of the Pebas system have played an important role in the speciation, extinction, and migration processes of Neotropical plant lineages (Antonelli et al., 2009; Hoorn et al., 2010; Antonelli and Sanmartín, 2011; Hughes et al., 2013; Luebert and Weigend, 2014). The rise of the Andes favoured the evolution of the Neotropical biodiversity through multiple mechanisms including the formation of new habitats, the separation of linages previously connected, the dispersal across the north-south pathway in South America, and more indirectly, the increase of the humidity in the lowlands both sides of the tropical Andes which facilitated the speciation of certain preexisting lineages (Antonelli et al., 2009; Hoorn et al., 2010; Luebert and Weigend, 2014). The age of the closure of the Isthmus of Panama remains controversial (Bacon et al., 2015; O'dea et al., 2016; Jaramillo et al., 2017). However, the profound impact of the massive land connection between North and South America on the history of life in the Neotropics is largely accepted. In addition, few phylogenetic studies have evaluated the influence of the Pebas system on the diversification of Neotropical angiosperm lineages. However, there is growing evidence that this aquatic system acted as a dispersal barrier for plant lineages between the Andes and western Amazonia from the middle Miocene until the late Miocene (Antonelli et al., 2009; Roncal et al., 2013).

Phylogenetic studies have also confirmed that the speciation, extinction and migration patterns in the Neotropics are strongly associated to the ecological attributes of the different biomes. For example, lineages mainly restricted to the Páramos have higher net diversification rates than lineages distributed in other biomes (Madriñán et al., 2013). Conversely, lineages distributed in the Neotropical rainforests have undergone significant variations in the diversification rates that might resemble museums and cradles through time (Eiserhardt et al., 2017).

More recently, innovative phylogenetic methods have assessed the impact of abiotic and biotic drivers on the diversification of Neotropical lineages, for example in the families Acanthaceae (*Ruellia* L.; Tripp and Tsai, 2017), Campanulaceae (Lobelioideae; Lagomarsino et al., 2016), and Orchidaceae (Cymbidieae and Pleurothallidinae; Pérez-Escobar et al., 2017), speciation and extinction rates are differently influenced by geological, climatic and ecological processes thought time. The phylogenetic evidence already available enables comparative studies on the contribution of dispersal to the configuration of the species diversity among different biomes and across the major lineages of the tree of life in the Neotropics (Antonelli et al., 2018). However, despite these fundamental insights in the origin

and evolution of angiosperm diversity in the Neotropics, numerous highly diverse lineages remain poorly studied from the phylogenetic perspective.

1.2. The family Araceae in the Neotropics

The Araceae (aroids) is a medium-sized angiosperm family in the early-diverging order Alismatales, with 144 genera and 3,645 currently accepted and ~6,500 estimated species (Boyce and Croat, 2018). Aroids are extremely diverse in terms of life forms including submerged, emergent, and free-floating aquatics, climbing and terrestrial plants, as well as epiphytes (Boyce and Croat, 2018). The family Araceae encompasses an extraordinary morphological diversity from the world's smallest seed plant (*Wolffia angusta* Landolt) with some individuals exhibiting 0.3 mm in width (Landolt, 1986) to the world's largest blooms [*Amorphophallus titanum* (Becc.) Becc. ex Arcang.], with pseudanthia rising above 3 m (Claudel et al., 2017). Aroids occur in tropical, subtropical and temperate regions but the family is, by far, most diverse in the perhumid tropics. The Palaeotropics have accumulated a considerably higher number of genera than the Neotropics. However, the latter contains the most species-rich genera *Anthurium* Schott with 1,041 accepted species (Govaerts et al., 2018) and ~2,000 estimated species (Boyce and Croat, 2018), and *Philodendron* Schott with 558 accepted species and ~700-1,000 estimated species (Govaerts et al., 2018), i.e. more than 40% of the entire species diversity of the family.

The most distinctive features of aroids are the leaf venation patterns and the inflorescences. Inflorescence typically consists of an unbranched axis with numerous flowers usually arranged in spirals called the spadix, surrounded by a bract called the spathe (Mayo et al., 1997; Cabrera et al., 2008). Flowers might be unisexual or bisexual. Phylogenetic studies on the family Araceae have consistently recovered the monophyly of both the bisexually-flowered species groups and the unisexually-flowered species groups (Cabrera et al., 2008; Cusimano et al., 2011; Henriquez et al., 2014). The unisexually-flowered clade includes two major lineages one of which corresponds to the subfamily Aroideae with 75 genera and 1,573 extant species (Henriquez et al., 2014). Within subfamily Aroideae, the *Philodendron* clade is one of the earlier diverging lineages which contain two subclades with a disjunct geographical distribution either in Asia or in the Neotropics (Cusimano et al., 2011; Nauheimer et al., 2012; Wong et al., 2013; Vasconcelos et al., 2018). The Asian subclade includes the genera

Furtadoa M. Hotta and *Homalomena* Schott and the Neotropical subclade includes the genera *Adelonema* Schott and *Philodendron.*

1.3. The genus *Philodendron* Schott

The genus *Philodendron* is one of the most characteristic components of Neotropical rainforests (Croat, 1997). *Philodendron* ranges from tropical Mexico to southern Brazil and the Caribbean islands (Mayo, 1990; Grayum, 1996; Croat, 1997). However, rainforests of the adjacent lowlands of the northern Andes harbor the largest proportion of its species diversity (e.g., the Chocó ecoregion and western Amazonia; Mayo, 1990; Croat, 1997). *Philodendron* is one of the most morphologically diverse genera in the aroids in terms of growth patterns and leaf morphology (Figures 1.1, 1.2). Growth patterns include terrestrials, vines and most commonly hemiepiphytes, and epiphytes (Croat, 1997). Leaf shape ranges from entire (from linear to cordate or sagittate), and variously lobed (trilobed and palmately-lobed) to compound (trisect and palmately-compound) leaves (Croat, 1997). Inflorescences vary from solitary to >10 per axil (Figure 1.2). The spathe is highly variable in terms of shape and colors; however, the secretion of resin from its inner surface is characteristic to *Philodendron* and unique among the aroids (Figure 1.2; Croat, 1997). The spadix includes the pistillate zone separated from the fertile staminate zone by a well-differentiated sterile staminate zone, and usually contained inside the spathe at anthesis (Figure 1.2). Floral morphology is diverse with the ovary divided in two to many separate locules and the number of ovules per locule ranges from one to many (>30) with axile or basal placentation (Croat, 1997). Floral morphology (e.g., locules/ovary, ovules/locule, and style structure) in conjunction with vegetative characters has been largely used for species delimitations and infrageneric classification within *Philodendron* (Schott, 1832; Engler, 1899; Krause, 1913; Bunting, 1979; Mayo, 1989; Grayum, 1996; Croat, 1997).

Figure 1.1. Growth patterns in *Philodendron.* A: terrestrial (*Philodendron mamei* André., Jardin Botanique du Montet, France), B: vine (*Philodendron palaciosii* Croat & Grayum, Croat 106128), C: hemiepiphyte (*Philodendron bonifaziae* Croat, Croat 104020), and D: epiphyte (*Philodendron insigne* Schott, French Guiana, N. Köster 1360). Images A-C copyright © David Scherberich and D © N. Köster.

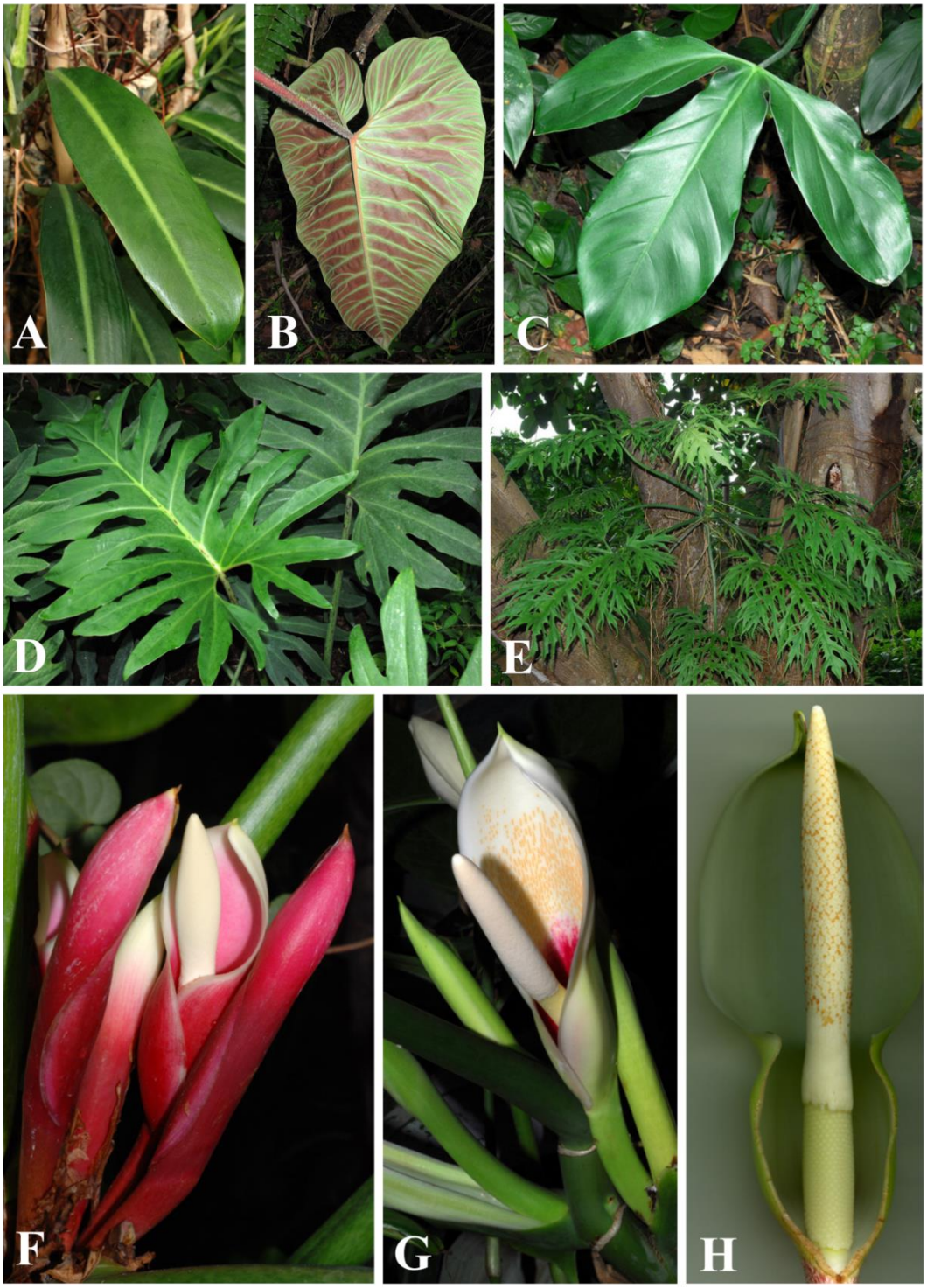

Figure 1.2. A-E, Examples of leaf morphological variation in *Philodendron*. A: linear to elliptic (*Philodendron glaziovii* Hook. f., Jardin Botanique de Lyon, France), B: cordate (*Philodendron verrucosum* L. Mathieu ex Schott, D. Scherberich), C: trilobed (*Philodendron holtonianum* Schott, Jardín Botánico de San Jorge, Colombia); D: palmately-lobed (*Philodendron pinnatifidum* (Willd.) Schott, Jardin Botanique de Lyon), E: palmately-compound (*Philodendron warszewiczii* K. Koch & C. D. Bouché, The Kampong, Miami, Florida), F: multiple inflorescences per axil in *Philodendron malesevichiae* Croat (Croat 74818), G: spathe with resin ducts in *Philodendron tripartitum* (Jacq.) Schott (Jardin Botanique de Lyon), and H: typical spadix zones in *Philodendron* (*Philodendron malesevichiae*, Croat 74818b). Images copyright © David Scherberich.

Despite receiving floral visitors of various insect groups, pollination of *Philodendron* seems to be accomplished exclusively by large scarab beetles of the tribe Cyclocephalini (Scarabaeidae, Dynastinae; Croat, 1997). Dispersal by birds, mammals (monkeys and bats?), and ants have been observed in *Philodendron* (Croat, 1997). Little is known about hybridization of *Philodendron* in nature, but natural hybrids are rarely found (Köster, pers. comm.). However, cultivars have been commonly produced for horticultural purposes (Devanand et al., 2004).

1.3.1. Systematics of the genus *Philodendron*

The first references to a member of the genus *Philodendron* might correspond to two illustrations of a plant known as "Huacalxochitl", elaborated in Mexico in the 16th century (Mayo, 1990). However, the first scientific account of *Philodendron* species (and in fact, of any Araceae from the New World) corresponds to the descriptions and drawings of four species elaborated by Charles Plumier during the last decade of the 17th century (Mayo, 1990). As result of the multiple explorations of the New World during the 18th and the earlier 19th centuries, additional species of *Philodendron* were described under the genera *Arum* L., *Caladium* Vent. and *Pothos* L., mainly by Jacquin, Browne, Rudge, Vellozo as well as Humboldt and Bonpland (see Mayo 1990; Grayum 1996; and Croat 1997 for a detailed account of the contributions made by other explorers before the formal description of the genus *Philodendron*).

1.3.1.1. Morphology-based taxonomic classifications of **Philodendron**

The genus *Philodendron* was circumscribed by Schott (1829) based on the morphology of the ovary and the stamens. Schott included eight species in the genus and established the respective new combinations for *P. grandifolium* (Jacq.) Schott (the type species), *P. hederaceum* (Jacq.) Schott, *P. lacerum* (Jacq.) Schott, *P. pinnatifidum* (Jacq.) Schott, and *P. tripartitum* (Jacq.) Schott, whereas *Philodendron bipinnatifidum* Schott ex Endl., *Philodendron imbe* Schott ex Kunth, and *P. laciniosum* Schott (now considered a synonym of *Philodendron pedatum* (Hook.) Kunth), were merely mentioned and later on validly described. In 1832, Schott published the first infrageneric arrangement of *Philodendron* consisting of four unranked groups, likewise based exclusively on floral characters:

Euphilodendron, *Calostigma*, *Meconostigma* and *Sphincterostigma* (Mayo, 1990; Croat, 1997). Subsequently, Schott (1856, 1860) recognized 99 (1856) and 135 (1860) species of *Philodendron* which he organized in 22 greges (plural of grex, a rank between genus and species), primarily based on variations of growth pattern, leaf shape, and venation pattern in combination with floral morphology and anatomy (Table 1; Mayo, 1990; Grayum, 1996). Engler (1878) rearranged the 22 greges proposed by Schott into ten sections and twelve subsections, putting special emphasis on the number of ovules per locule and the type of placentation (Mayo, 1990; Grayum, 1996; Croat, 1997). In his last revision, Engler (1899) circumscribed two subgenera in *Philodendron*: subgenus *Meconostigma* Engl. (which combined the former sections *Meconostigma* and *Sphincterostigma*), and the concomitant subgenus *Euphilodendron* (now subgenus *Philodendron*) which encompassed nine sections defined on the basis of the number of ovules per locule in combination with leaf shape and style type (Table 1.1; Mayo, 1990; Croat, 1997). In the last revision of the entire genus *Philodendron*, Krause (1913) followed the classification proposed by Engler in 1899, but added many new species (to a total of 222) and the new section *Camptogynium* Krause (Mayo, 1990).

Krause's infrageneric classification remained until Mayo (1986, 1988) identified three main lineages in *Philodendron* using a morphology-based phylogenetic approach. Mayo considered the three lineages as three morphologically and anatomically well-defined subgenera (Croat, 1997). The earlier diverged lineage corresponded to subgenus *Meconostigma* sister to a clade including the monophyletic subgenera *Philodendron* and *Pteromischum* (Schott) Mayo. Mayo (1986, 1988) hypothesized that subgenus *Meconostigma* originated in open environments in eastern Brazil and dispersed into the rainforests of western Amazonia. In contrast, the subgenera *Philodendron* and *Pteromischum* might have originated in the rainforests (Mayo, 1986, 1988; Croat, 1997).

For the three subgenera proposed by Mayo, taxonomic revisions have been published either for the complete subgenus within its entire range (e.g., subgenus *Meconostigma*; Mayo, 1989, 1991; Gonçalves and Salviani, 2002) or for parts of the subgenus within certain geographic areas (e.g., subgenus *Pteromischum* for Pacific and Caribbean tropical America; [Mayo, 1989, 1991; Grayum, 1996; Gonçalves and Salviani, 2002; Barbosa and Sakuragui, 2014], and subgenus *Philodendron* for Mexico and Central America [Croat, 1997]). Subgenus *Meconostigma* currently includes 21 accepted species (Gonçalves and Salviani, 2002). It consists of species with an arborescent habit, conspicuous petiole scars, a well-developed sterile intermediate zone in the inflorescence equal to or longer than the staminate zone, and

the gynoecium having stylar lobes (Mayo, 1991). Subgenus *Pteromischum* with 82 species divided in the sections *Pteromischum* (Schott) Engl. and *Fruticosa* Grayum, is primarily defined by the scandent habit, slender stems with several to many leaves usually terminated by a solitary inflorescence, and leaves with extensively sheathed petioles encircling the stem at the base (Grayum, 1996). Subgenus *Philodendron*, the largest subgenus with ~460 accepted species but many new species expected in underexplored regions of tropical America (Croat, pers. comm.), is primarily recognized by the absence of the characters observed in the subgenera *Meconostigma* and *Pteromischum* (Croat, 1997). Subgenus *Philodendron* is currently organized in ten sections: *Baursia* (Rchb. ex Schott) Engler, *Camptogynium*, *Dolichogynium* Croat and Köster, *Macrobelium* (Schott) Sakur., *Macrogynium* Engler, *Philodendron*, *Philopsammos* G. S. Bunting, *Polytomium* (Schott) Engler, *Schizophyllum* (Schott) Engler, and *Tritomophyllum* (Schott) Engler. Taxonomic revisions of the sections *Schizophyllum* and *Macrobelium* in Brazil have been published relatively recently (Sakuragui, 2012; Barbosa and Sakuragui, 2014; respectively).

Table 1.1. (next page) Main morphology-based taxonomic classifications of the genus *Philodendron*. * denotes an infrageneric category of interchanged rank. Number between brackets after subsection ranks correspond to the number of series proposed by Croat (1997).

Schott (1856, 1860)		**Engler (1899)**		**Krause (1913)**		**Mayo (1990)**		**Croat (1997)**	
		Subgenus *Euphilodendron*		**Subgenus *Euphilodendron***		**Subgenus *Philodendron***		**Subgenus *Philodendron***	
Grex	Baursia	Sect.	*Baursia*	Sect.	*Baursia*	Sect.	*Baursia*	Sect.	*Baursia*
		Sect.	*Macrogynium*	Sect.	*Macrogynium*	Sect.	*Macrogynium*	Sect.	*Macrogynium*
Grex	Macrolonchium	Sect.	*Macrolonchium*	Sect.	*Macrolonchium*				
		Sect.	*Polyspermium*	Sect.	*Polyspermium*	Sect.	*Philodendron*	Sect.	*Philodendron*
Grex	Achyropodium		*Achyropodium						Subsect. *Achyropodium*
Grex	Canniphyllum		*Canniphyllum						Subsect. *Canniphyllum*
Grex	Cardiobelium		*Cardiobelium						Subsect. *Macrolonchium*
Grex	Platypodium		*Platypodium						Subsect. *Platypodium*
Grex	Psoropodium		*Psoropodium						Subsect. *Psoropodium*
Grex	Solenosterigma		*Solenosterigma						Subsect. *Philodendron* (5)
									Subsect. *Solenosterigma*
		Sect.	*Oligospermium*	Sect.	*Oligospermium*	Sect.	*Calostigma*	Sect.	*Calostigma*
Grex	Doratophyllum		*Doratophyllum						Subsect. *Bulaoana*
Grex	Macrobelium		*Macrobelium						Subsect. *Eucardium*
			Eucardium						Subsect. *Glossophyllum* (2)
			Oligocarpidium						Subsect. *Macrobelium* (4)
									Subsect. *Oligocarpidium*
Grex	Polytomium	Sect.	*Polytomium*	Sect.	*Polytomium*	Sect.	*Polytomium*	Sect.	*Polytomium*
Grex	Schizophyllum	Sect.	*Schizophyllum*	Sect.	*Schizophyllum*	Sect.	*Schizophyllum*	Sect.	*Schizophyllum*
Grex	Tritomophyllum	Sect.	*Tritomophyllum*	Sect.	*Tritomophyllum*	Sect.	*Tritomophyllum*	Sect.	*Tritomophyllum*
				Sect.	*Camptogynium*	Sect.	*Camptogynium*	Sect.	*Camptogynium*
						Sect.	*Philopsammos*	Sect.	*Philopsammos*
Grex	Pteromischum	Sect.	*Pteromischum*	Sect.	*Pteromischum*	**Subgenus *Pteromischum***		**Subgenus *Pteromischum***	
Grex	Meconostigma	**Subgenus *Meconostigma***		**Subgenus *Meconostigma***		**Subgenus *Meconostigma***		**Subgenus *Meconostigma***	
Grex	Sphincterostigma								
Grex	Belocardium								
Grex	Cardiophylacium								
Grex	Eubelium								
Grex	Glossophyllum								
Grex	Imbea								
Grex	Oligophlebium								

1.3.1.2. Molecular-based phylogenetic studies on **Philodendron** *and recent taxonomic implications*

The evolutionary relationships of *Philodendron* have remained controversial since the earliest molecular-based phylogenetic studies on the family Araceae. The phylogenetic analyses conducted by Barabé et al. (2002) using plastid DNA markers (*trnL intron* and *trnL-trnF* spacer) and including only six species of *Philodendron* indicated that *Philodendron* might be paraphyletic with respect to the genus *Homalomena*, which appeared nested within *Philodendron*. Subsequently, the first molecular-based phylogenetic study on *Philodendron* (Gauthier et al., 2008) based on plastid (*rpl16* intron) and nuclear ribosomal DNA markers (external transcribed spacer - ETS, and internal transcribed spacer – ITS) provided two different hypotheses on the evolutionary relationships of the genus. Whilst the phylogenetic tree obtained with *rpl16* confirmed the hypothesis proposed by Barabé et al. (2002), the phylogenetic trees obtained with ETS and ITS recovered the monophyly of *Philodendron*. Subsequently, the phylogenetic studies on the genus *Homalomena* (Wong et al., 2013; 2016) involving 39 taxa of *Philodendron* corroborated the hypothesis proposed by Barabé et al. (2002) and separated all Neotropical *Homalomena* species in the resurrected genus *Adelonema* to render *Homalomena* monophyletic (Wong et al., 2016). A more recent study using a combined dataset of plastid and nuclear DNA markers (*rpl32-trnL, trnV-ndhC* and *trnQ-5'-rps16,* and ITS, respectively) recovered the monophyly of *Philodendron* (Vasconcelos, 2015). However, Loss-Oliveira et al. (2016) using a different combination of plastid and nuclear DNA markers (*matK*, *trnL* and *trnL-trnF*, and ETS, respectively) recovered the genus *Adelonema* in a polytomy with the three subgenera of *Philodendron.*

More recently, Sakuragui et al. (2018) based on both morphological (Mayo, 1991; Calazans et al., 2014) and previous phylogenetic studies (Barabé et al., 2002; Gauthier et al., 2008; Loss-Oliveira et al., 2014; Vasconcelos, 2015) proposed to separate the species attributed to subgenus *Meconostigma* in the genus *Thaumatophyllum* Schott. Following this view, *Philodendron* would correspond only to the subgenera *Philodendron* and *Pteromischum*, the latter of which has also been suggested to be split off as the resurrected genus *Elopium* Schott (Wong et al., 2016; Vasconcelos et al., 2018).

The results obtained in the present study based on comprehensive taxon sampling and a combined dataset of three plastid DNA markers and those recently obtained by Vasconcelos et al. (2018) based on a combined dataset of plastid and nuclear ribosomal DNA markers, consistently recovered the monophyly of *Philodendron* and its three subgenera. Therefore, in

the present study, *Philodendron* is considered as a single genus with three subgenera: *Meconostigma*, *Philodendron* and *Pteromischum.* A detailed discussion over the implications of recent nomenclature and taxonomic suggestions on subgenus *Meconostigma* (Sakuragui et al., 2018) and subgenus *Pteromischum* (Vasconcelos et al., 2018) is presented in Chapter 3 of this document.

1.4. Background, aims and outline of this study

There is a long tradition in the study of Araceae at the Botanic Garden and Botanical Museum Berlin (BGBM). During the direction of Adolf Engler from 1889 to 1921, the aroid family was one of the scientific priorities at the BGBM. During Engler‘s life time, the number of described Araceae nearly doubled from about 900 to around 1,800 species (Mayo et al., 1997), 90 of which corresponded to the genus *Philodendron*. Relatively shortly after publishing a revision of *Philodendron* himself (Engler, 1899), Engler assigned a new taxonomic revision of *Philodendron* within the series “Das Pflanzenreich” to Kurt Krause, who worked as a curator at the BGBM (Krause 1913). It was also Engler‘s assistant Krause who helped him to finish the monumental multi-volume monograph of the entire family as part of “Das Pflanzenreich” in 1920.

Although both Engler and Krause never observed *Philodendron* species in the wild, they could build their research based on an extensive living collection in the greenhouses of the botanic garden. Whilst most of the aroid vouchers escaped the fire of the herbarium in 1943 (including a high proportion of type specimens), probably none of the living plants studied by Engler and Krause survived the air attacks of World War II which destroyed most of the greenhouses. However, the living collection of Araceae at the BGBM has been rebuilt over the years and comprises currently more than 500 taxa with a total of nearly 800 different accessions. Based on its historical importance and its high species and genus diversity (including many large-sized taxa which cannot be easily cultivated in smaller botanic gardens), the aroid collection represents one of the taxonomic special collections of the BGBM and will be further expanded. Since 2011, the collection has been scientifically supervised and developed by Dr. Nils Köster, increasing the number of cultivated *Philodendron* from 60 to currently >100 species (and ~160 accessions) in the course of a research project.

Any attempt for a better understanding of the evolution of the species-rich genus *Philodendron* requires a broader taxon sampling, particularly across the Chocó ecoregion in Colombia, which corresponds to the area with the highest species diversity of *Philodendron*. The BGBM has recently established the basis of a scientific cooperation with the Botanical Garden of Bogotá (Jardín Botánico José Celestino Mutis) in order to contribute to the study of the extraordinary plant species diversity of Colombia from a phylogenetic perspective. Therefore, the present study enables integration of capabilities from both institutions using both living collections deposited at the BGBM and recent collections from Colombia.

Phylogenies illuminate the evolutionary relationships of taxa and, combined with palaeontological, environmental, and morphological data, they enable inferences on the age, distribution and diversification patterns of the species diversity through time (Pennington et al., 2006a; Eiserhardt et al., 2017). Evidence obtained from dated phylogenies also illuminates our knowledge of biome history at multiple temporal and spatial scales (Pennington et al., 2006a).

In this framework, a densely sampled, well resolved, and robustly supported phylogeny of the broadly distributed genus *Philodendron* is crucial for elucidating its evolutionary relationships and providing insights into the evolutionary history of the angiosperms in the tropics of the Americas. Consequently, this study explores the diversification of *Philodendron* in time and space using the first densely sampled and robustly generated phylogenetic hypothesis.

This document follows the cumulative format and therefore it contains five chapters. **Chapter 1** corresponds to the general introduction, Chapters 2 to 4 correspond to three research manuscripts, and Chapter 5 presents general conclusions. Chapters 2 to 4 are structured as journal articles and therefore, they contain their own summary, introduction, material and methods, results, discussion, conclusions, figures and tables. Chapter 2 corresponds to the paper entitled "Phylogeny and diversification history of the large Neotropical genus *Philodendron* (Araceae): Accelerated speciation in a lineage dominated by epiphytes" published in the *American Journal of Botany*, Chapter 3 corresponds to the manuscript entitled "Out of Amazonia and back again: Historical biogeography of the species-rich Neotropical genus *Philodendron* (Araceae)", recently submitted to the *Annals of the Missouri Botanical Garden*, Chapter 4 corresponds to a manuscript which will be submitted. All references are provided after Chapter 5. Appendices to the Chapters 2 to 4 are given at the end of this document.

Chapter 2 presents the first robustly generated phylogenetic tree of *Philodendron* based on three non-coding plastid DNA regions (*petD, rpl16,* and *trnK/matK*) and including 125 taxa (137 accessions). The phylogenetic tree obtained enables to [1] elucidate the relationships between *Philodendron* and the closely related genera *Adelonema* and *Homalomena*, and the evolutionary relationships among the three subgenera *Meconostigma, Philodendron* and *Pteromischum*, [2] infer timing of diversification of *Philodendron* and relate the ages obtained to the main geological changes in the Neotropics from the late Oligocene onwards, and [3] estimate diversification rate shifts and compare the findings on *Philodendron* with other species-rich lineages distributed in the Neotropics.

Evolution of the geographic range and inferences of the impact of the rise of the Andes on the diversification process of *Philodendron* are presented in **Chapter 3**. In order to achieve a more comprehensive geographic coverage, a total of 89 accessions of *Philodendron* were included into the plastid DNA dataset previously generated (Chapter 2). Consequently, the new phylogenetic tree including about one third of the species diversity of *Philodendron* was calibrated. This dated phylogeny enables to [1] investigate historical biogeography of *Philodendron* in the Neotropics and [2] assess the indirect impact of the uplift of the Andes on the diversification process of lineages mainly distributed in the adjacent lowlands of the northern Andes (e.g., the Chocó ecoregion and western Amazonia).

Chapter 4 presents the results on the evolution of morphological characters which have been used for the infrageneric circumscription of the genus *Philodendron*. The phylogenetic tree based on the plastid DNA dataset generated for the biogeographic analyses (Chapter 3) including 162 species of *Philodendron* and 4 species of its sister genus *Adelonema* enables to [1] infer the ancestral state of growth form in adult plants, persistence of cataphylls, blade shape, number of locules per ovary and number of ovules per locule in *Philodendron* and [2] compare the results obtained with the morphological evolution of other Neotropical plant lineages.

The last chapter of this document, **Chapter 5**, concludes main results obtained in this investigation and compares them with the results obtained in other studies.

Here no one who has any feeling of the magnificent and the sublime can be disappointed; the sombre shade, scarce illumined by a single direct ray even of the tropical sun, the enormous size and height of the trees, most of which rise like huge columns a hundred feet or more without throwing out a single branch, the strange buttresses around the base of some, the spiny or furrowed stems of others, the curious and even extraordinary creepers and climbers which wind around them, hanging in long festoons from branch to branch, sometimes curling and twisting on the ground like great serpents, then mounting to the very tops of the trees, thence throwing down roots and fibres which hang waving in the air, or twisting round each other form ropes and cables of every variety of size and often of the most perfect regularity. These, and many other novel features-the parasitic plants growing on the trunks and branches, the wonderful variety of the foliage, the strange fruits and seeds that lie rotting on the ground-taken altogether surpass description, and produce feelings in the beholder of admiration and awe. It is here, too, that the rarest birds, the most lovely insects, and the most interesting mammals and reptiles are to be found. Here lurk the jaguar and the boa-constrictor, and here amid the densest shade the bell-bird tolls his peal."

Wallace's letter to the members of the Mechanics' Institution in Neath, England in 1849
Wallace's book My Life, 1905.

Chapter 2. Phylogeny and diversification history of the species-rich genus *Philodendron*

2.1. Summary

Philodendron is a large genus of ~560 species and among the most conspicuous epiphytic components of Neotropical forests, yet its phylogenetic relationships, timing of divergence, and diversification history have remained unclear. We present a comprehensive phylogenetic study for *Philodendron* and investigate its diversification, including divergence-time estimates and diversification rate shift analyses. We performed the largest phylogenetic reconstruction for *Philodendron* to date, including 125 taxa with a combined dataset of three plastid DNA regions (*petD, rpl16,* and *trnK/matK*). We estimated divergence-times using Bayesian evolutionary analysis sampling trees and inferred shifts in diversification rates using Bayesian analysis of macroevolutionary mixtures. We found that *Philodendron,* its three subgenera, and the closely related genus *Adelonema* are monophyletic. Within *Philodendron* subgenus *Philodendron*, 12 statistically well-supported clades are recognized. The genus *Philodendron* originated ~25 mya and a diversification diversification-rate upshift was detected at the origin of subgenus *Philodendron* ~12 mya. *Philodendron* is a species-rich Neotropical lineage that diverged from *Adelonema* during the late Oligocene. Within *Philodendron,* the three subgenera currently accepted are recovered in two lineages: one contains the subgenera *Meconostigma* and *Pteromischum* and the other contains subgenus *Philodendron*. The lineage containing subgenera *Meconostigma* and *Pteromischum* underwent a consistent diversification rate. By contrast, a diversification-rate upshift occurred within subgenus *Philodendron* ~12 mya. This diversification-rate upshift is associated with the species radiation of the most speciose subgenus within *Philodendron*. The sections accepted within subgenus *Philodendron* are not congruent with the clades recovered. Instead, the clades are geographically defined.

2.2. Introduction

The Neotropical region (tropical America) is the most species-rich area on Earth comprising ~37% of extant seed plants (Richardson et al., 2001; Antonelli and Sanmartín, 2011). The origin of this exceptional diversity has attracted the attention of biogeographers, plant evolutionary biologists and systematists (Hughes et al., 2013; Pennington et al., 2015). The existence of angiosperm lineages that originated during the Eocene (or earlier) led to the hypothesis that Neotropical forests are "museums" of diversity, which have accumulated species over a long period (Davis et al., 2005; Couvreur et al., 2011; Lohmann et al., 2013; Pennington et al., 2015; Schneider and Zizka, 2017). The rationale for this hypothesis is that Neotropical forests are considered to have constituted stable environments that allowed the accumulation of species whilst extinction rates were low. In contrast, the discovery of lineages that diversified relatively recently from the late Miocene onward supports the hypothesis that the Neotropical forests are more likely "cradles" where species have evolved at high rates (Richardson et al., 2001; Kay et al., 2005; Erkens et al., 2007; Särkinen et al., 2007; Drew and Sytsma, 2013; Neupane et al., 2017). However, the "museum" and the "cradle" models are not mutually exclusive, and the high species diversity in the Neotropics may be explained by high species turnover at different geological periods (Mckenna and Farrell, 2006; Koenen et al., 2015). Therefore, this species diversity in Neotropical lineages may be explained by episodic bursts of high speciation and extinction rates through time (Pennington et al., 2015).

The genus *Philodendron* (Araceae) is among the most characteristic epiphytic components of the Neotropical rainforests, in terms of both species diversity and abundance of individuals (Croat, 1997). With ~560 currently accepted species and an estimated total of ~700 species (Govaerts et al., 2018), *Philodendron* is the second largest genus of the aroid family after *Anthurium*, with >1,000 species (Carlsen and Croat, 2013). In the Araceae, *Philodendron* is one of the most diverse genera in terms of both leaf morphology and life forms; the genus includes terrestrials, lianas, hemiepiphytes, and epiphytes (Croat, 1997; Croat et al., 2010). Despite the significant contribution of *Philodendron* to vascular epiphyte diversity in the Neotropics, phylogenetic studies to date have been based on limited taxon sampling and have resulted in partially resolved phylogenetic trees (Barabé et al., 2002; Gauthier et al., 2008; Loss-Oliveira et al., 2016).

Based on the phylogenetic studies of *Philodendron* available to date, which have used plastid DNA (partial *rpl16* intron, *matK* gene, *trnL* intron, and *trnL-trnF* spacer sequences) and nuclear ribosomal DNA (ETS and ITS), two contrasting hypotheses have been proposed with regard to the monophyly of the genus and its position with respect to the closely related genera *Adelonema* and *Homalomena*. The genus *Adelonema* was recently resurrected (Wong et al., 2016) and comprises 16 Neotropical species formerly assigned to *Homalomena*. The latter is therefore now considered a tropical Asian genus. The phylogenetic trees inferred by Barabé et al. (2002), based on the *trnL* intron and *trnL-trnF* spacer; by Gauthier et al. (2008), based on the *rpl16* intron; by Wong et al. (2013), based on the ITS; and by Wong et al. (2016), using ITS and *matK*, resolved subgenus *Pteromischum* as sister to *Adelonema*. In contrast, the phylogenetic trees inferred by Gauthier et al. (2008), based on ETS and ITS, and by Loss-Oliveira et al. (2016), based on ETS, *matK*, *trnL*, and *trnL-trnF*, recovered the entire genus *Philodendron* as a monophyletic group sister to *Adelonema*.

Morphological and anatomical characters of the inflorescences have been used for the infrageneric circumscription of *Philodendron* (Croat, 1997). Androecial characters were mostly used at the subgeneric level, and gynoecial characters at the sectional level (Engler, 1899; Mayo, 1988, 1989; Croat, 1997) . There are three subgenera in *Philodendron* that are morphologically and anatomically distinct from each other: subgenus *Meconostigma*, subgenus *Philodendron*, and subgenus *Pteromischum* (Mayo, 1986; Croat, 1997; Croat et al., 2016). The relationships among them, however, remain uncertain (Gauthier et al., 2008; Loss-Oliveira et al., 2016). *Philodendron* subgenus *Meconostigma*, which has recently been shown to be monophyletic, comprises 21 mostly terrestrial species distributed in Amazonia, the Mata Atlântica, and the Cerrado (Mayo, 1988; Braucks Calazans et al., 2014; Figure 2.1). *Philodendron* subgenus *Pteromischum* comprises two sections (sect. *Fruticosa*, and sect. *Pteromischum*), and includes 82 liana species distributed mostly in Central America and Amazonia (Grayum, 1996; Croat, 1997; Calazans and Sakuragui, 2013; Barbosa and Sakuragui, 2014; Figure 2.1). With 457 currently accepted species and an estimated total of >600 species, *Philodendron* subgenus *Philodendron* accounts for ~85% of the species diversity of the genus, mainly distributed in the Andes, Amazonia, Central America, and the Chocó ecoregion (Figure 2.1). Members of subgenus *Philodendron* are predominantly epiphytic (including facultative epiphytes and hemiepiphytes), although it is often difficult to attribute *Philodendron* species unequivocally to the epiphytic life form (Zotz, 2013). The currently accepted classification within subgenus *Philodendron* consists of 10 sections, 12 subsections, and 11 series mainly characterized by leaf morphology in combination with the

number of locules per ovary, the number of ovules per locule, the type of placentation, and the shape of the style (Croat, 1997; Köster and Croat, 2011). The monophyly of subgenus *Philodendron* is unclear; the phylogenetic trees inferred from analyses of ETS and ITS of 55 species recovered subgenus *Philodendron* as only a weakly supported monophyletic group (Gauthier et al., 2008).

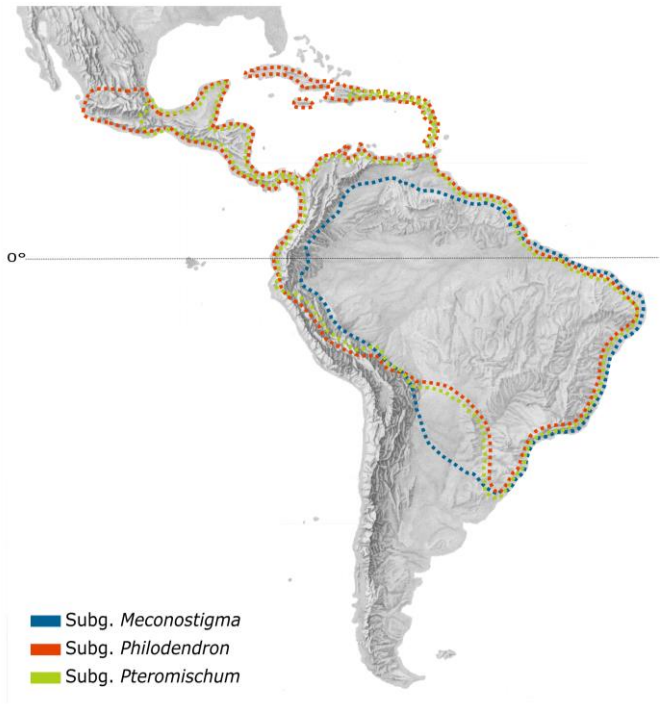

Figure 2.1. Distribution area of each of the three subgenera of *Philodendron*. Relief source: Herwig G. Schutzler, 1970.

The origin and divergence times of *Philodendron* remain subjects in need of further investigation. According to the fossil-calibrated phylogenetic tree inferred for the family Araceae (Nauheimer et al., 2012), the clade including *Adelonema*, *Furtadoa*, *Homalomena*, and *Philodendron* diverged from its sister clade ~25 mya (95% highest posterior density [HPD]: 11.8–39.4) in the late Oligocene, and *Philodendron* originated ~20.5 mya (95% HPD: 9.2–33.2) in the early Miocene. Loss-Oliveira et al. (2016) used fixed average substitution rates of plastid coding regions estimated in monocots to infer ages of *Philodendron*, and suggested that *Homalomena* diverged from its sister clade comprising *Adelonema* and *Philodendron* in the middle to late Miocene (95% HPD: 9.2–12.8, median age not given) and that *Philodendron* originated ~8.6 mya (95% HPD: 6.8–12.1). In both of the above studies,

however, the nodes critical for inferring the closest extant relatives of *Philodendron* are not well supported.

Well resolved, robustly supported, and time-calibrated phylogenetic trees of species-rich Neotropical lineages such as *Philodendron* are not only relevant to better understanding its origin and species radiation, but will provide the comparative basis to gain insights into the evolution of Neotropical plant lineages. Therefore, the goal of this investigation was to generate a well resolved and statistically supported phylogeny of *Philodendron* based on a broad taxon sampling that could also be used in divergence-time analyses. Consequently, we generated a dataset of three plastid group II introns for 125 taxa within the genus *Philodendron* to specifically [1] assess the monophyly of *Philodendron* and resolve relationships both between the genus *Philodendron* and the closely related genera *Adelonema* and *Homalomena* and between the subgenera within *Philodendron* (*Meconostigma*, *Philodendron*, and *Pteromischum*); [2] assess the relationships down to species level, in particular within the large subgenus *Philodendron*; and [3] estimate relative timing and diversification rate shifts throughout the history of *Philodendron*. In addition, we compare our findings in *Philodendron* with other Neotropical plant lineages and discuss them in the context of the scenarios for species diversification in the Neotropics (museum and cradle models; Koenen et al., 2015; Pennington et al., 2015).

2.3. Material and Methods

2.3.1. Taxon sampling, DNA extraction, amplification, sequencing, and alignment

The taxonomic treatment by Krause (1913) was the last complete revision of *Philodendron*. Therefore, we sampled as widely as possible across the genus, following regional taxonomic treatments and comparative studies of selected species groups (Mayo, 1991; Grayum, 1996; Croat, 1997; Köster and Croat, 2011). We covered both a broad range of morphological variation as well as the entire geographic range of the genus. We also included three species of both genera *Adelonema* and *Homalomena* in the ingroup because the relationships between *Adelonema* and the three subgenera of *Philodendron* remained to be resolved (Gauthier et al., 2008; Wong et al., 2013; 2016). Within *Philodendron*, we sampled

125 taxa (137 accessions), which represent all accepted subgenera and sections within subgenus *Philodendron*, including the type of the genus (Krause, 1913; Mayo, 1988, 1989, 1991; Grayum, 1996; Croat, 1997; Köster and Croat, 2011). Based on phylogenetic analyses of the entire Araceae (Cusimano et al., 2011; Nauheimer et al., 2012), we selected 11 taxa from 10 aroid genera as outgroups, including species from the subfamilies Pothoideae (*Anthurium hookeri* Kunth and *Anthurium scandens* [Aubl.] Engl.), Monsteroideae (*Spathiphyllum blandum* Schott), Lasioideae (*Urospatha sagittifolia* [Rudge] Schott), and Aroideae (*Aglaonema marantifolium* Blume, *Anchomanes difformis* [Blume] Engl., *Colocasia esculenta* [L.] Schott, *Montrichardia linifera* [Arruda] Schott, *Pseudohydrosme gabunensis* Engl., *Schismatoglottis calyptrata* [Roxb.] Zoll. & Moritzi, and *Zantedeschia rehmannii* Engl.; Appendix A1).

Genomic DNA was extracted from silica-dried leaf tissues using the CTAB method by of Doyle and Doyle (1987), with extraction of three fractions for each sample (Borsch et al., 2003). DNA stocks were kept at −20°C, and usually 1:10 working dilutions with water were used for polymerase chain reaction (PCR).

Plastid group II introns of *petD*, *rpl16*, and *trnK*, including the *matK* coding region, were selected on the basis of their utility at both deep and shallow phylogenetic levels in angiosperms (Kelchner, 2002; Borsch and Quandt, 2009). The *petD* region has not yet been used in phylogenetic analyses of *Philodendron*, and only short fragments of the *rpl16* intron (~500 bp) and *trnK/matK* (~450–1,600 bp) have been used to date (Gauthier et al., 2008; Loss-Oliveira et al., 2016). The *petD* and *rpl16* regions were amplified and sequenced by adding M13 tails to the amplification primers (Messing, 1983). The *petD* region was amplified and sequenced following Löhne and Borsch (2005), and *rpl16* with primers rpl16F and rpl16R (Campagna and Downie, 1998). The *trnK/matK* region was extended to *psbA* and amplified in two halves using the following primer combinations: trnKF Wicke and Quandt (2009) and ARAmatK655R (5′-GGATTCGCATTCGCAAACTACAT-3′; present study), and ARAmatK480F (Hilu et al., 2003) and psbA5'R (Shaw et al., 2005). Instead of primer ARAmatK480F, a further internal specific primer ARAmatK582F (5′-TTCACGAATATCATAATTGG-3′; present study) was designed for *Montrichardia linifera*.

PCR was performed in a peqSTAR Thermocycler 1107D (PeqLab, Erlangen, Germany). The mixture for one reaction for the *rpl16* and *trnK/matK* regions consisted of 10 µL of dNTPs 20 pm/µL, 5 µL of 10x *Taq*-buffer S, 3 µL of $MgCl_2$ with a concentration of 25 mM, 2 µL of each primer with a concentration of 20 pm/µL, 0.3 µL of *Taq* DNA Polymerase with 5 units/µL (PeqLab no. PEQL01-8120, Erlangen, Germany) and 4 µL of DNA template.

Ultrapure H_2O was added to obtain the final volume of 50 µL. The PCR mixture for the *petD* region included 4.9 µL of betaine (5M) in addition. Temperature profiles for the PCR amplification of *petD* and *trnK/matK* consisted of an initial denaturation of 1:30 min at 95°C, followed by 34 cycles of 30 s denaturation at 95°C, 1 min of primer annealing at 57°C and 1 min of extension at 72°C, and a final elongation period of 10 min at 72°C. For the *rpl16* region, the temperature profile consisted of an initial denaturation step of 1:30 min at 95°C, followed by 4 cycles of 1 min of primer annealing at 58°C and 1 min of extension at 72°C, 30 cycles of a 30 s denaturation step at 95°C, 1 min of primer annealing at 55°C and 1 min of extension at 72°C, followed by a final extension step at 72°C for 10 min. The PCR products were electrophoresed on 1.5% agarose gels in 1x Tris-acetate-EDTA (TAE) buffer (pH 8.0) and stained with SYBR-Gold (Life Technologies no. S11494, Carlsbad, California, USA). Bands were excised from the gel and cleaned using the GenepHlow Gel/PCR kit (Geneaid, New Taipei, Taiwan). Cycle sequencing was carried out by Macrogen Europe (Amsterdam, The Netherlands), using either the same primers as in the PCR reactions or M13. DNA samples are deposited at the Botanic Garden and Botanical Museum Berlin (BGBM) and are available via the Global Genome Biodiversity Network (GGBN; Droege et al., 2016).

Sequence files were edited and aligned manually using PhyDE version 0.9971 (Müller et al., 2005). Alignments were generated according to the similarity criteria for homology assessment and the the motif-alignment principles of Borsch et al. (2003) and Löhne and Borsch (2005). The alignment of *rpl16* sequences was not straightforward due to the occurrence of A/T-rich stem-loop elements. Regions of unclear homology such as many tandem repeats, mononucleotide repeats (microsatellites) and other hypervariable sections were excluded from the final alignment. Indels were coded as binary characters using the simple-indel-coding method (Simmons and Ochoterena, 2000) as implemented in SeqState version 1.4.1 (Müller, 2005). Final DNA sequences were submitted to ENA (www.ebi.ac.uk/ena) with the help of custom Python script (https://github.com/michaelgruenstaeudl/annonex2embl).

2.3.2. Phylogenetic analyses

Parsimony and likelihood analyses were conducted following the recommendations provided by Simmons and Freudenstein (2011). Parsimony analyses were conducted using the "parsimony ratchet" (Nixon, 1999) with PRAP version 2.0b3 (Müller, 2004) in conjunction

with PAUP* version 4.0b10 (Swofford, 2003) using the CIPRES portal (Miller et al., 2010). Ratchet settings included 200 iterations, unweighting 25% of the positions randomly (weight = 2), and 100 random addition cycles. A strict consensus tree was constructed from all saved trees. Jack-knife (JK) support was calculated in PAUP by performing a single heuristic search within each 10,000 JK pseudoreplicates using the tree bisection and reconnection (TBR) branch-swapping algorithm and a deletion of 36.79% characters in each replicate and saving 100 trees in each search. Starting trees were generated via stepwise addition with simple sequence addition.

The likelihood scores of potential models of sequence evolution for each partition and for the combined dataset were evaluated using jModelTest version 2.1.7 (Darriba et al., 2012). We selected the best-fitting model under Akaike's Information Criterion (AIC). For the initial tree search, the improved version of the neighbour-joining algorithm BIONJ (Saitou and Nei, 1987) was used (Gascuel, 1997).

Maximum likelihood tree was estimated using the graphical user interface (GUI) of RAxML version 1.5b1 (Silvestro and Michalak, 2012). Rapid bootstrap support (BS) was estimated based on the majority-rule consensus tree from 1,000 pseudoreplicates with 200 searches. The general time-reversible (GTR) + Γ and the binary (BIN) + Γ models were used for the nucleotide partition and indel partition, respectively.

The nucleotide data were partitioned for Bayesian inference as follows: (1) *petD*: three partitions (*petB* spacer with TVM + I, *petD* 5′ exon with F81, and *petD* intron with TPM1uf + Γ), (2) *rpl16*: one partition (*rpl16* intron with TIM2 + Γ), and (3) *trnK/matK*: 4 partitions (*matK* with TVM + I + Γ, *trnK* 3′ exon with JC, *trnK* 3′ intron with TVM + I, and *trnK* 5′ intron with TPM1uf + Γ). The corresponding indel matrices were added using the restriction site (binary) model (F81-like model) as recommended in Ronquist et al. (2011) for gaps and other binary characters. Bayesian inference analyses were conducted in MrBayes version 3.2 (Ronquist and Huelsenbeck, 2003) on CIPRES. Four runs each with four chains were performed for 50 million generations, sampling every 10,000 generations. Results were processed in Tracer version 1.6.0 (Bouckaert et al., 2014) to check for convergence. The first 10% of trees were discarded as burn-in; the remaining trees were used to construct a 50% majority-rule consensus tree.

The 50% majority-rule consensus tree obtained in MrBayes was processed in TreeGraph version 2.13.0-748 beta (Stöver and Müller, 2010). Support values obtained in maximum parsimony and maximum likelihood analyses were added with the function "Add support values" in TreeGraph. Simultaneously, this function allows the detection of conflicts

between nodes and branches obtained in the MrBayes tree and the maximum parsimony and maximum likelihood. Final PDF file was edited using the open source vector graphics editor Inkscape version 0.92 (The Inkscape Project, inkscape.org).

2.3.3. Divergence-time estimates

Testing of the optimal speciation tree prior for divergence-time estimates in *Philodendron* was conducted in BEAST version 1.8.2 (Xie et al., 2011). As a prior of the clock model (strict vs. uncorrelated lognormal relaxed clock [UCLN]; Drummond et al., 2006), we selected the UCLN. This model with a distinct rate along branches drawn from a lognormal distribution is considered more robust to avoid violation of assumptions about clock rate variation and has a better fit to simulated empirical datasets than the strict or the autocorrelated clock models (Crisp et al., 2014). Furthermore, in the UCLN analyses, a coefficient of variation higher than zero (>0.5) was obtained, which confirmed that the data did not fit a clock-like model (Drummond and Bouckaert, 2015). In order to select the appropriate branching process (speciation tree) prior to be used in subsequent divergence-time analyses, we conducted marginal likelihood estimation (MLE) using stepping-stone sampling (SSS) with 150 path steps in BEAST (Xie et al., 2011). The choice of branching process prior has been shown to bias node-age estimates (Condamine et al., 2015) and therefore we tested its effect under both birth-death and Yule speciation models separately. Each analysis was set with a chain length of one million iterations and using a simple model with two partitions: [1] the combined nucleotide and [2] the indel matrix under the GTR-Γ and the multistate stochastic Dollo model (Alekseyenko et al., 2008; Woodhams et al., 2013), respectively. Other parameters were set by default in the GUI application for generating BEAST XML files (BEAUTi). The MLE values were used to calculate log-Bayes factors (BFs); BF values above 5 indicated that one model was significantly favored over the other (Baele and Lemey, 2013). Based on the results of the MLE using the SSS analyses and BFs, the birth-death speciation prior best fit the data (139.93; Table 2.1). Therefore, all final analyses were conducted using a birth-death speciation prior under a UCLN.

Table 2.1. Values of the marginal likelihood estimates and Bayes factors analyses using stepping-stone sampling with 150 path steps. UCLN, uncorrelated lognormal model; ESS, effective sample size; MLE, marginal likelihood estimation; BFs, Bayes factors.

Speciation prior (under UCLN)	ESS	MLE	BFs
Birth-death model	>200	−25693.48	139, 93
Yule model	>200	−25833.41	

2.3.4. Divergence-time estimates in *Philodendron*: Calibration approaches

Molecular dating was performed in BEAST version 2.4.3 (Bouckaert et al., 2014), using the corresponding version of BEAUTi to set the parameters. We assessed two calibration approaches (Table 2.2): one consisted of three secondary constraints, and the other consisted of a fossil in combination with a secondary constraint (fossil+secondary constraint; Table 2.2). Here, we refer to a secondary calibration point as a divergence-time estimation that was derived from a molecular dataset on the basis of a primary external calibration point, usually one based on paleontological considerations (Shaul and Graur, 2002). The data partitions and substitution models were set according to jModelTest (*matK* = TVM + I +Γ, *petB* spacer and *trnK* 3′ intron = TVM + I, *petD* 5′ exon = F81, *petD* intron and *trnK* 5′ intron = TPM1uf + Γ, *trnK* 3′ exon = JC and *rpl16* intron = TIM2 + Γ). For all substitution models, rates of transitions were set in the XML file according to AIC values of jModelTest. For indels, we applied the multistate stochastic Dollo model.

Table 2.2. Parameters used in the secondary and fossil+secondary calibration approaches. Upper and lower values used are depicted in millions of years. UCLN, uncorrelated lognormal model; U, uniform prior; E, exponential prior; NA, not applicable; asterisk denotes nodes by Nauheimer et al. (2012).

Node	UCLN (secondary calibration)	UCLN (fossil+secondary calibration)
28*	80–100 Ma; U	NA
109*	54–81 Ma; U	NA
113*	11–39 Ma; U	11–39 Ma; U
Fossil (*Montrichardia aquatica*)	NA	Mean = 58.7 Ma (61.7–55.8 Ma); E

2.3.5. Node selection for the secondary calibration and the fossil+secondary calibration approaches

The use of secondary calibrations is the only source of calibration information for many groups, particularly for those in which the fossil record is scarce or non-existent, such as epiphytes in the wet tropics (Forest, 2009; Hipsley and Müller, 2014). To supplement secondary calibrations in studies of lineages where the focal group has no fossils, one option is to sample more distantly related clades that include paleontological records (Schenk, 2016). To date, no fossil has been attributed to *Philodendron* or its closely related genera (Mayo, 1991; Croat, 1997; Mayo et al., 1997; Loss-Oliveira et al., 2016). There is, however, one reliable fossil attributed to the Neotropical genus *Montrichardia* (Herrera et al., 2008) that is, like *Philodendron*, nested within subfamily Aroideae (Cusimano et al., 2011; Nauheimer et al., 2012). Previous phylogenetic studies including a broad taxon sampling across Araceae were conducted applying fossil calibration points, but this included only one species of *Philodendron* (Nauheimer et al., 2012). Our goal was, therefore, to test two calibration strategies: [1] secondary calibration and [2] fossil+secondary calibration.

We sampled as broadly as possible to include nodes strongly supported in the divergence-time analyses based on multiple fossil calibrations across the family Araceae by Nauheimer et al. (2012); nodes 28, 109, and 113 in Nauheimer et al. (2012) all received PP = 1.0. Thus, the following nodes correspond to those suitable for secondary calibration constraints given our taxon sampling: starting with the crown age of the *Philodendron* clade in Nauheimer et al. (2012; node 113) that includes the genera *Adelonema*, *Furtadoa*, *Homalomena*, and *Philodendron* according to Cusimano et al. (2011). A second constraint (node 109) corresponded to the crown age of one of the major lineages within the subfamily Aroideae represented in our study by *Anchomanes difformis* and *Pseudohydrosme gabunensis* from Nephthytideae, *Aglaonema marantifolium* from Aglaonemateae, and *Zantedeschia rehmannii* from the Zantedeschia clade and the *Philodendron* clade. To calibrate the root of our tree, we used the crown age of the split of the subfamilies Aroideae+Zamioculcadoideae and Lasioideae from Nauheimer et al. (2012; node 28). In order to incorporate a fossil calibration, we included the species *Montrichardia linifera* (Herrera et al., 2008) and two representatives of its closely related lineages (*Colocasia esculenta* and *Schismatoglottis calyptrata*) according to Nauheimer et al. (2012).

2.3.6. Parameters used in the secondary and fossil+secondary calibration approaches

In the secondary calibration approach, the three nodes were constrained under a uniform distribution prior (Table 2.2). This distribution is recommended for such calibrations, allowing every age between the upper and lower bounds to have equal prior probability (Schenk, 2016). We applied the mean and 95% HPD intervals obtained by Nauheimer et al. (2012) in the BEAST analysis under a UCLN model with a uniform prior and a Jukes-Cantor (JC) + Γ tree model. The following initial and upper values were applied: 80 Ma and 100 Ma (node 28), 54 Ma and 81 Ma (node 109), and 11 Ma and 39 Ma (node 113).

In the fossil+secondary calibration approach, two nodes were constrained (Table 2.2). The first node was constrained using the minimum age of a fossilized leaf identified as *Montrichardia aquatica* dated from the middle to late Paleocene 61.7–55.8 mya (Herrera et al., 2008). An exponential distribution prior was applied with an offset of 55.8 and a mean of 58.7, constraining the minimum age of the node with this fossil (*Colocasia esculenta*, *Montrichardia linifera*, and *Schismatoglottis calyptrata*). The mean value of 58.7 was selected based on the mean age estimated for the fossil. In an initial study, the fossil constraint was applied in combination with all three secondary points described above but the nodes calibrated with the ages of nodes 28 and 109 corresponded to the nodes prior and subsequent to the fossil calibrated node, respectively, in the BEAST MCC topology (Appendix A2). Given the range in calibration ages between these nodes (100 Ma and 81 Ma for the upper values of nodes 28 and 109, respectively) and their proximity to the fossil node, it was not possible to apply a fossil calibration and the entire set of three secondary constraints used in the secondary calibration approach to our dataset. Therefore, we applied the fossil calibration in combination with only one secondary calibration constraint to the ingroup (node 113) as described above (Table 2.2).

To assess the consistency of the BEAST results, three independent Markov chain Monte Carlo (MCMC) runs were conducted using the same dataset and the same parameters for both secondary and fossil+secondary calibration approaches. Each chain was run for 100 million generations logging parameters every 10,000 generations. Tracer version 1.6.0 (Bouckaert et al., 2014) was used to visualize log files, assess the stationarity on the log-likelihood curves, and determine the burn-in. The first 10% saved trees from each run were discarded, and the remaining trees were combined in Logcombiner version 2.4.3 (Drummond et al., 2012).

Treeannotator version 2.4.3 (Bouckaert et al., 2014) was used to estimate the maximum clade credibility (MCC) tree with posterior probability values (PP; limit set to 0.5) and mean node ages with the HPD of these ages. MCC trees estimated using different time calibration approaches were then compared in FigTree version 1.4.2 (Rambaut, 2012) and exported as with the phylogenetic trees described above.

2.3.7. Diversification rate shifts

Heterogeneity in rates of diversification processes (speciation and extinction) and in rate shifts across the genus *Philodendron* was estimated using BAMM version 2.5.0 (Rabosky, 2014; Rabosky et al., 2017). Speciation and extinction might vary through time and among lineages, in particular in clades such as *Philodendron*, where species diversity is imbalanced among subgenera. BAMM detects these rate shifts without a priori hypotheses on the number and location of these events based on a birth-death process. The MCC trees from the BEAST analyses with both secondary calibration and fossil+secondary calibration approach were used as input files without outgroup. The priors for the diversification rate analyses were set using the setBAMMPriors command in the BAMMtools-package version 2.1.6 (Rabosky, 2014) in R version 1.1.419 (R Core Team, 2013). Incomplete taxon sampling can bias inferences of diversification rates (Shi and Rabosky, 2015). We therefore specified the fraction of missing species in each subgenus of *Philodendron* under the assumption of random taxon sampling (Fitzjohn et al., 2009). The sampling fraction was calculated as a ratio of the number of species included divided by the total number of species currently accepted: *Meconostigma*: 3/21, *Pteromischum*: 8/82, and *Philodendron* 119 (126 accessions)/457, these proportions were used as inputs for the "SamplesProbsFilename" argument in the Control File. To test the sensitivity of the sampling fraction, we set two additional analyses for the MCC tree from the BEAST analysis with secondary calibrations where we assumed one smaller sampling fraction for each subgenus (0.05) and another with a larger one (0.5) (see also Shi and Rabosky, 2015). Given the ongoing debate on the theoretical foundations of the inference model in BAMM (Moore et al., 2016; Rabosky et al., 2017), we used the "BAMMlikelihood" function as recommended by Rabosky et al. (2017), which returns the log-likelihood for a given configuration of events on a phylogenetic tree. We used the same priors for the sampled fraction analysis and obtained a similar value for the log-likelihood of the final generation. According to Rabosky et al. (2017), similar or identical values indicate that BAMM is

correctly computing the likelihood. These analyses were conducted using a Poisson prior value of 1.0 for the "ExpectedNumberofShifts" as recommended by Rabosky (2014) and Shi and Rabosky (2015) that is more conservative and implies a null hypothesis of zero rate shifts across the phylogeny. BAMM was implemented in the C++ command line. We ran four parallel MCMCs for 50 million generations and sampled the results every 5,000 generations. The output files were analyzed in R, using the BAMMtools-package.

Convergence was assessed in the R-package "coda" (Plummer et al., 2006) by checking the ESS values for likelihood and number of shift events, the first 10% of the sampled generations were discarded as burn-in. Values >200 were considered indicative of convergence. Bayes factors were computed to compare the evidence for models with at least one rate shift to the evidence for the null model using the "computeBayesFactors" function. The event output files were analyzed by discarding 10% burn-in samples and assessing the distinct rate-shift configurations within the 95% credible set using the "credibleShiftSet" function. Subsequently, the position(s) of the significant rate shift was inferred by observing the nodes with the highest PP values (up to 95%) using the "distinctShiftConfigurations" function. To complement our analyses, we estimated rate shifts through time using the "credibleShiftSet" function. A burn-in of 10% was applied and a diversification rate plot through time was obtained using the "plotRateThroughTime" function. This analysis was carried out initially for the entire dataset and, in order to visualize separately the diversification process for the subgenera, we plotted two datasets separately: the clade corresponding to the subgenera *Meconostigma* and *Pteromischum* and the clade corresponding to subgenus *Philodendron*.

2.4. Results

2.4.1. Phylogenetic analyses

Individual matrices contained 154 new sequences for the *petD, rpl16,* and *trnK/matK* regions and 1,259, 2,898, and 3,197 aligned nucleotides, respectively. In cases of intraspecific variation in one, two, or three plastid regions, multiple sequences for the same species were maintained in the alignment. After excluding hotspots in each single region alignment (*petD*: a poly-A [positions 260–274]; *rpl16*: two poly-A [196–211; 320–330] and two hotspots [765–2,029; 2,933–2,998] and *trnK/matK* three poly-A [249–256; 875–881; 2,571–2,580], poly-T

[2,857–2,869] and poly-AT [2,934–2,998]), the combined plastid alignment contained 5204 aligned nucleotides (1,107 for *petD*, 1,185 for *rpl16*, and 2,912 for *trnK/matK*). Simple indel coding resulted in the addition of 267 binary characters (51 for *petD*, 114 for *rpl16*, and 102 for *trnK/matK*).

Sequence statistics, models of sequence evolution (AIC) and tree statistics for the individual marker alignments and the combined plastid dataset are presented in Appendix A3. Bayesian inference, maximum likelihood, and maximum parsimony analyses of the combined plastid dataset produced nearly identical topologies with the exception of two inconsistent placements of the species *Colocasia esculenta*, *Montrichardia linifera*, *Schismatoglottis calyptrata*, and *Zantedeschia rehmannii* and inconsistences found within the subgenus *Philodendron* (clades 5–14) (displayed in square brackets in Figure 2.2).

2.4.2. Phylogenetic relationships between the genera *Adelonema*, *Homalomena*, and *Philodendron*

The MrBayes 50% majority-rule consensus tree based on the analysis of the combined plastid dataset with node support values for maximum likelihood, maximum parsimony, and Bayesian inference is shown in Figure 2.2. *Homalomena* is supported as monophyletic (BS = 100, JK = 100, PP = 1.0) and resolved as sister to a clade consisting of the Neotropical genera *Adelonema* and *Philodendron* (BS = 83, JK = 85, PP = 0.83). The genera *Adelonema* and *Philodendron* are both resolved as monophyletic groups (BS = 91, JK = 96, PP = 1.0 and BS = 94, JK = 92, PP = 1.0, respectively).

2.4.3. Relationships within the genus *Philodendron*

Within *Philodendron*, two major lineages are found (lineages A and B; Figure 2.2). Lineage A (BS = 90, JK = 94, PP = 0.92) contains the subgenera *Meconostigma* (BS = 100, JK = 100, PP = 1.0; clade 1) and *Pteromischum* (BS = 100, JK = 100, PP = 1.0; clade 2) and lineage B (BS = 100, JK = 100, PP = 1.0) corresponds to the larger subgenus *Philodendron*. Within subgenus *Philodendron*, there are 12 well-supported clades (clades 3–14; Figure 2.2). The first clade (clade 3) consists of species from different geographical regions of the Neotropics, including *P. hederaceum* (Jacq.) Schott, the most widespread *Philodendron* species, which essentially covers the entire range of the genus. The next branching clade

(clade 4) comprises species endemic to the Guianas, with the single exception of the very widespread species *P. fragrantissimum* (Hook.) G. Don. Clades 5–14 form the highly supported core of subgenus *Philodendron* (BS = 100, JK = 100, PP = 1.0; Figure 2.2).

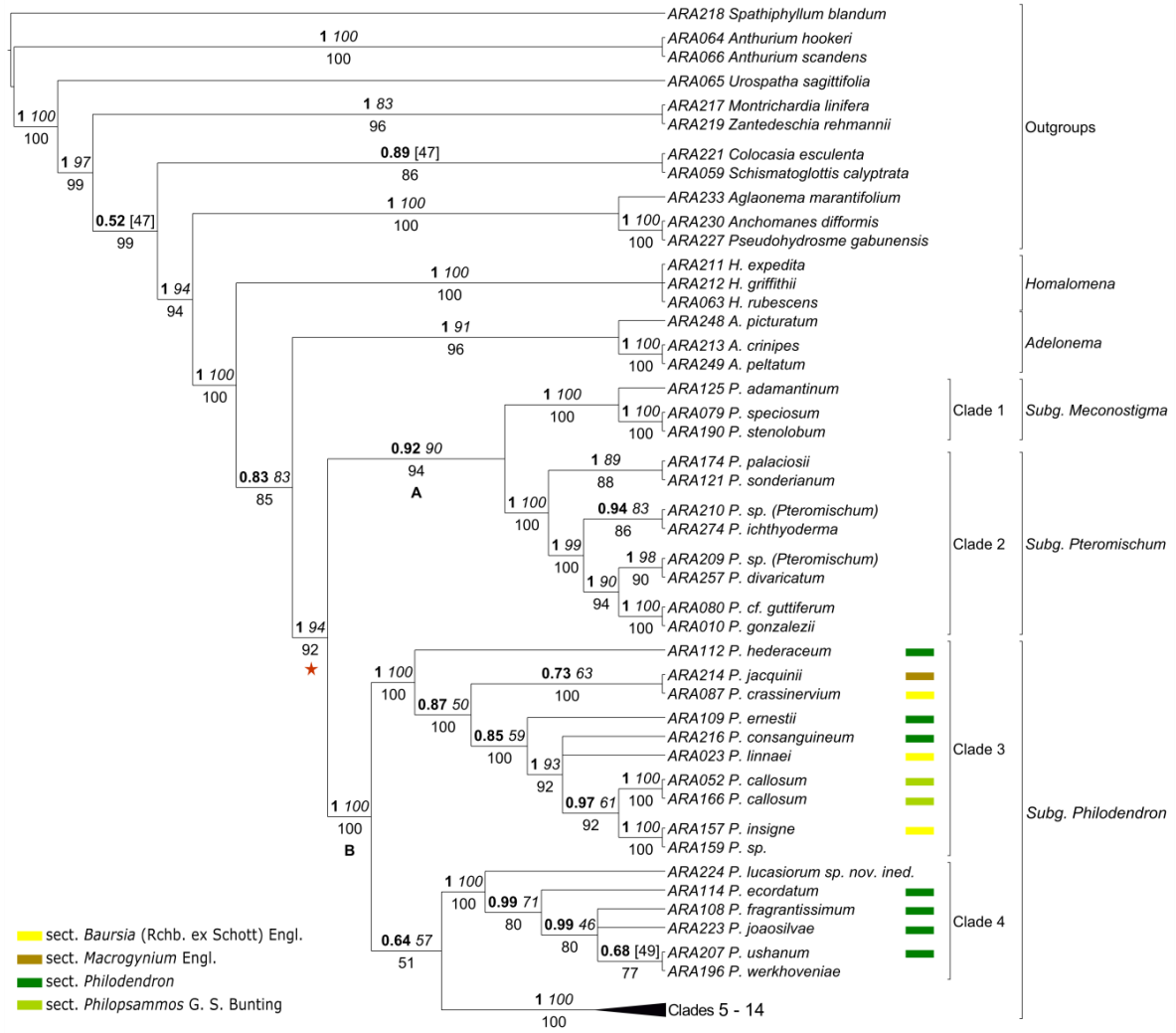

Figure 2.2. (a) Bayesian 50% majority-rule consensus tree of *Philodendron* with three plastid markers (*petD*, *rpl16*, and *trnK/matK*). Values above branches indicate posterior probability (bold) and bootstrap (italic) supports, and values below branches indicate Jack-knife support. Values in square brackets indicate conflicting topologies between Bayesian inference and maximum likelihood (above branches) and maximum parsimony (below branches) detected in TreeGraph. Node tips are labelled with DNA number and species names. Star = genus *Philodendron*; A = subgenera *Meconostigma* + *Pteromischum*; B = subgenus *Philodendron*. Key, bottom left: sections recognized within subgenus *Philodendron* (Croat, 1997; Köster and Croat, 2011). Colored boxes next to tips indicate the sectional attribution, which is unknown or ambiguous for species without boxes.

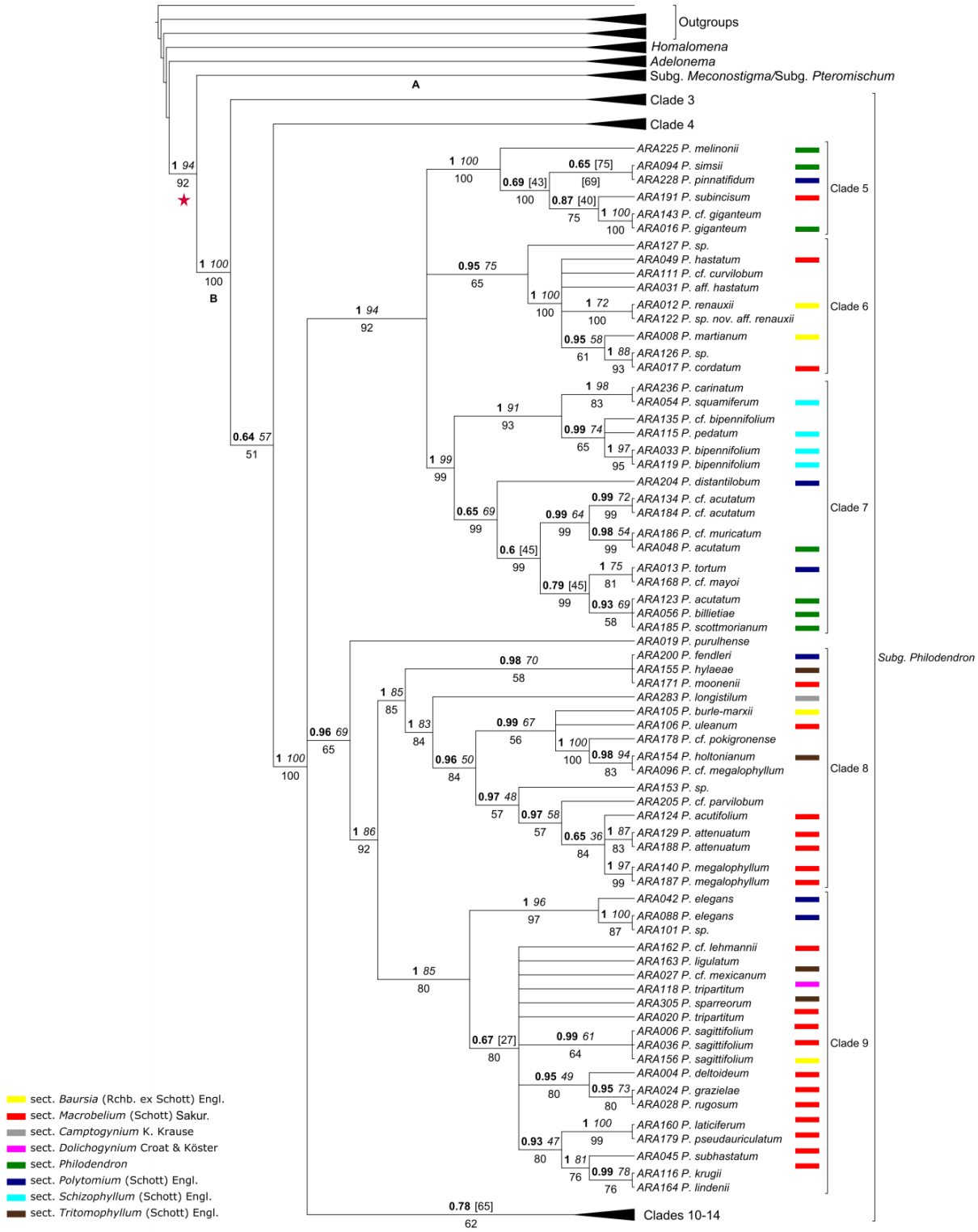

Figure 2.2. (b, continued)

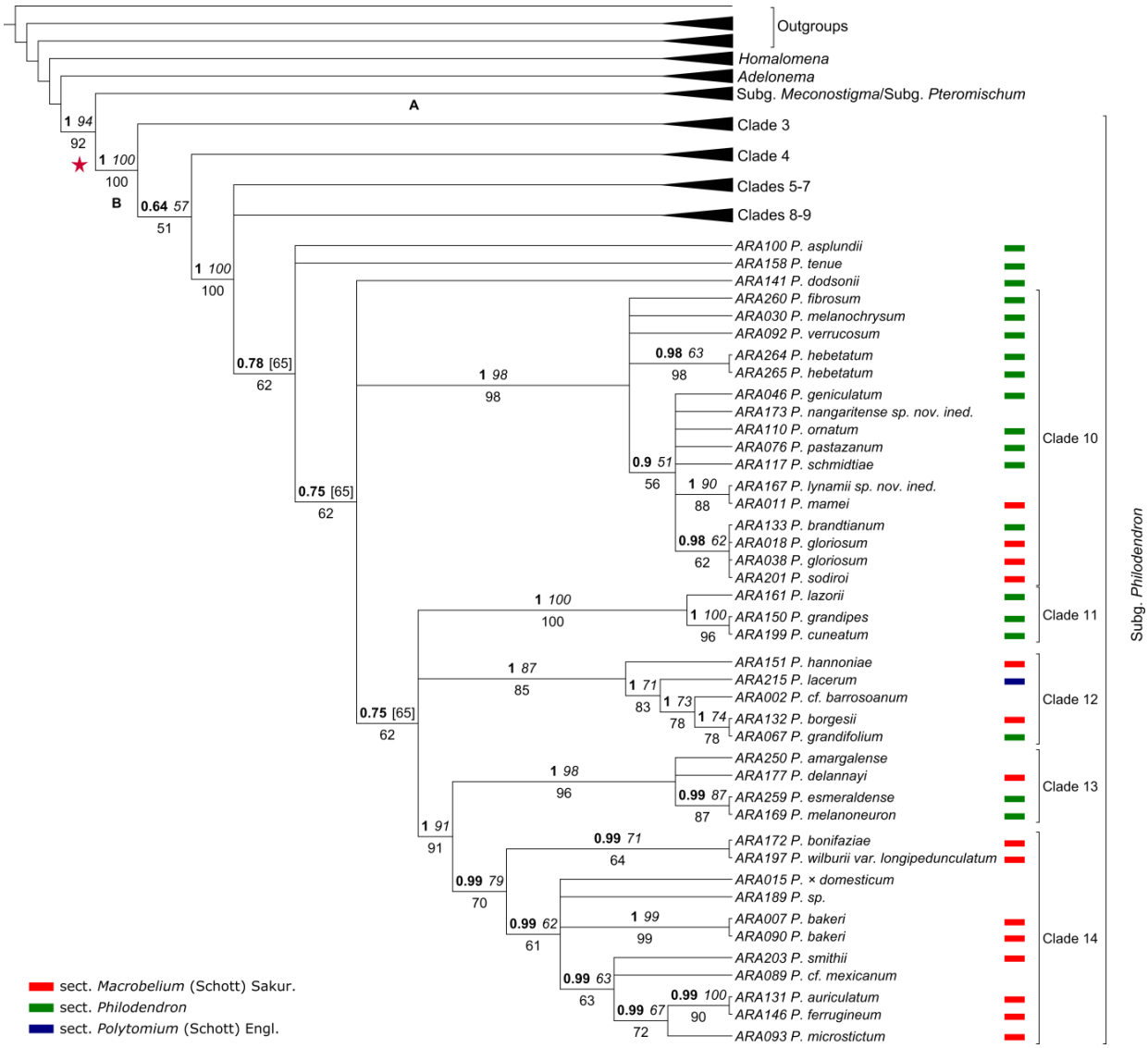

Figure 2.2. (c, continued)

2.4.4. Divergence-time estimates in the secondary calibration approach

The BEAST tree based on the secondary calibration approach is presented in Figure 2.3 with crown and stem node age estimates for the clades proposed in Table 2.3. Stem ages of ~111.14 Ma (95% HPD: 81.75–148.17) for the clade consisting of subfamilies Pothoideae and

Monsteroideae and of ~87.74 Ma (95% HPD: 80.1–97.51) for the clade including subfamilies Lasioideae and Aroideae+Zamioculcadoideae were estimated. The stem age of the ingroup containing *Homalomena*, *Adelonema*, and *Philodendron* was estimated ~53.28 Ma (95% HPD: 39.18–66.23). The stem age of the clade containing *Adelonema* and *Philodendron* was inferred to be ~27.31 Ma (95% HPD: 18.9–36.64). The diversification of *Philodendron* and *Adelonema* occurred ~25.53 mya (95% HPD: 17.81–33.94), in the late Oligocene.

Within genus *Philodendron*, the split between subgenus *Philodendron* and the clade consisting of subgenera *Meconostigma* and *Pteromischum* was estimated as ~22.1 mya (95% HPD: 15.48–29.79) in the early Miocene. The crown nodes of the subgenera *Meconostigma*, *Pteromischum*, and *Philodendron* were estimated to be ~6.66 Ma (95% HPD: 2.55–11.88), ~14.56 Ma (95% HPD: 8.64–20.54) and ~18.06 Ma (95% HPD: 12.3–24.44), respectively. Within subgenus *Philodendron*, in contrast to Bayesian inference, maximum likelihood, and maximum parsimony trees, clade 12 was recovered as sister to a major clade containing clades 5–14 in the BEAST analyses (Figures 2.2 and 2.3; Appendix A2). Clades 5, 6 and 11 were not supported. The remaining clades within subgenus *Philodendron* diversified during the past 11 Ma (Figure 2.3 and crown ages in Table 2.3).

2.4.5. Divergence-time estimates in the fossil+secondary calibration approach

Inferences with the fossil+secondary calibration approach resulted in overall younger ages compared to the ages inferred with the secondary calibration approach (Table 2.3; Appendices A2 and A4). The stem age of the node consisting of subfamilies Pothoideae and Monsteroideae was estimated to be ~87.1 Ma (95% HPD: 57.14–121.31); the stem age of subfamilies Lasioideae and Aroideae+Zamioculcadoideae was estimated to be ~72.91 Ma (95% HPD: 59.24–87.46). The stem age of the ingroup containing *Homalomena*, *Adelonema*, and *Philodendron* was estimated at ~45.23 Ma (95% HPD: 32.84–56.95). The stem age of the clade containing *Adelonema* and *Philodendron* was inferred to be ~21.55 Ma (95% HPD: 13.87–29.89). The diversification of *Philodendron* and *Adelonema* occurred ~18.61 mya (95% HPD: 12.19–26.12), in the early Miocene.

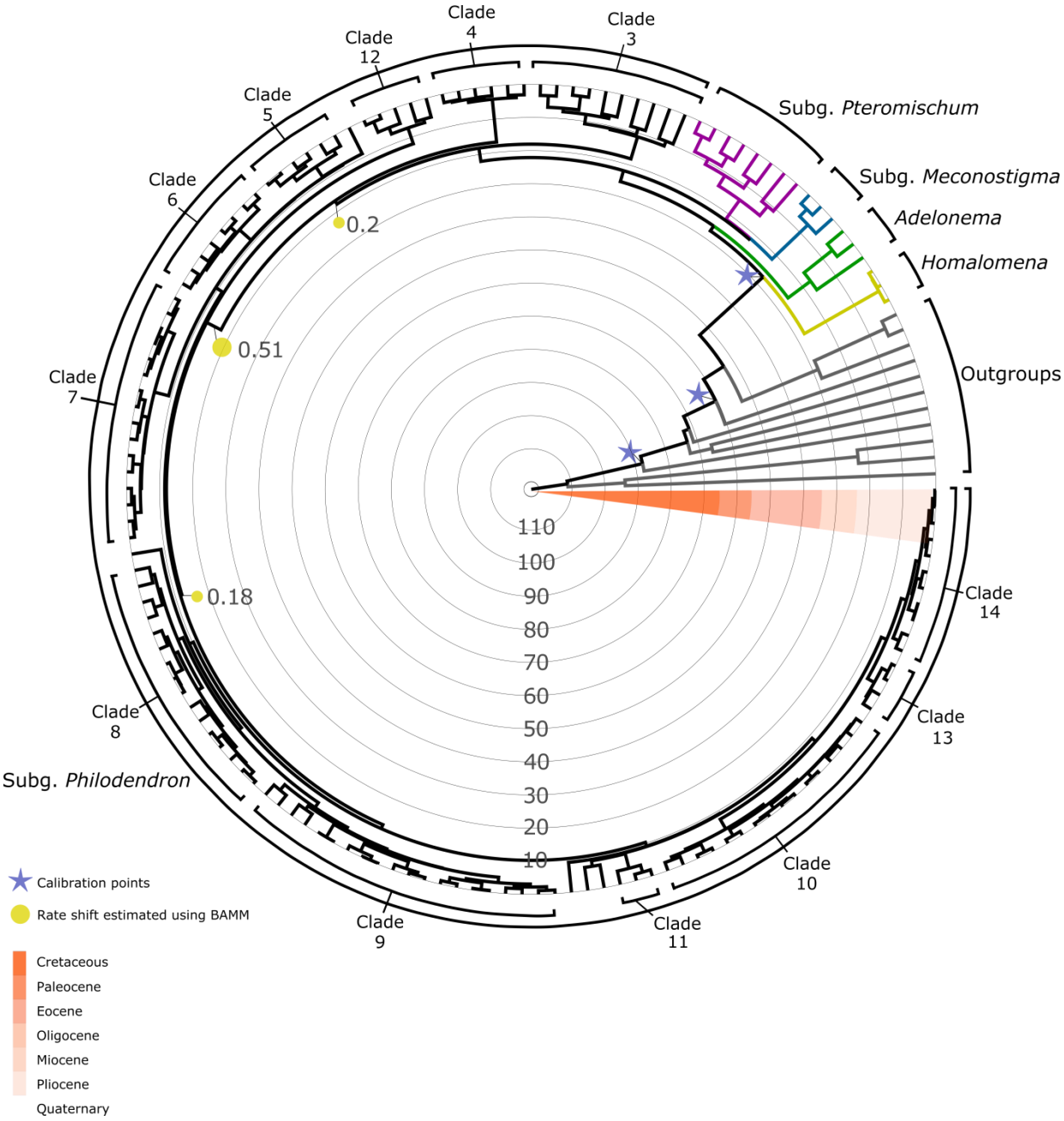

Figure 2.3. Maximum clade credibility (MCC) chronogram obtained in BEAST based on three plastid markers (*petD*, *rpl16*, and *trnK/matK*) with age estimates with three secondary calibration constraints. Time intervals in millions of years ago are indicated by black circles. Geologic time scale is indicated by the orange gradient band. Violet stars correspond to secondary calibration points to specific nodes referred to in the text. Yellow circles correspond to three posterior distributions of the diversification rate shift estimated with BAMM. Refer to Table 2.3 for details of %HPD values for divergence-time estimates.

Table 2.3. Branch supports and divergence-time estimates (Ma) using BEAST under birth-death speciation prior. UCLN, uncorrelated lognormal model; C, crown node; S, stem node; PP, posterior probability; HPD, 95% intervals; asterisk, not calculated given the low statistic support; NA, not applicable; NS, not sampled in Nauheimer et al. (2012). Names between brackets in the first column indicate nodes calibrated in each approach.

								Divergence-time estimates obtained by Nauheimer et al. (2012). UCLN model with a uniform prior and a Jukes-Cantor + Γ tree model.	
		Secondary constraint approach			**Fossil+secondary constraint approach**				
		BEAST			**BEAST**				
Clade	**Node**	**PP**	**Mean**	**HPD**	**PP**	**Mean**	**HPD**	**Mean**	**HPD**
Pothoideae + Monsteroideae	S	1.00	1111.14	81.75–148.17	1.00	87.1	57.14–121.31	96.73	86.62–107.06
	C	0.75	93.81	46.03–121.14	0.82	68.46	29.48–95.05	81.06	68.3–93.68
Lasioideae (Secondary constraint approach)	S	1.00	87.74	80.1–97.51	0.68	72.91	59.24–87.46	90.23 (Node 28)	80.09–100.68
	C	NA (Single terminal node)			NA (Single terminal node)				
Aroideae	S	1.00	87.74	80.1–97.51	0.68	72.91	59.24–87.46	86.95	77.1–97.03
	C	1.00	72.99	59.64–83.53	0.95	60.91	55.89–67.77	82.12	73.24–92.28
Anchomanes difformis, *Pseudohydrosme gabunensis*, *Aglaonema marantifolium* and *Zantedeschia rehmannii* + Philodendron clade (Secondary constraint approach)	S	1.00	71.21	59.39–81.49	0.98	51.82	39.88–62.63	68.17 (Node 109)	54.06–81
	C	1.00	60.51	47.07–73.78	0.97	45.23	32.84–56.95	40.69	24.48–57.71
Montrichardia (Fossil+secondary constraint approach)	S	1.00	72.99	59.64–83.53	1.00	57.6	55.8–61.22	Not supported	
	C	1.00	66.25	50.11–81.07	0.99	52.16	40.58–60.64	NS	
Philodendron clade (Both approaches)	S	0.96	53.28	39.18–66.23	0.97	45.23	32.84–56.95	NS	
	C	1.00	27.31	18.9–36.64	1.00	23	15.01–32.53	25 (Node 113)	11.88–39.4
Homalomena	S	1.00	27.31	18.9–36.64	1.00	23	15.01–32.53	NS	
	C	1.00	1.41	0.2–3.12	1.00	1.2	0.17–2.7	NS	
Adelonema	S	0.79	25.53	17.81–33.94	0.76	21.55	13.87–29.89	NS	
	C	1.00	17.05	8.76–26.26	1.00	14.23	6.91–22.39	NS	
Philodendron	S	0.79	25.53	17.81–33.94	0.76	21.55	13.87–29.89	NS	
	C	1.00	22.1	15.48–29.79	1.00	18.61	12.19–26.12	NS	
Subg. *Meconostigma*	S	0.37	21.69	*	1.00	18.61	12.19–26.12	NS	
	C	1.00	6.66	2.55–11.88	1.00	5.61	1.94–9.98	NS	
Subg. *Pteromischum*	S	0.37	21.69	*	0.37	18.32	*	NS	
	C	1.00	14.56	8.64–20.54	1.00	12.22	7.11–18.05	NS	
Subg. *Philodendron*	S	1.00	22.1	15.48–29.79	0.37	18.32	*	NS	
	C	1.00	18.06	12.3–24.44	1.00	15.19	9.64–21.26	NS	
Clade 3	S	1.00	18.06	12.3–24.44	1.00	15.19	9.64–21.26	NS	
	C	1.00	11.1	6.85–15.63	1.00	9.34	5.34–13.6	NS	
Clade 4	S	0.85	16.91	11.2–22.65	0.85	14.21	8.9–19.87	NS	
	C	1.00	3.93	1.75–6.66	1.00	3.28	1.39–5.66	NS	
Clade 5	S	0.18	8.8	*	0.17	7.6	*	NS	
	C	0.18	5.15	*	1.00	4.34	2.21–6.81	NS	
Clade 6	S	0.18	9.03	*	0.17	7.6	*	NS	
	C	1.00	4.33	2.21–6.81	0.25	7.25	*	NS	
Clade 7	S	1.00	9.13	5.81–12.85	1.00	7.7	4.63-11.22	NS	
	C	1.00	4.69	2.56–7.09	1.00	3.95	2.05–6.21	NS	
Clade 8	S	0.96	7.87	4.95–11.01	0.96	6.64	4–03.9.61	NS	
	C	1.00	6.25	3.76–8.95	1.00	5.27	3.04–7.76	NS	
Clade 9	S	0.96	7.87	4.95–11.01	0.96	6.64	4–03.9.61	NS	
	C	1.00	6.08	3.59–8.82	1.00	5.12	2.91–7.7	NS	
Clade 10	S	0.76	7.46	4.56–10.47	0.74	6.3	3.69–9.02	NS	
	C	1.00	4.08	2.15–6.16	1.00	3.44	1.78–5.35	NS	
Clade 11	S	0.17	8.65	*	0.96	7.65	4.77–11	NS	
	C	0.18	4.1	*	1.00	3.44	1.48–5.84	NS	
Clade 12	S	1.00	12.03	7.87–16.37	0.23	9.98	*	NS	
	C	1.00	6.97	3.13–11.01	1.00	5.81	2.98–9.47	NS	
Clade 13	S	1.00	5.71	3.24–8.34	1.00	4.81	2.65–7.23	NS	
	C	1.00	3.35	1.58–5.43	1.00	2.8	1.24–4.59	NS	
Clade 14	S	1.00	5.71	3.24–8.34	1.00	4.81	2.65–7.23	NS	
	C	1.00	4.1	2.1–6.39	1.00	3.45	1.69–5.48	NS	

The topology of the BEAST analysis based on the fossil+secondary calibration approach differs from that of the BEAST tree based on the secondary calibration approach in resolving subgenus *Meconostigma* as sister to a clade consisting of the subgenera *Philodendron* and *Pteromischum* (Appendix A2). The split between subgenus *Meconostigma* and the clade containing subgenera *Philodendron* and *Pteromischum* was estimated to be ~18.61 Ma (95% HPD: 12.19–26.12). Within subgenus *Philodendron*, the node of the clades 5, 6, and 12 were not supported.

2.4.6. Diversification rate shifts

The likelihood of the BAMM MCMC reached convergence, and the post-burn-in ESS values were >200 for rate-shift analyses of both the fossil+secondary and the secondary calibration approaches (Appendix A5). A model with one shift received a higher BF in comparison to the models with zero, two, three, and four shifts for trees of both calibration approaches (Table 2.4). Different values used for the sampling fractions in the BAMM analyses showed no effect on the number of evolutionary shifts or on the estimation of speciation and extinction rates. BAMM results of the 95% credible set of shift configurations under the three sampling-fraction assumptions identified a diversification rate shift within subgenus *Philodendron* (Appendix A6). According to the analysis accounting for the random taxon sampling (Appendix A6), three of the four configurations within the 95% credible set (posterior distributions = 0.51, 0.18, and 0.2) showed a rate shift occurring near the base of subgenus *Philodendron*. The shift with 0.2 posterior distribution occurred on the branch prior to the divergence of clades 2–12, the shift with the highest posterior distribution (0.51) was located on the branch prior to the divergence of clades 3–12, and the shift with 0.18 posterior distribution was located on the branch prior to the divergence of clades 3–12 (excluding clade 10) (Figure 2.4; Appendix A6). In Figure 2.4, the blue line corresponds to the diversification process of subgenus *Philodendron* beginning ~18 mya, whereas the dark green line corresponds to the diversification process of the lineage including the subgenera *Meconostigma* and *Pteromischum* beginning ~21 mya. The diversification process of the two lineages begun with a similar speciation rate (~0.30 events/Ma/lineage), subsequently (by ~12 mya) the speciation rate of subgenus *Philodendron* had increased to ~0.55 events/Ma/lineage, whereas the diversification of the lineage containing the subgenera *Meconostigma* and *Pteromischum* remained ~0.30 events/Ma/lineage. The diversification rate of subgenus

Philodendron dropped slightly at ~10 mya to 0.48 events/Ma/lineage, followed by another increase to ~0.58 events/Ma/lineage at ~8.5 mya; from that time to the present day, the diversification rate has continued to increase. The current diversification rate of subgenus *Philodendron* was estimated to be ~0.73 events/Ma/lineage, whereas the diversification rate of the subgenera *Meconostigma* and *Pteromischum* remained relatively stable and increased by ~0.05 events/Ma/lineage to ~0.35 events/Ma/lineage.

Table 2.4. Bayes factors comparison of the models with posterior or prior greater than zero under the two calibration approaches. BFs, Bayes factors.

Calibration approach	Expected number of shifts	BFs
Fossil+secondary calibration	0	1.0
	1	33.11
	2	8.88
	3	1.42
	4	1.06
Secondary calibration	0	1.0
	1	14.46
	2	2.98
	3	0.88
	4	0.16

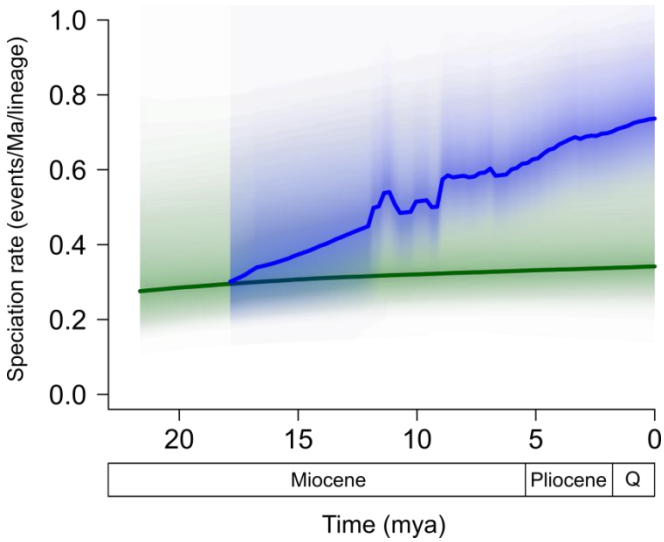

Figure 2.4. *Philodendron* speciation rate through time (events/Ma/lineage) according to BAMM analysis using the MCC calibrated with three secondary constraints. Color density shading area indicates 95% Bayesian credible region of the distribution of rates. Blue line corresponds to the speciation rate of subgenus *Philodendron*. Dark green line corresponds to the speciation rate of the subgenera *Meconostigma* and *Pteromischum*. Q, Quaternary.

2.5. Discussion

2.5.1. Phylogenetic relationships between the genera *Adelonema*, *Homalomena*, and *Philodendron*

In the present study, the Asian genus *Homalomena* is resolved as sister group to a clade including the Neotropical genera *Adelonema* and *Philodendron* (Figures 2.2 and 2.3). This result is congruent with the maximum parsimony trees based on nuclear DNA data (ETS and ITS with 48 and 31 species of *Philodendron*, respectively) obtained by Gauthier et al. (2008) and the topologies obtained by Wong et al. (2013) with ITS; by Wong et al. (2016) with ITS and *trnK/matK* partial sequences; and by Loss-Oliveira et al. (2016) with ETS, *trnL-trnF*, and partial *trnK/matK*. Our results lend support to the monophyly of the genera *Adelonema* and *Philodendron*. This result is not congruent with the maximum parsimony tree based on *rpl16* partial sequences with 45 species (Gauthier et al., 2008), the maximum likelihood tree by Wong et al. (2013) based on ITS, or the Bayesian inference tree by Wong et al. (2016) using ITS and *matK*, which recovered *Philodendron* as a non-monophyletic group with *Philodendron* subgenus *Pteromischum* sister to *Adelonema*. Based on the phylogenetic relationships within *Philodendron*, our results lend support to the taxonomic concept of *Philodendron* subgenus *Pteromischum* as an entity within *Philodendron* (Schott, 1856; Engler, 1899; Krause, 1913; Mayo, 1986; Grayum, 1996). Wong et al. (2013, 2016) documented some morphological similarities supporting a closer phylogenetic relationship between *Adelonema* and subgenus *Pteromischum* (e.g., anisophyllous sympodial growth with several or many leaves per stem article, absent or highly inconspicuous cataphylls, and sheathing petioles). However, apart from the different life forms (species of subgenus *Pteromischum* are lianas while *Adelonema* species are strictly terrestrial herbs), floral characters used in the taxonomic circumscription of the genus *Philodendron* (e.g., shape and vascularization patterns in the stamens, style morphology, and number of ovules per locule; Grayum, 1996) as well as certain anatomical characters (e.g., presence of three types of raphide cells; Klimko et al., 2014) are evidence for a closer relationship of *Philodendron* subgenus *Pteromischum* to the other two subgenera of the genus *Philodendron* than to *Adelonema*.

The monophyly of *Philodendron* is strongly supported by our results. Although there is no single morphological feature that unambiguously distinguishes *Philodendron* from closely related genera, the combination of the following characters supports its monophyly: plants usually climbing or epiphytic (if terrestrial herbs, adult plants with conspicuous cataphylls and petiolar sheath much reduced); inflorescences secreting resin at anthesis, either from the adaxial canals of the spathe or from the spadix, rarely from both; spadix with distinct sterile staminate zone between pistillate zone and fertile staminate zone; endothecium nearly always with cell wall thickenings; female flowers without staminodes; ovary with two to many completely separate locules, with axile to basal placentation; and ovules one to many per locule, usually hemiorthotropous, rarely hemianatropous (Grayum, 1996; Croat, 1997; Klimko et al., 2014).

2.5.2. Relationships within the genus *Philodendron*

Analyses of a combination of the *petD*, *rpl16*, and *trnK/matK* regions and the substantially increased sampling (>20% of total species diversity) in the present study provide a more comprehensive hypothesis on the phylogenetic relationships within *Philodendron*, yielding a distinctly higher number of resolved and well-supported clades compared to previous studies(Gauthier et al., 2008; Loss-Oliveira et al., 2016).

The three subgenera of *Philodendron* were recovered as monophyletic groups, although the sister relationship between the subgenera *Meconostigma* and *Pteromischum* is weakly supported (Figure 2.2). *Meconostigma* and *Pteromischum* were resolved as monophyletic groups based on ITS and *matK* (Wong et al., 2016), and ETS and ITS (Gauthier et al., 2008). The monophyly of subgenus *Meconostigma* is additionally supported by at least four morphological synapomorphies: a thickened spathe, a well-developed intermediate staminodial zone subequal to longer than staminate portion, the presence of stylar lobes, and an axial vascular system independent of the funicle supply (Braucks Calazans et al., 2014; clade 1; Figure 2.2a).

2.5.3. Phylogenetic relationships within subgenus *Philodendron*: clades recovered and inconsistencies with the current infrageneric classification

Within subgenus *Philodendron*, 12 strongly supported clades are recognized (Clades 3–14; Figure 2.2). Some of these clades have similar species composition to lineages recognized in the ETS and ITS trees by Gauthier et al. (2008; e.g., *P. ecordatum* Schott and *P. fragrantissimum*, clade 4; *P. melinonii* Brongn. ex Regel and *P. pinnatifidum* (Willd.) Schott, clade 5; and *P. gloriosum* André and *P. ornatum* Schott, clade 10; Figure 2.2).

No section from the currently accepted infrageneric classification of subgenus *Philodendron* was recovered as monophyletic, and morphological synapomorphies for the individual clades have not been found. Nevertheless, most of the species with <10 ovules/locule (traditionally attributed to sect. *Macrobelium* [Schott] Sakur. and sect. *Tritomophyllum*) are resolved in two divergent monophyletic clades: one contains both clades 8 and 9, and the other is clade 14 (Figure 2.2). Species with >10 ovules/locule (mostly members of sect. *Philodendron*) are grouped in clades 4, 11, 12, and 13 (Figure 2.2). Therefore, this character appears to be polyphyletic.

With the exception of clade 3, most of the clades (clades 4–14; Figure 2.2) identified within subgenus *Philodendron* are consistent with geographic patterns rather than with the current taxonomic classification based on morphology. Clades that are geographically defined but inconsistent with the morphological classification have also been documented in *Anthurium* (Carlsen and Croat, 2013), and they are commonly found in recent species-rich Neotropical lineages such as *Costus* (Kay et al., 2005) and *Inga* (Richardson et al., 2001).

Clade 3 (BS = 100, JK = 100, PP = 1.0; Figure 2.2a) contains species from different regions (Caribbean, Amazon basin, Guianas, and southeast Brazil), many of which are assigned to sect. *Baursia* in the current taxonomic classification (Croat, 1997), and *P. consanguineum* Schott, *P. ernestii* Engl. and *P. hederaceum*, traditionally attributed to sect. *Philodendron* and *P. jacquinii* Schott of the monotypic sect. *Macrogynium* (Croat, 1997). Clade 4 (BS = 100, JK = 100, PP = 1.0; Figure 2.2) comprises range-restricted species from the lowland rainforests of the Guianas, with the exception of *P. fragrantissimum*, which occurs from Belize and Cuba through to southeast Brazil. With *P. joaosilvae* Croat, A. Cardoso & Moonen, and *P. werkhoveniae* Croat, this clade includes two terrestrial species among the otherwise appressed-climbing hemiepiphytes or vines.

The remaining clades (5–14; Figures 2.2b, c) are organized in three major lineages: clades 5–7; clades 8 and 9; and clades 10–14 and three monospecific branches corresponding to the species *P. asplundii* Croat & M. L. Soares and *P. tenue* K. Koch & Augustin (sisters to clades 10–14) and *P. dodsonii* Croat & Grayum (sister to clade 10). Clade 5 (BS = 100, JK = 100, PP = 1.0) includes epiphytic species from South America and the Caribbean, with the exception of *P. subincisum* Schott, a species endemic to northern Veracruz in Mexico (Croat, 1997). All species of clade 5 have persistent cataphylls decaying as fibers, a character state that has been used in combination with others for the circumscription of subsections *Macrolonchium* and *Philodendron* (Croat, 1997). However, this character state is also found in species nested in other clades containing members of the series *Fibrosa* Croat within sect. *Philodendron* (e.g., *P. tenue* K. Koch & Augustin in clade 10, *P. grandipes* K. Krause in clade 11). Clade 6 (BS = 75, JK = 65, PP = 0.95) includes epiphytes, appressed-climbing hemiepiphytes and procumbent terrestrial species, all endemic to southeast Brazil (Sakuragui et al., 2005; 2011). Clade 7 (BS = 99, JK = 99, PP = 1.0) represents a group of appressed-climbing hemiepiphytes from the Amazon Basin and the Guianas with often three-lobed or deeply incised-lobate leaf blades (traditionally assigned to sect. *Polytomium* [Schott] Engl. or sect. *Schizophyllum* [Schott] Engl.) or at least with blades featuring well-developed posterior lobes (sect. *Philodendron*, the largest group within the subgenus).

Philodendron purulhense Croat is endemic to southern Mexico (Chiapas) and Honduras (Croat, 1997) and was resolved sister to clades 8 and 9 (Figure 2.2b). These two clades contain members from seven different sections, including the representatives of the small sections *Camptogynium* K. Krause, *Dolichogynium* Croat & Köster and *Tritomophyllum*. As far as has been documented, most species in clades 8 and 9 are characterized by a solitary ovule per locule. Clade 8 (BS = 85, JK = 85, PP = 1.0) comprises mostly species distributed in the Amazon basin along with three species restricted to northern Venezuela (*P. fendleri* K. Krause) or the Guianas (*P. moonenii* Croat and *P.* cf. *pokigronense* Croat). Apart from *P. krugii* Engl. from Tobago and northern Venezuela (Engler, 1899), clade 9 (BS = 85, JK = 80, PP = 1.0) includes species occurring in Central America, the Chocó ecoregion, and the northern Andes.

Clades 10–14 (Figure 2.2c) contain species mostly assigned to sect. *Macrobelium* and sect. *Philodendron* (Figure 2.2c). Species of sect. *Macrobelium* have basal or sub-basal placentation and typically solitary or few ovules per locule, while species of sect. *Philodendron* are characterized by having axile placentation and many ovules per locule (Croat, 1997). Clade 10 (BS = 98, JK = 98, PP = 1.0) includes species mainly of sect.

Philodendron and represents mostly those species with conspicuously velvety or at least completely matt adaxial leaf surfaces, which are often ornamented (mottled or with much paler veins). Apart from *P. ornatum*, which is widely distributed in South America, the species of this clade are restricted to the northern Andes and the Chocó ecoregion (with *P. verrucosum* L. Mathieu ex Schott reaching Costa Rica). Clade 11 (BS = 100, JK = 100, PP = 1.0) comprises three species from Central America and the Chocó ecoregion (Engler, 1905; Coelho et al., 2015). Clade 12 (BS = 87, JK = 85, PP = 1.0) comprises species occurring in northern South America with *P. lacerum* (Jacq.) Schott from the Greater Antilles (Schott, 1829; Acevedo-Rodríguez and Strong, 2012). Clade 13 (BS = 98, JK = 96, PP = 1.0) contains species endemic to the Chocó ecoregion recently described by Croat and Mora (2004) and Croat et al. (2016), whereas clade 14 (BS = 79, JK = 70, PP = 0.99) is made up of members of sect. *Macrobelium* from Central America.

2.5.4. Time-calibrating the phylogenetic tree of *Philodendron*

Node ages estimated with the fossil+secondary calibration approach (using one fossil and a single secondary constraint) deviate from the ages estimated in Nauheimer et al. (2012) more than the ages calculated with three secondary calibration approach (Table 2.3). These discrepancies between the ages calculated with the fossil+secondary calibration approach and the ages previously reported by Nauheimer et al. (2012) might be explained by different factors. Secondary calibration points could only be applied to nodes that were well-supported in the Araceae fossil calibrated phylogeny by Nauheimer et al. (2012) and received statistical support in the present study. These correspond to three nodes: 28, 109, and 113 (Figure 2.3; Appendix A2). In order to test a fossil-calibration approach, we included the closest outgroup taxon to *Philodendron* with a reliable fossil (*Montrichardia aquatica*; Herrera et al., 2008). However, this node is resolved sister to two of the three nodes (28 and 109) that could be used for secondary calibration points. Given the topological proximity between these nodes (Appendix A2), initial tests in divergence-time analyses (data not shown) revealed that it was not possible to combine all three secondary constraints and the fossil constraint since the priors applied to each node contradict one another. Therefore, in the fossil+secondary calibration approach it was only possible to calibrate two nodes: one fossil calibration for the lineage including *M. linifera* and one secondary calibration to node 113 (Table 2.3). The clade containing the taxon with a fossil record (*Montrichardia* + *Schismatoglottis*) in our study

represents a much larger clade according to Nauheimer et al. (2012). Sparse taxon sampling affects age estimates, particularly in combination with a single fossil calibration (Schulte, 2013); therefore, the use of single species for a fossil calibration to represent larger clades in our outgroup may explain why the fossil+secondary-calibration approach resulted in younger ages, compared to the results in Nauheimer et al. (2012; Table 2.3). Furthermore, even though paleontological calibrations have been recommended for estimating evolutionary divergence times (Schenk, 2016), adding branches to the phylogeny in order to accommodate a fossil calibration when the focal group lacks paleontological evidence, as is the case with *Philodendron*, is more likely to bias divergence-time estimates than to accurately estimate the evolutionary history (Hipsley and Müller, 2014). Therefore, we focus our discussion on the ages obtained using the secondary calibration approach (Figure 2.3 and Table 2.3).

2.5.5. Diversification history of *Philodendron* in the context of Neotropical plant evolution

Studies in other Neotropical species-rich lineages have corroborated either the "museum" model, with a steady and consistent accumulation of species diversity (e.g., Quiinoideae; Schneider and Zizka, 2017) or the cradle model, with higher diversification rates during short periods (e.g., *Inga*, Richardson et al., 2001; *Costus* subgenus *Costus*, Kay et al., 2005). The present study indicates that the diversification history of the genus *Philodendron* is a complex process characterized by lineage-specific diversification rate shift within subgenus *Philodendron*. A recent acceleration in the diversification rate occurred in the species-rich and predominantly epiphytic lineage corresponding to subgenus *Philodendron* from 0.55 to 0.73 events/Ma/lineage ~12 mya to the present (Figure 2.4). In contrast, its sister lineage containing the subgenera *Meconostigma* and *Pteromischum* diversified at a relatively low, consistent diversification rate from 0.30 to 0.35 events/Ma/lineage since its origin ~22 mya to the present (Figure 2.4). Based on the differences in the species diversification process between these sister lineages, we consider that a single model of diversification (cradle or museum) fails to explain the species radiation at the genus level for *Philodendron*. Therefore, our results are more in line with the idea that high species diversity in Neotropical lineages such as *Philodendron* can be explained by periods of episodic species turnover or, in this case, a "burst" of species diversification for one lineage (Koenen et al., 2015; Pennington et al., 2015).

The recent geological dynamics in the Neotropics are likely to have been a driver of speciation in numerous plant lineages, including epiphytes, herbs, lianas, and trees (Hoorn et al., 2010; Antonelli and Sanmartín, 2011; Hughes et al., 2013; Lohmann et al., 2013; Givnish et al., 2014). The origin of *Philodendron* co-occurred with the beginning of the mountain uplift of the central and northern Andes in the late Oligocene to the early Miocene. The uplift of the Andes coincides with the diversification of the first modern montane plant and animal genera in the Neotropics (~23 mya; Hoorn et al., 2010). Most *Philodendron* species arose within the past 10 Ma and are resolved within subgenus *Philodendron*, and this coincides with the most intense orogenic periods of the Andean region (~12 and ~4.5 mya; Hoorn et al., 2010). It is likely that the orogenic activity in the Andes during that period facilitated the diversification of *Philodendron* by creating new habitats (Antonelli and Sanmartín, 2011; Luebert and Weigend, 2014), as has been found in many other recently evolved Neotropical lineages, such as *Costus* (Kay et al., 2005), *Guarea* and *Trichilia* (Koenen et al., 2015), *Guatteria* (Erkens et al., 2007), *Inga* (Richardson et al., 2001; Nicholls et al., 2015)), *Renealmia* (Särkinen et al., 2007), Bromeliaceae (Givnish et al., 2014), and Orchidaceae (Givnish et al., 2015).

Croat (1997) indicated that widely distributed species of *Philodendron* may have strong dispersal abilities or an ancient origin, perhaps predating the Miocene and the Pliocene and, therefore, evolving over a longer period in which the species could have dispersed across broad geographic ranges. The oldest lineage within subgenus *Philodendron* diversified ~11 mya (clade 3; Table 2.3) and includes some of the most widespread species, in particular *P. hederaceum*, which occurs in the Greater Antilles and from Mexico throughout Central and South America (Croat, 1997; Figures 2.2 and 2.3). However, our results indicate that some widely distributed species arose more recently, ~4 mya (*P. fragrantissimum* in clade 4 and *P. ornatum* in clade 10; Table 2.3; Figures 2.2 and 2.3). Thus, widespread species are found both in older and in more recent clades, indicating that intrinsic factors such as dispersal abilities may have helped these widespread *Philodendron* species to colonize their habitats.

Within *Philodendron*, epiphytism is found almost exclusively in subgenus *Philodendron* and its geographic diversity patterns resemble those found in other lineages that contain predominantly vascular epiphytes in the Neotropics. These epiphytic lineages constitute a major portion of the species richness in the Neotropical forests, especially lineages of the families Araceae, Bromeliaceae, Orchidaceae, and Polypodiaceae (Gentry and Dodson, 1987; Givnish et al., 2011; 2014; Zotz, 2013; 2016; Sundue et al., 2015). In contrast to the diversification history of ferns (Sundue et al., 2015), studies on bromeliads and orchids

have shown that epiphytic lineages have higher net rates of diversification compared to their terrestrial relatives (Givnish et al., 2014; 2015). The epiphytic life form arose in the late Eocene in orchids and in the Miocene in bromeliads (Givnish et al., 2014; 2015). In the genus *Philodendron*, a lineage-specific diversification-rate upshift occurred after the origin of the predominantly epiphytic subgenus *Philodendron* ~12 mya and it coincides with one of the most intense periods of mountain uplift in the Andes (Figures 2.3 and 2.4). We therefore hypothesize that the high diversification rate in subgenus *Philodendron* compared to the other subgenera of *Philodendron* is associated with the colonization of perhumid forests in the Andes and their foothills that likely promoted the evolution of the epiphytic habit. However, this remains to be robustly tested, since understanding the epiphytism in *Philodendron* requires further morphological and ecological studies. In contrast to subgenus *Philodendron*, its sister lineage showed a low diversification rate (Figures 2.1 and 2.4) and has gradually accumulated terrestrial species (subgenus *Meconostigma*) distributed in open environments in lowland forests in Amazonia and southeast Brazil as well as lianas (subgenus *Pteromischum*), occurring in the dense rainforests of Amazonia, the Chocó ecoregion, and Central America (Figures 2.1 and 2.4). Although the taxon sampling for subgenera *Meconostigma* and *Pteromischum* is scarce, our study provides insights into the diversification history of a widely distributed angiosperm lineage in the Neotropics. However, we provide a robust phylogenetic framework and divergence-time estimates analysis to enable future testing of hypotheses that may explain the accelerated diversification rate within subgenus *Philodendron* compared to the rest of the genus *Philodendron*.

2.6. Conclusions

No section from the currently accepted infrageneric classification of subgenus *Philodendron* was recovered as monophyletic. The present study represents another example of a recent species radiation in the Neotropics that lends support to the global model of episodic periods of high species turnover (Koenen et al., 2015; Pennington et al., 2015) rather than endorsing the traditional models of diversification (cradle and museum models). Most of the species diversity in the genus *Philodendron* originated rapidly and recently within subgenus *Philodendron*. It will be beneficial to test the biotic and abiotic factors that may have influenced the speciation pattern found in *Philodendron*. The present study provides a basis for investigating the historical geographic ranges and the evolution of *Philodendron*,

one of the most diverse genera in the Neotropical rainforests but one that is poorly understood.

"Die dem Aequator nahe Gebirgsgegend [...] ist der Theil der Oberfläche unseres Planeten, wo im engsten Raume die Mannigfaltigkeit der Natureindrücke ihr Maximum erreicht. In der tiefgefurchten Andeskette von Neu-Granada und Quito ist es dem Menschen gegeben alle Gestalten der Pflanzen und alle Gestirne des Himmels gleichzeitig zu schauen."

"The mountainous region near the equator [...] is the part of earth's surface where the variety of natural impressions reaches its maximum on a very small area. In the deeply furrowed Andean cordillera of Nueva Granada [nowadays: Columbia] and Quito people can see all the shapes of the plants and all the stars of the sky at the same time."

Alexander von Humboldt: Kosmos. Entwurf einer physischen Weltbeschreibung. – Erster Band (1845).

Chapter 3. Historical biogeography of the genus *Philodendron*

3.1. Summary

The origin of Neotropical species diversity is strongly associated with the geological history of South America. Since the Miocene, a number of species radiations across different Neotropical lineages coincided with the rise of the Andes and the formation of the Isthmus of Panama. The species-rich genus *Philodendron* (Araceae) is widely distributed across Neotropical rainforests, originating in the late Oligocene and diversified more intensely from the Miocene onwards. It is likely that its diversification process and distribution patterns are associated with recent geological changes in the Americas. To test this hypothesis, we sampled the species diversity of *Philodendron* across its entire geographic range and used a combination of three non-coding plastid regions (*petD, rpl16* and *trnK/matK*) to obtain a comprehensive time-calibrated phylogeny, we then inferred geographic range evolution, and explored the impact of the Andean orogeny on speciation, extinction and dispersal. The genus *Philodendron* originated ~29 mya and experienced the earliest diversification events ~25 mya in the pan-Amazonian rainforests. From the middle Miocene onwards, multiple geographic range expansion events occurred from Amazonia to southeast Brazil and to the area which would become the Chocó and the northern Andes. From the Pliocene onwards, *Philodendron* reached Central America and the Caribbean islands and Andean lineages recolonized and diversified in Amazonia. In *Philodendron*, higher diversification rates are revealed in the adjacent lowland rainforests of the northern Andes compared to other regions in the Neotropics, this demonstrates a potential indirect impact of the uplift of the Andes on species radiations in lowland regions

3.2. Introduction

The biogeographic history of the Americas is fundamental for understanding the origin of Neotropical biota (Hoorn et al., 2010). During the last 60 Ma, geological processes resulted in two major changes in the Neotropics: [1] the formation of the Andes (Hoorn et al., 2010),

and [2] the massive land connection between North and South America through the Isthmus of Panama (Bacon et al., 2015; O'dea et al., 2016; Jaramillo et al., 2017).

The Andes harbor ~15% of the extant flowering plant species of the world, half of which are endemic to the region (Myers et al., 2000). These mountain ranges have favored the evolution of the Neotropical biodiversity through multiple processes (Hoorn et al., 2010; Antonelli and Sanmartín, 2011; Luebert and Weigend, 2014). New habitats that arose during the uplift of the mountains are proposed to have fostered the evolution of new lineages, such as in bromeliads (Givnish et al., 2014) and bellflowers (Lagomarsino et al., 2016). The mountain uplift in the Andes likely also separated distributional ranges of plants that were previously connected, as shown for the tribes Cinchoneae and Isertieae in the coffee family (Antonelli et al., 2009), and the genera *Brunfelsia* L. (Filipowicz and Renner, 2012), and *Bomarea* Mirb. (Chacón et al., 2012). On the other hand, the Andean cordilleras have also been proposed to have facilitated dispersal across the north-south pathway in South America such as in the genera *Solanum* L. (Simon et al., 2011), and *Oreobolus* R. Br. (Chacón et al., 2006). The rising Andes increased precipitation and humidity in the Chocó ecoregion and in western Amazonia and therefore, the mountains indirectly favored the speciation of lineages already in Amazonia, such as the genus *Inga* (Richardson et al., 2001; Antonelli et al., 2009; Luebert and Weigend, 2014).

The closure of the Isthmus of Panama facilitated one of the most extraordinary events in the history of life, namely the biotic interchange between North and South America involving many groups of organisms across the tree of life (Bacon et al., 2015; Jaramillo et al., 2017). Over the last 30 Ma, episodic dispersal from South America to Central America is found in the genera *Hechtia* Klotzsch (Givnish et al., 2011), and *Bernardia* Houst. ex Mill. (Cervantes et al., 2016). In addition to the biotic interchange between North and South America, the Caribbean islands as the most important insular system in the Neotropics (Maunder et al., 2018) have experienced biotic interchange among each other and with continental America since the Eocene (Nieto-Blázquez et al., 2017).

The species-rich genus *Philodendron* inhabits continental America from tropical Mexico to southern Brazil, and the Caribbean islands (Mayo, 1991; Grayum, 1996; Croat, 1997). The genus is among the most characteristic epiphytic and hemiepiphytic components throughout Neotropical rainforests (Croat, 1997; Canal et al., 2018). However, the perhumid rainforests in the Chocó ecoregion and western Amazonia accumulated the highest proportion of its species diversity. *Philodendron* comprises ~560 accepted species and an estimated total of 700-1,000 species (Boyce and Croat, 2018; Govaerts et al., 2018). Recently, two species-

level phylogenetic studies, both representing slightly more than 20% of the species diversity, have confirmed the monophyly of *Philodendron*; in Canal et al. (2018) based on three plastid DNA markers and in Vasconcelos et al. (2018) based on both separate and combined analyses of four plastid markers and the nuclear ribosomal DNA (ITS2). According to both studies, there are three major lineages within *Philodendron* which correspond to the three subgenera currently recognized *Meconostigma*, *Pteromischum* and *Philodendron*. Subgenus *Meconostigma* comprises 21 mostly terrestrial species distributed in Amazonia, the Mata Atlântica and the Cerrado (Mayo, 1988, 1991; Braucks Calazans et al., 2014). Subgenus *Pteromischum* includes 82 species of vines distributed mostly in Central America, the Chocó ecoregion and Amazonia (Grayum, 1996; Croat, 1997; Calazans and Sakuragui, 2013; Barbosa and Sakuragui, 2014; Canal et al., 2018). With ~460 accepted species and an estimated number of >600, subgenus *Philodendron* has accumulated the highest species diversity of the genus. Its species are mainly epiphytes and hemiepiphytes, with centers of diversity in Central America, the Chocó ecoregion, the northern Andes and the Amazon basin.

The taxonomic implications of the infrageneric relationships within *Philodendron* are currently the subject of debate. Sakuragui et al. (2018) resurrected the genus *Thaumatophyllum* to encompass the species of subgenus *Meconostigma*. This view was adopted by Vasconcelos et al. (2018), who additionally suggested reinstating the genus *Elopium* for the species attributed to subgenus *Pteromischum.* In contrast, Canal et al. (2018), that was published prior to those studies, maintained all three subgenera within a single genus *Philodendron*. Since the monophyly of the genus *Philodendron* is undisputed according to the most recent and comprehensive phylogenetic studies (Canal et al., 2018; Vasconcelos et al., 2018), and in view of the results of the present study, we deem it prudent to refrain from unnecessarily segregating any of the subgenera as a separate genus for the time being and, consequently, treat *Philodendron* as a single genus in the following (see discussion for further reasoning).

The genus *Philodendron* originated ~25 mya and most of its diversification occurred from the late Miocene onwards (Canal et al., 2018). *Philodendron* therefore represents a potential model to investigate the impact of geological changes since the late Oligocene on the diversification of species-rich lineages that are prominent in the Neotropics. The uplift of the Andes is proposed to be a major abiotic driver of species radiations in the Neotropics (Hoorn et al., 2010; Antonelli and Sanmartín, 2011; Luebert and Weigend, 2014). Furthermore, the Andean orogeny would have created perhumid conditions in the lowlands of the Chocó ecoregion and western Amazonia, which indirectly provided opportunities for

diversification, leading to high species richness in those regions (Richardson et al., 2001; Antonelli et al., 2009; Luebert and Weigend, 2014). Species diversity of *Philodendron* is highest in the lowland regions adjacent to the northern Andes (Chocó ecoregion and Western Amazonia). This allows us to test the indirect impact of the Andean uplift on the diversification of *Philodendron*.

By expanding the taxon sampling of Canal et al. (2018), the species diversity across the entire geographic range of the genus is included and a phylogeny is estimated using three plastid markers (*petD, rpl16* and *trnK/matK*). In light of this new phylogenetic backbone, the present study aims [1] to conduct robust biogeographic range expansion analyses of *Philodendron* in the Neotropics using BioGeography with Bayesian (and likelihood) Evolutionary Analysis in R (BioGeoBEARS), based on a time-calibrated phylogeny, using three secondary calibration points, and [2] to measure and compare diversification rates between species in the Chocó ecoregion and western Amazonia regions and species occurring outside of these regions using Geographic State Speciation and Extinction (GeoSSE) in order to test the indirect effect of the uplift of the Northern Andes on the diversification of *Philodendron*.

3.3. Material and Methods

3.3.1. Taxon sampling, DNA sequencing, alignment, and phylogenetic analyses

In order to achieve a more complete geographic coverage for the genus *Philodendron*, we expanded the sampling of Canal et al. (2018) across the whole genus by including accessions recently collected in Colombia, Cuba and French Guiana. This augmented sampling comprises a total of 221 accessions belonging to 173 *Philodendron* taxa, as compared to 137 accessions of *Philodendron* from 125 taxa in Canal et al. (2018) As a consequence, the sampling for the genus' center of diversity in northwest South America has been largely improved, together with a much deeper sampling within South American species of subgenus *Pteromischum*. However, species of subgenus *Pteromischum* that are endemic to Central America could not be included in the sampling, because this subgenus is generally poorly represented in living collections, and additional field collections in Central America in

the course of the present work was not possible. From the additional samples, we generated a total of 267 new sequences of the three non-coding plastid regions *petD*, *rpl16* and *trnK/matK*, representing 89 accessions within *Philodendron*. DNA extraction, PCR amplification, sequencing, gene alignments and phylogenetic analyses (maximum parsimony - MP, maximum likelihood - ML, and Bayesian inference - BI) were conducted as described in Canal et al. (2018). See Supplemental Data with the online version of this article for voucher information and the National Center for Biotechnology Information (NCBI) accession numbers (Appendix B1). DNA samples are available via the Global Genome Biodiversity Network (GGBN; Droege et al., 2016). Based on the most recent taxonomic treatments (Mayo, 1991; Grayum, 1996; Croat, 1997; Sakuragui et al., 2018), and the World Checklist of Selected Plant Families (Govaerts et al., 2018), we calculated the fraction of species included for each subgenus. Our taxon sampling includes 6/21 species accepted in subgenus *Meconostigma*, 144/~460 species of subgenus *Philodendron* and 23/82 species of subgenus *Pteromischum*. Thus, it corresponds to a proportion of nearly one third of the entire species diversity of *Philodendron*. In addition, we sampled 4/16 species of the Neotropical sister genus *Adelonema* and 5/~140 species of the Asian genus *Homalomena*, which is sister to the clade combining *Adelonema* and *Philodendron*.

3.3.2. Divergence-time estimates

Multiple specimens for each species would bias geographic range inferences (Matzke, 2013). We therefore, removed multiple accessions of each species from the final concatenated alignment to estimate divergence-times and to infer the biogeographic range evolution for *Philodendron*. The final concatenated plastid DNA dataset resulted in a total of 5,363 characters (1,134 for *petD*, 1,272 for *rpl16* and 2,957 for *trnK/matK*). We calibrated the phylogenetic tree of *Philodendron* according to the most appropriate approach for *Philodendron* found by Canal et al. (2018): three secondary calibration points guided by multiple fossil-calibrated phylogenetic analyses obtained by Nauheimer et al. (2012; Nodes 28, 109 and 113). Therefore, we included the 11 outgroup species used by Canal et al. (2018) and applied the same priors for rate heterogeneity among lineages (Drummond et al., 2006; Uncorrelated Lognormal Relaxed Clock – UCLN), and speciation tree process (birth-death model - BD). The data partitions and substitution models were set according to jModelTest version 2.1.7 (*matK* = TVMef + I + Γ, *petB* spacer and *trnK* 3’ intron = TVM + Γ, *petD* 5’

exon = JC, *petD* intron and *trnK* 5' intron = TPM1uf + Γ, *trnK* 3' exon = K80, and *rpl16* intron = TIM2 + Γ; Darriba et al., 2012). For all substitution models, rates of transitions were set according to AIC values obtained in jModelTest. All parameters described were set in the XML file in BEAST 2.4.7 (Bouckaert et al., 2014) using the corresponding version of BEAUTi. A coefficient of variation higher than zero (> 0.45) was obtained in the UCLN analysis, which confirms that our data does not fit a clock-like model (Drummond and Bouckaert, 2015).

To assess the consistency of the BEAST results, three independent MCMC runs were conducted using a different random seed on the CIPRES Science Gateway (Miller et al., 2010). Each chain was run for 50 million generations logging parameters every 5,000 generations. Tracer version 1.6.0 (Bouckaert et al., 2014) was used to visualize log files, assess both convergence using effective sample size (ESS) and the stationarity on the log-likelihood curves and determine the burn-in. The first 10% saved trees from each run were discarded and the remaining trees were combined in LogCombiner version 2.4.3 (Drummond et al., 2012). Treeannotator version 2.4.3 (Bouckaert et al., 2014) was used to estimate the Maximum Clade Credibility Tree (MCCT) with posterior probability values (PP; limit set to 0.5) and mean node ages with the 95% Highest Posterior Density – HPD intervals of these ages. The MCCT estimated was visualized in FigTree version 1.4.2 (Rambaut, 2012) and edited using the vector graphics editor Inkscape version 0.92 (The Inkscape Project, inkscape.org; Appendix B2).

3.3.3. Ancestral range estimation

Species distribution data were obtained from taxonomic monographs, floras and checklists (Mayo, 1991; Grayum, 1996; Croat, 1997; Croat and Mora, 2004; Croat et al., 2010; Croat et al., 2016; Govaerts et al., 2018) as well as from species protologues and locality data of voucher labels (Tropicos.org). Species of *Philodendron* occur predominantly in humid forests of tropical lowlands, lower mountain ranges or at mid-elevations of higher mountains. In the Andes, only very few species are found in high-elevation forests >2,000 m. Since many *Philodendron* species are shared between lowland forests of the Chocó ecoregion and mid-elevation forests of the Andes, we followed the example of other studies dealing with lowland rainforest lineages and combined both areas (Schley et al., 2018). Likewise, we merged the coastal cordillera of Venezuela into Amazonia, since both areas showed strong

biogeographic relationships with respect to *Philodendron* species. Species were coded for presence/absence in five operational areas, which were based on and adapted from the level 2 area units of the World Geographical Scheme for Recording Plant Distributions (Brummitt et al., 2001). These areas are partially congruent with the areas used in biogeographic studies of other Neotropical plant lineages (Givnish et al., 2011; Nieto-Blázquez et al., 2017; Pérez-Escobar et al., 2017) and are here defined as follows (given from northwest to southeast): Central America (ranging from tropical Mexico to the Isthmus of Panama); Caribbean islands (Greater and Lesser Antilles, and the Bahamas; Nieto-Blázquez et al., 2017); Chocó & Andes (including the Chocó ecoregion and >1,000 m in the northern and central Andes); Amazonia (including the Amazon and Orinoco basins, the Guiana Shield, the coastal cordillera of Venezuela and the eastern cordillera of the Andes <1,000 m); and Southeast Brazil (including the Caatinga, the Cerrado, the Chaco in Argentina and the Mata Atlântica).

Undetermined species were coded only for the areas where the collection was made. Although a certain source of error, this approach should be acceptable since the vast majority of *Philodendron* species has rather restricted distribution ranges belonging to only one of our five operational areas (Figure 3.2), and this is especially true for less known or even hitherto undescribed species which should represent the majority of our undetermined species. The highest species overlap between two areas corresponds to Central America and the Chocó & Andes region, because a number of species occurs in the wet forests both northwest and southeast of the Isthmus of Panama. Particularly in subgenus *Pteromischum*, of which our analyses contains several undetermined species due to a high proportion of sterile specimens in the sampling, a distribution pattern of species ranging from central or southern Central America southwards to as far as central or southern Ecuador is very common (Grayum, 1996). However, disjunct species distributions between Central America and the Chocó & Andes region on one side and the Amazon basin on the other side are extremely scarce (Croat, 1997) or, as in the case of subgenus *Pteromischum*, non-existent (Grayum, 1996). Therefore, the distributions in the clades in question should be taken with some caution, although the presence of a certain amount of undetermined species in the sampling should not affect our general conclusions from the results.

We focused our investigation on ancestral distribution patterns of the genus *Philodendron* and its sister genus *Adelonema*. Therefore, the Asian genus *Homalomena* and outgroups were excluded from the MMCT obtained in BEAST. We estimated ancestral ranges using the R-package BioGeography with Bayesian (and likelihood) Evolutionary Analysis in R (BioGeoBEARS version 0.2.1; Matzke, 2014) in R version 3.2.4 (R Core Team,

2013). BioGeoBEARS estimates geographical ranges through time accounting for anagenetic and cladogenetic processes such as dispersal, extinction, founder-event speciation, and vicariance (Matzke, 2013; 2014; Matthew and Matzke, 2016). We evaluated the following models: BAYAREALIKE, DEC and DIVALIKE and compared them using AIC values and likelihood ratio tests (LRTs). Subsequently, we compared each model with and without the +J parameter, using AIC values and likelihood ratio tests (LRTs).

3.3.4. Geographical state-dependent analyses

In order to assess the impact of the Andean orogeny on the speciation, extinction and dispersal of *Philodendron*, we used the Geographic State Speciation and Extinction - GeoSSE model (Goldberg et al., 2011) as implemented in the R-package Diversitree version 0.9-10 (Fitzjohn, 2012) in RStudio version 1.1.419 (R Core Team, 2013). The GeoSSE model differs from the Binary State Speciation and Extinction model (BiSSE; Maddison et al., 2007) by including a parameter to account for diversification and range shifts among two regions (Goldberg et al., 2011). We coded three geographical regions: [A] species found in the central and northern Andes and/or the adjacent lowlands (i.e. the Chocó ecoregion and western Amazonia); [B] species found neither in the Andes nor in the adjacent lowlands (i.e. only in Central America, the Caribbean islands, central/eastern Amazonia and/or southeast Brazil); [AB] species widely distributed in the Neotropics (occurring both in the Andes & adjacent lowlands and outside of this area). In order to account for the indirect effect of the Andean uplift by means of highly increased precipitation in the adjacent lowlands, the Chocó ecoregion and western Amazonia were included in the geographical state A; therefore the coding differs slightly from that used in our biogeographic analyses. We compared three different models based on Goldberg et al. (2011). [1] full model (Goldberg et al., 2011); [2] without between-region speciation (sAB = 0); and [3] speciation and extinction are equal in regions A and B (sA = sB; xA = xB). We specified the fraction of missing species of *Philodendron* under the assumption of random taxon sampling (Fitzjohn et al., 2009). The sampling fraction was calculated as a ratio of the number of species included divided by the total number of species estimated for each region: A = 53/280, B = 65/180 and AB = 43/90. Subsequently, we used MCMC on the MCCT to estimate the best-fitting GeoSSE model parameters, running 1 million generations with broad exponential priors (rate = 0.1). The GeoSSE model with the lowest AIC value was selected. BiSSE and associated state-

speciation and extinction models inferences might include high Type I error rates (Maddison and Fitzjohn, 2015), in particular for phylogenetic trees with less than 300 terminals and for states present in <10% of the species sampled (Davis et al., 2013). Therefore, we conducted additional analyses by redistributing the coded areas randomly onto the MCCT as conducted by Pérez-Escobar et al. (2017; Appendix B3).

3.4. Results

3.4.1. Phylogenetic analyses

The clades recovered in the ML, MP and BI analyses are largely consistent with those found by Canal et al. (2018; see discussion for the evolutionary relationships of the species newly sampled in this study). Sequence statistics, models of sequence evolution (with AIC values) and tree statistics for the combined plastid DNA dataset are presented in the Supplemental Data (Appendix B4). The resulting cladogram of the MrBayes 50% majority-rule consensus tree with node support values obtained in ML and MP analyses is shown in Figure 3.1 and Supplemental Data (Appendix B5). Within subgenus *Pteromischum*, the species *P. surinamense* (Miq.) Engl. was resolved as sister to two newly recovered, well-supported clades (Clade A: BS = 97, JK = 98, PP = 1.0, and Clade B: BS = 82, JK = 60, PP = 0.99; Figure 3.1). Both clades recovered within subgenus *Pteromischum* contain species inhabiting the adjacent lowlands of the northern Andes (the Chocó ecoregion and western Amazonia).

3.4.2. Divergence-time estimates

The chronogram and the divergence times for each node and their corresponding 95% HPDs obtained in BEAST based on the divergence time analyses using three secondary calibration priors are presented in Figure 3.2 and Appendix B2. Divergence-time analyses resulted in older estimated ages than those obtained in Canal et al. (2018) that involved the same calibration approach but with a reduced taxon and geographic range sampling. In the present study, the genus *Philodendron* diverged from its sister genus *Adelonema* ~28.40 mya (95% HPD = 20.90-36.16) and started to diversify ~24.72 mya (95% HPD = 17.80-32.09) in

the late Oligocene (Figure 3.2, Appendix B4). In the MCCT subgenus *Pteromischum* is resolved sister to an unsupported clade including the subgenera *Meconostigma* and *Philodendron.* Within genus *Philodendron,* subgenus *Meconostigma* diversified ~8.68 mya (95% HPD = 4.32-13.35; Figure 3.2), subgenus *Pteromischum* ~19.21 mya (95% HPD = 12.47-25-46; Figure 3.2), and subgenus *Philodendron* ~20.37 mya (95% HPD = 14.03-26.54; Figure 3.2). Stem nodes of the clades 4, 5 and 10 and crown node of clade 3 were not supported (Table 3.1; Figure 3.2). Major clades within subgenera *Pteromischum* and *Philodendron* diversified from the middle Miocene onwards (crown ages in Table 3.1 and Appendix B2).

Figure 3.1. Bayesian 50% majority-rule consensus tree of *Philodendron* Schott with three plastid DNA markers (*petD*, *rpl16* and *trnK/matK*). Values above branches indicate posterior probability of Bayesian inference (BI) analyses (bold, left), and Jack-knife supports of maximum parsimony (MP) analyses (right). Values below branches indicate bootstrap support of maximum likelihood (ML) analyses. Values in square brackets indicate conflicting topologies between BI and ML detected in TreeGraph. Node tips are labelled with DNA number and species names, refer to Appendix B1 for specimen details. Star = *Philodendron*. Refer to Appendix B5 for the entire phylogenetic tree.

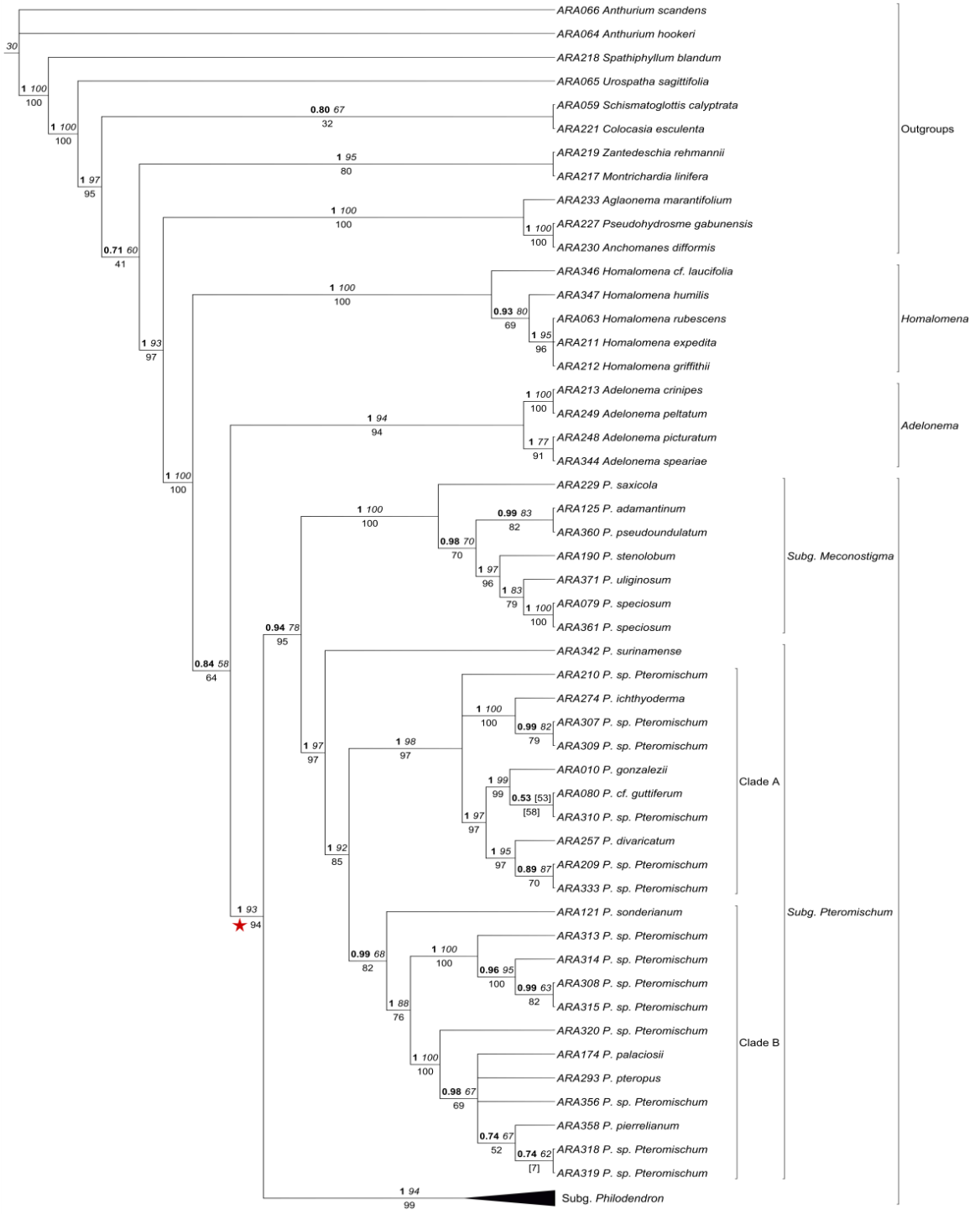

Table 3.1. Comparison of the ages obtained by Canal et al. (2018) and the present study, both using the same three secondary calibration priors, Birth-Death (BD) speciation prior and uncorrelated lognormal model (UCLN) in BEAST. Branch supports (PP, posterior probability), mean ages of the stem and crown nodes (in Ma) and Highest Posterior Density (HPD) 95% intervals are shown. C, crown node; S, stem node; *, not calculated given the low statistic support; NA, not applicable. Calibrated nodes in both studies are labeled as "Secondary constraint". Numbers between brackets in the first column correspond to the number of the clades in Canal et al. (2018).

Clade	Node	Canal et al. (2018)			Present study		
		PP	Mean	HPD	PP	Mean	HPD
Pothoideae + Monsteroideae	S	1.00	1111.14	81.75-148.17	1.00	104.96	82.18-132.20
	C	0.75	93.81	46.03-121.14	0.87	86.37	51.32-113.22
Lasioideae (Secondary constraint)	S	1.00	87.74	80.1-97.51	1.00	88.58	80.10-98.28
	C	NA (Single terminal node)			NA (Single terminal node)		
Aroideae	S	1.00	87.74	80.1-97.51	1.00	88.58	80.10-98.28
	C	1.00	72.99	59.64-83.53	1.00	77.21	65.43-89.74
Anchomanes difformis, *Pseudohydrosme gabunensis*, *Aglaonema marantifolium* and *Zantedeschia rehmannii* + Philodendron clade (Secondary constraint)	S	1.00	71.21	59.39-81.49	0.15	76.57	*
	C	1.00	60.51	47.07-73.78	1.00	64.52	54.50-75.27
Philodendron clade (Secondary constraint)	S	0.96	53.28	39.18-66.23	0.98	56.74	45.16-68.63
	C	1.00	27.31	18.9-36.64	1.00	30.49	22.82-38.85
Homalomena	S	1.00	27.31	18.9-36.64	1.00	30.49	22.82-38.85
	C	1.00	1.41	0.2-3.12	1.00	5.2	1.90-9.36
Adelonema	S	0.79	25.53	17.81-33.94	0.91	28.40	20.90-36.16
	C	1.00	17.05	8.76-26.26	1.00	19.74	11.75-28.02
Philodendron	S	0.79	25.53	17.81-33.94	0.91	28.40	20.90-36.16
	C	1.00	22.1	15.48-29.79	1.00	24.72	17.80-32.09
Subgenus *Meconostigma* (1)	S	0.37	21.69	*	0.27	24.53	*
	C	1.00	6.66	2.55-11.88	1.00	8.68	4.32-13.35
Subgenus *Pteromischum* (2)	S	0.37	21.69	*	1.00	24.72	17.80-32.09
	C	1.00	14.56	8.64-20.54	1.00	19.21	12.47-25.46
Clade A	S	NA	NA	NA	1.00	15.29	9.77-20.08
	C	NA	NA	NA	1.00	11.86	7.46-16.33
Clade B	S	NA	NA	NA	1.00	15.29	9.77-20.08
	C	NA	NA	NA	1.00	11.39	6.79-16.12
Subgenus *Philodendron*	S	1.00	22.1	15.48-29.79	0.27	24.53	*
	C	1.00	18.06	12.3-24.44	1.00	20.37	14.03-26.54
Clade 1 (3)	S	1.00	18.06	12.3-24.44	1.00	20.37	14.03-26.54
	C	1.00	11.1	6.85-15.63	1.00	12.34	7.72-17.17
Clade 2 (4)	S	0.85	16.91	11.2-22.65	0.88	18.87	12.82-24.69
	C	1.00	3.93	1.75-6.66	1.00	6.34	3.12-10.17
Clade 3 (5)	S	0.18	8.8	*	1.00	9.84	6.36-13.53
	C	0.18	5.15	*	0.18	9.49	*
Clade 4 (6)	S	0.18	9.03	*	0.21	9.32	*
	C	1.00	4.33	2.21-6.81	1.00	4.32	2.20-6.66
Clade 5 (7)	S	1.00	9.13	5.81-12.85	0.21	9.32	*
	C	1.00	4.69	2.56-7.09	1.00	4.86	2.63-7.48
Clade 6 (8)	S	0.96	7.87	4.95-11.01	0.94	8.49	5.45-11.60
	C	1.00	6.25	3.76-8.95	0.99	6.70	4.17-9.46
Clade 7 (9)	S	0.96	7.87	4.95-11.01	0.94	8.49	5.45-11.60
	C	1.00	6.08	3.59-8.82	1.00	6.52	4.12-9.22
Clade 8 (10)	S	0.76	7.46	4.56-10.47	0.98	10.35	7.00-13.95
	C	1.00	4.08	2.15-6.16	0.54	9.77	5.82-12.84
Clade 9 (11)	S	0.17	8.65	*	0.98	9.32	6.27-12.68
	C	0.18	4.1	*	1.00	6.48	3.97-9.20
Clade 10 (12)	S	1.00	12.03	7.87-16.37	0.38	12.55	*
	C	1.00	6.97	3.13-11.01	1.00	8.12	4.27-12.29
Clade 11 (13)	S	1.00	5.71	3.24-8.34	1.00	7.42	4.70-10.19
	C	1.00	3.35	1.58-5.43	1.00	5.99	3.59-8.43
Clade 12 (14)	S	1.00	5.71	3.24-8.34	1.00	7.42	4.70-10.19
	C	1.00	4.1	2.1-6.39	1.00	5.48	3.01-8.15

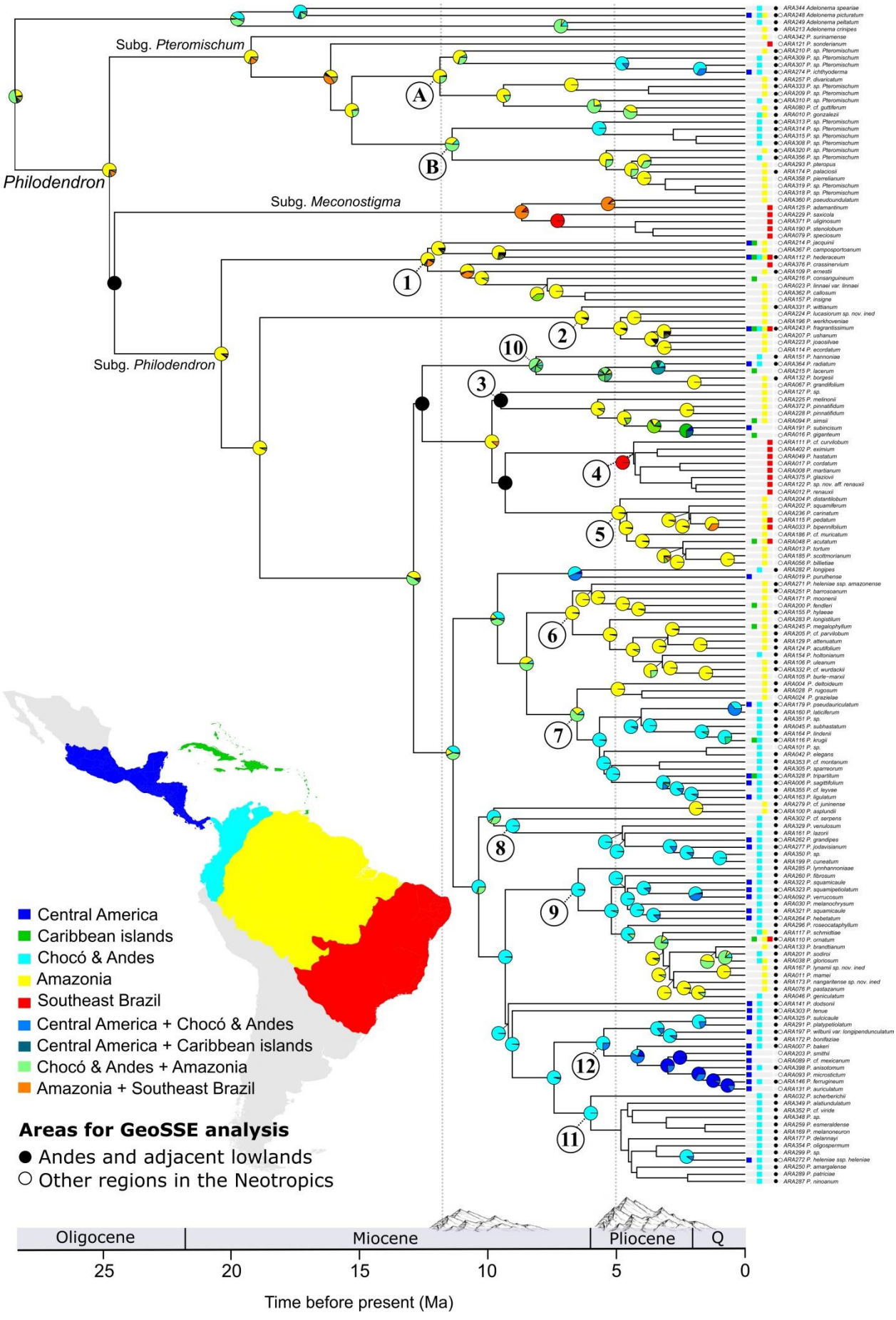
Subg. Pteromischum
Philodendron
Subg. Meconostigma
Subg. Philodendron
A
B
1
2
10
3
4
5
6
7
8
9
12
11
Central America
Caribbean islands
Chocó & Andes
Amazonia
Southeast Brazil
Central America + Chocó & Andes
Central America + Caribbean islands
Chocó & Andes + Amazonia
Amazonia + Southeast Brazil
Areas for GeoSSE analysis
Andes and adjacent lowlands
Other regions in the Neotropics
Oligocene
Miocene
Pliocene
Q
25
20
15
10
5
0
Time before present (Ma)

Figure 3.2. (previous page) Biogeographic history of *Philodendron* Schott. Maximum Clade Credibility tree obtained from BEAST analyses of three plastid DNA markers (*petD, rpl16* and *trnK/matK*) showing the estimated ancestral biogeographic history of the genus. Time intervals in million years ago (mya) are indicated by the timescale with the geologic periods. Pie charts at each node represent ancestral geographic ranges instantaneously before cladogenesis as inferred in BioGeoBEARS. Black pie charts correspond to unsupported nodes. Vertical dashed lines indicate the most intense periods of the uplift of the Andes. Letters or numbers at the internal nodes indicate clades identified within subgenus *Pteromischum* (Clades A and B) and subgenus Philodendron (Clades 1 to 12). Operational areas defined for the biogeographic ranges analysis in BioGeoBEARS (Central America, Caribbean islands, Chocó & Andes, Amazonia and Southeast Brazil) are based on and adapted from the level 2 area units of the World Geographical Scheme for Recording Plant Distributions (Brummitt et al., 2001). Refer to Table 3.1 for details of divergence-time % HPD values.

3.4.3. Ancestral range estimates

The Dispersal-Extinction-Cladogenesis model with founder speciation events (DEC+J) was estimated as the best-fitting model for *Philodendron* based on AIC, comparing LnL values across all models and LRT analyses comparing the nested null model (DEC) with DEC+J (LnL -285.6, LRT < 0.05; Tables 3.2 and Appendix B6). Values for range expansion, range extinction and founder event parameters were 0.014, 0 and 0.011, respectively (Table 3.2). This result indicates that the best-fitting model relied on range expansion and founder events more than on extinction.

Ancestral range estimates at each node in Figure 3.2 represent the ranges instantaneously before each cladogenesis event according to the DEC+J model.

The stem node of the genus *Philodendron* had an estimated divergence time of ~29 mya, during the early Oligocene and the ancestral geographic range for this node was estimated to be both operational areas: Amazonia and Chocó & Andes (~50% support). There was ~25% support that the ancestral area of this node corresponded only to Amazonia. Amazonia was estimated to be the ancestral geographic range of the crown node of *Philodendron* with the highest probability (~75%; Figure 3.2) ~25 mya during the late Oligocene. In *Philodendron*, the first geographic range expansion from Amazonia into southeastern Brazil occurred within subgenus *Pteromischum* during the early Miocene. During the middle Miocene, multiple events of geographic range expansion from Amazonia towards the Chocó & Andes region occurred independently within subgenera *Philodendron* and *Pteromischum*. During the late Miocene, three geographic range expansions occurred independently from Amazonia into southeastern Brazil within subgenera *Meconostigma* and

Philodendron. During the same period of time, geographic range expansions from Amazonia to the Chocó & Andes were estimated within subgenera *Philodendron* and *Pteromischum*. In the Miocene-Pliocene transition period, lineages of subgenera *Philodendron* and *Pteromischum* underwent geographic range expansion from the Chocó & Andes region to Central America. From the early Pliocene onwards, multiple lineages experienced geographic range expansion from South America to the Caribbean islands. The origin and the corresponding geographic range evolution of the three subgenera *Meconostigma, Philodendron* and *Pteromischum* are addressed in the discussion.

Table 3.2. Comparison of the models evaluated in BioGeoBEARS version 0.2.1 (Matzke, 2014) using Akaike Information Criterion (AIC) values. Model in bold corresponds to the best-fitting model obtained. LnL, Log-likelihood; d, dispersal; e, extinction; j, founder; AICwt, AIC weight.

Model	LnL	# of parameters	d	e	j	AIC	AICwt
DEC	-291.4	2	0.015	1.0e-12	0	586.7	0.0086
DEC+J	**-285.6**	**3**	**0.014**	**1.0e-12**	**0.011**	**577.3**	**0.99**
DIVALIKE	-294.7	2	0.018	1.0e-12	0	593.3	0.0003
DIVALIKE+J	-290.7	3	0.016	1.0e-12	0.010	587.5	0.0059
BAYAREALIKE	-319.4	2	0.011	0.056	0	642.9	5.5e-15
BAYAREALIKE+J	-297.4	3	0.010	0.0014	0.026	600.8	7.5e-06

3.4.4. Geographical state-dependent analyses

Following GeoSSE analyses that tested models associated with differences in speciation rates between areas A (Andes & adjacent lowlands, i.e., the Chocó ecoregion and western Amazonia), B (Central America, Caribbean islands, central or eastern Amazonia, Southeast Brazil, collectively called "other regions in the Neotropics"), likelihood scores and AIC values supported the model with differences in rates of speciation (sA – sB) between regions A and B (Table 3.3). Posterior probability distributions for the best-fitting GeoSSE model using the MCCT obtained in BEAST and the differences of the speciation, extinction and dispersal rates between the two regions are shown in Figure 3.3. The speciation and dispersal rates in the Andes & adjacent lowlands [A] are notably higher (than for species restricted to all other regions in the Neotropics (B; Figure 3.3). Extinction rate within the Andes & adjacent lowlands region [A] is similar to the extinction rate estimated for the rest of the regions [B].

Table 3.3. Results of GeoSEE. Full model with free speciation, extinction and dispersal between areas resulted in the best-fitting model. Df, degrees of freedom; lnLik, log-likelihood; ChiSq, chi-square values; Pr(>IChiI), probability of greater chi-square value; Full, full model; No. sAB, without between-regions speciation; Eq.div, speciation and extinction are equal in regions A and B.

Model	Df	lnLik	AIC	ChiSq	Pr(>IChiI)
Full	7	-584.76	1183.5		
No. sAB	6	-584.76	1181.5	-0.0009	1.0000000
Eq.div	5	-592.07	1194.2	14.6243	0.0006674

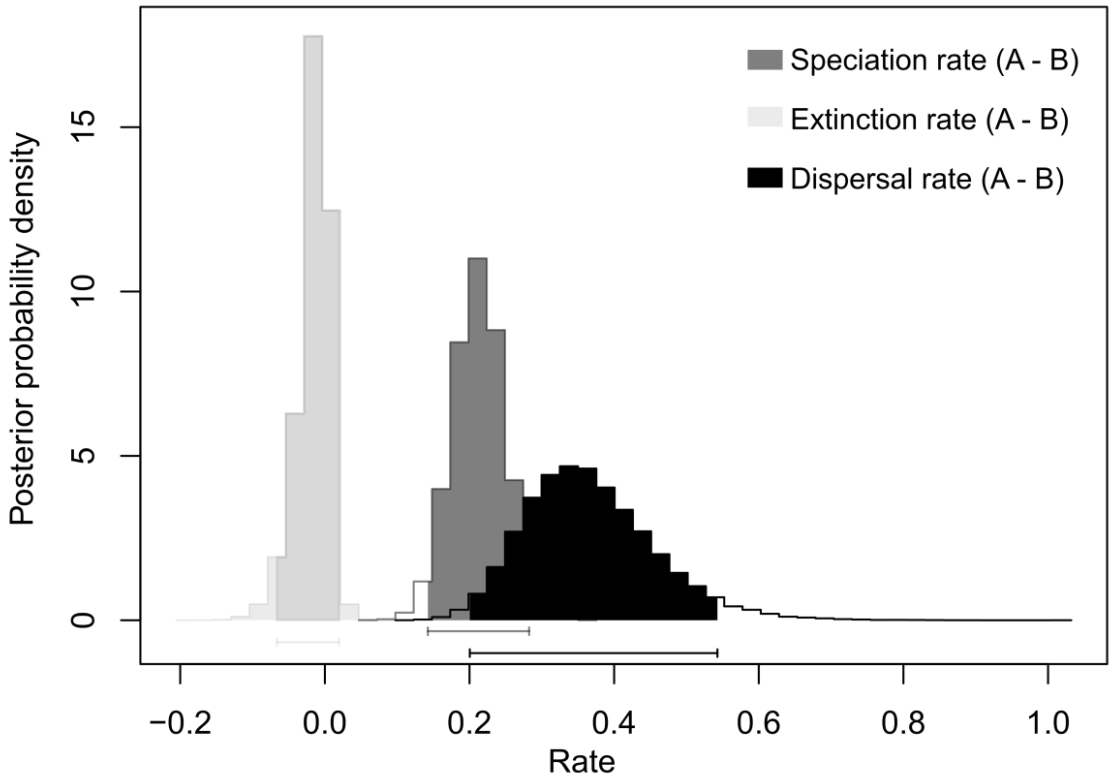

Figure 3.3. Density probability plots of the differences between areas A and B in rates of speciation (s), extinction (x) and dispersal (d) identified by GeoSSE. Area A refers to species found in the central and northern Andes and/or the adjacent lowlands (i.e. the Chocó ecoregion and western Amazonia), and area B refers to species found neither in the Andes nor in the adjacent lowlands (i.e. only in Central America, the Caribbean islands, central/eastern Amazonia and/or southeast Brazil). Horizontal bars below the figure represent 95% confidence intervals estimated using Markov chain Monte Carlo. Rates are in events per millions of years.

3.5. Discussion

3.5.1. Differences between the phylogenetic tree of *Philodendron* and previous phylogenetic studies

The phylogenetic trees obtained (Figure 3.1) are highly congruent with those presented by Canal et al. (2018). However, the evolutionary relationships at the deepest level of the phylogeny of *Philodendron* differ from the relationships recovered by Sakuragui et al. (2018) based on a sampling of 67 *Philodendron* taxa and Vasconcelos et al. (2018; 129 *Philodendron* taxa). In the present study, the genus *Philodendron* is monophyletic. In contrast, Sakuragui et al. (2018) recovered subgenus *Meconostigma* (genus *Thaumatophyllum* sensu Sakuragui et al., 2018) in a polytomy together with two clades containing *Adelonema* and *Philodendron* subgenus *Philodendron*, respectively (the latter clade also including several species of subgenus *Pteromischum* scattered among species of subgenus *Philodendron*). Similar to the present study, Vasconcelos et al. (2018) recovered the monophyly of *Philodendron*. Within this clade, however, subgenus *Meconostigma* (as genus *Thaumatophyllum*) was resolved as sister to a clade including the two monophyletic subgenera *Pteromischum* and *Philodendron*. Causes of the topological discrepancies between our study and the studies conducted by Sakuragui et al. (2018) and Vasconcelos et al. (2018) are likely due to the differences in the taxon sampling strategy and the genomic regions analyzed. We used a combination of plastid DNA markers (*petD*, *rpl16* and *trnK/matK*), Sakuragui et al. (2018) used nrETS and Vasconcelos et al. (2018) used a combination of plastid and ribosomal nuclear DNA markers (*atpF-atpH*, *rpl32-trnL*, *trnQ-5'-rps16* and *trnV-ndhC* and ITS2, respectively). Nuclear ribosomal ETS and ITS are known to be multi-copy and subject to reticulate evolution, whilst it is important to have information about the nuclear genome, interpretation of such results should be taken with caution (Poczai and Hyvönen, 2010).

Sakuragui et al. (2018) present an overview conveniently summarizing the phylogenetic relationships among *Adelonema*, *Homalomena* and *Philodendron* resulting from previous studies (Barabé et al., 2002; Gauthier et al., 2008; Wong et al., 2013; Loss-Oliveira et al., 2016; Wong et al., 2016). Together with the results presented in the "supertree" in Sakuragui et al. (2018), the outcomes of these studies suggest a possible paraphyly of the genus *Philodendron*, leading to the conclusion of separating subgenus *Meconostigma* as genus

Thaumatophyllum. Like Sakuragui et al. (2018), however, all previous phylogenetic studies of *Philodendron* mentioned above have a relatively limited taxon sampling, and the relevant clades are in general poorly supported. In contrast, the results of the present study, those by Canal et al. (2018), and Vasconcelos et al. (2018), based on comprehensive taxon sampling and providing high levels of resolution in the phylogenetic trees, support the monophyly of the genus *Philodendron* and each of its three subgenera. The relationships among the three subgenera remain unclear however, as indicated by the low statistical support at the backbone of the genus *Philodendron* between the subgenera in our BEAST tree (Figure 3.2); taxonomic and nomenclatural conclusions within *Philodendron* should therefore be made with caution.

From a taxonomic perspective, the subgenera *Meconostigma* and *Pteromischum* are morphologically well-defined (Mayo, 1991; Grayum, 1996; Calazans et al., 2014; Sakuragui et al., 2018). In contrast, the largest subgenus *Philodendron* is morphologically extremely variable and essentially defined by the absence of the morphological attributes characterizing the subgenera *Meconostigma* and *Pteromischum* (Mayo, 1989; Croat, 1997). Thus, the separation of these two subgenera would leave the remainder of the genus *Philodendron* (i.e., the current subgenus *Philodendron*) without clear morphological characters for its taxonomic delimitation. From a nomenclatural perspective, it is stated in the preamble of the International Code of Nomenclature for algae, fungi, and plants that "the useless creation of names should be avoided" (Turland et al., 2018). This could be the case if the subgenera *Meconostigma* and *Pteromischum* were separated, furthermore there would be little further practical benefit. Finally, the recognition of subgenus *Meconostigma* as a separate genus would also unnecessarily lead to identification difficulties for field botanists less experienced with aroids, therefore further reducing the practical benefits of changing the nomenclature. Therefore, until analyses based on extensive sampling across the genus and incorporating multiple low copy nuclear markers, for example by using target enrichment (Weitemier et al., 2014) provide more informative phylogenetic hypotheses, we strongly recommend maintaining *Philodendron* as a single genus with three subgenera.

In order to streamline the further discussion, we will focus on the new clades recovered within subgenus *Pteromischum* and the differences in comparison to Canal et al. (2018), which are mostly caused by the phylogenetic position of the taxa that are newly included in the present study. Subgenus *Pteromischum* consists of the two sections *Fruticosa* and *Pteromischum* (Grayum, 1996; Croat, 1997). Section *Pteromischum* includes strictly appressed-climbing, relatively slender vines producing compound inflorescences with cataphylls (Grayum, 1996). In contrast, section *Fruticosa* includes lianescent vines with

divergent flowering shoots bearing mostly solitary inflorescences without cataphylls (Grayum, 1996). Newly added species in the present study since Canal et al. (2018; i.e. *P. pteropus* Mart. ex Schott and *P. pierrelianum* Scherberich, Croat, M. M. Mora & G. Ferry), are assigned to sect. *Pteromischum* and were resolved in a clade that is sister to a clade including species assigned to sect. *Fruticosa* (including *P. divaricatum* K. Krause, *P. gonzalezii* Grayum, *P. guttiferum* Kunth, *P. ichthyoderma* Croat & Grayum, and *P. sonderianum* Schott); thus lending support to the recognition of the two morphologically distinct sections. However, further sampling is required for a critical assessment of the phylogenetic relationships of subgenus *Pteromischum* and a number of sterile *Pteromischum* specimens were difficult to determine to species level due to missing characters (*P.* sp. *Pteromischum*, Figure 3.2). Within subgenus *Philodendron*, the present study recovers all the clades previously recognized Canal et al. (2018). Newly added species assigned to different taxonomic sections further indicate the groups that were previously defined based on morphology alone are not supported (Croat, 1997; Köster & Croat, 2011). Therefore, the results of the present study support the current classification at the sectional level in subgenus *Pteromischum* but not within subgenus *Philodendron*. This might reflect the high morphological plasticity in the relatively young and rapidly diversifying subgenus *Philodendron*, a common feature of Neotropical plant lineages (Richardson et al., 2001).

3.5.2. Taxon sampling and its impact on divergence time estimates in *Philodendron*

The slight discrepancies between the ages estimated in this study and the ages previously documented (Canal et al., 2018) might be attributed to the differences in the taxon sampling density. The ages (means of the stem nodes and the crown nodes) were comparatively older in the present study than in Canal et al. (2018). However, their corresponding 95% HPD values overlap in both studies (Table 3.1). These ages differ from the ages previously estimated for the stem node of both genera *Adelonema* and *Philodendron* (~25.53 Ma; HPD = 17.81-33.94; Canal et al., 2018) and the crown node of *Philodendron* (~22.1 Ma; HPD = 15.48-29.79; Canal et al., 2018). Likewise, differences are found within the genus *Philodendron*. The subgenera *Meconostigma*, *Philodendron* and *Pteromischum* diversified earlier than previously estimated (Canal et al., 2018). For a comparison of the ages estimated for the clades defined in Canal et al. (2018) please refer to Table 3.1.The

differences between the ages obtained for the stem nodes range from a minimum of 0.19 Ma for the stem node of Clade 7 to 2.31 Ma for the stem node of Clade 3. Larger differences are found for the ages of the crown nodes than for the stem nodes, ranging from a minimum of 1.24 Ma for the crown age of Clade 3 to a maximum of 5.69 Ma for the crown node of Clade 10 (Table 3.1). Under the same calibration priors, bias in divergence-time estimates might be attributed to the sampling density and the distance of the clades from the node calibrated (Linder et al., 2005). Since both studies relied on the same priors to account for rate heterogeneity among lineages, speciation tree process and calibration constraints, we consider that the present study based on a comparatively larger fraction of the species diversity of *Philodendron* (161 vs 125 species in Canal et al., 2018), provides more reliable age estimates than previously documented.

3.5.3. Origin of *Philodendron* and earliest diversification events

The evolutionary history of *Philodendron* is strongly associated with the major geological events in the Neotropics since the late Oligocene. The origin of *Philodendron* ~29 mya (stem node of *Philodendron*; Table 3.1) coincides with the last period of the Amazonian-lowland to the Andean-highland landscape transition in northwest South America (~33-23 mya; Hoorn et al., 2010). Our analysis suggested that the most likely ancestral geographic range for the stem node of the genera *Adelonema* and *Philodendron* is either the combination of the current Chocó & Andes region and Amazonia (50%) or just Amazonia (~25%; Figure 3.2). Before the late Miocene, the Chocó and Northern Andean regions were part of a larger area known as the pan-Amazonian region (until ~10 mya; Hoorn et al., 2010). Therefore, our analysis indicates that the pan-Amazonian region is likely to be the ancestral geographic range for *Adelonema* and *Philodendron*.

Subsequently, the Oligocene-Miocene transition (~24 mya) corresponds to the first period of diversification within the genus *Philodendron* and the origin of the three subgenera *Meconostigma*, *Philodendron* and *Pteromischum* (Figure 3.2). Amazonia is recovered as the most likely ancestral geographic range for the node containing a polytomy of the three subgenera (Figure 3.2). This is in line with the geographic origin of the genus and the area of its earliest diversification inferred by Loss-Oliveira et al. (2016), although the timing differs substantially from that obtained in our results [see Canal et al. (2018) for a detailed comparison of results of the two studies]. This is in accordance with the hypothesis of

Amazonia being the main source of plant and animal lineages in the Neotropics (Antonelli et al., 2018). The rate of dispersal out of Amazonia is higher than out of any other region in the Neotropics (Antonelli et al., 2018). Dispersal events out of Amazonia have significantly increased the species diversity of other Neotropical regions for the last 60 Ma (Antonelli et al., 2018). Amazonian rainforests are proposed to be the primary source for the Andean diversity in orchids (Pérez-Escobar et al., 2017). From the middle Miocene onwards, the genus *Philodendron* underwent multiple geographic range expansions from Amazonia to northwest South America (Chocó & Andes region), southeast Brazil (including the Caatinga, the Cerrado, the Chaco and the Mata Atlântica), and the Caribbean islands (Figure 3.2). Therefore, the earliest geographic range expansion in the evolution of *Philodendron* further supports the importance of Amazonia for the configuration of Neotropical species diversity (Pérez-Escobar et al., 2017; Antonelli et al., 2018). This species radiation coincides with the origin of the species diversity of other Neotropical rainforest lineages such as *Inga* (Richardson et al., 2001), *Costus* (Kay et al., 2005), *Renealmia* L. f. (Särkinen et al., 2007), and *Guarea* and *Trichilia* (Koenen et al., 2015).

3.5.4. From the Amazonia rainforest to the seasonally dry tropical forests (SDTFs) in South America

The geographic range expansion of *Philodendron* started during the Miocene (Figure 3.2). The earliest dispersal events from Amazonia into southeast Brazil occurred in subgenus *Pteromischum* during the early-middle Miocene transition ~16 mya (Figure 3.2). Afterwards, geographic range expansion from Amazonia towards southeast Brazil was inferred in the subgenera *Meconostigma* and *Philodendron* ~10 mya during the late Miocene (Figure 3.2). In contrast, the ages calculated by Loss-Oliveira et al. (2016) for the dispersal events from Amazonia into southeast Brazil are much younger (i.e., 3.7 Ma in subgenus *Meconostigma* and 4.1 Ma in subgenus *Philodendron*). In our study, southeast Brazil corresponds to the Dry Diagonal (Caatinga: tropical semi-arid thorn woodlands; the Cerrado: seasonal woody savannas and the Chaco: subtropical/tropical semi-arid thorn woodlands; Neves et al., 2015) and to the perhumid rainforests of the Mata Atlântica. The geographic range expansion from Amazonian rainforests to SDTFs in southeast Brazil might be associated with independent habitat shifts within all three subgenera within *Philodendron* from humid to drier habitats. Species of *Adelonema* (terrestrial herbs), subgenus *Pteromischum* (mostly vines) and

subgenus *Philodendron* (mostly epiphytes or hemiepiphytes) predominantly occur in dense rainforests where they have accumulated extraordinarily high species diversity (Croat, 1997), members of the much less diverse subgenus *Meconostigma* (mostly terrestrial or saxicolous) typically inhabit open SDTFs or inselbergs. Further studies on modeling the climatic niche evolution for *Philodendron* would allow a better understanding of the colonization of different Neotropical biomes through time.

3.5.5. The impact of the Andean uplift on the history of *Philodendron*

The present study indicates that subgenus *Philodendron* experienced a geographic range expansion from Amazonia to the Choco & Andes region ~12 mya during the middle Miocene (Figure 3.2). This period coincides with the first intense mountain uplift of the northern Andes (covering the Ecuadorian and Colombian cordilleras; Bermúdez et al., 2015). Geological evidence indicates that the paleoelevations in the northern Andes reached 2,000 m during the Miocene-Pliocene transition ~5 mya (Gregory-Wodzicki, 2000). Therefore, the elevations of the northern Andes during the middle Miocene should not have represented a critical barrier for the dispersal of the lineages of *Philodendron* distributed in northwest Amazonia. From the middle Miocene until the late Miocene, the rise of the eastern cordillera of the central Andes indirectly promoted the formation of a large wetland (Pebas system) in western Amazonia (~23-10 mya; Antonelli et al., 2009; Hoorn et al., 2010; Antonelli and Sanmartín, 2011). This dispersal barrier between the Andes and western Amazonia is also probably reflected by the geographic range evolution observed within the genera *Astrocaryum* G. Mey. and *Geonoma* Willd. (Roncal et al., 2013) and the tribe Cinchoneae in the coffee family (Antonelli et al., 2009). The dispersal of *Philodendron* from Amazonia to the Chocó & Andes region is estimated to have occurred around the terminal phase of the Pebas system (~12 mya; Figure 3.2) and the onset of the Amazon drainage period (Salas-Gismondi et al., 2015). Therefore, it is likely that the dispersal of *Philodendron* from western Amazonia to the Andes occurred when the Pebas system represented a network of fragmented wetlands (Antonelli et al., 2009; Hoorn et al., 2010). Such a landscape would not represent a barrier for birds and bats anymore, probably the most important seed dispersal agents for *Philodendron* species (Grayum, 1996; Croat, 1997).

The geographic range shift from Amazonia to the northern Andes and the Chocó ecoregion coincides with the net diversification rate upshift detected near the base of the clade formed by the largest subgenus *Philodendron* (Canal et al., 2018). Within subgenus *Philodendron* (~460 species accepted), the diversification rate increased from ~0.55 to 0.73 events/Ma/ lineage ~12 mya (Canal et al., 2018). The GeoSSE analyses in the present study aimed to robustly test the importance of the Andes & adjacent lowlands (Chocó ecoregion to the west, and western Amazonia to the east) for the species radiation of the genus *Philodendron*. The Andes are proposed to have influenced the diversification of lineages particularly diverse in both sides of the Andes in the Chocó ecoregion and western Amazon such as *Inga* (Richardson et al., 2001) and in the tribe Bignonieae (Bignoniaceae; Lohmann et al., 2013). The lowland rainforests on both sides of the Andes have accumulated the highest proportion of the species diversity of *Philodendron*. Therefore, the areas coded GeoSSE analyses differ from the operational areas in the biogeographic analysis (see Figure 3.2 for details). According to our results, lineages of *Philodendron* distributed in the rainforests of the Andes & adjacent lowlands have experienced higher speciation and dispersal rates but similar extinction rates as lineages distributed in other regions of the Neotropics (Figure 3.3). The episodic surface uplift of the Andes is a driver of speciation, extinction and dispersal especially for high altitude Andean lineages such as bellflowers (Lagomarsino et al., 2016), and orchids (Pérez-Escobar et al., 2017). The genus *Philodendron* represents an exceptional group because, in contrast to other diverse plant lineages studied in the Neotropics, it is particularly diverse outside of the Andes in the lowland rainforests of the Chocó ecoregion and western Amazonia adjacent to the Andes, rather than in higher altitudes within the Andes. We reveal the indirect impact of the Andean uplift on the development of extremely humid lowland rainforests that, in *Philodendron*, likely facilitated the higher diversification rates in the Andes & adjacent lowlands compared to other areas.

Many lineages in Neotropical rainforests do not show geographical phylogenetic structure (geographical proximity among closely related lineages; Pennington et al., 2006b), such as in the woody genera *Clusia* L., *Guatteria* and *Inga* (Hughes et al., 2013). However, with the exception of the clades recovered within subgenus *Pteromischum* and clade 1 of subgenus *Philodendron* (Figures 3.1, 3.2), clades within subgenus *Philodendron* are in fact geographically defined (i.e. clades 11 and 12 mainly distributed in the Chocó ecoregion and Central America, respectively; Figures. 3.1, 3.2). In contrast to the diversification process of other species-rich Neotropical lineages distributed across the rainforests such as *Inga* (30% of the species originated during the last 2 Ma; Richardson et al., 2001), the stem and crown ages

of the clades of *Philodendron* predate the Pliocene, a period which corresponds to the most intense phase of surface uplift in the northern Andes (reaching elevations above ~2,500 m; Gregory-Wodzicki, 2000). Sympatry is common in *Philodendron*, in particular in the rainforests of the Chocó ecoregion and the westernmost part of the Amazon basin. For, example Croat et al. (2016) identified a total of 69 species of *Philodendron* (11 in subgenus *Pteromischum* and 58 in subgenus *Philodendron*) continually distributed between Lita and San Lorenzo (~50 km apart) in Esmeraldas Province - Ecuador. Kreft et al. (2004) found 30 species of *Philodendron* within an area of 650 ha in the Amazonian rainforest of Yasuní in Orellana Province (Ecuador); and within a plot of only 0.1 ha; they found the striking number of 25 *Philodendron* species (Köster and Kreft, unpublished data). It is notable that, although closely related species co-occur, hybridization between species of *Philodendron* is not common (Croat, unpublised data; Köster, unpublised data). Therefore, recently diverged *Philodendron* species appear to have developed reproductive barriers. Investigation into the drivers of reproductive isolation between recently diverges lineages would be highly valuable for understanding the origins of the high species diversity and endemism in *Philodendron*. Although more riguorous analyses would be required, it is likely that the diversification process of *Philodendron* clades geographically structured resembles the diversification process proposed by Pennington et al. (2006b; 2009; 2015) for lineages predominantly distributed in the SDTFs. Among others, the increased elevations of the Andes might have represented a critical geographical barrier that restricted the migration of species and therefore, the clades have diversified in areas geographically confined over time.

Increasing the taxon sampling density in particular in the clades comprising vines (subgenus *Pteromischum*), and terrestrial species (subgenus *Meconostigma*) of *Philodendron* would benefit the investigation of the role of the biotic drivers of the species diversification process in the entire genus (e.g., life form). For example, clades of lianas of the tribe Bignonieae (Bignoniaceae) tend to have wider geographical distributions than other plant groups in the Neotropics (Hughes et al., 2013; Lohmann et al., 2013). This is in line with the fact that the most widespread species of subgenus *Philodendron* also tend to be vines [e.g., *P. acutatum* Schott, *P. fragrantissimum* (Hook.) G. Don, *P. hederaceum* (Jacq.) Schott and *P. jacquinii* Schott].

3.5.6. The Caribbean islands in the geographic range expansion of *Philodendron*

Adjacent land masses of Mexico, Central and South America are proposed to be the main source of plant and animal lineages for the Caribbean islands (Iturralde-Vinent and Macphee, 1999; Santiago-Valentín and Olmstead, 2004). Dispersal from South America is primary explained by the preexistence of a land connection (Aves Ridge) between the Greater Antilles (Cuba, Hispaniola and Puerto Rico) and South America during the Eocene-Oligocene transition ~34 mya (GAARlandia model; Iturralde-Vinent and MacPhee, 1999). In contrast, migrations from Central America are explained by oversea dispersals from the Oligocene-Miocene transition onwards (Cervantes et al., 2016; Nieto-Blázquez et al., 2017). In *Philodendron*, multiple independent oversea dispersal events (overwater or animal dispersion might be advocated) from the late Miocene onwards were inferred out of Central America, the Chocó & Andes region and Amazonia to the Caribbean (Figure 3.2). The earliest dispersal event to the Caribbean islands is estimated ~7 mya (*P. consanguineum* Schott; 95% HPD = 4.22-11.45; Figure 3.2), although the most intense period of the geographic range expansion from South America to the Caribbean islands started not earlier than the early Pliocene ~4 mya (Figure 3.2). This took place, however, in the form of many independent dispersal events, without any notable significant subsequent radiation of a monophyletic Caribbean *Philodendron* lineage on the islands. Further research into the special genetic structure within more widespread species may shed light on migration routes.

The Caribbean islands harbor 19 *Philodendron* taxa of which seven are endemic to the islands [e.g, *P. consanguineum, P. dussii* Engl., *P. giganteum* Schott, *P. lacerum* (Jacq.) Schott, *P. lingulatum* (L.) K. Koch, *P. schottii* K. Koch ssp. *schottii* and *P. simmondsii* Mayo; Acevedo-Rodríguez & Strong, 2012; Govaerts et al., 2018]. The remaining species are also widely distributed in continental America [e.g., *P. fragrantissimum* (Hook.) G. Don, *P. hederaceum* (Jacq.) Schott, *P. jacquinii* Schott and *P. tripartitum* (Jacq.) Schott; Croat, 1997]. Widely distributed species are estimated to have originated either in the middle Miocene (e.g., *P. jacquinii* and *P. hederaceum*, Figure 3.2) or more recently from the early Pliocene on (e.g., *P. fragrantissimum;* Figure 3.2). Our data, however, do not allow for estimating their time of arrival on the islands. Although an extensive revision of the reproductive biology of the species of *Philodendron* remains to be achieved, the recurrent geographic range expansion of widely distributed species from South America to the Caribbean islands might be associated

with the existence of advantages in their reproductive biology. Phenological observations in subgenus *Philodendron* in Central America, for example, indicate that widespread species tend to have longer flowering periods (Croat, 1997).

For the 11 species that occur in the Caribbean and included in our analyses [e.g., *P. acutatum, P. consanguineum, P. fendleri* K. Krause, *P. fragrantissimum, P. giganteum, P. hederaceum, P. jacquinii, P. krugii* Engl., *P. megalophyllum* Schott, *P. ornatum* Schott, and *P. simsii* (Hook.) Kunt], the closest relatives occur in South America. Furthermore, the biogeographic ranges, for the ancestral nodes of those clades that contain Caribbean and South American species, are estimated as either Amazonia or the Chocó ecoregion. This gives evidence of dispersal events from the northern coast of South America to the Caribbean islands. In many of these cases, dispersal took place only as far as to the rainforests of Trinidad (e.g., *P. acutatum, P. fendleri, P. krugii, P. ornatum* and *P. simsii*) or the Lesser Antilles (e.g., *P. giganteum* and *P. megalophyllum*). Two species (e.g., *P. lacerum* and *P. tripartitum*) have their closest relatives in Central America and/or the Chocó & Andes region, arguing for dispersal events from these areas directly to the Greater Antilles. It is likely that *P. subincisum* Schott represents an isolated case of recolonization of the Central American mainland by a Caribbean lineage. However, Croat (1997) has proposed a hybrid origin for this taxon, which would possibly involve *P. giganteum* as one parent (compare Figure 3.2). Therefore, interpretation of this result should be taken with caution.

Seasonally Dry Tropical Forests (SDTFs) are one of the most characteristic biomes in southeast Brazil and the Caribbean coasts of Colombia and Venezuela also occurring in the islands of Cuba, Hispaniola, Puerto Rico and Jamaica and the Lesser Antilles (Pennington et al., 2006b). Therefore, the geographic range expansion from South America to the Caribbean islands might represent another example of a habitat shift from dense rainforests to the more open SDTFs similar to the geographic range expansion of *Philodendron* subgenus *Meconostigma* from Amazonia into habitats of the Dry Diagonal of southeast Brazil. We hypothesize that, for several vine species in the SDTFs of the Greater Antilles (e.g., *P. consanguineum, P. hederaceum, P. jacquinii* and *P. lacerum*), this habitat shift might have occurred in the SDTFs of the northern coast of Colombia and Venezuela pre-dating the dispersal to the Caribbean islands.

3.5.7. Episodic geographic range expansion into Central America

From the Miocene-Pliocene transition onwards, lineages of subgenera *Philodendron* and *Pteromischum* experienced geographic range expansion from the Chocó & Andes region to Central America (Figure 3.2). Although contrasting ages have been proposed for the closure of the Isthmus of Panama (~23-7 mya; Bacon et al., 2015; and ~2.8 mya; O'Dea et al., 2016), our study supports the earlier closure documented by Bacon et al. (2015) and recently supported by Jaramillo et al. (2017). Within subgenus *Philodendron*, the most recently diverged clades (clades 11 and 12; crown ages ~6 Ma; Figure 3.2) comprise species restricted to the Chocó ecoregion in Colombia and/or Central America, respectively. Therefore, the Chocó ecoregion is the main source for lineages of *Philodendron* inhabiting Central America. Another example of episodic dispersal from South America to Central America was found in the species radiation process of the genus *Bernardia* Houst. ex Mill. ~13 mya (Cervantes et al., 2016).

Within subgenus *Philodendron,* ~100 species inhabit Central America (Croat, 1997), whilst only 16 species occur in the Caribbean islands (Acevedo-Rodríguez and Strong, 2012; Govaerts et al., 2018). In contrast to a probable habitat shift during the colonization of the Caribbean islands (from dense rainforests to open SDTFs), it is likely that rainforest lineages of *Philodendron* in western Colombia have experienced dispersal to similar habitats in Central America. Similarly, rainforest clades in the genera *Guarea* and *Trichilia* (Meliaceae) experienced significantly higher speciation rates compared to non-rainforest lineages (Koenen et al., 2015).

3.5.8. From the Andes and Chocó ecoregion back to Amazonia

In contrast to the earliest dispersal pathway from Amazonia to the Chocó & Andes region ~12 mya during the middle Miocene (Figure 3.2), *Philodendron* also shows dispersal back from the Andes to western Amazonia ~4 mya. Evidence of a recent dispersal from the Chocó & Andes region to Amazonia is found within clade 10 and the clade consisting of the species *P. asplundii* Croat & M. L. Soares and *P. juninense* Engl., both within subgenus *Philodendron*. Within clade 9, species distributed in western Amazonia (e.g., *P. mamei* André, *P. nangaritense* Croat and *P. pastazanum* K. Krause) are estimated to have an Andean ancestor (Figure 3.2). The surface uplift of the northern Andes during the Miocene-Pliocene

transition has promoted speciation in western Amazonia in the genus *Inga* (Richardson et al., 2001), in the extra-Andean tribe Bignonieae (Bignoniaceae; Lohmann et al., 2013), and the tribe Cinchoneae (Rubiaceae; Antonelli et al., 2009). For vascular epiphytes, it has been shown that predominantly Andean taxa tend to extend their ranges into the most humid parts of the western Amazon basin (Kreft et al., 2004). Accordingly, *Philodendron* lineages adapted to the extraordinarily high precipitation in the Chocó & Andes region might have been able to recolonize the perhumid lowlands of western Amazonia. Thus, the dispersal from the Chocó & Andes region to Amazonia in subgenus *Philodendron* confirms that Amazonian lowland diversity is a combination of both old and more recently originated lineages from ~40-6 mya (Hoorn et al., 2010; Antonelli et al., 2018).

3.6. Conclusions

The expanded taxon sampling across the entire geographic range of *Philodendron* in the Neotropics enabled the most comprehensive phylogenetic hypothesis for this genus to date. Based on the phylogenetic relationships recovered here, we confirm the monophyly of *Philodendron*, *Adelonema* and *Homalomena*. Within *Philodendron*, our study contributes a set of relationships among the three subgenera *Meconostigma*, *Philodendron* and *Pteromischum* that have recently been debated. Based on the time-calibrated phylogenetic tree and the biogeographic analysis, we found that the evolution of *Philodendron* is highly congruent with the main geological changes in the Neotropics during the last 30 Ma. We conclude that *Philodendron* originated and underwent the earliest diversification events in the pan-Amazonia landscapes ~29-25 mya. From the middle Miocene onwards, the genus *Philodendron* underwent multiple geographic range expansion events from Amazonia to southeast Brazil and the Chocó & Andes region. From the Pliocene onwards, *Philodendron* reached Central America and the Caribbean islands. During the same period of time, lineages distributed in the Chocó & Andes region underwent dispersal back to Amazonia. The diversification process of *Philodendron* occurs simultaneously with the species radiation of other species-rich plant lineages distributed in the Neotropical rainforests including trees, understory shrubs, lianas and epiphytes. According to the speciation, extinction and dispersal rate analyses the Andes and the adjacent lowlands (including the Chocó ecoregion and western Amazonia) have higher speciation and dispersal rates than all other regions combined. Therefore, our study shows how the Andean uplift indirect facilitated the

diversification of *Philodendron* in the Andes and adjacent lowlands through the development of perhumid lowland rainforests. Interestingly, *Philodendron* lineages have undergone various species radiations in almost all of the geographical areas, except for the Caribbean islands, in which current species diversity of *Philodendron* was built up completely by multiple and independent colonization events.

"Nennt man überhaupt Gattung, den Inbegriff der Merkmale mehrer, unter einander verwandter Arten; so vergesse man nicht dabei zu bemerken, dass diese, so wie überhaupt alle systematischen Eintheilungen, keinen andern Zwekk haben, als die große Menge der natürlichen Körper leichter übersehn zu können, oder uns eine dauerendere Kenntniss von denselben, nach gewissen Merkmalen, leichter zu verschaffen. Diesem Zwekke gemäß muss man bei Errichtung einer neuen Gattung verfahren: die Anzahl der Gattungen in einem Systeme muss nicht zu groß sein; aber es müssen auch nicht zu viele Arten unter einem gemeinschaftlichen Begriffe zusammengedrängt sein. In beiden Fällen wird der Zwekk, einen gegebenen Körper mit andern, deren man sich sogleich wieder erinnert, zu einem Begriffe zu vereinigen, oder ihn zu erkennen, verfehlt."

"With regard to the genus, the quintessence of the characters of related species, one should not forget that this like all other systematic divisions has no purpose other than to make the plethora of natural entities easier to survey or to provide us with an enduring knowledge of them according to certain characters. The erection of new genera has to be carried out according to this purpose: the number of genera within a system must not be too large but neither must there be too many species crowded under a common term. In both cases, the purpose – to unite a given entity with others that are readily recognized under one term – will be missed."

Jacob Christian Gustav Karsten (1781–1866)

Chapter 4. Insights into the morphological character evolution of *Philodendron*

4.1. Summary

In the aroids, *Philodendron* is one of the most morphologically diverse genera in terms of growth patterns and leaf morphology. Morphological and anatomical characters have been used for the recognition of three subgenera within *Philodendron: Meconostigma, Philodendron* and *Pteromischum*. The origin and evolution of the morphological diversity of *Philodendron* have not been studied yet. We inferred the ancestral character-state of five morphological characters of *Philodendron* including growth form in adult plants, persistence of cataphylls, blade shape, number of locules per ovary and number of ovules per locule using BayesTraits and taking into account a recent comprehensive species-level phylogenetic tree which comprises one third of the species diversity of the genus and includes representatives of the three subgenera and the sections recognized. Character-state inferences reveal that *Philodendron* is an ancestrally climbing lineage, without cataphylls, with cordate blades, few locules per ovary and many ovules per locule. In contrast to clades recovered within subgenera *Meconostigma* and *Pteromischum*, major clades within subgenus *Philodendron* are morphologically diverse. Clades morphologically diverse are common in other recent Neotropical plant lineages that have experienced higher diversification rates.

4.2. Introduction

The genus *Philodendron* is one of the most characteristic components of the Neotropical rainforests ranging from tropical Mexico to southern Brazil, and the Caribbean islands (Mayo, 1990; Grayum, 1996; Croat, 1997). However, the adjacent lowland of both sides of the northern Andes harbor the largest proportion of its species diversity (e.g., the Chocó ecoregion and western Amazonia; Mayo, 1990; Croat, 1997). With 558 accepted species and estimated above 700-1,000 species (Govaerts et al., 2018), *Philodendron* is the second largest genus in the family Araceae after *Anthurium* with 1,041 accepted (Govaerts et al., 2018) and ~2,000 estimated species (Boyce and Croat, 2018). The species-level

phylogenetic trees by Canal et al. (2018) based on a combination of three plastid DNA markers (*petD, rpl16* and *trnK/matK*) and ~20% of the species diversity, and by Vasconcelos et al. (2018) based on a combination of plastid (*atpF-atpH, rpl32-trnL, trnQ-5'-rps16* and *trnV-ndhC*) and ribosomal (ITS2) nuclear DNA markers and ~23% of the species diversity, have consistently confirmed the monophyly of *Philodendron*. The genus *Philodendron* originated in the late Oligocene ~29 mya and diversified more recently from the middle Miocene ~12 mya onwards (Canal et al., 2018).

In the aroids, *Philodendron* is one of the most morphologically diverse genera in terms of growth patterns and leaf morphology. Growth patterns include terrestrials, vines and most commonly hemiepiphytes, and epiphytes (Croat, 1997). Leaf shape ranges from entire (from linear to cordate or sagittate), and variously lobed (trilobed and palmately-lobed) to compound (trisect and palmately-compound) leaves (Croat, 1997). Inflorescences vary from 1 to >10 per axil. The spathe is highly variable in terms of shape and colors; however, the secretion of resin from its inner surface is characteristic to *Philodendron* and unique among the aroids (Croat, 1997). The spadix includes the proximal pistillate zone separated from the fertile staminate zone by a well-differentiated sterile staminate, and usually contained inside the spathe at anthesis. Floral morphology is highly diverse with the ovary divided in two to many (47) separate locules and the number of ovules per locule ranges from one to many (>30) with axile or basal placentation. Morphological and anatomical characters were used for the recognition of three subgenera within *Philodendron* (*Meconostigma, Pteromischum* and *Philodendron*; Engler, 1899; Mayo, 1989; Grayum, 1996; Croat, 1997). Subgenus *Meconostigma* (recently recognized as genus *Thaumatophyllum*; Sakuragui et al., 2018; Vasconcelos et al., 2018), includes 21 species characterized by the arborescent habit, conspicuous petiole scars, a well-developed sterile intermediate zone in the inflorescence equal or longer than the staminate zone, and a gynoecium having stylar lobes (Mayo, 1989, 1991; Croat et al., 2016). Subgenus *Pteromischum* includes 82 species recognized by usually scandent habit, slender stems, with several to many leaves terminated by a solitary or several inflorescences, and leaves with extensively sheathed petioles encircling the stem at the base (Grayum, 1996). Subgenus *Philodendron* with ~460 accepted species corresponds to the most diverse subgenus both in terms of species and morphology. Species of subgenus *Philodendron* are mostly hemiepiphytes and epiphytes , and sometimes vines and terrestrial species (e.g., *Philodendron hederaceum* (Jacq.) Schott, and *Philodendron grandipes* K. Krause, respectively; Croat 1997). The species diversity of subgenus *Philodendron* is organized in ten sections primarily defined on the basis of leaf shape, blade venation patterns

and floral morphology (i.e. number of locules/ovary, ovules/locule and type of placentation; Croat, 1997; Köster and Croat, 2011): *Baursia*, *Camptogynium*, *Dolichogynium*, *Macrobelium*, *Macrogynium*, *Philodendron*, *Philopsammos*, *Polytomium*, *Schizophyllum*, and *Tritomophyllum*. However, recent phylogenetic studies indicate that these sections are non-monophyletic (Canal et al., 2018; Vasconcelos et al., 2018).

The origin and evolution of the extraordinary morphological diversity of *Philodendron* have not been studied yet. Therefore, we aim to [1] infer the ancestral character-state of five morphological characters of *Philodendron* including growth form in adult plants, persistence of cataphylls, blade shape, number of locules/ovary, and number of ovules/locule using BayesTraits and taking into account a recent comprehensive species-level phylogenetic tree which comprises one third of the species diversity of *Philodendron* and [2] compare the results obtained with the morphological evolution of other Neotropical plant lineages.

4.3. Material and Methods

4.3.1. Phylogenetic framework

Phylogenetic analyses were conducted using the species of the genera *Adelonema* and *Philodendron* included in the alignment of three plastid DNA regions (*petD, rpl16***,** and *trnK/matK*) used for inferences of geographic range evolution of *Philodendron* (see material and methods in Chapter 3 of this document). Final matrix includes 166 taxa (162 of *Philodendron* and four of *Adelonema*) and a total of 5,002 aligned nucleotides (998 for *petD*, 1,149 for *rpl16* and 2,855 for *trnK/matK*) and 148 indels coded as binary characters following Simmons and Ochoterena (2000). The combined matrix of three non-coding plastid DNA regions was reanalyzed using Bayesian inference (BI) in MrBayes version 3.2.6 (Ronquist and Huelsenbeck, 2003) following Canal et al. (2018). Clades names and numbers follow Chapter 3 of the present document.

4.3.2. Character and character-state selection

We selected morphological characters based on both their variability and importance in the infrageneric classification of *Philodendron* (Krause, 1913; Mayo, 1988, 1991; Grayum,

1996; Croat, 1997). We defined and treated morphological characters for ancestral character-state inferences as proposed by Sauquet et al. (2017). Therefore, we reconstructed the ancestral character-state of five secondary characters which are derived from five primary characters. Primary characters are transformed into secondary characters by reduction of states from discrete primary characters or from modification of continuous primary characters into discrete classes of variation (Sauquet et al., 2017). Primary characters scores were mainly obtained from the literature including taxonomic revisions and protologues and complemented with personal observations of different living collections in Europe, particularly at the Botanischer Garden und Botanisches Museum Berlin (BGBM). We included polymorphic data (two or more states co-exist in any given species) and treated inapplicable data as missing data according to Sauquet et al. (2017). The final matrix with five primary characters and their corresponding secondary characters is provided as Supplemental Data (Appendix 4.1). Primary characters and their corresponding secondary characters are described as follow: [1] *Growth form in adult plants*. Species of *Philodendron* are arborescents, terrestrials, hemiepiphytes, appressed-climbing vines, and epiphytes (Mayo, 1991; Grayum, 1996; Croat, 1997). In this study, we aimed to reduce the number of states in order to reduce the estimates of number of transitions rates from one state to another as suggested by Sauquet et al. (2017). Therefore, we identified three states for the growing form in adult plants in *Philodendron*: strictly terrestrials (i.e. horizontal creeping, shortly upright or arborescent), climbing [vertically creeping, i.e. appressed climbing (nomadic) vines or hemiepiphytes], and rosulate (very short internodes, trash-basket epiphytes). [2] *Persistence of cataphylls*. Cataphylls are defined as bract-like modified leaves which protect newly emerging leaves (Croat, 1997). Cataphylls are found in subgenus *Meconostigma* and *Philodendron* but they are missing in subgenus *Pteromischum.* Cataphylls may persist either intact or as fibers (Croat, 1997). Therefore, we identified five states: absent, deciduous (still ± green when falling off), shortly persistent (only on upper nodes), persistent ± intact, and persistent as fibers. [3] *Overall blade outline.* Adult blade outline in *Philodendron* is extremely diverse (Croat, 1997). Therefore, we aimed to reduce the number of states to only four states: narrow (with ± cuneate to truncate base including the outlines lanceolate, elliptic, oblong, ovate and obovate), cordate (with ± pronounced basal lobes including the outlines sagittate, triangular and hastate), tripartite, and multiply incised [including (bi) pinnatifid or pedate]. [4] *Number of locules/ovary,* and [5] *Number of ovules/locules*. Sections of subgenus *Philodendron* have been defined on the basis of number of locules per ovary and number of ovules per locule (Engler, 1899; Krause, 1913; Croat, 1997). In this study, we discretized

these two characters in the states used in the literature (Engler, 1899; Krause, 1913; Croat, 1997). Thus, few (1-6), and many (6-47) for number of locules/ovary and solitary, few (>1 and ≤10), and many (>10) for number of ovules/locules.

4.3.3. Ancestral character-state reconstruction

Parsimony-based, maximum likelihood and Bayesian inference methods allow reconstruction of ancestral states. However, Bayesian methods enable the inference of character evolution while simultaneously accounting for phylogenetic, transition rate and model uncertainty (Pagel et al., 2004; Pagel and Meade, 2006). Therefore, we estimated ancestral states using Bayesian approach in BayesTraits version 2.0 (Pagel et al., 2004; Pagel and Meade, 2006). We produce a maximum clade credibility tree (MCCT) using the distribution of trees obtained in the four t.files from the BI analysis after discarding the first 25% of the trees as a burn-in in the program TreeAnnotator version 1.8.4 (Bouckaert et al., 2014). We inferred the probable ancestral state for the stem and crown node of *Philodendron*, its three subgenera and the clades named by Canal et al. (2018). We generated a command line for the inference of the ancestral character-state in the program TreeGraph version 2.13.0-748 beta (Stöver and Müller, 2010) using the MrBayes 50% majority-rule consensus tree obtained in the BI analysis. We used the reversible-jump Markov chain Monte Carlo (rj-MCMC) approach to integrate phylogenetic uncertainty as well as the uncertainty in the estimate of ancestral state and model parameters. This approach is particularly recommended for ancestral state inferences of multistate discrete characters (Sauquet et al., 2017). Each rj-MCMC analysis was run with an exponential hyperprior (mean on a uniform interval from 0 to 1) to reduce model uncertainty and arbitrariness as performed by Sauquet et al. (2017). Analyses were conducted using MCMC 1 million generations, sampling parameters and ancestral states from the posterior every 1,000 generations and discarding the first 25% as a burn-in. Apparent stationary was checked in the program Tracer version 1.6.0 (Bouckaert et al., 2014). Probable ancestral character-states of five characters obtained were plotted on the MCCT using the option “Import BayesTraits data” in TreeGraph version 2.13.0-748 beta (Stöver and Müller, 2010).

4.4. Results

4.4.1. Phylogenetic analyses

The present study corroborates the evolutionary relationships within *Philodendron* previously obtained (Canal et al., 2018). Thus, the genus *Philodendron* consists of two main lineages, a lineage including subgenera *Meconostigma* and *Pteromischum* sister to a lineage corresponding to subgenus *Philodendron.* See Chapter 3 for a detailed discussion of discrepancies between the topology obtained in this study and the topologies obtained in other recent phylogenetic analyses conducted by Vasconcelos et al. (2018).

4.4.2. Ancestral character-state reconstruction

The inferred ancestral states of selected nodes are plotted in Figure 4.1, with BayesTraits posterior probability (BPP) values given in the Table 4.1.

Growth form in adult plants: overall, inferences on the growth form in adult plants resulted in one of the three states with the highest BPP at the stem nodes and the crown nodes of clades previously defined (Chapter 3; Table 3.1, Figure 4.1). The terrestrial state has the highest BPP for the stem node of *Philodendron* (BPP = 0.71; in Table 4.1; Figure 4.1). A first shift in the growth form was inferred at the crown node of *Philodendron* with the highest BPP at the climbing state (BPP = 0.99 in Table 4.1; Figure 4.1). After the earliest diversification event of *Philodendron* in two major lineages (one including the subgenera *Meconostigma* and *Pteromischum* and the other corresponding to subgenus *Philodendron*), the ancestral state of growth form at the stem nodes of the three subgenera are most likely to have remained climbing (BPP = 0.79, BPP = 0.79, BPP = 1.0 in Table 4.1; respectively; Figure 4.1). Subsequently, a shift from climbing to terrestrial is likely to have occurred at the crown node of subgenus *Meconostigma* (BPP = 1.0 in Table 4.1 and Figure 4.1). In contrast, crown nodes of the subgenera *Pteromischum* and *Philodendron* are more likely to have retained the climbing habit (BPP = 1.0, and PP = 0.97 in Table 4.1; respectively; Figure 4.1). Subsequently, the ancestral character-state of the stem and crown nodes of major clades within subgenus *Philodendron* are more likely to have remained climbing with a shift to

rosulate at the crown nodes of clades 2 and 3 (BPP = 0.86, and BPP = 0.95 in Table 4.1; respectively; Figure 4.1).

Persistence of cataphylls. Inferences on the persistence of cataphylls resulted in one of the five states with the highest BPP at the stem and crown nodes of the clades previously defined except for clades 1 and 3 to 5 (Table 4.1). Cataphylls are more likely to have independently originated in the subgenera *Meconostigma* and *Philodendron* after the earliest diversification event of *Philodendron* (Figure 4.1; Table 4.1). Cataphylls have remained deciduous within subgenus *Meconostigma*. In contrast, they have diversified into at least four different character-states within subgenus *Philodendron*. The ancestral character-state of cataphylls remains ambiguous at the crown node of subgenus *Philodendron* (Table 4.1; Figure 4.1). Deciduous cataphylls are more likely to have originated multiple times within subgenus *Philodendron* (see BPP of the crown nodes of clades 1, 5, 6, 7 and 12 in Table 4.1 and Figure 4.1). In contrast, persistent intact cataphylls are likely to have originated once at the crown node of clade 2 (Figure 4.1, Table 4.1). Cataphylls persistent as fibers are likely to have originated at least three times within subgenus *Philodendron* in clades 3, 8 and 9 (see crown nodes in Figure 4.1 and Table 4.1). They are also likely to evolve to shortly persistent at clades 10 and 11 (see crown nodes in Figure 4.1, Table 4.1).

Overall blade outline. Inferences on blade outline indicate that the most likely ancestral character-state is cordate at both the stem and crown nodes of *Philodendron* (BPP = 0.67 and PP = 0.76; respectively; Figure 4.1, Table 4.1). A shift from cordate blade to narrow blade is likely to have occurred at the stem node of subgenera *Meconostigma* and *Pteromischum* (Figure 4.1, Table 4.1). In contrast, cordate blade remains to be the ancestral state of blade shape at both the stem and crown nodes of subgenus *Philodendron* (Figure 4.1, Table 4.1). Whilst a shift from narrow blade to cordate blade is inferred at the crown node of subgenus *Meconostigma*, ancestral narrow blade state is likely to have remained at the crown node of subgenus *Pteromischum*. Within subgenus *Philodendron*, narrow blade shape is likely to have originated multiple times from a cordate ancestor (clades 3, 6 and 10; Figure 4.1). Character-states of overall blade outline corresponding to multiply incised is more likely to have originated once at the crown node of clade 5 from an ancestrally cordate blade lineage (Figure 4.1). In addition, multiply incised and tripartite blades are likely to have arisen recently multiple times across subgenus *Philodendron* (Figure 4.1).

Locules/Ovary. The most recent common ancestor of *Philodendron* is inferred to have had few locules per ovary (see BPP of the stem and crown nodes in Table 4.1 and Figure 4.1). A first shift from few locules per ovary (1-6) to many locules per ovary (6-47) is likely to

have occurred at the crown node of subgenus *Meconostigma* (Figure 4.1, Table 4.1). Likewise, a shift from few locules per ovary to many locules per ovary is likely to have occurred at the node containing clades 2-12 within subgenus *Philodendron* (Figure 4.1, Table 4.1). Subsequently, a shift from few locules per ovary to many locules per ovary has occurred independently at the crown node of clade 3 and the base of the node including clades 6-12 (Figure 4.1). A shift from locules per ovary many locules to few locules per ovary is inferred to have occurred at the crown nodes of clades 9 and 12 (Figure 4.1, Table 4.1).

Ovules/Locule. The most recent common ancestor of *Philodendron* is more likely to have had many ovules per locule (see BPP of the stem and crown nodes in Table 4.1 and Figure 4.1). Subsequently, a first shift from many ovules per locule (>10) to few ovules per locule (>1 and $\leq$10) is likely to have occurred at the crown node of subgenus *Meconostigma* (see BPP at the Table 4.1; Figure 4.1). Likewise, a shift from many to few ovules per locule is inferred at the node including clades 1-12 within subgenus *Philodendron*. Subsequently, a shift from few to many ovules per locule is inferred at the node including clades 6-12 (Figure 4.1, Table 4.1). Another shift from many to few ovules per locule is likely to have occurred at the node containing clades 11 and 12 (Figure 4.1, Table 4.1).

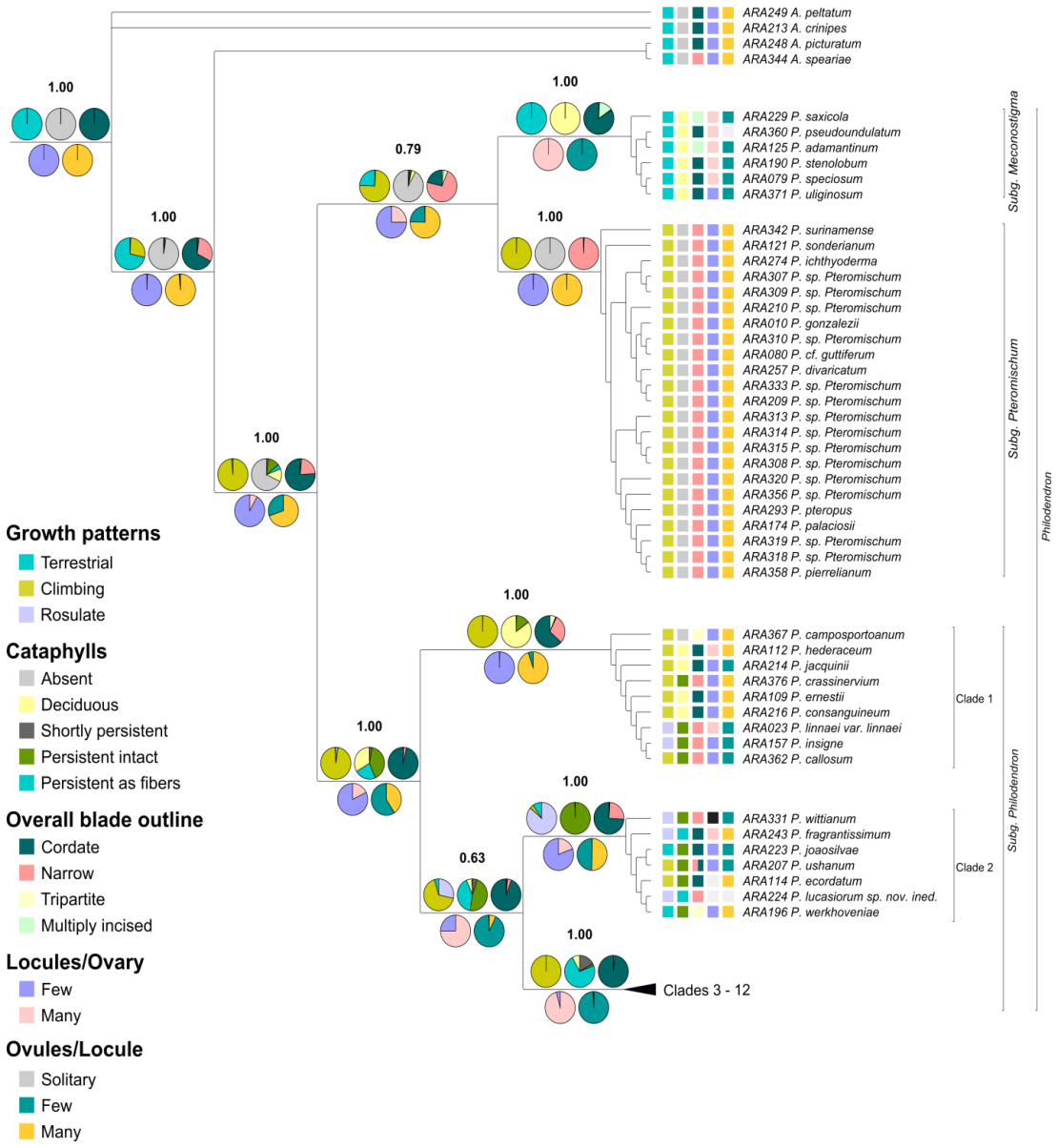

Figure 4.1. (a-c) Bayesian inference of ancestral character-state reconstruction of five morphological characters of *Philodendron* plotted in the maximum clade credibility tree with Bayesian posterior probabilities (PP) above branches. Reconstructed ancestral character-state are represented as pie charts at the stem and crown nodes of major clades within *Philodendron* including the three subgenera *Meconostigma*, *Philodendron* and *Pteromischum* and the 12 clades identified by Canal et al. (2018). For BayesianTraits posterior probabilities (BPP) of each node refer to Table 4.1. Pie charts above branches correspond to growth form in adult plants (left), persistence of cataphylls (middle), and overall blade outline (right). Pie charts below branches correspond to locules/ovary (left) and ovules/locule (right). The corresponding states of each character are indicated in the legend. Squares indicate species character-state. Light grey squares before species names indicate missing data and black squares correspond to unknown character-state.

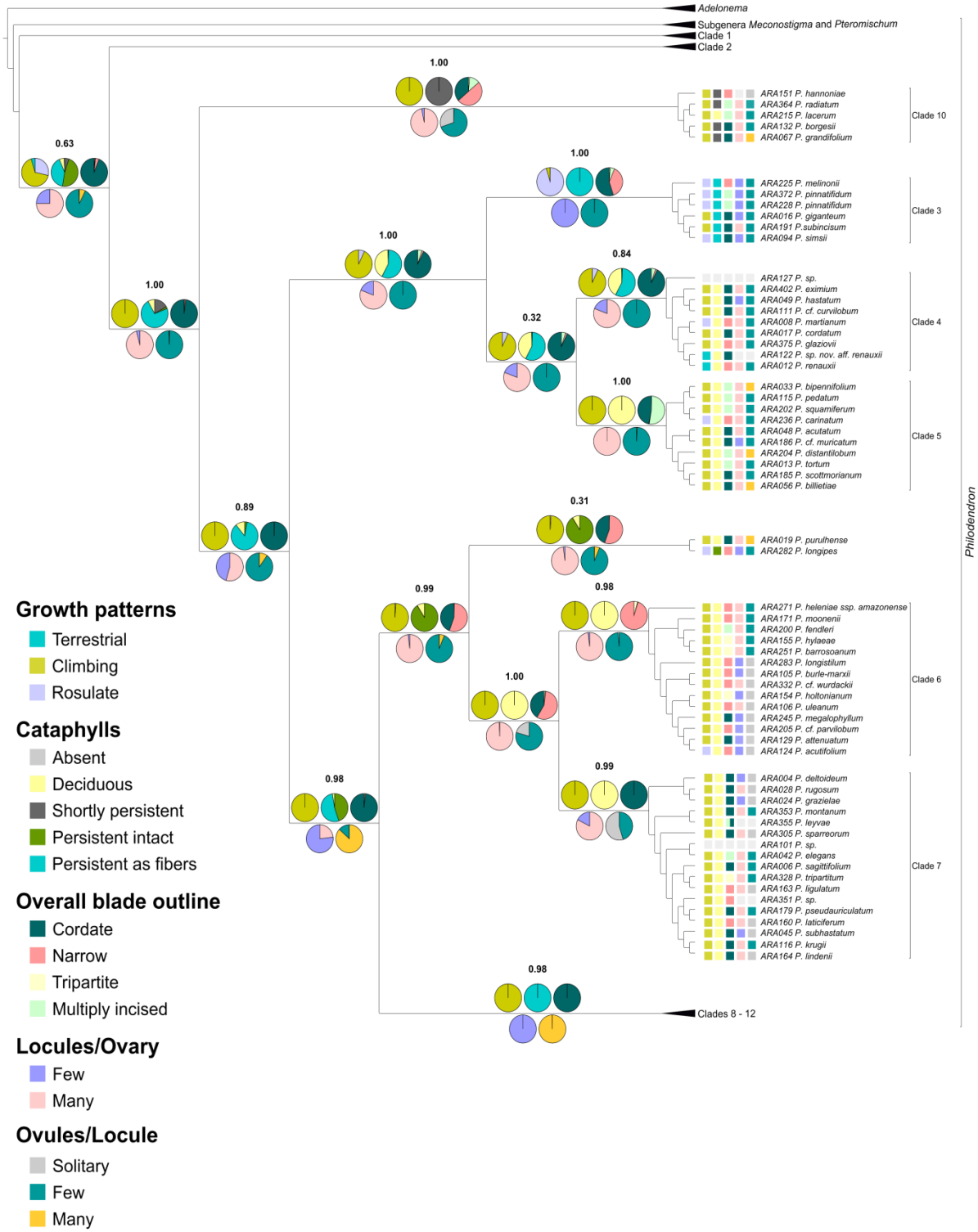

Figure 4.1. (b, continued)

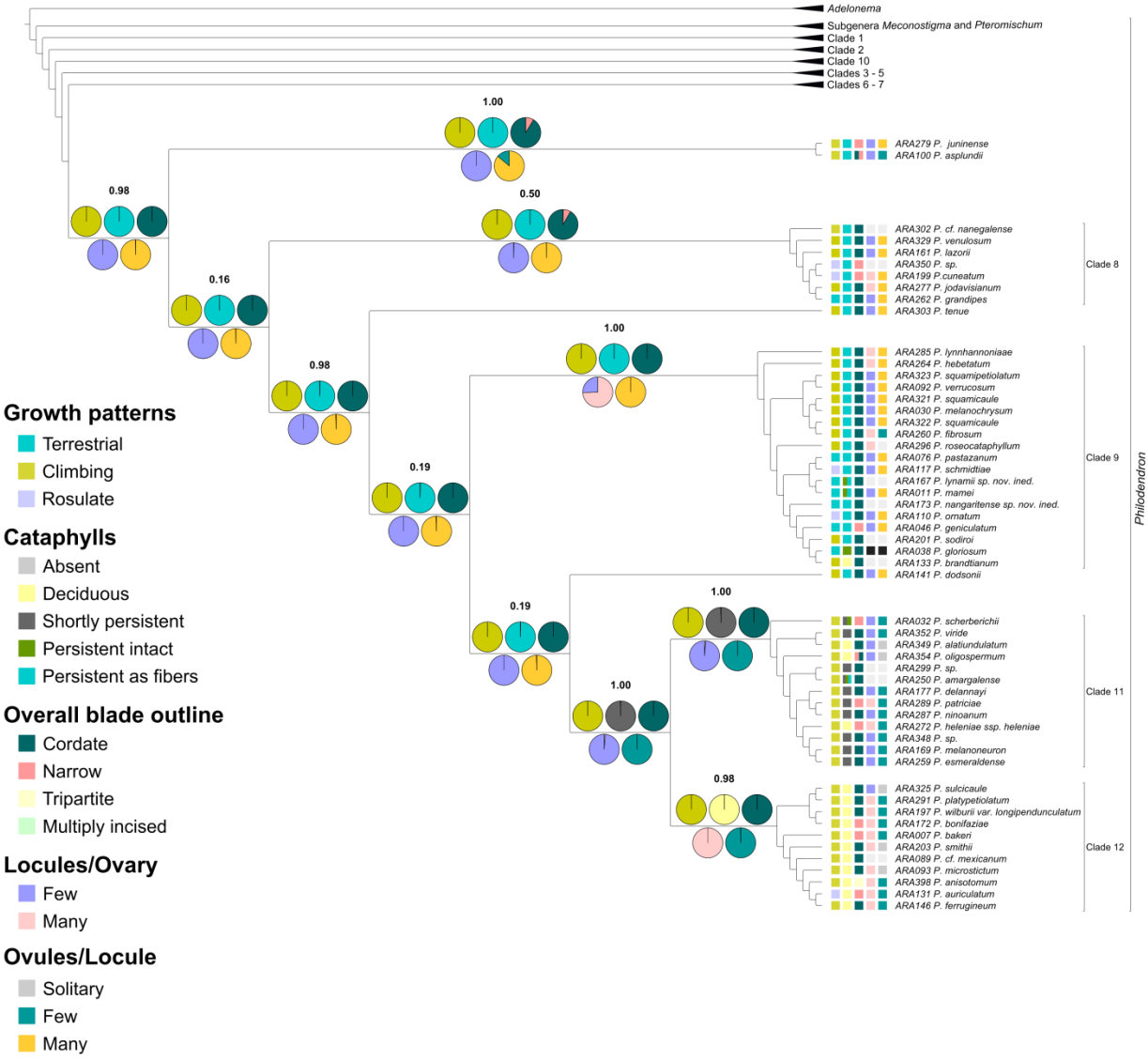

Figure 4.1. (c, continued)

Table 4.1. (next page) BayesTraits posterior probabilities (BPP) of the ancestral character-state of five morphological characters in *Philodendron* at nodes previously selected using BayesTraits version 2.0. Growth form in adult plants: C, climbing; R, rosulate; T, terrestrial. Persistence of cataphylls: A, absent; D, deciduous; Pf, persistent as fibers; Pi, persistent intact; Ps, shortly persistent. Overall blade outline: Co, cordate; Na, narrow; Mu, multiply incised; Tr, tripartite. Locules/Ovary: F, few; M, many. Ovules/Locule: F, few; M, many; S, solitary; C, crown node; S, stem node; PP, Bayesian posterior probability.

Clade	Node	PP	Growth form in adult plants			Persistence of cataphylls					Overall blade outline				Locules/Ovary		Ovules/Locule		
			C	R	T	A	D	Pf	Pi	Ps	Co	Mu	Na	Tr	F	M	S	F	M
Philodendron	S	1.00	0.28	0.01	0.71	0.98	0.01	0	0.01	0.01	0.67	0	0.31	0	1.00	0	0	0.01	0.99
	C	1.00	0.99	0	0.01	0.68	0.13	0.05	0.12	0.02	0.76	0.01	0.22	0	0.92	0.08	0	0.30	0.70
Subg. *Meconostigma*	S	0.77	0.79	0.01	0.24	0.92	0.04	0	0	0.01	0.72	0.05	0.21	0.01	0.75	0.25	0	0.24	0.75
	C	1.00	0	0	1.00	0	1.00	0	0	0	0.84	0.15	0.01	0.01	0	1.00	0	1.00	0
Subg. *Pteromischum*	S	0.77	0.79	0.01	0.24	0.92	0.04	0	0	0.01	0.21	0.05	0.72	0.01	0.75	0.25	0	0.24	0.75
	C	1.00	1.00	0	0	1.00	0	0	0	0	0.01	0	0.99	0	1.00	0	0	0	1.00
Subg. *Philodendron*	S	1.00	1.00	0	0	0.68	0.13	0.05	0.12	0.02	0.76	0	0.22	0.01	0.92	0.08	0	0.30	0.70
	C	1.00	0.97	0.02	0	0	0.33	0.23	0.41	0.03	0.96	0	0.03	0	0.82	0.18	0	0.59	0.41
Clade 1	S	1.00	0.97	0.02	0	0	0.33	0.23	0.41	0.03	0.63	0.01	0.29	0.06	0.82	0.18	0	0.59	0.41
	C	1.00	1.00	0	0	0	0.85	0	0.15	0	0.94	0.01	0.04	0.01	1.00	0	0	0.05	0.95
Clade 2	S	0.63	0.67	0.29	0.05	0.01	0.06	0.41	0.47	0.05	0.94	0.01	0.04	0.01	0.25	0.75	0	0.92	0.07
	C	1.00	0.04	0.86	0.10	0	0	0.01	0.99	0	0.74	0.01	0.25	0.01	0.81	0.19	0	0.49	0.51
Clade 3	S	1.00	0.93	0.07	0	0	0.42	0.57	0	0	0.93	0	0.02	0.05	0.19	0.81	0	1.00	0
	C	1.00	0.05	0.95	0	0	0	1.00	0	0	0.55	0.05	0.39	0.01	1.00	0	0	1.00	0
Clade 4	S	0.32	0.93	0.07	0	0	0.42	0.57	0	0	0.93	0	0.02	0.05	0.19	0.81	0	1.00	0
	C	0.84	0.93	0.07	0	0	0.42	0.57	0	0	0.93	0	0.02	0.05	0.19	0.81	0	1.00	0
Clade 5	S	0.32	0.93	0.07	0	0	0.42	0.57	0	0	0.93	0	0.02	0.05	0.19	0.81	0	1.00	0
	C	1.00	1.00	0	0	0	1.00	0	0	0	0.47	0.52	0.01	0	0	1.00	0	0.99	0.01
Clade 6	S	1.00	1.00	0	0	0	1.00	0	0	0	0.41	0	0.57	0.01	0.01	0.99	0.55	0.45	0
	C	0.98	1.00	0	0	0	1.00	0	0	0	0	0	0.95	0.04	0.02	0.98	0	0.99	0.01
Clade 7	S	1.00	1.00	0	0	0	1.00	0	0	0	0.41	0	0.57	0.01	0.01	0.99	0.21	0.79	0
	C	0.99	1.00	0	0	0	1.00	0	0	0	0	0	1.00	0	0.17	0.83	0.55	0.45	0
Clade 8	S	0.16	1.00	0	0	0	0	1.00	0	0	1.00	0	0	0	1.00	0	0	0	1.00
	C	0.50	1.00	0	0	0	0	1.00	0	0	0.92	0	0.08	0	1.00	0	0	0	1.00
Clade 9	S	0.19	1.00	0	0	0	0	1.00	0	0	1.00	0	0	0	1.00	0	0.01	0.99	0
	C	1.00	1.00	0	0	0	0	1.00	0	0	1.00	0	0	0	0.26	0.74	0	0	1.00
Clade 10	S	0.63	1.00	0	0	0	0.08	0.73	0.02	0.17	0.98	0	0.01	0	0.04	0.96	0.01	0.99	0
	C	1.00	1.00	0	0	0	0	0	0	1.00	0.36	0.13	0.50	0.01	0.03	0.97	0.30	0.69	0
Clade 11	S	1.00	1.00	0	0	0	0	0	0	1.00	1.00	0	0	0	0.99	0.01	0	1.00	0
	C	1.00	1.00	0	0	0	0	0	0	1.00	1.00	0	0	0	0.99	0.01	0	1.00	0
Clade 12	S	1.00	1.00	0	0	0	0	0	0	1.00	1.00	0	0	0	0.99	0.01	0	1.00	0
	C	0.98	1.00	0	0	0	1.00	0	0	0	1.00	0	0	0	0	1.00	0	1.00	0

4.5. Discussion

4.5.1. Ancestral character-state reconstruction in *Philodendron*

The present results reveal the evolution of morphological characters traditionally used in the taxonomic delimitation of *Philodendron*. Character-state inferences reveal that *Philodendron* is an ancestrally climbing lineage, without cataphylls, with cordate blades, few locules per ovary and many ovules per locule. Within *Philodendron*, subgenus *Pteromischum* retains plesiomorphic states. In contrast, subgenera *Meconostigma* and *Philodendron* have accumulated derived states. Within subgenus *Philodendron*, major clades are morphologically diverse. This might be associated with the comparatively recent and faster diversification process of subgenus *Philodendron* (Canal et al., 2018), a common feature of other Neotropical plant lineages such as *Costus* (Kay et al, 2005) and *Inga* (Richardson et al., 2001). Since the evolutionary relationships among the three subgenera remain unclear as indicated by the low statistical support at the backbone of the phylogenetic tree, interpretation of the evolutionary history of certain phenotypic characters should be made with caution.

4.5.1.1. The climbing ancestral habit and the multiple origins of other growth patterns in **Philodendron**

The BayesianTraits ancestral character-state inferences indicate that *Philodendron* is an ancestrally terrestrial lineage, which is likely to have shifted to climbing at the crown node of *Philodendron*. Subsequently, the climbing growth form is most likely to have shifted to terrestrial in the descendent lineages corresponding to subgenera *Meconostigma* and *Philodendron*. Shifts from ancestrally climbing to self-supporting descendent lineages are likely to have occurred in the family Apocynaceae (Fishbein et al., 2012), and in the genus *Aristolochia* Juss. subgenus *Isometra* (Wagner et al., 2012). In *Isometra*, this transition is proposed to be associated to biomechanical and anatomical shifts of the stem such as increase in diameter and stiffness (Wagner et al., 2012). Similar shifts are likely to have occurred in the transition from climbing ancestor to terrestrial descendent in *Philodendron*. However, the impact of biomechanical and anatomical properties of the stem on the evolution of *Philodendron* should be rigorously tested.

According to the results obtained in the geographic range evolution analyses (see Chapter 3), the genus *Philodendron* is most likely to have originated and diversified in the humid rainforests of the pan-Amazonian region ~29 to 24 mya. The lineage corresponding to subgenus *Meconostigma* is most likely to have colonized the seasonally dry tropical forests (SDTFs) during the late Miocene ~10 mya. Although the phylogenetic relationships among the subgenera of *Philodendron* remain unclear, the shift from climbing ancestor to terrestrial descendent within subgenus *Meconostigma* coincides with the habitat shift from the humid rainforests to dry forest of the SDTFs. However, a correlation between the growth form shift and a potential adaptation to the seasonality of the SDTFs require further analyses.

Anatomically, stems of genus *Philodendron* contain simple (subgenus *Pteromischum*) or more commonly compound vascular bundles (subgenera *Meconostigma* and *Philodendron*; Tenorio et al., 2012). Multiple bundles increase absorption and transport of water and other components. Therefore, they are thought to represent an ecological advantage in the subgenera *Meconostigma* and *Philodendron* (Tenorio et al., 2012). Although the evolution of the stem remains unknown in *Philodendron*, two evolutionary scenarios might be proposed on the basis of the present results: [1] the climbing ancestor of *Philodendron* might have simple bundles and subsequently, a shift to compound bundles occurred independently in the subgenera *Meconostigma* and *Philodendron*, and [2] compound bundles are plesiomorphic in *Philodendron* and subsequently, a shift to simple bundles occurred within subgenus *Pteromischum*. A shift from low number of bundles to more complex bundles is inferred in the character transition from climbing to shrub-like habit in the evolution of *Isometra* (Wagner et al., 2012). It is likely that similar anatomical shifts have played an important role in the evolution of *Philodendron*. However, anatomical studies are required in order to elucidate the evolution of the stem and its implications on the diversification process of *Philodendron*.

4.5.1.2. Diversification of cataphylls in the most speciose lineage of **Philodendron**

Emerging leaves are protected by cataphylls in the family Araceae and therefore, cataphylls are thought to be primitive among the aroids (Grayum, 1996). In *Philodendron*, cataphylls are not plesiomorphic and they are more likely to have independently originated in the subgenera *Meconostigma* and *Philodendron* (Figure 4.1). In contrast to the deciduous cataphylls within subgenus *Meconostigma*, cataphylls have highly diversified in subgenus *Philodendron* including shortly persistent, persistent intact or as fibers. In the present study,

the ancestor of subgenus *Philodendron* is more likely to have persisting intact cataphylls (Figure 4.1). Subsequently, cataphylls are likely to have shifted either to persistent as a fibers, deciduous or shortly persistent. Within subgenus *Philodendron,* shifts in cataphylls are inferred more commonly after the geographic range expansion event from Amazonia to the Andes ~12 mya (see Chapter 3). The rise of the Andes during the last 10 Ma is thought to have triggered the diversification process of subgenus *Philodendron* trough different mechanisms (see Chapter 3 for a detailed description). Species of subgenus *Philodendron* are more commonly hemiepiphytes and epiphytes distributed in the rainforests in the Andes and adjacent lowlands both sides of the Andes (Croat, 1997). Hemiepiphytes and epiphytes species of *Philodendron* are thought to be exposed to severe environmental conditions in the rainforests (Croat, 1997). Cataphylls protect emerging leaves from damage and desiccation and therefore, it is likely that the gain of cataphylls in subgenus *Philodendron* might be associated with the species diversification of hemiepiphytes and epiphytes within subgenus *Philodendron.*

The gain of cataphylls might be related to structural changes in the growth patterns within *Philodendron*. Studies on stem anatomy on *Philodendron* indicate that articles (growth units produced by a single meristem) are either anisophyllous or homeophyllous (Ray, 1987, 1988). In contrast to anisophyllous articles with a variable number of leaves, homeophyllous articles have fixed number of leaves from which one corresponds to a cataphyll (Grayum, 1996). While anisophyllous articles characterized subgenus *Pteromischum*, homeophyllous are presents in the subgenera *Meconostigma* and *Philodendron* (Grayum, 1996). Reconstruction of the ancestral articles might contribute to a better understating of the growth patterns and the origin and evolution of the cataphylls in *Philodendron.*

4.5.1.3. Multiple independent origins of similar blade forms within subgenus **Philodendron**

Probably no morphological feature is more diverse in the genus *Philodendron* than blade shape (Croat, 1997). Within subgenus *Philodendron,* adult blade shape is extremely diverse encompassing more morphological variation than in the subgenera *Meconostigma* and *Pteromischum* (Croat, 1997). Within subgenus *Philodendron,* multiple independent origins of the same blade forms are likely to have occurred across its major clades (e.g., narrow blades in clades 3, 6 and 10 or multiply incised blades in clades 3 to 7 and 10; Figure 4.1). Overall, the evolution of the blade shape resulted highly homoplasic within subgenus *Philodendron*. Our results do not allow us to assume any evolutionary process underlying the diversification

of blade shape within *Philodendron* (convergent evolution?; Stayton, 2015). However, in the Neotropical rainforests, it is common that clades rapidly diversified are morphologically diverse (Hughes et al., 2013). As many other lowland Neotropical plant lineages such as *Inga* (Richardson et al., 2001) and *Costus* subgenus *Costus* (Kay et al., 2005), the species radiation of subgenus *Philodendron* occurred comparatively faster than the other subgenera of *Philodendron* (Canal et al., 2018). Causes of this phylogenetic pattern remain to be rigorously assessed.

4.5.1.4. Insights into the evolution of the female flowers in Philodendron

Ancestrally, the genus *Philodendron* is inferred to have few locules per ovary (1-6). Subsequently, a shift from few to many locules per ovary (6-47) is likely to have occurred independently at the crown node of subgenus *Meconostigma* and within subgenus *Philodendron* after the divergence of clade 1 (Figure 4.1). Within subgenus *Philodendron*, a reversal from many to few locules per ovary is likely to have occurred at the crown node of clade 3 and the crown node of lineage including clades 8-12 (Figure 4.1). In contrast to the number of locules per ovary, *Philodendron* is inferred to be a lineage with many ovules per locule (>10) at both the stem and crown nodes (Figure 4.1). The plesiomorphic state has remained in the subgenus *Pteromischum*. Conversely, a shift from many to few ovules per locule (>1 to ≤10) is inferred at the crown node of subgenus *Meconostigma* and the node containing clades 2 to12 within subgenus *Philodendron* (Figure 4.1). Subsequently, solitary ovules per locule are more likely to have independently originated in the clades 6, 7, 11 and 12 from an ancestor with few ovules per locule (Figure 4.1). The present results might suggest an evolutionary reduction in the number of ovules per locule in *Philodendron*. Within subgenus *Philodendron*, not all ovules are successfully pollinated and therefore, the number of seeds is often smaller than the number of ovules per locule (Croat, 1997). Whether this reduction represents an adaptation remain to be rigorously investigated.

4.6 Conclusions

Inferences of the ancestral character-state of morphological characters traditionally used in the taxonomic circumscription of *Philodendron* (e.g., growth form in adult plants, persistence of cataphylls, overall blade outline, number of locules/ovary, and number of

ovules/locules) indicate that *Philodendron* is an ancestrally climbing lineage without cataphylls, with cordate blades, few locules per ovary and many ovules per locule. Progress in inferring ancestral character-states in *Philodendron* might benefit from the potential utility of anatomical and structural characters. In addition, further analyses on the evolution of *Philodendron* might explore the impact of the character-state shifts on speciation and extinction rates.

Chapter 5. General conclusions

5.1. Implications of the present study on the taxonomy of the genus *Philodendron*

The results obtained in the present study constitute the first well resolved and statistically supported phylogenetic hypothesis of the genus *Philodendron* including a representative sampling of its species diversity (about one third) and multiple plastid genomic regions. The phylogenetic analyses using maximum parsimony, maximum likelihood and Bayesian inference approaches have consistently recovered *Philodendron* as a monophyletic group sister to the Neotropical genus *Adelonema.*

The present studies recover the monophyly of the three subgenera *Meconostigma Pteromischum* and *Philodendron*. This result is consistent with previous phylogenetic studies conducted by Barabé et al. (2002), Gauthier et al. (2008) and Wong et al. (2016). Within subgenus *Pteromischum,* the present study supports the monophyly of the two sections recognized (sect. *Pteromischum* and sect. *Fruticosa*; Grayum, 1996). In contrast, the 12 well-supported clades recovered within subgenus *Philodendron* do not correspond to the ten sections recognized: *Baursia, Camptogynium*, *Dolichogynium*, *Macrobelium*, *Macrogynium*, *Philodendron*, *Philopsammos*, *Polytomium*, *Schizophyllum*, and *Tritomophyllum* (Croat, 1997; Köster and Croat 2011).

Taxonomists and systematists are aware of the importance of providing a natural classification for *Philodendron* (Mayo, 1986; Grayum, 1996; Croat, 1997; Barabé et al., 2002; Gauthier et al., 2008; Wong et al., 2016; Canal et al., 2018; Vasconcelos et al., 2018). The results obtained in the present study represent the largest phylogenetic tree of *Philodendron* to date and therefore, enable further studies towards a better classification of the entire genus.
Whereas the evolutionary relationships among the three subgenera of *Philodendron*: *Meconostigma*, *Philodendron* and *Pteromischum* remain unclear, their monophyly is well established. Subgenera *Meconostigma* and *Pteromischum* are morphologically well-defined (Mayo, 1991; Grayum, 1996; Calazans et al., 2014; Sakuragui et al., 2018). In contrast, the largest subgenus *Philodendron* is morphologically extremely variable and essentially defined by the absence of the morphological attributes characterizing the subgenera *Meconostigma* and *Pteromischum* (Mayo, 1989; Croat, 1997; Govaerts et al., 2018). Therefore, the

separation of these two subgenera as recently suggested by Sakuragui et al. (2018) for subgenus *Meconostigma* and Vasconcelos et al. (2018) for subgenus *Pteromischum*, would leave the remainder of the genus *Philodendron* (i.e., the current subgenus *Philodendron*) without clear morphological characters for its taxonomic delimitation.

Within subgenus *Philodendron*, the present study identified 12 well supported clades that do not correspond to the sections proposed (Croat, 1997; Köster and Croat, 2011). However, these clades allow further taxonomic and phylogenetic studies towards a natural sectional classification of the largest subgenus of *Philodendron*.

5.2. Evolution of *Philodendron* in the Neotropics

Divergence-time inferences using a Bayesian approach reveal that the genus *Philodendron* originated ~29 mya during the Oligocene and diversified most intensely during the Miocene onwards. During the same period, multiple Neotropical plant lineages distributed in the lowland rainforests diversified including trees, understory shrubs, vines, lianas and epiphytes.

Time-dependent diversification rate shifts analyses reveal that the diversification process of *Philodendron* combines elements of two traditional models used to explain the origin of the extraordinary species diversity in the Neotropics. Thus, a comparatively more recent and faster diversification process ("cradle" model in subgenus *Philodendron*) parallel to a relatively older and more constant diversification process ("museum" model in the subgenera *Meconostigma* and *Pteromischum*). Within *Philodendron*, epiphytism is found almost exclusively in subgenus *Philodendron* and its distribution resembles those found in other Neotropical plant lineages that contain vascular epiphytes such as bromeliads and orchids. Studies on bromeliads and orchids have shown that epiphytic lineages have higher net rates of diversification compared to their terrestrial relatives (Givnish et al., 2014; 2015). In the genus *Philodendron*, a diversification-rate upshift occurred after the origin of the predominantly epiphytic subgenus *Philodendron* ~12 mya and it coincides with one of the most intense periods of mountain uplift in the Andes (Gregory-Wodzicki, 2000). The potential correlation between the comparatively higher diversification rate of subgenus *Philodendron* and biotic factors such as the origin of the epiphytism or abiotic factors such as the colonization of the Andes remain to be rigorously assessed.

Ancestral range inferences using Bayesian and likelihood approaches reveal that the evolutionary history of *Philodendron* is strongly associated with the most intense period of the uplift of the Andes and the formation of the Isthmus of Panama. The genus *Philodendron* originated ~29 mya in the pan-Amazonian region (preexisting landscape corresponding to the current Chocó ecoregion, northern Andes and western Amazonia; Hoorn et al., 2010). Subsequently, the three subgenera of *Philodendron* (*Meconostigma, Philodendron* and *Pteromischum*) are likely to have originated ~24 mya. Overall, the species radiation and the current geographic distribution of *Philodendron* is the result of multiple geographic range expansion through time: from Amazonia to northwest South America and southeast Brazil from the middle Miocene, and more recently from the Chocó ecoregion to Central America and from South America to the Caribbean islands during the Miocene-Pliocene transition.

Within subgenus *Philodendron*, the geographic range expansion from Amazonia to the northern Andes coincides with a diversification-rate upshift ~12 mya. Therefore, the present study reveals that the extraordinary species radiation of subgenus *Philodendron* is associated to the colonization of the Andes. Furthermore, the geographical state-speciation and extinction model analyses demonstrate the indirect impact of the Andes on the diversification process of *Philodendron* in the adjacent lowlands both sides of the northern Andes. Thus, the rise of the northern Andes from the middle Miocene accelerated speciation and dispersal rates of *Philodendron* in the lowland rainforests of the Chocó ecoregion and western Amazonia. Causes of the comparatively higher speciation and dispersal rates founded in the adjacent lowlands of the northern Andes remain unknown. However, mountain uplift of the Andes may have triggered the diversification process of plant lineages distributed in the adjacent lowlands of the Andes by increasing precipitation and nutrient deposition (Antonelli and Sanmartín, 2011).

In contrast to the two clades obtained within subgenus *Pteromischum*, the 12 clades recovered within subgenus *Philodendron* show geographic phylogenetic structure (geographical proximity among lineages closely related; Pennington et al., 2006a). Geographic phylogenetic structure is thought to be strongly associated to the history of the biomes in the Neotropics. For example, lineages distributed in the confined seasonally dry tropical forests such as *Coursetia* DC., *Poissonia* Baill., and *Ruprechtia* C. A. Mey. tend to accumulate more endemic species and therefore, show higher geographic phylogenetic structure than lineages distributed in the comparatively larger rainforests such as *Clusia, Guatteria, Inga,* and *Renealmia* (Pennington et al., 2006a; Hughes et al., 2013). In addition, high or low geographic phylogenetic structure is thought to be associated to low or high

migration rates, respectively (Pennington et al., 2006a). While the origin and diversification processes of other plant species-rich lineages distributed in the Amazonian rainforest postdate the most intense period of the uplift of the Andes, the origin and earliest diversification of *Philodendron* predate the most intense period of the uplift of the Andes. Therefore, the contrasting higher geographic phylogenetic structure of subgenus *Philodendron* across the lowland Neotropical rainforests might be explained by the comparatively older origin of the genus in the Neotropics ~29 mya and the impact of the formation of the northern Andes and the dry diagonal in Brazil (~7-5 mya; Werneck et al., 2012) as dispersal barriers from the middle Miocene ~12 mya (Hoorn et al., 2010).

References

Acevedo-Rodríguez, P., and M. T. Strong. 2012. Catalogue of seeds plants of the West Indies. Smithsonian Contributions to Botany. Smithsonian Institution Scholarly Press. Washington, D.C. USA.

Alekseyenko, A. V., C. J. Lee, and M. A. Suchard. 2008. Wagner and Dollo: a stochastic duet by composing two parsimonious solos. *Systematic Biology* 57: 772–784.

Antonelli, A., and I. Sanmartín. 2011. Why are there so many plant species in the Neotropics? *Taxon* 60: 403-414.

Antonelli, A., J. A. A. Nylander, C. Persson, and I. Sanmartín. 2009. Tracing the impact of the Andean uplift on Neotropical plant evolution. *Proceedings of the National Academy of Sciences of the United States of America* 106: 9749-9754.

Antonelli, A., G. Zizka, F. Antunes Carvalho, R. Scharn, C. D. Bacon, D. Silvestro, and F. L. Condamine. 2018. Amazonia is the primary source of Neotropical biodiversity. *Proceedings of the National Academy of Sciences*: 1-6.

Bacon, C. D., D. Silvestro, C. Jaramillo, B. T. Smith, P. Chakrabarty, and A. Antonelli. 2015. Biological evidence supports an early and complex emergence of the Isthmus of Panama. *Proceedings of the National Academy of Sciences of the United States of America* 112: 6110–6115.

Baele, G., and P. Lemey. 2013. Bayesian evolutionary model testing in the phylogenomics era: matching model complexity with computational efficiency. *Bioinformatics* 29: 1970–1979.

Barabé, D., A. Bruneau, F. Forest, and C. Lacroix. 2002. The correlation between development of atypical bisexual flowers and phylogeny in the Aroideae (Araceae). *Plant Systematics and Evolution* 232: 1-19.

Barbosa, J. F., and C. M. Sakuragui. 2014. Taxonomy and conservation of the Brazilian extra-Amazonian species of *Philodendron* subg. *Pteromischum* (Araceae). *Phytotaxa* 191: 45-65.

Bermúdez, M. A., C. Hoorn, M. Bernet, M. Carillo, P. A. Van Der Beek, J. L. Garver, J. L. Mora, and K. Mehrkian. 2015. The detrital record of late-Miocene to Pliocene surface uplift and exhumation of the Venezuelan Andes in the Maracaibo and Barinas foreland basins. *Basin Research*: 1-26.

Borsch, T., and D. Quandt. 2009. Mutational dynamics and phylogenetic utility of noncoding chloroplast DNA. *Plant Systematics and Evolution* 282: 169-199.

Borsch, T., K. W. Hilu, D. Quandt, V. Wilde, C. Neinhuis, and W. Barthlott. 2003. Noncoding plastid *trnT-trnF* sequences reveal a well resolved phylogeny of basal angiosperms. *Journal of Evolutionary Biology* 16: 558-576.

Bouckaert, R., J. Heled, D. Kuhnert, T. Vaughan, C. H. Wu, D. Xie, M. A. Suchard, et al. 2014. BEAST 2: A software platform for Bayesian evolutionary analysis. *Plos Computational Biology* 10.

Boyce, P. C., and T. Croat. 2018. The Überlist of Araceae, totals for published and estimated number of species in aroid genera http://www.aroid.org/genera. Retrieved 30 November 2018.

Braucks Calazans, L. S., C. M. Sakuraguia, and S. J. Mayo. 2014. From open areas to forests? The evolutionary history of *Philodendron* subgenus *Meconostigma* (Araceae) using morphological data. *Flora* 209: 117–121.

Brummitt, R. K., F. Pando, S. Hollis, and N. A. Brummitt. 2001. World geographical scheme for recording plant distributions. *Hunt Institute for Botanical Documentation* Pittsburgh, PA.

Bunting, G. 1979. Sinopsis de las Araceae de Venezuela. *Revista de la Facultad de Agronomía* 10: 139-290.

Cabrera, L. I., G. A. Salazar, M. W. Chase, S. J. Mayo, J. Bogner, and P. Dávila. 2008. Phylogenetic relationships of aroids and duckweeds (Araceae) inferred from coding and noncoding plastid DNA. *American Journal of Botany* 95: 1153-1165.

Calazans, L. S. B., and C. M. Sakuragui. 2013. A new species of *Philodendron* (Araceae) and a key to Brazilian Atlantic Forest species of P. subgenus *Pteromischum*. *Phytotaxa* 94 49–55.

Calazans, L. S. B., C. M. Sakuragui, and S. J. Mayo. 2014. From open areas to forest? The evolutionary history of *Philodendron* subgenus *Meconostigma* using morphological data. *Flora* 209: 117–121.

Campagna, M. L., and S. R. Downie. 1998. The intron in chloroplast gene *rpl16* is missing from the flowering plant families Geraniaceae, Goodeniaceae, and Plumbaginaceae. *Transactions of the Illinois State Academy of Science* 91: 1-11.

Canal, D., N. Köster, K. E. Jones, N. Korotkova, T. B. Croat, and T. Borsch. 2018. Phylogeny and diversification history of the large Neotropical genus *Philodendron* (Araceae): Accelerated speciation in a lineage dominated by epiphytes. *American Journal of Botany* 105: 1035-1052.

Carlsen, M., and T. B. Croat. 2013. A molecular phylogeny of the species-rich Neotropical genus *Anthurium* (Araceae) based on combined chloroplast and nuclear DNA. *Systematic Botany Monographs* 38 576–588.

Cervantes, A., S. Fuentes, J. Gutiérrez, S. Magallón, and T. Borsch. 2016. Successive arrival since the Miocene shaped the diversity of the Caribbean Acalyphoideae (Euphorbiaceae). *Journal of Biogeography* 43: 1773-1785.

Chacón, J., S. Madriñán, M. W. Chase, and J. J. Bruhl. 2006. Molecular phylogenetics of *Oreobolus* (Cyperaceae) and the origin and diversification of the American species. *Taxon* 55: 359-366.

Chacón, J., M. C. De Assis, A. W. Meerow, and S. S. Renner. 2012. From east Gondwana to Central America: historical biogeography of the Alstroemeriaceae. *Journal of Biogeography* 39: 1806-1818.

Claudel, C., S. Buerki, L. W. Chatrou, A. Antonelli, N. Alvarez, and W. Hetterscheid. 2017. Large-scale phylogenetic analysis of *Amorphophallus* (Araceae) derived from nuclear and plastid sequences reveals new subgeneric delineation *Botanical Journal of the Linnean Society* 184: 32-45.

Coelho, M. A. N., M. L. Soares, L. S. B. Calazans, E. G. Gonçalves, I. M. Andrade, T. A. De Pontes, C. M. Sakuragui, et al. 2015. Araceae in lista de espécies da Flora do Brasil. Flora do Brasil 2020. Available at http://floradobrasil.jbrj.gov.br/

Condamine, F. L., N. S. Nagalingum, C. R. Marshall, and H. Morlon. 2015. Origin and diversification of living cycads: a cautionary tale on the impact of the branching process prior in Bayesian molecular dating. *BMC Evolutionary Biology* 15: 65.

Couvreur, T. L. P., and W. J. Baker. 2011. Origin and global diversification patterns of tropical rain forests: inferences from a complete-genus level phylogeny of palms. *BMC Evolutionary Biology* 9: 1-12.

Couvreur, T. L. P., P. M. D., L. W. Chatrou, R. M. K. Saunders, Y. C. F. Su, J. E. Richardson, and R. H. J. Erkens. 2011. Early evolutionary history of the flowering plant family Annonaceae: steady diversification and boreotropical geodispersal. *Journal of Biogeography* 38: 664-680.

Crisp, M. D., N. B. Hardy, and L. G. Cook. 2014. Clock model makes a large difference to age estimates of long-stemmed clades with no internal calibration: a test using Australian grasstrees. *Evolutionary Biology* 14: 1-17.

Croat, T. B. 1997. A revision of *Philodendron* subgenus *Philodendron* (Araceae) for Mexico and Central America. *Annals of the Missouri Botanical Garden* 84: 311-704.

Croat, T. B., and M. M. Mora. 2004. New taxa of Araceae from Cabo Corrientes in Chocó Department of Colombia. *Aroideana* 27: 90-129.

Croat, T. B., P. Huang, J. Lake, and C. V. Kostelac. 2010. Araceae of the Flora of La Planada, Nariño Department, Colombia. *Aroideana* 33: 75-142.

Croat, T. B., X. Delannay, S. Duncan, and C. V. Kostelac. 2016. Revision of *Philodendron* from the Lita-San Lorenzo Region (Esmeraldas Province, Ecuador). *Aroideana* 39: 26-315.

Cusimano, N., J. Bogner, S. J. Mayo, P. C. Boyce, S. Y. Wong, M. Hesse, W. L. A. Hetterscheid, et al. 2011. Relationships within the Araceae: Comparison of morphological patterns with molecular phylogenies. *American Journal of Botany* 98: 654-668.

Darriba, D., G. L. Taboada, R. Doallo, and D. Posada. 2012. jModelTest 2: more models, new heuristics and parallel computing. *Nature Methods* 9: 772-772.

Davis, C. C., C. O. Webb, K. J. Wurdack, C. A. Jaramillo, and M. J. Donoghue. 2005. Explosive radiation of Malpighiales supports a Mid-Cretaceous origin of modern tropical rain forests. *The American Naturalist* 165: 36-65.

Davis, M. P., P. E. Midford, and W. P. Maddison. 2013. Exploring power and parameter estimation of the BiSSE method for analyzing species diversification. *BMC Evolutionary Biology* 13: 38.

Devanand, P. S., J. Chen, R. J. Henny, and T. C. Chih-Cheng. 2004. Assessment of genetic relationships among *Philodendron* cultivars using AFLP markers. *Journal of the American Society for Horticultural Science* 129: 690-697.

Doyle, J. J., and J. L. Doyle. 1987. A rapid DNA isolation procedure for small quantities of fresh leaf tissue. [Sonderdr. - Maschinenschr. Veröffentlichung] ed. Phytochemical Sect., Bronx, NY.

Drew, B. T., and K. Sytsma. 2013. The South American radiation of *Lepechinia* (Lamiaceae): phylogenetics, divergence times and evolution of dioecy. *Botanical Journal of the Linnean Society* 171: 171-190.

Droege, G., K. Barker, O. Seberg, J. Coddington, E. Benson, W. G. Berendsohn, B. Bunk, et al. 2016. The global genome biodiversity network (GGBN) data standard specification. *Nucleic Acids Research* 42(D1): D607-D612.

Drummond, A. J., and R. Bouckaert. 2015. Bayesian evolutionary analysis with BEAST. Cambridge University Press, United Kingdom.

Drummond, A. J., S. Y. W. Ho, M. J. Phillips, and A. Rambaut. 2006. Relaxed phylogenetics and dating with confidence. *PLoS Biology* 4: 699-710.

Drummond, A. J., M. A. Suchard, D. Xie, and A. Rambaut. 2012. Bayesian phylogenetics with BEAUti and the BEAST 1.7 *Molecular Biology and Evolution* 29: 1969-1973.

Eiserhardt, W. L., T. L. P. Couvreur, and W. J. Baker. 2017. Plant phylogeny as a window on the evolution of hiperdiversity in the tropical rainforest biome. *New Phytologist* 214: 1408-1422.

Engler, A. 1878. Araceae. *In* Martius, C.F.P. von. *Flora Brasiliensis* 3: 25-224 tt. 222–252.

Engler, A. 1899. Beiträge zur Kenntnis der Araceae. IX. 16. Revision der Gattung *Philodendron* Schott. Botanische Jahrbücher für Systematik, Pflanzengeschichte und Pflanzengeographie. 26: 509-564.

Engler, A. 1905. Beiträge zur Kenntnis der Araceae. X. 18. Botanische Jahrbücher für Systematik, Pflanzengeschichte und Pflanzengeographie. 37: 110-143.

Erkens, R. H. J., L. W. Chatrou, J. W. Maas, T. Van Der Niet, and V. Savolainen. 2007. A rapid diversification of rainforest trees (*Guatteria*; Annonaceae) following dispersal from Central into South America. *Molecular Phylogenetics and Evolution* 44: 399–411.

Filipowicz, N., and S. S. Renner. 2012. *Brunfelsia* (Solanaceae): a genus evenly divided between South America and radiations on Cuba and other Antillean islands. *Molecular Phylogenetics and Evolution* 64: 1-11.

Fishbein, M., T. Livshultz, C. K. S. Straub, A. O. Simões, J. Boutte, A. Mcdonnell, and A. Foote. 2012. Evolution on the backbone: Apocynaceae phylogenomics and new perspectives on growth forms, flowers, and fruits. *American Journal of Botany* 105: 495-513.

Fitzjohn, R. G. 2012. Diversitree: comparative phylogenetic analysis of diversification in R. *Methods in Ecology and Evolution* 3: 1084-1092.

Fitzjohn, R. G., W. P. Maddison, and S. P. Otto. 2009. Estimating trait-dependent speciation and extintion rates from incompletely resolved phylogenies. *Systematic Biology* 58: 595-611.

Forest, F. 2009. Calibrating the Tree of Life: fossils, molecules and evolutionary timescales. *Annals of Botany* 104: 789–794.

Gascuel, O. 1997. BIONJ: An improved version of the NJ algorithm based on a simple model of sequence data. *Molecular Biology and Evolution* 14: 685-695.

Gauthier, M. P. L., D. Barabe, and A. Bruneau. 2008. Molecular phylogeny of the genus *Philodendron* (Araceae): delimitation an infrageneric classification. *Botanical Journal of the Linnean Society* 156: 13-27.

Gentry, A. H., and C. H. Dodson. 1987. Diversity and biogeography of Neotropical vascular epiphytes. *Annals of the Missouri Botanical Garden* 74: 205-233.

Givnish, T. J., D. Spalink, M. Ames, S. P. Lyon, S. J. Hunter, A. Zuluaga, W. J. D. Iles, et al. 2015. Orchid phylogenomics and multiple drivers of their extraordinary diversification. *Proceedings of the Royal Society B* 282.

Givnish, T. J., M. H. J. Barfuss, B. V. Ee, R. Riina, K. Schulte, R. Horres, P. A. Gonsiska, et al. 2011. Phylogeny, adaptative radiation, and historical biogeography in Bromeliaceae: insights from an eight-locus plastid phylogeny. *American Journal of Botany* 98: 872-895.

Givnish, T. J., M. H. J. Barfuss, B. Van Ee, R. Riina, K. Schulte, R. Horres, P. A. Gonsiska, et al. 2014. Adaptative radiation, correlated and contingent evolution, and net species diversification in Bromeliaceae. *Molecular Phylogenetics and Evolution* 71: 55-78.

Goldberg, E., L. Lancaster, and R. H. Ree. 2011. Phylogenetic inference of reciprocal effects between geographic range evolution and diversification. *Systematic Biology* 60: 451-465.

Gonçalves, E. G., and E. R. Salviani. 2002. New species and changing concepts of *Philodendron* subgenus *Meconostigma* (Araceae). *Aroideana* 25: 2-15.

Govaerts, R., J. Bogner, J. Boos, P. Boyce, B. Cosgriff, T. B. Croat, E. Gonçalves, et al. 2018. World Checklist of Araceae. Facilitated by the Royal Botanic Gardens, Kew. Published on the Internet; http://wcsp.science.kew.org. Retrieved 22 November 2018.

Grayum, M. H. 1996. Revision of *Philodendron* subgenus *Pteromischum* (Araceae) for Pacific and Caribbean Tropical America. *Systematic Botany Monographs* 47: 1-233.

Gregory-Wodzicki, K. M. 2000. Uplift history of the Central and Northern Andes: a review. *GSA Bulletin* 112: 1091-1105.

Henriquez, C. L., T. Arias, J. C. Pires, T. B. Croat, and B. A. Schaal. 2014. Phylogenomics of the plant family Araceae. *Molecular Phylogenetics and Evolution* 75: 91-102.

Herrera, F. A., C. A. Jaramillo, D. L. Dilcher, S. L., S. L. Wing, and C. Gómez-N. 2008. Fossil Araceae from a Paleocene neotropical rainforest in Colombia. *American Journal of Botany* 95: 1569–1583.

Hilu, K. W., T. Borsch, K. Muller, D. E. Soltis, P. S. Soltis, V. Savolainen, M. W. Chase, et al. 2003. Angiosperm phylogeny based on *matK* sequence information. *American Journal of Botany* 90: 1758-1776.

Hipsley, C. A., and J. Müller. 2014. Beyond fossil calibrations: realities of molecular clock practices in evolutionary biology. *Frontiers in Genetics* 5.

Hoorn, C., F. P. Wesselingh, H. Ter Steege, M. A. Bermudez, A. Mora, J. Sevink, I. Sanmartin, et al. 2010. Amazonia through time: Andean uplift, climate change, landscape evolution, and biodiversity. *Science* 330: 927–931.

Hughes, C. E., R. T. Pennington, and A. Antonelli. 2013. Neotropical plant evolution: assembling the big picture. *Botanical Journal of the Linnean Society* 171: 1-18.

Iturralde-Vinent, M., and R. D. Macphee. 1999. Paleogeography of the Caribbean region: Implications for Cenozoic biogeography. *Bulletin of the American Museum of Natural History* 238: 1-95.

Jaramillo, C., M. J. Rueda, and G. Mora. 2006. Cenozoic plant diversity in the Neotropics. *Science* 311: 1893-1896.

Jaramillo, C., C. Montes, A. Cardona, D. Silvestro, A. Antonelli, and C. D. Bacon. 2017. Comment (1) on "Formation of the Isthmus of Panama" by O'Dea et al. *Science Advances* 3: 1.8.

Kay, K. M., P. A. Reeves, R. G. Olmstead, and D. W. Schemske. 2005. Rapid speciation and evolution of humminbird pollination in neotropical *Costus* subgenus *Costus* (Costaceae): evidence from nrDNA ITS and ETS sequences. *American Journal of Botany* 92: 1899-1910.

Kelchner, S. A. 2002. Group II introns as phylogenetic tools: structure, function, and evolutionary constraints. *American Journal of Botany* 89: 1651-1669.

Klimko, M., M. Wawrzyńska, and J. Wiland-Szymańska. 2014. Comparative leaf morphology and anatomy of some neotropical *Philodendron* Schott (Araceae) species. *Steciana* 18: 159-171.

Koenen, E. J. M., J. J. Clarkson, T. D. Pennington, and L. W. Chatrou. 2015. Recently evolved diversity and convergent radiations of rainforest mahoganies (Meliaceae) shed new light on the origins of rainforest hyperdiversity. *New Phytologist* 207: 327–339.

Köster, N., and T. B. Croat. 2011. A new section and a new species of *Philodendron* (Araceae) from Ecuador. *Willdenowia* 41.

Krause, K. 1913. Araceae-Philodendroideae-Philodendreae-Philodendrinae. Engler, A. & K. Krause (eds), Das Pflanzenreich Regni Vegetabilis Conspectus. W. Engelmann, Leipzig, Germany. IV: 1-143.

Kreft, H., N. Köster, W. Küper, J. Nieder, and W. Barthlott. 2004. Diversity and biogeography of vascular epiphytes in Western Amazonia, Yasuní, Ecuador. *Journal of Biogeography* 31: 1463-1476.

Lagomarsino, L. P., F. L. Condamine, A. Antonelli, A. Mulch, and C. C. Davis. 2016. The abiotic and biotic drivers of rapid diversification in Andean bellflowers (Campanulaceae). *New Phytologist* 210: 1430-1442.

Landolt, E. 1986. Biosystematic investigations in the family of duckweeds (Lemnaceae), volume 2. The family of Lemnaceae - a monographic study, volume 1. *Zürich: Veröffentlichungen des Geobotanischen Institutes der ETH, Stiftung Rübel, in Zürich (71 Heft)*.

Linder, H. P., C. R. Hardy, and F. Rutschmann. 2005. Taxon sampling effects in molecular clock dating: an example from African Restionaceae. *Molecular Phylogenetics and Evolution* 35: 569-582.

Lohmann, G. L., D. C. Bell, F. M. Calio, and C. R. Winkworth. 2013. Pattern and timing of biogeographical history in the Neotropical tribe Bignonieae (Bignoniaceae). *Botanical Journal of the Linnean Society* 171: 155-170.

Löhne, C., and T. Borsch. 2005. Molecular evolution and phylogenetic utility of the *petD* group II intron: A case study in basal angiosperms. *Molecular Biology and Evolution* 22: 317-332.

Loss-Oliveira, L., C. Sakuragui, M. De Lourdes Soares, and C. G. Schrago. 2016. Evolution of *Philodendron* (Araceae) species in Neotropical biomes. *Peerj* 4: 1-18.

Loss-Oliveira, L., L. S. B. Calazans, E. B. Morais, S. J. Mayo, C. E. G. Schrago, and C. M. Sakuragui. 2014. Floral evolution of *Philodendron* subgenus *Meconostigma* (Araceae). *Plos One* 9: e89701.

Luebert, F., and M. Weigend. 2014. Phylogenetic insights into Andean plant diversification. *Frontiers in Ecology and Evolution* 2: 1-17.

Maddison, W. P., and R. G. Fitzjohn. 2015. The unsolved challenge to phylogenetic correlation tests for categorical characters. *Systematic Biology* 64.

Maddison, W. P., P. E. Midford, and S. P. Otto. 2007. Estimating a binary character's effect on speciation and extinction. *Systematic Biology* 56: 701-710.

Madriñán, S., A. J. Cortés, and J. E. Richardson. 2013. Páramo is the world's fastest evolving and coolest biodiversity hotspot. *Frontiers in Genetics* 4: 1-7.

Matthew, V. D., and N. J. Matzke. 2016. Evaluating the influence of connectivity and distance on biogeographic patterns in the south-western deserts of North America. *Journal of Biogeography* 43: 1514-1532.

Matzke, N. J. 2013. BioGeoBEARS: BioGeography with Bayesian (and likelihood) evolutionary analysis in R scripts, CRAN: The Comprehensive R Archive Network, Berkeley, CA.

Matzke, N. J. 2014. Model selection in historical biogeography reveals that founder-event speciation is a crucial process in island clades. *Systematic Biology* 63: 951-970.

Maunder, M., A. Leiva, E. Santiago-Valentín, D. W. Stevenson, P. Acevedo-Rodriguez, A. W. Meerow, M. Mejía, et al. 2018. Plan conservation in the Caribbean island biodiversity hotspot *Botanical Review* 74: 197–207.

Mayo, S. 1990. History and infrageneric nomenclature of *Philodendron* (Araceae). *Kew Bulletin* 45: 37-71.

Mayo, S. J. 1986. Systematics of *Philodendron* Schott (Araceae) with special reference to inflorescence characters. Ph.D. Thesis, University of Reading, U.K.

Mayo, S. J. 1988. Aspectos da evolução e da geografia do gênero *Philodendron* Schott (Araceae). *Acta Botanica Brasilica* 1: 27-40.

Mayo, S. J. 1989. Observations of gynoecial structure in *Philodendron* (Araceae). *Botanical Journal of the Linnean Society* 100: 139-172.

Mayo, S. J. 1991. A revision of *Philodendron* subgenus *Meconostigma* (Araceae). *Kew Bulletin* 46: 601-681.

Mayo, S. J., J. Bogner, and P. C. Boyce. 1997. The genera of Araceae. The Trustees, Royal Botanic Gardens, Kew. UK.

Mckenna, D. D., and B. D. Farrell. 2006. Tropical forests are both evolutionary cradles and museums of leaf beetle diversity. *Proceedings of the National Academy of Sciences* 103: 10947–10951.

Messing, J. 1983. New M13 vectors for cloning. *Methods in Enzymology* 101: 20–78.

Miller, M. A., W. Pfeiffer, and T. Schwartz. 2010. "Creating the CIPRES Science Gateway for inference of large phylogenetic trees" in Proceedings of the Gateway Computing Environments Workshop (GCE). 14 Nov. 2010, New Orleans, LA pp 1 - 8.

Moncrieff, G. R., T. Hicker, and S. I. Higgins. 2015. Intercontinental divergence in the climate envelope of major plant biomes. *Global Ecology and Biogeography* 24: 324-334.

Moore, B. R., S. Höhna, M. R. May, B. Rannala, and J. P. Huelsenbeck. 2016. Critically evaluating the theory and performance of Bayesian analysis of macroevolutionary mixtures. *Proceedings of the National Academy of Sciences* 113: 9569-9574.

Morrone, J. J. 2014. Cladistic biogeography of the Neotropical region: identifying the main events in the diversification of the terrestrial biota. *Cladistics* 30: 202-214.

Müller, K. 2004. PRAP-computation of Bremer support for large data sets. *Molecular Phylogenetics and Evolution* 31: 780-782.

Müller, K. 2005. SeqState – primer design and sequence statistics for phylogenetic DNA data sets. *Applied Bioinformatics* 4: 65–69.

Müller, K., D. Quandt, J. Müller, and C. Neinhuis. 2005. PhyDE, Version 0.92: Phylogenetic data editor.

Myers, N., R. A. Mittermeier, C. G. Mittermeier, G. A. B. Fonseca, and J. Kent. 2000. Biodiversity hotspots for conservation priorities. *Nature* 403: 853-858.

Nauheimer, L., D. Metzler, and S. S. Renner. 2012. Global history od the ancient monocot family Araceae inferred with models accounting for past continental positions and previous ranges based on fossils. *New Phytologist* 195: 938-950.

Neupane, S., P. O. Lewis, S. Dessein, H. Shanks, S. Paudyal, and F. Lens. 2017. Evolution of woody life form on tropical mountains in the tribe Spermacoceae (Rubiaceae). *American Journal of Botany* 104: 419-438.

Neves, D. M., K. G. Dexter, R. T. Pennington, M. L. Bueno, and A. T. Oliveira Fihlo. 2015. Environmental and historical controls of floristic composition across the South American Dry Diagonal. *Journal of Biogeography* 42: 1566-1576.

Nicholls, J. A., R. T. Pennington, E. J. M. Koenen, C. E. Hughes, J. Hearn, L. Bunnefeld, K. G. Dexter, et al. 2015. Using targeted enrichment of nuclear genes to increase phylogenetic resolution in the neotropical rain forest genus *Inga* (Leguminosae: Mimosoideae). *Frontiers in Plant Science* 6: 1-20.

Nieto-Blázquez, M. E., A. Antonelli, and J. Roncal. 2017. Historical biogeography of endemic seed plant genera in the Caribbean: did GAARlandia play a role? *Ecology and Evolution*: 1-17.

Nixon, K. C. 1999. The Parsimony Ratchet, a new method for rapid parsimony analysis. *Cladistics* 15: 407-414.

O'dea, A., A. L. Harilaos, A. G. Coates, R. I. Eytan, S. A. Restrepo-Moreno, A. L. Cione, L. S. Collins, et al. 2016. Formation of the Isthmus of Panama. *Science Advances* 2: e1600883.

Olson, D. M., E. Dinerstein, E. D. Wikramanayake, N. D. Burguess, G. V. N. Powell, E. C. Underwood, J. A. D'amico, et al. 2001. Terrestrial ecoregions of the world: a new map of life on Earth. *BioScience* 51: 933-938.

Pagel, M., and A. Meade. 2006. Bayesian analysis of correlated evolution of discrete characters by reversible-jump Markov chain Monte Carlo. *American Naturalist* 167: 808-825.

Pagel, M., A. Meade, and D. Barker. 2004. Bayesian estimation of ancestral character states on phylogenies. *Systematic Biology* 53: 673-684.

Pennington, R. T., J. E. Richardson, and M. Lavin. 2006a. Insights into the historical construction of species-rich biomes from dated plant phylogenies, neutral ecological theory and phylogenetic community structure. *New Phytologist* 172: 605-616.

Pennington, R. T., J. A. Ratter, and G. P. Lewis. 2006b. Neotropical savannas and seasonally dry forests: plant biodiversity, biogeography and conservation. Boca Raton, Florida: CRC Press.

Pennington, R. T., M. Levin, and A. T. Oliveira Fihlo. 2009. Woody plant diversity, evolution, and ecology in the Tropics: perspectives from seasonally dry tropical forests. *Annual Review of Ecology, Evolution, and Systematics* 40: 437-457.

Pennington, R. T., M. Hughes, and P. W. Moonlight. 2015. The origins of tropical rainforest hyperdiversity. *Trends in Plant Science* 20: 693-695.

Pennington, R. T., M. Lavin, T. Särkinen, P. L. Gwilym, B. B. Klitgaard, and C. E. Hughes. 2010. Contrasting plant diversification histories within the Andean biodiversity hotspot. *Proceedings of the National Academy of Sciences* 107: 13783-13787.

Pérez-Escobar, O. A., G. Chomicki, F. L. Condamine, A. P. Karremans, D. Bogarín, N. J. Matzke, D. Silvestro, and A. Antonelli. 2017. Recent origin and rapid speciation of Neotropical orchids in the world's richest plant biodiversity hotspot. *New Phytologist* 215: 891-905.

Plummer, M., N. Best, K. Cowles, and K. Vines. 2006. CODA: convergence diagnosis and output analysis for MCMC. *R News* 6: 7-11.

Poczai, P., and J. Hyvönen. 2010. Nuclear ribosomal spacer regions in plant phylogenetics: problems and prospects. *Molecular Biology Reports* 37: 1897–1912.

Rabosky, D. L. 2014. Automatic detection of key innovations, rate shifts, and diversity-dependence on phylogenetic trees. *Plos One* 9: e89543.

Rabosky, D. L., J. S. Mitchell, and J. Chang. 2017. Is BAMM flawed? theoretical and practical concerns in the analysis of multi-rate diversification models. *Systematic Biology* 66: 477-498.

Rambaut, A. 2012. FigTree v1.4. Molecular evolution, phylogenetics and epidemiology. University of Edinburgh, Institute of Evolutionary Biology, Edinburgh, UK.

R Core Team. 2013. R: A language and environment for statistical computing. R Foundation for Statistical Computing, Vienna, Austria. http://www.R-project.org/.

Ray, T. S. 1987. Diversity of shoot organization in the Araceae. *American Journal of Botany* 74: 1373-1387.

Ray, T. S. 1988. Survey of shoot organization in the Araceae. *American Journal of Botany* 75: 56-84.

Richardson, J. E., R. T. Pennington, T. D. Pennington, and P. M. Hollingsworth. 2001. Rapid diversification of a species-rich genus of neotropical rain forest trees. *Science* 293: 2242-2245.

Roncal, J., F. Kahn, B. Millan, T. L. P. Couvreur, and J.-C. Pintaud. 2013. Cenozoic colonization and diversification patterns of tropical American palms: evidence from *Astrocaryum* (Arecaceae). *Botanical Journal of the Linnean Society* 171: 120-139.

Ronquist, F., and J. P. Huelsenbeck. 2003. MrBayes 3: Bayesian phylogenetic inference under mixed models. *Bioinformatics* 19: 1572-1574.

Ronquist, F., J. Huelsenbeck, and M. Teslenko. 2011. MrBayes version 3.2 manual: tutorials and model summaries. Available at http://mrbayes.sourceforge.net/mb3.2_manual.pdf.

Saitou, N., and M. Nei. 1987. The neighbor-joining method: a new method for reconstruction of phylogenetic trees. *Molecular Biology and Evolution* 4: 406-425.

Sakuragui, C. 2012. Two new species and a revised key for *Philodendron* section *Schizophyllum* (Araceae). *Systematic Botany* 37: 43-47.

Sakuragui, C. M., S. J. Mayo, and D. C. Zappi. 2005. Taxonomic revision of Brazilian species of *Philodendron* section *Macrobelium*. *Kew Bulletin* 60: 465-513.

Sakuragui, C. M., L. S. Braucks Calazans, É. Barroso De Morais, M. A. Nadruz Coelho, and M. O. De Oliveira Pellegrini. 2011. Diversity and conservation of *Philodendron* Schott (Araceae) in Atlantic Forest of Rio de Janeiro State, Brazil. *Feddes Repertorium* 122 472– 496.

Sakuragui, C. M., L. S. Braucks Calazans, L. Loss De Oliveira, E. Barroso De Morais, A. M. Benko-Iseppon, S. Vasconcelos, C. E. Guerra Schrago, and S. J. Mayo. 2018. Recognition of the genus *Thaumatophyllum* Schott − formerly *Philodendron* subg. *Meconostigma* (Araceae) −based on molecular and morphological evidence. *PhytoKeys* 98: 51-71.

Salas-Gismondi, R., J. J. Flynn, P. Baby, J. V. Tejada-Lara, F. P. Wesselingh, and P. O. Antoine. 2015. A Miocene hyperdiverse crocodylian community reveals peculiar trophic dynamics in proto-Amazonian mega-wetlands. *Proceedings of the Royal Society B: Biological Sciences* 282: 20142490.

Santiago-Valentín, E., and R. G. Olmstead. 2004. Historical biogeography of Caribbean plants: introduction to current knowledge and possibilities from a phylogenetic perspective. *Taxon* 53: 299-319.

Särkinen, T. E., M. F. Newman, P. J. M. Maas, H. Maas, A. D. Poulsen, D. J. Harris, J. E. Richardson, et al. 2007. Recent oceanic long-distance dispersal and divergence in the amphi-Atlantic rain forest genus *Renealmia* L.f. (Zingiberaceae). *Molecular Phylogenetics and Evolution* 44: 968-980.

Sauquet, H., M. Von Balthazar, S. Magallón, J. A. Doyle, P. K. Endress, E. J. Bailes, É. Barroso De Morais, et al. 2017. The ancestral flower of angiosperms and its early diversification. *Nature Communications* 8: 1-10.

Schenk, J. J. 2016. Consequences of secondary calibrations on divergence time estimates. *Plos One* 11: e0148228. doi:0148210.0141371.

Schley, R. J., M. De La Estrella, O. A. Pérez-Escobar, A. Bruneau, T. Barraclough, F. Forest, and B. Klitgård. 2018. Is Amazonia a "museum" for Neotropical trees? The evolution of the Brownea clade (Detarioideae, Leguminosae). *Molecular Phylogenetics and Evolution* 126: 279-292.

Schneider, J. V., and G. Zizka. 2017. Phylogeny, taxonomy and biogeography of Neotropical Quiinoideae (Ochnaceae s.l.). *Taxon* 66: 855-867.

Schott, H. W. 1829. Für Liebhaber der Botanik. Wiener Zeitschrift für Kunst, Literatur, Theater und Mode 1829. 3: 779-780.

Schott, H. W. 1832. Araceae. In H. Schott and S. Endlicher, Meletemata botanica. Typis Caroli Gerold, Vienna.

Schott, H. W. 1856. Synopsis Aroidearum, 140 pp. Typis Congregationis Mechitharisticae. Viena.

Schott, H. W. 1860. Prodromus systematis Aroidearum, 602 pp. Typis congregationis mechitharisticae, Vienna.

Schulte, J. A. 2013. Undersampling taxa will underestimate molecular divergence dates: an example from the South American lizard clade Liolaemini. *International Journal of Evolutionary Biology* 2013: 12.

Shaul, S., and D. Graur. 2002. Playing chicken (*Gallus gallus*): methodological inconsistencies of molecular divergence date estimates due to secondary calibration points. *Gene* 300.

Shaw, J., E. B. Lickey, J. T. Beck, S. B. Farmer, Liu W, J. Miller, K. C. Siripun, et al. 2005. The tortoise and the hare II: relative utility of 21 noncoding chloroplast DNA sequences for phylogenetic analysis. *American Journal of Botany* 92: 142-166.

Shi, J. J., and D. L. Rabosky. 2015. Speciation dynamics during the global radiation of extant bats. *Evolution* 69: 1528-1545.

Silvestro, D., and I. Michalak. 2012. raxmlGUI: a graphical front-end for RAxML. *Organisms Diversity & Evolution* 12: 335-337.

Simmons, M. P., and H. Ochoterena. 2000. Gaps as characters in sequence-based phylogenetic analyses. *Systematic Biology* 49: 369-381.

Simmons, M. P., and J. V. Freudenstein. 2011. Spurious 99% bootstrap and jackknife support for unsupported clades. *Molecular Phylogenetics and Evolution* 61.

Simon, R., A. F. Fuentes, and D. M. Spooner. 2011. Biogeographic implications of the striking discovery of a 4,000 kilometer disjunct population of the wild potato *Solanum morelliforme* in South America. *Systematic Botany* 36: 1062-1067.

Stayton, C. T. 2015. What does convergent evolution mean? The interpretation of convergence and its implications in the search for limits to evolution. *InterFace Focus* 5: 1-8.

Stebbins, G. L. 1974. Evolution above the species level. Cambridge, Massachussets: Harvard University Press.

Stöver, B. C., and K. F. Müller. 2010. TreeGraph 2: Combining and visualizing evidence from different phylogenetic analyses. *BMC Bioinformatics* 11.

Sundue, M. A., W. L. Testo, and T. A. Ranker. 2015. Morphological innovation, ecological, opportunity, and the radiation of a major vascular epiphyte lineage. *Evolution* 69: 2482-2495.

Swofford, D. L. 2003. PAUP*. Phylogenetic analyses using parsimony (*and other methods).

Tenorio, V., C. Sakuragui, and R. Cardoso Vieira. 2012. Stem anatomy of *Philodendron* Schott (Araceae) and its contribution to the systematics of the genus. *Plant Systematics and Evolution* 298: 1337-1347.

Tripp, E. A., and Y.-H. E. Tsai. 2017. Disentangling geographical, biotic, and abiotic drivers of plant diversity in neotropical *Ruellia* (Acanthaceae). *Plos One* 12: 1-17.

Turland, N. J., J. H. Wiersema, F. R. Barrie, W. Greuter, D. L. Hawksworth, P. S. Herendeen, S. Knapp, et al. 2018. International Code of Nomenclature for algae, fungi, and plants (Shenzhen Code) adopted by the Nineteenth International Botanical Congress Shenzhen, China, July 2017. Regnum Vegetabile 159. Glashütten: Koeltz Botanical Books. DOI https://doi.org/10.12705/Code.2018.

Vasconcelos, S. 2015. Filogenia e evolução cariotípica do gênero *Philodendron* (Araceae), com ênfase para espécies da Amazônia brasileira. PhD Thesis, Universidade Federal de Pernambuco, Brazil.

Vasconcelos, S., M. Lourdes Soares, C. Sakuragui, T. B. Croat, G. Oliveira, and A. M. Benko-Iseppon. 2018. New insights on the phylogenetic relationships among the traditional *Philodendron* subgenera and the other groups of the *Homalomena* clade (Araceae). *Molecular Phylogenetics and Evolution* 127: 168-178.

Wagner, S. T., S. Isnard, N. P. Rowe, M.-S. Samain, C. Neinhuis, and S. Wanke. 2012. Escaping the lianoid habit: evolution of shrub-like growth forms in *Aristolochia* subgenus *Isotrema* (Aristolochiaceae). *American Journal of Botany* 99: 1609-1629.

Wang, W., R. D. C. Ortiz, F. M. B. Jacques, X.-G. Xiang, H.-L. Li, L. Lin, R.-Q. Li, et al. 2012. Menispermaceae and the diversification of tropical rainforests near the Cretaceous-Paleogene boundary. *New Phytologist* 195: 470-478.

Weitemier, K., S. C. K. Straub, R. C. Cronn, M. Fishbein, R. Schmickl, A. Mcdonnell, and A. Liston. 2014. Hyb-Seq: Combining target enrichment and genome skimming for plant phylogenomics. *Applications in Plant Sciences* 2: 1400042.

Werneck, F., T. Gamble, G. R. Colli, M. T. Rodrigues, and J. W. Sites. 2012. Deep diversification and long-term persistence in the South American' Dry Diagonal: integrating continent-wide phylogeography and distribution modeling of geckos. *Evolution* 66: 3014-3034.

Wicke, S., and D. Quandt. 2009. Universal primers for the amplification of the plastid *trn*K/*mat*K region in land plants. *Anales del Jardín Botánico de Madrid* 66: 285-288.

Wong, S. J., A. W. Meerow, and T. B. Croat. 2016. Resurrection and new species of the Neotropical genus *Adelonema* (Araceae: Philodendron Clade). *Systematic Botany* 41: 32-48.

Wong, S. J., T. P. Jean, N. K. Kiaw, A. S. Othman, H. L. Boon, B. F. Ahmad, and C. P. Boyc. 2013. Phylogeny of Asian *Homalomena* (Araceae) based on the ITS region combined with morphological and chemical data. *Systematic Botany Monographs* 38: 589-599.

Woodhams, M., D. A. Steane, R. C. Jones, D. Nicolle, V. Moulton, and B. R. Holland. 2013. Novel distances for Dollo data. *Systematic Biology* 62: 62–77.

Xie, W., P. O. Lewis, Y. Fan, L. Kuo, and M.-H. Chen. 2011. Improving marginal likelihood estimation for Bayesian phylogenetic model selection. *Systematic Biology* 60: 150–160.

Zotz, G. 2013. The systematic distribution of vascular epiphytes – a critical update. *Botanical Journal of the Linnean Society* 171: 453-481.

Zotz, G. 2016. Plants on plants. The biology of vascular epiphytes, Berlin Heidelberg New York, Springer.

List of publications and own contributions

Chapter 2

Canal, D., N. Köster, K. E. Jones, N. Korotkova, T. B. Croat, and T. Borsch. 2018. Phylogeny and diversification history of the large Neotropical genus *Philodendron* (Araceae): Accelerated speciation in a lineage dominated by epiphytes. *American Journal of Botany* 105(6): 1035–1052.
https://doi.org/10.1002/ajb2.1111

Own contribution: Performed field work (together with Dr. Nils Köster), laboratory work, data analyses and wrote the manuscript.

Chapter 3

Canal, D., N. Köster, M. Celis, T. B. Croat, T. Borsch, and K. E. Jones. Out of Amazonia and back again: historical biogeography of the species-rich genus *Philodendron* (Araceae). Submitted to the *Annals of the Missouri Botanical Garden.*

Own contribution: Performed field work (together with Dr. Nils Köster), laboratory work, data analyses and wrote the manuscript.

Appendices

Appendix A. Supplementary material for Chapter 2

Appendix A1. Taxa used for molecular data and their details (Taxon and authorities, ID, DNA bank number, locality/provenience of sample, collector(s) and collector number, specimen voucher and NCBI accession numbers for *trnK/matK*, *rpl16* and *petD*, respectively). All sequences were newly generated in this study. Accessions that could not be identified to species level were submitted to NBCI with the abbreviation *sp*. followed by the code DC2018 and an alphabetic character. Herbaria acronyms for voucher locations follow Index Herbariorum (Thiers, B. [continuously updated]. Index Herbariorum: A global directory of public herbaria and associated staff. New York Botanical Garden's Virtual Herbarium. http://sweetgum.nybg.org/science/ih/). Species names are used following Govaerts et al. (2018). Accessions are listed in alphabetic order. Abbreviations: s.n. = sine numero (without number).

Outgroups: ***Aglaonema marantifolium*** Blume, ARA233, DB 29791, Cultivated, *Cubr 30432* (B 10 0746890, B 10 0746891), LT995112, LT996397, LT996579; ***Anchomanes difformis*** (Blume) Engl., ARA230, DB 29788, Togo, *Ern, Hein & Pircher 195* (B 10 0746889), LT995111, LT996396, LT996578; ***Anthurium hookeri*** Kunth, ARA064, DB 29622, Cultivated, *Schwerdtfeger 21482* (B 10 0746885, B 10 0746886), LT995002, LT996287, LT996469; ***Anthurium scandens*** (Aubl.) Engl., ARA066, DB 29624, Mexico, *s.n.* (B 10 0746880, B 10 0746881, B 10 0746882), LT995004, LT996289, LT996471; ***Colocasia esculenta*** (L.) Schott, ARA221, DB 29779, Cultivated, *s.n.* (B 10 0746875, B 10 0746876), LT995105, LT996390, LT996572; ***Montrichardia linifera*** (Arruda) Schott, ARA217, DB 29775, Colombia, *Koenen 153a* (B 10 0746877, B 10 0746878, B 10 0746879), LT995102, LT996387, LT996569; ***Pseudohydrosme gabunensis*** Engl., ARA227, DB 29785, Gabun, *s.n.* (B 10 0746887, B 10 0746888), LT995109, LT996394, LT996576; ***Schismatoglottis calyptrata*** (Roxb.) Zoll. & Moritzi, ARA059, DB 29617, Cultivated, *Schwerdtfeger 10946* (B 10 0746864), LT995000, LT996285, LT996467; ***Spathiphyllum blandum*** Schott, ARA218, DB 29776, Guatemala, *Welz s.n.* (B 10 0746883, B 10 0746884), LT995103, LT996388, LT996570; ***Urospatha sagittifolia*** (Rudge) Schott, ARA065, DB 29623, Venezuela, *Große s.n.* (B 10 0394682), LT995003, LT996288, LT996470; ***Zantedeschia rehmannii*** Engl., ARA219, DB 29777, Cultivated, *s.n.* (B 10 0746892, B 10 0746893), LT995104, LT996389, LT996571; **Ingroup:** ***Adelonema crinipes*** (Engl.) S.Y. Wong & Croat, ARA213, DB 29771, Ecuador, *s.n.* (BG München), LT995098, LT996383, LT996565; ***Adelonema peltatum*** (Mast.) S.Y. Wong & Croat, ARA249, DB 29807, Colombia, *M. Celis DC600* (JBB), LT995115, LT996400, LT996582; ***Adelonema picturatum*** (Linden & André) S.Y. Wong & Croat, ARA248, DB 29806, Colombia, *M. Celis DC735* (JBB), LT995114, LT996399, LT996581; ***Homalomena expedita*** A. Hay & Hersc., ARA211, DB 29769, Malaysia, *Bogner s.n.* (B 10 0746844), LT995096, LT996381, LT996563; ***Homalomena griffithii*** (Schott) Hook. f., ARA212, DB 29770, Malaysia,

Bogner s.n. (B 10 0746845), LT995097, LT996382, LT996564; ***Homalomena rubescens*** (Roxb.) Kunth, ARA063, DB 29621, Cultivated, *s.n.* (B 10 0746871, B 10 0746872), LT995001, LT996286, LT996468; ***Philodendron*** **subgenus** ***Meconostigma***: ***Philodendron adamantinum*** Mart. ex Schott, ARA125, DB 29683, Cultivated, *T.B. Croat 90271* (MO 2295367), LT995038, LT996323, LT996505; ***Philodendron speciosum*** Schott ex Endl., ARA079, DB 29637, Cultivated, *s.n.* (B 10 0746914, B 10 0746915), LT995007, LT996292, LT996474; ***Philodendron stenolobum*** E.G. Gonç., ARA190, DB 29748, Brazil: Espírito Santo, *T.B. Croat 98074* (MO 2037712, MO 2037713), LT995083, LT996368, LT996550; ***Philodendron*** **subgenus** ***Philodendron****:* ***Philodendron*** **×** ***domesticum*** G.S. Bunting, ARA015, DB 29573, Cultivated, *s.n.* (B 10 0746940, B 10 0746941, B 10 0746942, B 10 0746943), LT994977, LT996262, LT996444; ***Philodendron acutatum*** Schott, ARA048, DB 29606, Brazil: Amazonas, *Chmelar s.n.* (B 10 0746863), LT994995, LT996280, LT996462; ***Philodendron acutatum*** Schott, ARA123, DB 29681, Guyana, *T.B. Croat 101623* (MO 2119734, MO 2119735), LT995036, LT996321, LT996503; ***Philodendron acutifolium*** K. Krause, ARA124, DB 29682, Ecuador, *T.B. Croat 75430* (MO 1213762, MO 1473271, MO 2922694), LT995037, LT996322, LT996504; ***Philodendron*** **aff.** ***hastatum*** K.Koch & Sello, ARA031, DB 29589, Costa Rica, *Cl. Horich s.n.* (B 10 0746903, B 10 0746904), LT994988, LT996273, LT996455; ***Philodendron amargalense*** Croat & M.M. Mora, ARA250, DB 29808, Colombia, *M. Celis DC509* (JBB), LT995116, LT996401, LT996583; ***Philodendron asplundii*** Croat & M.L. Soares, ARA100, DB 29658, Ecuador, *M. Schwerdtfeger 96082127* (B 10 0746894), LT995019, LT996304, LT996486; ***Philodendron attenuatum*** Croat, ARA129, DB 29687, Ecuador, *T.B. Croat 87076* (MO 1349740), LT995041, LT996326, LT996508; ***Philodendron auriculatum*** Standl. & L.O. Williams, ARA131, DB 29689, Costa Rica, *T.B. Croat 32956* (MO 1021900, MO 1021907, MO 1021909), LT995042, LT996327, LT996509; ***Philodendron bakeri*** Croat & Grayum, ARA007, DB 29565, Costa Rica, *Cl. Horich s.n.* (B 10 0054992), LT994971, LT996256, LT996438; ***Philodendron bakeri*** Croat & Grayum, ARA090, DB 29648, Costa Rica, *Cl. Horich s.n.* (B 10 0747000), LT995012, LT996297, LT996479; ***Philodendron billietiae*** Croat, ARA056, DB 29614, French Guiana, *F. Billiet 5740* (B 10 0120370, B 10 0120371, B 10 0120372, B 10 0120373), LT994999, LT996284, LT996466; ***Philodendron bipennifolium*** Schott, ARA033, DB 29591, Costa Rica, *Cl. Horich s.n.* (B 10 0715023), LT994989, LT996274, LT996456; ***Philodendron bipennifolium*** Schott, ARA119, DB 29677, Malaysia?, *s.n.* (B 10 0746850), LT995033, LT996318, LT996500; ***Philodendron bonifaziae*** Croat, ARA172, DB 29730, Ecuador, *T.B. Croat 82295* (MO 1600968), LT995070, LT996355, LT996537; ***Philodendron borgesii*** G.S. Bunting, ARA132, DB 29690, Venezuela, *T.B. Croat 54957* (MO 1241116, MO 2353654, MO 2353655), LT995043, LT996328, LT996510; ***Philodendron brandtianum*** K. Krause, ARA133, DB 29691, Bolivia, *T.B. Croat 84556* (MO 1241202), LT995044, LT996329, LT996511; ***Philodendron burle-marxii*** G.M. Barroso, ARA105, DB 29663, Colombia, *Leppard 1396* (B 10 0746858), LT995021, LT996306, LT996488; ***Philodendron callosum*** K. Krause, ARA052, DB 29610, Venezuela, *Lohse 88-G-267* (B 10 0746862), LT994997, LT996282, LT996464; ***Philodendron callosum*** K. Krause, ARA166, DB 29724, French Guiana, *T.B. Croat 103536* (MO 2353064, MO 2353065), LT995065, LT996350, LT996532; ***Philodendron carinatum*** E.G. Gonç., ARA236, DB 29794, French Guiana, *N. Köster 2908* (B 10 0746973), LT995113, LT996398, LT996580; ***Philodendron*** **cf.** ***acutatum*** Schott, ARA134, DB 29692, Brazil, *T.B. Croat 53585* (MO 2295369), LT995045, LT996330, LT996512; ***Philodendron*** **cf.** ***acutatum*** Schott, ARA184, DB 29742, Cultivated, *T.B. Croat 72007* (MO 2295374), LT995077, LT996362, LT996544; ***Philodendron*** **cf.** ***attenuatum*** Croat, ARA188, DB 29746, Ecuador, *T.B. Croat 75374* (MO 2353880, MO 2744116), LT995081,

LT996366, LT996548; ***Philodendron* cf. *barrosoanum*** G.S. Bunting, ARA002, DB 29560, Venezuela, *Lohse s.n.* (B), LT994968, LT996253, LT996435; *Philodendron cf. bipennifolium* Schott, ARA135, DB 29693, French Guiana, *T.B. Croat 103036* (MO 2295370), LT995046, LT996331, LT996513; ***Philodendron* cf. *curvilobum*** Schott, ARA111, DB 29669, Cultivated, *s.n.* (B 10 0746902), LT995026, LT996311, LT996493; ***Philodendron* cf. *giganteum*** Schott, ARA143, DB 29701, Cultivated, *s.n.* (MO), LT995049, LT996334, LT996516; ***Philodendron* cf. *lehmannii*** Engl., ARA162, DB 29720, Cultivated, *T.B. Croat 100572* (MO 2295371), LT995062, LT996347, LT996529; ***Philodendron* cf. *mayoi*** E.G. Gonç., ARA168, DB 29726, Cultivated, *T.B. Croat 101523* (MO 2295372), LT995067, LT996352, LT996534; ***Philodendron* cf. *megalophyllum*** Schott, ARA096, DB 29654, Colombia, *Bauer s.n.* (B 10 0746909), LT995016, LT996301, LT996483; ***Philodendron* cf. *mexicanum*** Engl., ARA027, DB 29585, Cultivated, *s.n.* (B 10 0746927, B 10 0746928, B 10 0746929, B 10 0746930, B 10 0746931), LT994985, LT996270, LT996452; ***Philodendron* cf. *mexicanum*** Engl., ARA089, DB 29647, Costa Rica, *G. Schoser s.n.* (B 10 0746926), LT995011, LT996296, LT996478; ***Philodendron* cf. *muricatum*** Willd. ex Schott, ARA186, DB 29744, Venezuela, *T.B. Croat 95562A* (MO 2295364), LT995079, LT996364, LT996546; ***Philodendron* cf. *parvilobum*** Croat, ARA205, DB 29763, Ecuador, *T.B. Croat 87310* (MO 1356780), LT995092, LT996377, LT996559; ***Philodendron* cf. *pokigronense*** Croat, ARA178, DB 29736, Suriname, *T.B. Croat 102167* (MO 2119940, MO 2119941, MO 2119942), LT995075, LT996360, LT996542; ***Philodendron consanguineum*** Schott, ARA216, DB 29774, Cuba, *T. Borsch et al. 5259* (B 10 0746848), LT995101, LT996386, LT996568; ***Philodendron cordatum*** Kunth ex Schott, ARA017, DB 29575, Cultivated, *s.n.* (B 10 0746936, B 10 0746937), LT994979, LT996264, LT996446; ***Philodendron crassinervium*** Lindl., ARA087, DB 29645, Cultivated, *s.n.* (B 10 0746861), LT995009, LT996294, LT996476; ***Philodendron cuneatum*** Engl., ARA199, DB 29757, Colombia, *T.B. Croat 80926* (MO 1219664, MO 1219665), LT995087, LT996372, LT996554; ***Philodendron delannayi*** Croat, ARA177, DB 29735, Ecuador, *T.B. Croat 83113A* (MO 2295365), LT995074, LT996359, LT996541; ***Philodendron deltoideum*** Poepp., ARA004, DB 29562, Cultivated, *s.n.* (B 10 0746952, B 10 0746953), LT994969, LT996254, LT996436; ***Philodendron distantilobum*** K. Krause, ARA204, DB 29762, Bolivia, *T.B. Croat 84546* (MO 1219440, MO 1219441), LT995091, LT996376, LT996558; ***Philodendron dodsonii*** Croat & Grayum, ARA141, DB 29699, Ecuador, *T.B. Croat 82065* (MO 1240418, MO 1240419), LT995048, LT996333, LT996515; ***Philodendron ecordatum*** Schott, ARA114, DB 29672, French Guiana, *A.L. Haigh, S.J. Mayo & D. Barabé 8* (K000099735), LT995028, LT996313, LT996495; ***Philodendron elegans*** K. Krause, ARA042, DB 29600, Cultivated, *s.n.* (B 10 0746944, B 10 0746945, B 10 0746946, B 10 0746947), LT994992, LT996277, LT996459; ***Philodendron elegans*** K. Krause, ARA088, DB 29646, Cultivated, *s.n.* (B 10 0746860), LT995010, LT996295, LT996477; ***Philodendron ernestii*** Engl., ARA109, DB 29667, Ecuador, *Davis s.n.* (B 10 0746856), LT995024, LT996309, LT996491; ***Philodendron esmeraldense*** Croat, ARA259, DB 29817, Colombia, *M. Celis DC527* (JBB), LT995118, LT996403, LT996585; ***Philodendron fendleri*** K. Krause, ARA200, DB 29758, Venezuela, *Manfred Speckmaier s.n.* (BG Wien), LT995088, LT996373, LT996555; ***Philodendron ferrugineum*** Croat, ARA146, DB 29704, Panama, *T.B. Croat 76607* (MO 1073120), LT995050, LT996335, LT996517; ***Philodendron fibrosum*** Sodiro ex Croat, ARA260, DB 29818, Colombia, *M. Celis DC671* (JBB), LT995119, LT996404, LT996586; ***Philodendron fragrantissimum*** (Hook.) G. Don, ARA108, DB 29666, Brazil: Bahia, *Leppard s.n.* (B 10 0746857), LT995023, LT996308, LT996490; ***Philodendron geniculatum*** Bogner & Croat, ARA046, DB 29604, Cultivated, *s.n.* (B 10 0479859, B 10 0479860), LT994994, LT996279, LT996461; ***Philodendron giganteum***

Schott, ARA016, DB 29574, Guadeloupe: Basse Terre., *Urban s.n.* (B 10 0746938, B 10 0746939), LT994978, LT996263, LT996445; ***Philodendron gloriosum*** André, ARA018, DB 29576, Cultivated, *s.n.* (B 10 0746846), LT994980, LT996265, LT996447; ***Philodendron gloriosum*** André, ARA038, DB 29596, Cultivated, *s.n.* (B 10 0746916, B 10 0746917, B 10 0746918, B 10 0746919), LT994991, LT996276, LT996458; ***Philodendron grandifolium*** (Jacq.) Schott, ARA067, DB 29625, French Guiana, *Leuenberger & Hagemann s.n.* (GH 28047, 50301), LT995005, LT996290, LT996472; ***Philodendron grandipes*** K. Krause, ARA150, DB 29708, Cultivated, *s.n.* (MO), LT995051, LT996336, LT996518; ***Philodendron grazielae*** G.S. Bunting, ARA024, DB 29582, Cultivated, *s.n.* (B 10 0746933), LT994984, LT996269, LT996451; ***Philodendron hannoniae*** Croat, ARA151, DB 29709, Ecuador, *T.B. Croat 82294* (MO 2744386), LT995052, LT996337, LT996519; ***Philodendron hastatum*** K.Koch & Sello, ARA049, DB 29607, Cultivated, *GH 27664, 35596* (B 10 0746958, B 10 0746959, B 10 0746956, B 10 0746955, B 10 0746954), LT994996, LT996281, LT996463; ***Philodendron hebetatum*** Croat, ARA264, DB 29822, Colombia, *M. Celis DC492* (JBB), LT995120, LT996405, LT996587; ***Philodendron hebetatum*** Croat, ARA265, DB 29823, Colombia, *M. Celis DC564* (JBB), LT995121, LT996406, LT996588; ***Philodendron hederaceum*** (Jacq.) Schott, ARA112, DB 29670, Cultivated, *s.n.* (B 10 0746854), LT995027, LT996312, LT996494; ***Philodendron holtonianum*** Schott, ARA154, DB 29712, Colombia, *T.B. Croat & P.A. Silverstone-Sopkin 98000* (MO 2330378, MO 2330379), LT995054, LT996339, LT996521; ***Philodendron hylaeae*** G.S. Bunting, ARA155, DB 29713, French Guiana, *T.B. Croat 102857* (MO 2119964, MO 2119965), LT995055, LT996340, LT996522; ***Philodendron insigne*** Schott, ARA157, DB 29715, Venezuela, *R.L. Liesner 19121* (MO 1255387), LT995057, LT996342, LT996524; ***Philodendron jacquinii*** Schott, ARA214, DB 29772, Cuba, *T. Borsch et al. 5200* (B 10 0746849), LT995099, LT996384, LT996566; ***Philodendron joaosilvae*** Croat, A. Cardoso & Moonen, ARA223, DB 29781, French Guiana, *N. Köster 2905* (B 10 0746970), LT995106, LT996391, LT996573; ***Philodendron krugii*** Engl., ARA116, DB 29674, Trinidad and Tobago, *S.J. Mayo 148* (B 10 0746852), LT995030, LT996315, LT996497; ***Philodendron lacerum*** (Jacq.) Schott, ARA215, DB 29773, Cuba, *T. Borsch et al. 5258* (B 10 0605979, B 10 06055980, B 10 06055981), LT995100, LT996385, LT996567; ***Philodendron laticiferum*** Croat & M.M. Mora, ARA160, DB 29718, Colombia, *T.B. Croat 83719* (MO 1310744), LT995060, LT996345, LT996527; ***Philodendron lazorii*** Croat, ARA161, DB 29719, Panama, *T.B. Croat 69833* (MO 1073704, MO 1073705, MO 150445, MO 150446, MO 150447), LT995061, LT996346, LT996528; ***Philodendron ligulatum*** Schott, ARA163, DB 29721, Panama, *T.B. Croat 77041* (MO 1072715), LT995063, LT996348, LT996530; ***Philodendron lindenii*** Schott, ARA164, DB 29722, Venezuela, *T.B. Croat 54879* (MO 1243547), LT995064, LT996349, LT996531; ***Philodendron linnaei*** **var. *linnaei*** Kunth, ARA023, DB 29581, Cultivated, *s.n.* (B 10 0746934, B 10 0746935), LT994983, LT996268, LT996450; ***Philodendron longistilum*** K. Krause, ARA283, DB 29841, Colombia, *M. Celis DC710* (JBB), LT995123, LT996408, LT996590; ***Philodendron lucasiorum*** **sp. nov. ined**. Croat, ARA224, DB 29782, French Guiana, *N. Köster 2904* (B 10 0746971), LT995107, LT996392, LT996574; ***Philodendron lynamii*** **sp. nov. ined**. Croat, ARA167, DB 29725, Peru, *T.B. Croat 58107* (MO 1259014, MO 1281954, MO 1473193), LT995066, LT996351, LT996533; ***Philodendron mamei*** André, ARA011, DB 29569, Cultivated, *s.n.* (B 10 0746950, B 10 0746951), LT994974, LT996259, LT996441; ***Philodendron martianum*** Engl., ARA008, DB 29566, Venezuela, *Große s.n.* (B 10 0746900, B 10 0746901), LT994972, LT996257, LT996439; ***Philodendron megalophyllum*** Schott, ARA140, DB 29698, Venezuela, *T.B. Croat 54252* (MO 1243829), LT995047, LT996332, LT996514; ***Philodendron megalophyllum*** Schott, ARA187, DB 29745, Suriname, *T.B. Croat 61123*

(MO 1255683), LT995080, LT996365, LT996547; ***Philodendron melanochrysum*** Linden & André, ARA030, DB 29588, Cultivated, *s.n.* (B 10 0746922), LT994987, LT996272, LT996454; ***Philodendron melanoneuron*** Croat, ARA169, DB 29727, Ecuador, *T.B. Croat 93354* (MO 1211671, MO 1211672), LT995068, LT996353, LT996535; ***Philodendron melinonii*** Brongn. ex Regel, ARA225, DB 29783, French Guiana, *N. Köster 2893* (B 10 0746847), LT995108, LT996393, LT996575; ***Philodendron microstictum*** Standl. & L.O. Williams, ARA093, DB 29651, Costa Rica, *Cl. Horich s.n.* (B 10 0746912), LT995014, LT996299, LT996481; ***Philodendron moonenii*** Croat, ARA171, DB 29729, French Guiana, *T.B. Croat 103359* (MO 2330190, MO 2330191), LT995069, LT996354, LT996536; ***Philodendron nangaritense*** **sp. nov. ined.** Croat, ARA173, DB 29731, Ecuador, *T.B. Croat 98757* (MO 2295373), LT995071, LT996356, LT996538; ***Philodendron ornatum*** Schott, ARA110, DB 29668, Brazil: Espirito Santo, *J. Plummer 214* (B 10 0746855), LT995025, LT996310, LT996492; ***Philodendron pastazanum*** K. Krause, ARA076, DB 29634, Cultivated, *s.n.* (B 10 0543096, B 10 0543097), LT995006, LT996291, LT996473; ***Philodendron pedatum*** (Hook.) Kunth, ARA115, DB 29673, Peru, *s.n.* (B 10 0746853), LT995029, LT996314, LT996496; ***Philodendron pinnatifidum*** (Jacq.) Schott, ARA228, DB 29786, French Guiana, *N. Köster 2906* (B 10 0746972), LT995110, LT996395, LT996577; ***Philodendron pseudauriculatum*** Croat, ARA179, DB 29737, Panama, *T.B. Croat 33526* (MO 1072916, MO 1072917, MO 1072918, MO 1072919), LT995076, LT996361, LT996543; ***Philodendron purulhense*** Croat, ARA019, DB 29577, Guatemala, *A. Rieger 22* (B 10 0746961), LT994981, LT996266, LT996448; ***Philodendron renauxii*** Reitz, ARA012, DB 29570, Cultivated, *s.n.* (B 10 0746992, B 10 0746993, B 10 0746994), LT994975, LT996260, LT996442; ***Philodendron rugosum*** Bogner & G.S. Bunting, ARA028, DB 29586, Ecuador, *J. Brenner s.n.* (B 10 0746924, B 10 0746925), LT994986, LT996271, LT996453; ***Philodendron sagittifolium*** Liebm., ARA006, DB 29564, Costa Rica, *Cl. Horich s.n.* (B 10 0746979, B 10 0746980, B 10 0746981, B 10 0746974), LT994970, LT996255, LT996437; ***Philodendron sagittifolium*** Liebm., ARA036, DB 29594, Costa Rica, *Cl. Horich s.n.* (B 10 0746975, B 10 0171515), LT994990, LT996275, LT996457; ***Philodendron sagittifolium*** Liebm., ARA156, DB 29714, Panama, *T.B. Croat 67111* (MO 1072462, MO 1072463), LT995056, LT996341, LT996523; ***Philodendron schmidtiae*** Croat & Cerón, ARA117, DB 29675, Ecuador, *Hodgson s.n.* (B 10 0746851), LT995031, LT996316, LT996498; ***Philodendron scottmorianum*** Croat & Moonen, ARA185, DB 29743, French Guiana, *T.B. Croat 33531* (MO 993600, MO 993603), LT995078, LT996363, LT996545; ***Philodendron simsii*** (Hook.) Sweet ex Kunth, ARA094, DB 29652, Trinidad and Tobago, *Cubr (Köster) 50971* (B 10 0746910, B 10 0746911), LT995015, LT996300, LT996482; ***Philodendron smithii*** Engl., ARA203, DB 29761, Mexico, *T.B. Croat 40079* (MO 440740, MO 440741, MO 440764), LT995090, LT996375, LT996557; ***Philodendron sodiroi*** N.E.Br., ARA201, DB 29759, Cultivated, *s.n.* (MO KBCC 7234), LT995089, LT996374, LT996556; ***Philodendron sp.***, ARA101, DB 29659, *s.n.* (B 10 0746859), LT995020, LT996305, LT996487; ***Philodendron sp***., ARA126, DB 29684, Cultivated, *T.B. Croat 90166* (MO 2295368), LT995039, LT996324, LT996506; ***Philodendron sp.***, ARA127, DB 29685, Venezuela, *T.B. Croat 69765* (MO 2119513, MO 2119514), LT995040, LT996325, LT996507; ***Philodendron sp.,*** ARA153, DB 29711, Peru, *T.B. Croat 81921* (MO 1243265), LT995053, LT996338, LT996520; ***Philodendron sp.***, ARA159, DB 29717, Brazil: Rio de Janeiro, *T.B. Croat 71917* (MO 1255444, MO 1255445, MO 2500795), LT995059, LT996344, LT996526; ***Philodendron sp.***, ARA189, DB 29747, Cultivated, *T.B. Croat 101529* (MO 2295375), LT995082, LT996367, LT996549; ***Philodendron*** **sp. nov. aff.** ***renauxii***, ARA122, DB 29680, Brazil: Santa Catarina, *S.J. Mayo, A.K. Mayo, H.C. de Lima & P.R. Reitz 578* (B 10

0746960, K001239981, K001239982), LT995035, LT996320, LT996502; ***Philodendron sparreorum*** Croat, ARA305, DB 29863, Colombia, *M. Celis DC706* (JBB), LT995124, LT996409, LT996591; ***Philodendron squamiferum*** Poepp., ARA054, DB 29612, Cultivated, *GH 14523*, (B 10 0746923), LT994998, LT996283, LT996465; ***Philodendron subhastatum*** K.Krause, ARA045, DB 29603, Cultivated, *s.n.* (B 10 0746983, B 10 0746989, B 10 0746988, B 10 0746991, B 10 0746990), LT994993, LT996278, LT996460; ***Philodendron subincisum*** Schott, ARA191, DB 29749, Cultivated, *T.B. Croat 107788* (MO 2295363), LT995084, LT996369, LT996551; ***Philodendron tenue*** K. Koch & Augustin, ARA158, DB 29716, Panama, *T.B. Croat 38039* (MO 1073657), LT995058, LT996343, LT996525; ***Philodendron tortum*** M.L. Soares & Mayo, ARA013, DB 29571, Cultivated, *s.n.* (B 10 0746948, B 10 0746949), LT994976, LT996261, LT996443; ***Philodendron tripartitum*** (Jacq.) Schott, ARA020, DB 29578, Cultivated, *s.n.* (B 10 0746965, B 10 0746966, B 10 0746967), LT994982, LT996267, LT996449; ***Philodendron tripartitum*** (Jacq.) Schott, ARA118, DB 29676, Mexico: Chiapas, *S.J. Mayo 26* (B 10 0746899), LT995032, LT996317, LT996499; ***Philodendron uleanum*** Engl., ARA106, DB 29664, Ecuador, *Hodgson 51* (B 10 0746895), LT995022, LT996307, LT996489; ***Philodendron ushanum*** Croat & Moonen, ARA207, DB 29765, French Guiana, *T.B. Croat 102968* (MO 2119961), LT995093, LT996378, LT996560; ***Philodendron verrucosum*** L. Mathieu ex Schott, ARA092, DB 29650, Panama, *R. Mangelsdorff RMP 265* (B 10 0746913), LT995013, LT996298, LT996480; ***Philodendron werkhoveniae*** Croat, ARA196, DB 29754, Suriname, *T.B. Croat 79413* (MO 1295132), LT995085, LT996370, LT996552; ***Philodendron wilburii*** **var.** ***longipedunculatum*** Croat & Grayum, ARA197, DB 29755, Panama, *T.B. Croat 77083* (MO 1043267), LT995086, LT996371, LT996553; ***Philodendron*** **subgenus** ***Pteromischum: Philodendron*** **cf.** ***guttiferum*** Kunth, ARA080, DB 29638, Ecuador, *M. Schwerdtfeger s.n.* (B 10 0715002, B 10 0715003), LT995008, LT996293, LT996475; ***Philodendron divaricatum*** K. Krause, ARA257, DB 29815, Colombia, *M. Celis DC709* (JBB), LT995117, LT996402, LT996584; ***Philodendron gonzalezii*** Grayum, ARA010, DB 29568, Venezuela, *Lohse 96-G-107* (B 10 0413590, B 10 0413591, B 10 0029000, B 10 0028999), LT994973, LT996258, LT996440; ***Philodendron ichthyoderma*** Croat & Grayum, ARA274, DB 29832, Colombia, *M. Celis DC559* (JBB), LT995122, LT996407, LT996589; ***Philodendron palaciosii*** Croat & Grayum, ARA174, DB 29732, Ecuador, *L. Hannon 96-108* (MO 1691144), LT995072, LT996357, LT996539; ***Philodendron sonderianum*** Schott, ARA121, DB 29679, Brazil: Parana, *G. Hatschbach 46079* (K001183368), LT995034, LT996319, LT996501; ***Philodendron sp.*** **(Pteromischum)**, ARA209, DB 29767, French Guiana, *N. Köster 2872* (B 10 0746968), LT995094, LT996379, LT996561; ***Philodendron sp.*** **(Pteromischum)**, ARA210, DB 29768, French Guiana, *N. Köster 2873*, (B 10 0746969), LT995095, LT996380, LT996562.

Appendix A2. Maximum clade credibility trees obtained in BEAST. (a) Tree obtained with three secondary constraints (nodes 28, 109 and 113). Values above branches correspond to the Posterior probability.

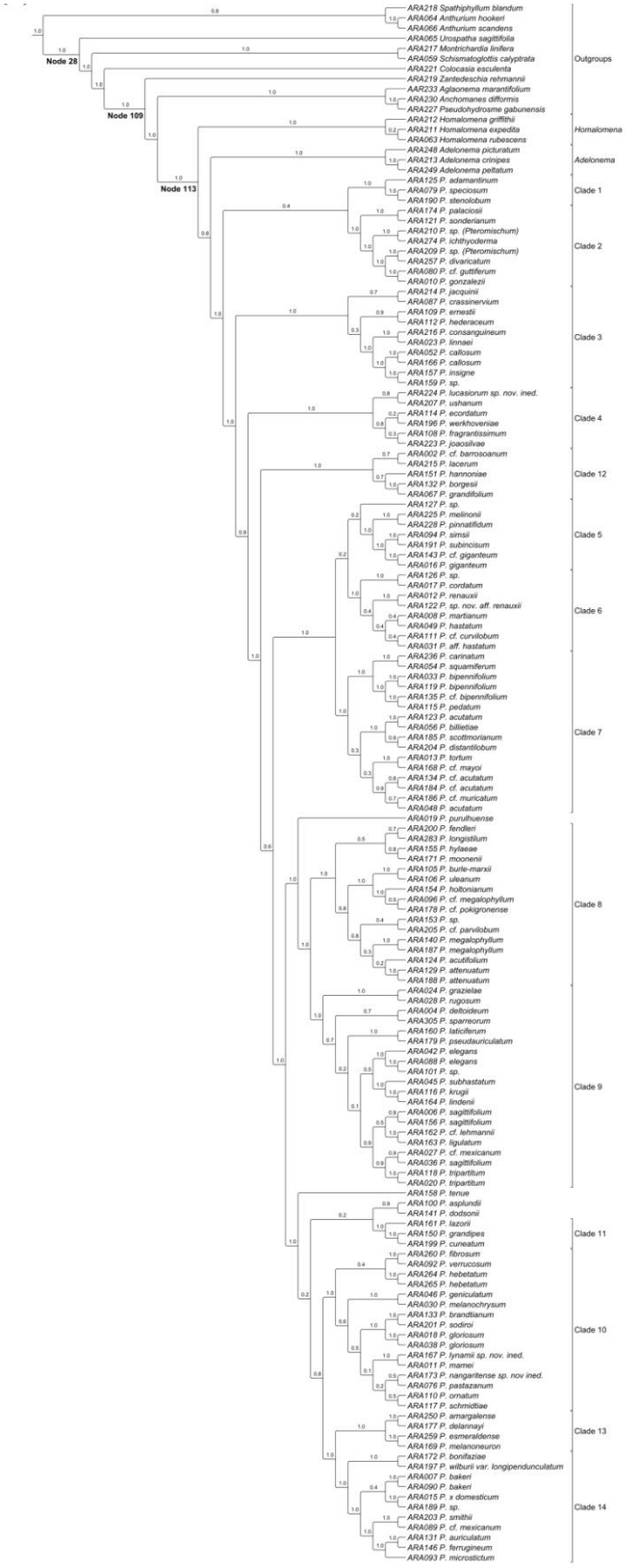

Appendix A2. (b) Tree obtained with a fossil constraint (*Montrichardia aquatica*) and a single secondary constraint (node 113). Values above branches correspond to the Posterior probability. NA, Not applicable.

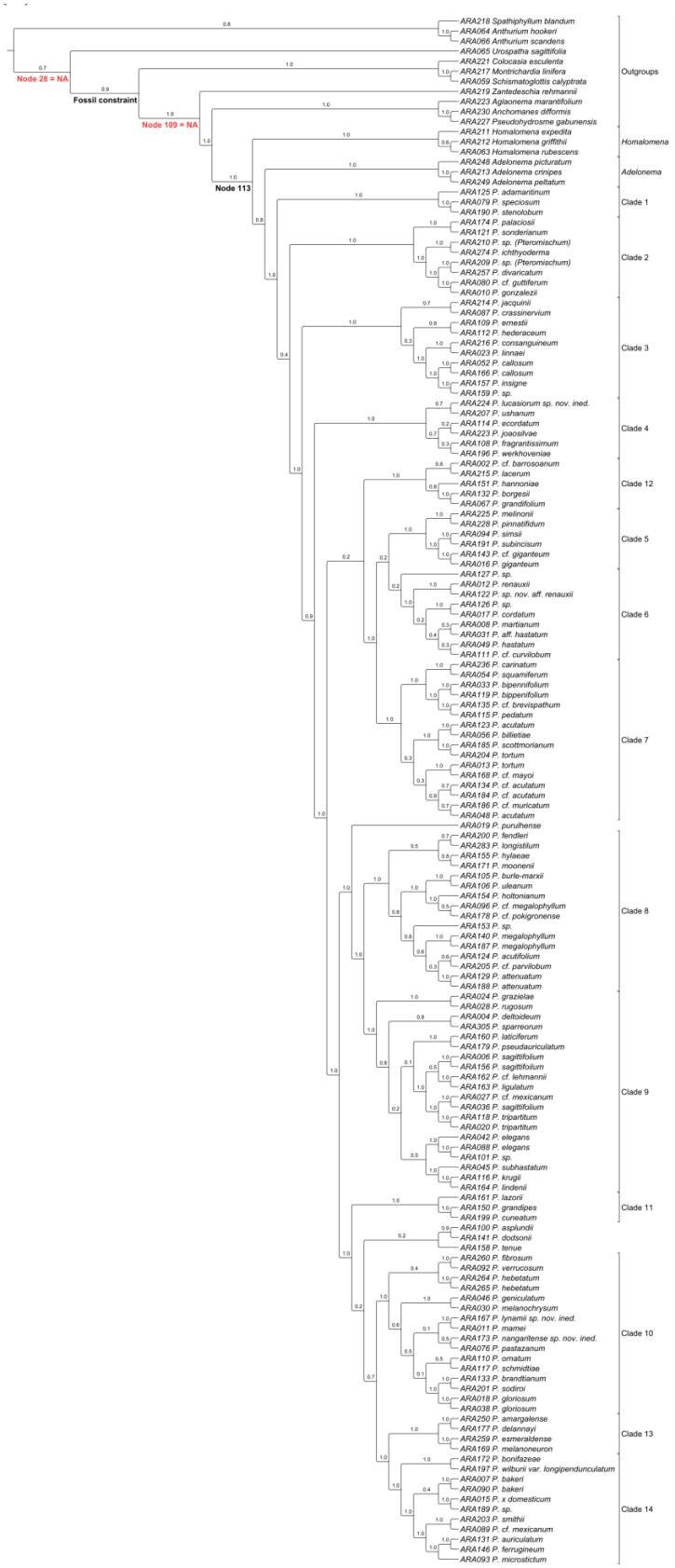

Appendix A3. Summary of character statistics, evolutionary models and trees statistics for each dataset under maximum parsimony, maximum likelihood, and Bayesian inference. [a] The number of accessions included for each data matrix was *N*=154. [b] Including the corresponding indel coded matrix. [c] L: length of the most parsimonious tree; CI: consistency index; RI: retention index. [d] The number of moderate to strong supported nodes by ≥75 maximum parsimony - MP (Jack-knife), ≥75 maximum likelihood - ML (Bootstrap) and ≥0.95 Bayesian inference - BI (Posterior probability). [1] Combined matrix of *petD, rpl16* and *trnK/matK*. [2] Models of sequence evolution obtained for each partition were maintained as described in the row Substitution model (BI analyses).

	petD	***rpl16***	***trnK/matK***	**Combined plastid DNA[1]**
Aligned length[a]	1107	1185	2912	5204
No. variable sites[b]	263	480	825	1566
MP analyses				
No. parsimony-informative sites[b]	135	204	414	753
No. MP trees	161	186	95	100
L[c]	374	719	1308	2436
CI[c]	0.781	0.769	0.716	0.730
RI[c]	0.873	0.851	0.833	0.835
No. supp. nodes[d]	18	24	46	70
ML analyses				
Substitution model	GTR + Γ	GTR + Γ	GTR + Γ	GTR + Γ
No. supp. nodes[d]	23	34	56	70
BI analyses				
Partition	*petB* Spacer *petD* 5' exon *petD* intron	*rpl16* intron	*matK* *trnK* 3' exon *trnK* 3' intron *trnK* 5' intron	8
Substitution model	TVM + I F81 TPM1uf + Γ	TIM2 + Γ	TVM + I + Γ JC TVM + I TPM1uf + Γ	Partitioned[2]
No. supp. nodes[c]	29	39	71	90

Appendix A4. Maximum clade credibility (MCC) chronogram obtained in BEAST based on three plastid markers (*petD*, *rpl16*, and *trnK/matK*) with age estimates with three secondary calibration constraints. Time intervals in millions of years ago are indicated by black circles. Geologic time scale is indicated by the orange gradient band. Light green star corresponds to the fossil point to a specific node referred to in the text. Light violet star corresponds to secondary calibration point to a specific node referred to in the text. Refer to Table 2.3 for details of %HPD values for divergence-time estimates.

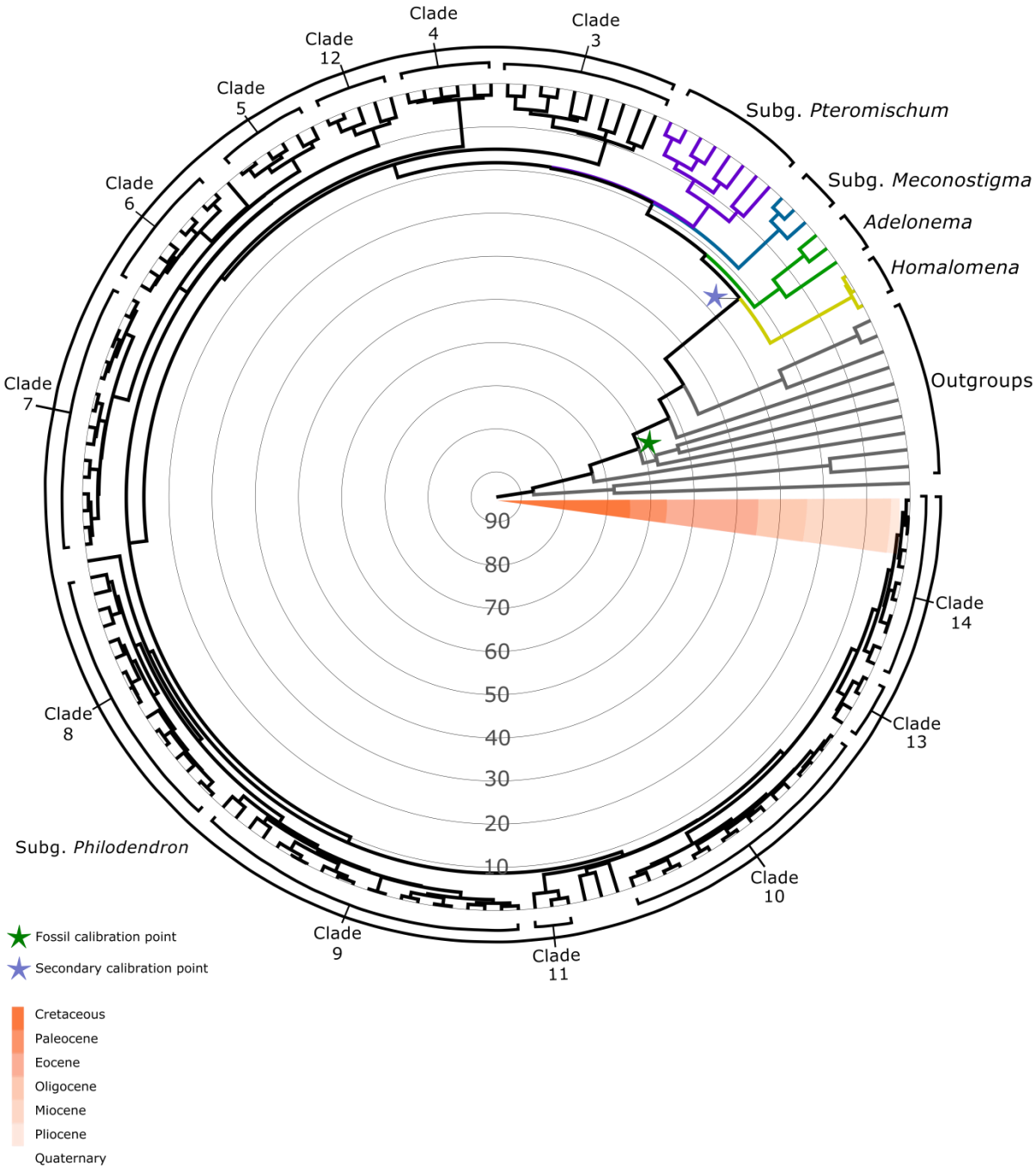

Appendix A5. Effective sample sizes (ESS) of the log-likelihood and the number of shift events using two different calibration approaches in BAMM.

Calibration approach	**ESS of the Log-likelihood**	**ESS of the number of shift events**
Fossil+secondary calibration	706.04	750.35
Secondary calibration	726.73	794.99

Appendix A6. Rate shift configurations within the 95% credible sets obtained in BAMM. (a) 95% credible set obtained with the BEAST MCC tree under the fossil+secondary calibration approach. (b) 95% credible set obtained with the BEAST MCC tree under the secondary calibration approach.

(a)

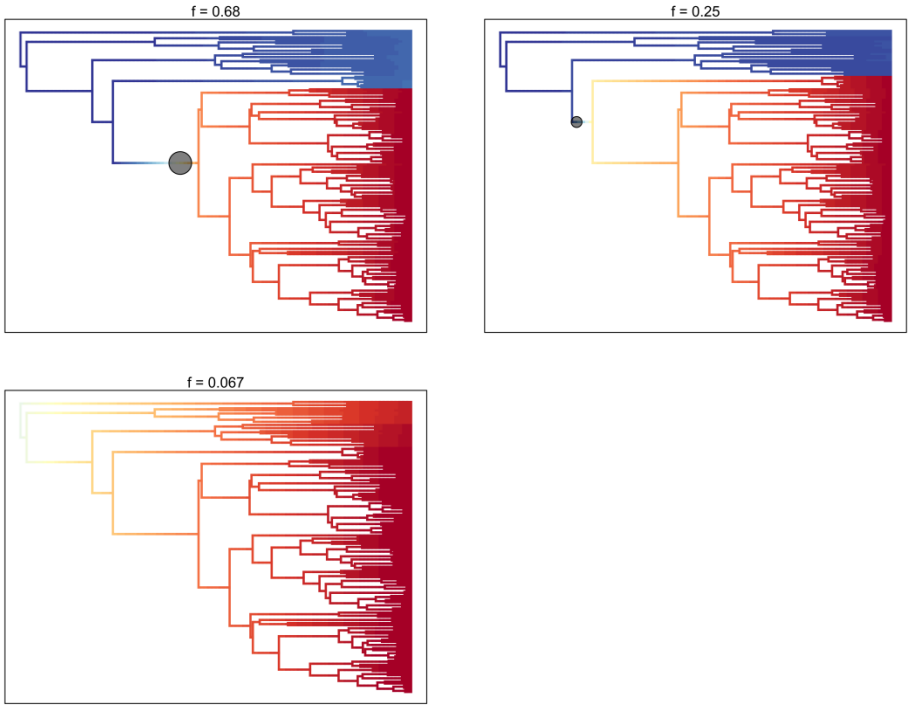

(b)

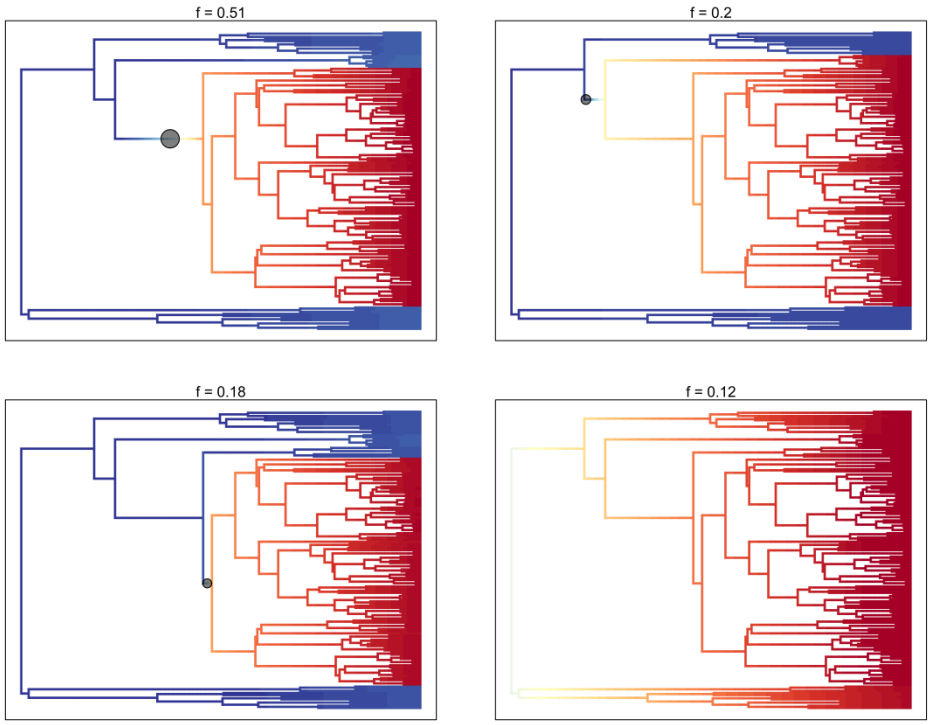

Appendix A6. (Continued) (c) 95% credible set obtained with the BEAST MCC tree under the secondary calibration approach with a proportion of 0.5 for the sampling fraction of each subgenus. (d) 95% credible set obtained with the BEAST MCC tree under the secondary calibration approach with a proportion of 0.05 for the sampling fraction of each subgenus.

(c)

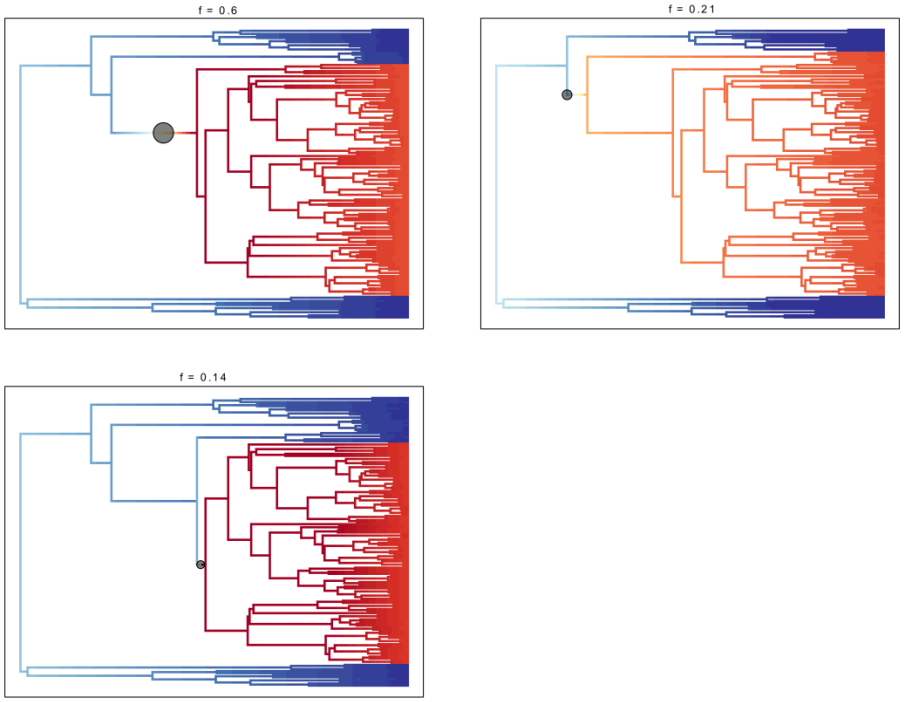

(d)

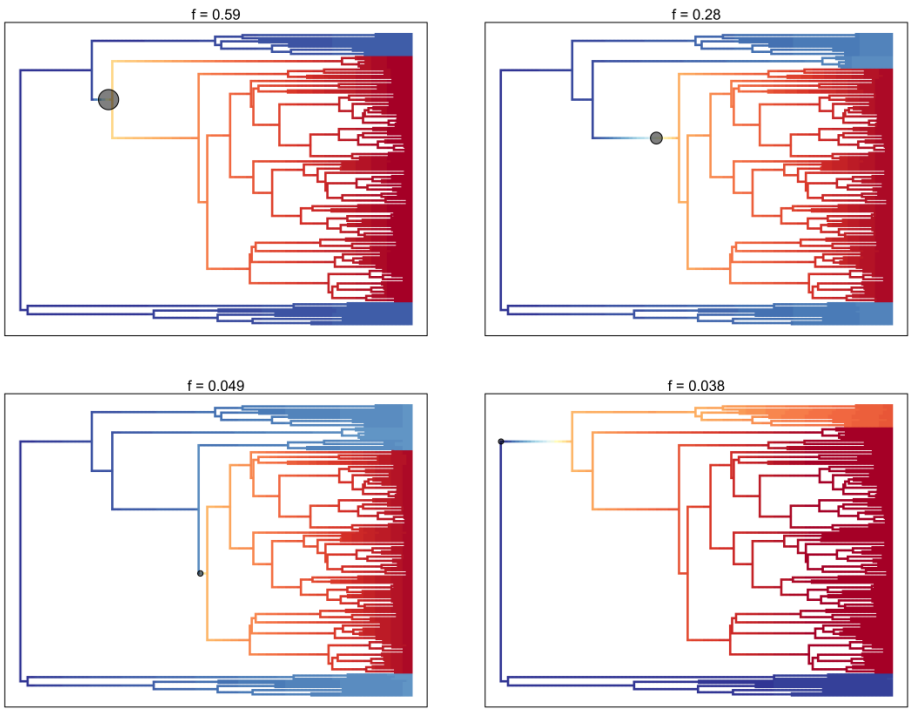

Appendix B. Supplementary material for Chapter 3

Appendix B1. Taxa used for molecular data and their details (Taxon, ID, DNA bank number, locality/provenience of sample, collector(s) and collector number, specimen voucher and NCBI accession numbers for *trnK/matK*, *rpl16* and *petD*, respectively). Sequences newly generated have hyphen (-) for accessions numbers. Accessions that could not be identified to species level were submitted to NBCI with the abbreviation *sp*. followed by the code DC2018 and an alphabetic character. Herbaria acronyms for voucher locations follow Index Herbariorum (Thiers, B. [continuously updated]. Index Herbariorum: A global directory of public herbaria and associated staff. New York Botanical Garden's Virtual Herbarium. http://sweetgum.nybg.org/science/ih/). Species names are used following Govaerts et al. (2018). Accessions are listed in alphabetic order. Abbreviations: s.n. = sine numero (without number).

Outgroup: ***Aglaonema marantifolium***, ARA233, DB 29791, (B 10 0746890, B 10 0746891), *Cubr 30432*, Cultivated in Botanical Garden of Berlin, LT995112, LT996397, LT996579; ***Anchomanes difformis***, ARA230, DB 29788, (B 10 0746889), *Ern, Hein & Pircher 195*, Togo, LT995111, LT996396, LT996578; ***Anthurium hookeri***, ARA064, DB 29622, (B 10 0746885, B 10 0746886), *Schwerdtfeger 21482*, Cultivated in Botanical Garden of Berlin, LT995002, LT996287, LT996469; ***Anthurium scandens***, ARA066, DB 29624, (B 10 0746880, B 10 0746881, B 10 0746882), *s.n.*, Mexico, LT995004, LT996289, LT996471; ***Colocasia esculenta***, ARA221, DB 29779, (B 10 0746875, B 10 0746876), *s.n.*, Cultivated in Botanical Garden of Berlin, LT995105, LT996390, LT996572; ***Montrichardia linifera***, ARA217, DB 29775, (B 10 0746877, B 10 0746878, B 10 0746879), *Koenen 153a*, Colombia, LT995102, LT996387, LT996569; ***Pseudohydrosme gabunensis***, ARA227, DB 29785, (B 10 0715006, B 10 0715007), *s.n.*, Gabun, LT995109, LT996394, LT996576; ***Schismatoglottis calyptrata***, ARA059, DB 29617, (B 10 0746864), *Schwerdtfeger 10946*, Cultivated in the Botanical Garden of Berlin, LT995000, LT996285, LT996467; ***Spathiphyllum blandum***, ARA218, DB 29776, (B 10 0191040, B 10 0191041), *Welz s.n.*, Guatemala, LT995103, LT996388, LT996570; ***Urospatha sagittifolia***, ARA065, DB 29623, (B 10 0394682), *Große s.n.*, Venezuela, LT995003, LT996288, LT996470; ***Zantedeschia rehmannii***, ARA219, DB 29777, (B 10 0746892, B 10 0746893), *s.n.*, Cultivated in Botanical Garden of Berlin, LT995104, LT996389, LT996571. **Ingroup*:*** ***Adelonema crinipes***, ARA213, DB 29771, (BG München), *s.n.*, Ecuador, LT995098, LT996383, LT996565; ***Adelonema peltatum***, ARA249, DB 29807, (UNO), *M. Celis DC 600*, Colombia, LT995115, LT996400, LT996582; ***Adelonema picturatum***, ARA248, DB 29806, (UNO), *M. Celis DC 735*, Colombia, LT995114, LT996399, LT996581; ***Adelonema speariae***, ARA344, DB 29902, (B 10), *Elaine Spear s.n.*, -, -, -, -; ***Homalomena* cf. *lancifolia***, ARA346, DB 29904, (B 10), *s.n.*, -, -, -, -; ***Homalomena expedita***, ARA211, DB 29769, (B 10 0746844), *Bogner s.n.*, Malaysia, LT995096, LT996381, LT996563; ***Homalomena griffithii***, ARA212, DB 29770, (B 10 0746845), *Bogner s.n.*, Malaysia, LT995097, LT996382, LT996564; ***Homalomena humilis***, ARA347, DB 29905, (B 10), -, -, -, -, -; ***Homalomena rubescens***, ARA063, DB 29621, (B 10 0746871, B 10 0746872), *s.n.*, Cultivated in Botanical Garden of Berlin, LT995001, LT996286, LT996468; ***Philodendron* subgenus *Meconostigma***: ***Philodendron pseudoundulatum***, ARA360,

DB 29918, (B 10 0746977, B 10 0746978), *U. Urban s.n.*, -, -, -, -; ***Philodendron adamantinum***, ARA125, DB 29683, (MO-2295367), *T.B. Croat 90271*, Unknown, LT995038, LT996323, LT996505; ***Philodendron saxicola***, ARA229, DB 29787, (B 10 0746889), *N. Köster 2909*, -, -, -, -; ***Philodendron uliginosum***, ARA371, DB 29929, (B 10 0746870), *J. Bogner s.n.*, - , -, -, -; ***Philodendron stenolobum***, ARA190, DB 29748, (MO-2037712, MO-2037713), *T.B. Croat 98074*, Brazil: Espírito Santo, LT995083, LT996368, LT996550; ***Philodendron speciosum***, ARA079, DB 29637, (B 10 0746914, B 10 0746915), *s.n.*, Cultivated in Botanical Garden of Berlin, LT995007, LT996292, LT996474; ***Philodendron speciosum***, ARA361, DB 29919, (B 10), -, -, -, -, -; ***Philodendron* subgenus *Philodendron***: ***Philodendron* × *domesticum***, ARA015, DB 29573, (B 10 0746940, B 10 0746941, B 10 0746942, B 10 0746943), *s.n.*, Cultivated in Botanical Garden of Berlin, LT994977, LT996262, LT996444; ***Philodendron acutatum***, ARA048, DB 29606, (B 10 0746863), *Chmelar s.n.*, Brazil: Amazonas, LT994995, LT996280, LT996462; ***Philodendron acutatum***, ARA123, DB 29681, (MO-2119734, MO-2119735), *T.B. Croat 101623*, Guyana, LT995036, LT996321, LT996503; ***Philodendron acutatum***, ARA365, DB 29923, (B 10), -, -, -, -, -; ***Philodendron acutifolium***, ARA124, DB 29682, (MO-1213762, MO-1473271, MO-2922694), *T.B. Croat 75430*, Ecuador, LT995037, LT996322, LT996504; ***Philodendron* aff. *hastatum***, ARA031, DB 29589, (B 10 0746903, B 10 0746904), *Cl. Horich, s.n.*, Costa Rica, LT994988, LT996273, LT996455; ***Philodendron* aff. *tenue***, ARA327, DB 29885, (UNO), *M. Celis DC 727*, Colombia, -, -, -; ***Philodendron alatiundulatum***, ARA349, DB 29907, (MO-), *T.B. Croat 106676*, -, -, -, -; ***Philodendron amargalense***, ARA250, DB 29808, (UNO), *M. Celis DC 509*, Colombia, LT995116, LT996401, LT996583; ***Philodendron anisotomum***, ARA398, DB 29956, (B 10 0746905), -, -, -, -, -; ***Philodendron asplundii***, ARA100, DB 29658, (B 10 0746894), *M. Schwerdtfeger 96082127*, Ecuador, LT995019, LT996304, LT996486; ***Philodendron attenuatum***, ARA129, DB 29687, (MO-1349740), *T.B. Croat 87076*, Ecuador, LT995041, LT996326, LT996508; ***Philodendron auriculatum***, ARA131, DB 29689, (MO-1021900, MO-1021907, MO-1021909), *T.B. Croat 32956*, Costa Rica, LT995042, LT996327, LT996509; ***Philodendron bakeri***, ARA007, DB 29565, (B 10 0054992), *Cl. Horich, s.n.*, Costa Rica, LT994971, LT996256, LT996438; ***Philodendron bakeri***, ARA090, DB 29648, (B 10 0747000), *Cl. Horich, s.n.*, Costa Rica, LT995012, LT996297, LT996479; ***Philodendron barrosoanum***, ARA251, DB 29809, (UNO), *M. Celis DC 726*, -, -, -, -; ***Philodendron billietiae***, ARA056, DB 29614, (B 10 0120370, B 10 0120371, B 10 0120372, B 10 0120373), *F. Billiet 5740*, French Guiana, LT994999, LT996284, LT996466; ***Philodendron billietiae***, ARA334, DB 29892, (B 10 0746907), *N. Köster 2882*, -, -, -, -; ***Philodendron billietiae***, ARA335, DB 29893, (B 10 0746906), *N. Köster 2898*, -, -, -, -; ***Philodendron bipennifolium***, ARA033, DB 29591, (B 10 0715023), *Cl. Horich, s.n.*, Costa Rica, LT994989, LT996274, LT996456; ***Philodendron bipennifolium***, ARA119, DB 29677, (B 10 0746850), *s.n.*, Malaysia?, LT995033, LT996318, LT996500; ***Philodendron bonifaziae***, ARA172, DB 29730, (MO-1600968), *T.B. Croat 82295*, Ecuador, LT995070, LT996355, LT996537; ***Philodendron borgesii***, ARA132, DB 29690, (MO-1241116, MO-2353654, MO-2353655), *T.B. Croat 54957*, Venezuela, LT995043, LT996328, LT996510; ***Philodendron brandtianum***, ARA133, DB 29691, (MO-1241202), *T.B. Croat 84556*, Bolivia, LT995044, LT996329, LT996511; ***Philodendron burle-marxii***, ARA105, DB 29663, (B 10 0746858), *Leppard 1396*, Colombia, LT995021, LT996306, LT996488; ***Philodendron callosum***, ARA052, DB 29610, (B 10 0746862), *Lohse 88-G-267*, Venezuela, LT994997, LT996282, LT996464; ***Philodendron callosum***, ARA166, DB 29724, (MO-2353064, MO-2353065), *T.B. Croat 103536*, French Guiana, LT995065, LT996350, LT996532; ***Philodendron callosum***, ARA362, DB 29920, (B 10), *B.E. Leuenberger & I. Hagemann s.n.*, -, -, -, -;

Philodendron camposportoanum, ARA367, DB 29925, (B 10 0746976), *P. Ibisch s.n.*, -, -, -, -; ***Philodendron carinatum***, ARA236, DB 29794, (B 10 0746973), *N. Köster 2908*, French Guiana, LT995113, LT996398, LT996580; ***Philodendron* cf. *acutatum***, ARA134, DB 29692, (MO-2295369), *T.B. Croat 53585*, Brazil, LT995045, LT996330, LT996512; ***Philodendron* cf. *acutatum***, ARA184, DB 29742, (MO-2295374), *T.B. Croat 72007*, Cultivated in Missouri Botanical Garden, LT995077, LT996362, LT996544; ***Philodendron* cf. *attenuatum***, ARA188, DB 29746, (MO-2353880, MO-2744116), *T.B. Croat 75374*, Ecuador, LT995081, LT996366, LT996548; ***Philodendron* cf. *barrosoanum***, ARA002, DB 29560, (GH-Beleg 40167), *Lohse s.n.*, Venezuela, LT994968, LT996253, LT996435; ***Philodendron* cf. *bipennifolium***, ARA135, DB 29693, (MO-2295370), *T.B. Croat 103036*, French Guiana, LT995046, LT996331, LT996513; ***Philodendron* cf. *bipennifolium***, ARA240, DB 29798, (B 10 0746908), *N. Köster 2899*, -, -, -, -; ***Philodendron* cf. *cuneatum***, ARA256, DB 29814, (UNO), *M. Celis DC 646*, -, -, -, -; ***Philodendron* cf. *curvilobum***, ARA111, DB 29669, (B 10 0746902), *s.n.*, -, LT995026, LT996311, LT996493; ***Philodendron* cf. *giganteum***, ARA143, DB 29701, (MO-), *s.n.*, Unknown, LT995049, LT996334, LT996516; ***Philodendron* cf. *juninense***, ARA279, DB 29837, (UNO), *M. Celis DC 712*, Colombia, -, -, -; ***Philodendron* cf. *laticiferum***, ARA280, DB 29838, (UNO), *M. Celis DC 451*, Colombia, -, -, -; ***Philodendron* cf. *laticiferum***, ARA292, DB 29850, (UNO), *M. Celis DC 506*, Colombia, -, -, -; ***Philodendron* cf. *lehmannii***, ARA162, DB 29720, (MO-2295371), *T.B. Croat 100572*, Cultivated at the Missouri Botanical Garden, LT995062, LT996347, LT996529; ***Philodendron* cf. *mayoi***, ARA168, DB 29726, (MO-2295372), *T.B. Croat 101523*, Unknown, LT995067, LT996352, LT996534; ***Philodendron* cf. *megalophyllum***, ARA096, DB 29654, (B 10 0746909), *Bauer s.n.*, Colombia, LT995016, LT996301, LT996483; ***Philodendron* cf. *megalophyllum***, ARA366, DB 29924, (B 10), *J. Nieder 193*, -, -, -, -; ***Philodendron* cf. *mexicanum***, ARA027, DB 29585, (B 10 0746927, B 10 0746928, B 10 0746929, B 10 0746930, B 10 0746931), *s.n.*, Cultivated in Botanical Garden of Berlin, LT994985, LT996270, LT996452; ***Philodendron* cf. *mexicanum***, ARA089, DB 29647, (B 10 0746926), *G. Schoser, s.n.*, Costa Rica, LT995011, LT996296, LT996478; ***Philodendron* cf. *montanum***, ARA353, DB 29911, (MO-), *T.B. Croat 106685*, -, -, -, -; ***Philodendron* cf. *muricatum***, ARA186, DB 29744, (MO-2295364), *T.B. Croat 95562A*, Venezuela, LT995079, LT996364, LT996546; ***Philodendron* cf. *parvilobum***, ARA205, DB 29763, (MO-1356780), *T.B. Croat 87310*, Ecuador, LT995092, LT996377, LT996559; ***Philodendron* cf. *pokigronense***, ARA178, DB 29736, (MO-2119940, MO-2119941, MO-2119942), *T.B. Croat 102167*, Suriname, LT995075, LT996360, LT996542; ***Philodendron* cf. *serpens***, ARA302, DB 29860, (UNO), *M. Celis DC 682*, Colombia, -, -, -; ***Philodendron* cf. *viride***, ARA352, DB 29910, (MO-), *T.B. Croat 106684*, -, -, -; ***Philodendron* cf. *wurdackii***, ARA332, DB 29890, (UNO), *M. Celis DC 728*, Colombia, -, -, -; ***Philodendron consanguineum***, ARA216, DB 29774, (B 10 0746848), *T. Borsch et al. 5259*, Cuba, LT995101, LT996386, LT996568; ***Philodendron cordatum***, ARA017, DB 29575, (B 10 0746936, B 10 0746937), *s.n.*, Cultivated in Botanical Garden of Berlin, LT994979, LT996264, LT996446; ***Philodendron crassinervium***, ARA087, DB 29645, (B 10 0746861), *s.n.*, Cultivated, LT995009, LT996294, LT996476; ***Philodendron crassinervium***, ARA376, DB 29934, (B 10 0746905), *S.J. Mayo 215*, -, -, -; ***Philodendron cuneatum***, ARA199, DB 29757, (MO-1219664, MO-1219665), *T.B. Croat 80926*, Colombia, LT995087, LT996372, LT996554; ***Philodendron cuneatum***, ARA254, DB 29812, (UNO), *M. Celis DC 575*, -, -, -; ***Philodendron delannayi***, ARA177, DB 29735, (MO-2295365), *T.B. Croat 83113A*, Ecuador, LT995074, LT996359, LT996541; ***Philodendron deltoideum***, ARA004, DB 29562, (B 10 0746952, B 10 0746953), *GH-Beleg 10918*, Cultivated in Botanical Garden of Berlin, LT994969, LT996254, LT996436;

Philodendron distantilobum, ARA204, DB 29762, (MO-1219440, MO-1219441), *T.B. Croat 84546*, Bolivia, LT995091, LT996376, LT996558; ***Philodendron distantilobum***, ARA359, DB 29917, (B 10 0605633), -, -, -, -; ***Philodendron dodsonii***, ARA141, DB 29699, (MO-1240418, MO-1240419), *T.B. Croat 82065*, Ecuador, LT995048, LT996333, LT996515; ***Philodendron ecordatum***, ARA114, DB 29672, (K000099735), *A.L. Haigh, S.J. Mayo & D. Barabé 8*, French Guiana, LT995028, LT996313, LT996495; ***Philodendron ecordatum***, ARA241, DB 29799, (B 10 0746889), *N. Köster 2870*, -, -, -, -; ***Philodendron elegans***, ARA042, DB 29600, (B 10 0746944, B 10 0746945, B 10 0746946, B 10 0746947), *s.n.*, Cultivated in Botanical Garden of Berlin, LT994992, LT996277, LT996459; ***Philodendron elegans***, ARA088, DB 29646, (B 10 0746860), *s.n.*, Cultivated, LT995010, LT996295, LT996477; ***Philodendron ernestii***, ARA109, DB 29667, (B 10 0746856), *Davis s.n.*, Ecuador, LT995024, LT996309, LT996491; ***Philodendron esmeraldense***, ARA259, DB 29817, (UNO), *M. Celis DC 527*, Colombia, LT995118, LT996403, LT996585; ***Philodendron eximium***, ARA402, DB 29960, (B 10 0746905), -, -, -, -; ***Philodendron fendleri***, ARA200, DB 29758, (BG Wien), *Manfred Speckmaier s.n.*, Venezuela, LT995088, LT996373, LT996555; ***Philodendron ferrugineum***, ARA146, DB 29704, (MO-1073120), *T.B. Croat 76607*, Panama, LT995050, LT996335, LT996517; ***Philodendron fibrosum***, ARA260, DB 29818, (UNO), *M. Celis DC 671*, Colombia, LT995119, LT996404, LT996586; ***Philodendron fragrantissimum***, ARA108, DB 29666, (B 10 0746857), *Leppard s.n.*, Brazil: Bahia, LT995023, LT996308, LT996490; ***Philodendron fragrantissimum***, ARA243, DB 29801, (B 10 0746889), *N. Köster 2889*, -, -, -, -; ***Philodendron fragrantissimum***, ARA261, DB 29819, (UNO), *M. Celis DC 429*, Colombia, -, -, -; ***Philodendron geniculatum***, ARA046, DB 29604, (B 10 0479859, B 10 0479860), *s.n.*, Cultivated in Botanical Garden of Berlin, LT994994, LT996279, LT996461; ***Philodendron giganteum***, ARA016, DB 29574, (B 10 0746938, B 10 0746939), *Urban s.n.*, Guadeloupe: Basse Terre., LT994978, LT996263, LT996445; ***Philodendron glaziovii***, ARA369, DB 29927, (B 10 0746870), *Cubr (Köster) 50709*, -, -, -, -; ***Philodendron glaziovii***, ARA375, DB 29933, (B 10 0746870), *J. Plummer 144*, -, -, -, -; ***Philodendron gloriosum***, ARA018, DB 29576, (B 10 0746846), *s.n.*, Cultivated in Botanical Garden of Berlin, LT994980, LT996265, LT996447; ***Philodendron gloriosum***, ARA038, DB 29596, (B 10 0746916, B 10 0746917, B 10 0746918, B 10 0746919), *s.n.*, Cultivated in Botanical Garden of Berlin, LT994991, LT996276, LT996458; ***Philodendron grandifolium***, ARA067, DB 29625, (GH-Beleg 28047, 50301), *Leuenberger & Hagemann s.n.*, French Guiana, LT995005, LT996290, LT996472; ***Philodendron grandifolium***, ARA242, DB 29800, (B 10 0746889), *N. Köster 2881*, -, -, -, -; ***Philodendron grandipes***, ARA150, DB 29708, (MO-), *s.n.*, Unknown, LT995051, LT996336, LT996518; ***Philodendron grandipes***, ARA262, DB 29820, (UNO), *M. Celis DC 452*, Colombia, -, -, -; ***Philodendron grazielae***, ARA024, DB 29582, (B 10 0746933), *s.n.*, Cultivated in Botanical Garden of Berlin, LT994984, LT996269, LT996451; ***Philodendron hannoniae***, ARA151, DB 29709, (MO-2744386), *T.B. Croat 82294*, Ecuador, LT995052, LT996337, LT996519; ***Philodendron hastatum***, ARA049, DB 29607, (B 10 0746958, B 10 0746959, B 10 0746956, B 10 0746955, B 10 0746954), *GH-Beleg 27664, 35596*, Cultivated in Botanical Garden of Berlin, LT994996, LT996281, LT996463; ***Philodendron hebetatum***, ARA264, DB 29822, (UNO), *M. Celis DC 492*, Colombia, LT995120, LT996405, LT996587; ***Philodendron hebetatum***, ARA265, DB 29823, (UNO), *M. Celis DC 564*, Colombia, LT995121, LT996406, LT996588; ***Philodendron hederaceum***, ARA112, DB 29670, (B 10 0746854), *s.n.*, LT995027, LT996312, LT996494; ***Philodendron heleniae* ssp. *amazonense***, ARA271, DB 29829, (UNO), *M. Celis DC 730*, Colombia, -, -, -; ***Philodendron heleniae* ssp. *heleniae***, ARA272, DB 29830, (UNO), *M. Celis DC 460*, Colombia, -, -, -; ***Philodendron holtonianum***, ARA154, DB 29712, (MO-2330378,

MO-2330379), *T.B. Croat & P.A. Silverstone-Sopkin 98000*, Colombia, LT995054, LT996339, LT996521; ***Philodendron hylaeae***, ARA155, DB 29713, (MO-2119964, MO-2119965), *T.B. Croat 102857*, French Guiana, LT995055, LT996340, LT996522; ***Philodendron hylaeae***, ARA336, DB 29894, (B 10), *N. Köster 2903*, -, -, -, -; ***Philodendron insigne***, ARA157, DB 29715, (MO-1255387), *R.L. Liesner 19121*, Venezuela, LT995057, LT996342, LT996524; ***Philodendron jacquinii***, ARA214, DB 29772, (B 10 0746849), *T. Borsch et al. 5200*, Cuba, LT995099, LT996384, LT996566; ***Philodendron joaosilvae***, ARA223, DB 29781, (B 10 0746970), *N. Köster 2905*, French Guiana, LT995106, LT996391, LT996573; ***Philodendron jodavisianum***, ARA277, DB 29835, (UNO), *M. Celis DC 465*, Colombia, -, -, -; ***Philodendron krugii***, ARA116, DB 29674, (B 10 0746852), *S.J. Mayo 148*, Trinidad and Tobago, LT995030, LT996315, LT996497; ***Philodendron lacerum***, ARA215, DB 29773, (B 10 0605979, B 10 06055980, B 10 06055981), *T. Borsch et al. 5258*, Cuba, LT995100, LT996385, LT996567; ***Philodendron laticiferum***, ARA160, DB 29718, (MO-1310744), *T.B. Croat 83719*, Colombia, LT995060, LT996345, LT996527; ***Philodendron lazorii***, ARA161, DB 29719, (MO-1073704, MO-1073705, MO-150445, MO-150446, MO-150447), *T.B. Croat 69833*, Panama, LT995061, LT996346, LT996528; ***Philodendron leyvae***, ARA355, DB 29913, (MO-), *T.B. Croat 106687*, -, -, -, -; ***Philodendron ligulatum***, ARA163, DB 29721, (MO-1072715), *T.B. Croat 77041*, Panama, LT995063, LT996348, LT996530; ***Philodendron lindenii***, ARA164, DB 29722, (MO-1243547), *T.B. Croat 54879*, Venezuela, LT995064, LT996349, LT996531; ***Philodendron linnaei var. linnaei***, ARA023, DB 29581, (B 10 0746934, B 10 0746935), *s.n.*, Cultivated in Botanical Garden of Berlin, LT994983, LT996268, LT996450; ***Philodendron longipes***, ARA282, DB 29840, (UNO), *M. Celis DC 576*, Colombia, -, -, -; ***Philodendron longistilum***, ARA283, DB 29841, (UNO), *M. Celis DC 710*, Colombia, LT995123, LT996408, LT996590; ***Philodendron lucasiorum* sp.nov. ined.**, ARA224, DB 29782, (B 10 0746971), *N. Köster 2904*, French Guiana, LT995107, LT996392, LT996574; ***Philodendron lynamii sp. nov. ined.***, ARA167, DB 29725, (MO-1259014, MO-1281954, MO-1473193), *T.B. Croat 58107*, Peru, LT995066, LT996351, LT996533; ***Philodendron lynnhannoniae***, ARA285, DB 29843, (UNO), *M. Celis DC 677*, Colombia, -, -, -; ***Philodendron mamei***, ARA011, DB 29569, (B 10 0746950, B 10 0746951), *s.n.*, Cultivated in Botanical Garden of Berlin, LT994974, LT996259, LT996441; ***Philodendron martianum***, ARA008, DB 29566, (B 10 0746900, B 10 0746901), *Große s.n.*, Venezuela, LT994972, LT996257, LT996439; ***Philodendron megalophyllum***, ARA140, DB 29698, (MO-1243829), *T.B. Croat 54252*, Venezuela, LT995047, LT996332, LT996514; ***Philodendron megalophyllum***, ARA187, DB 29745, (MO-1255683), *T.B. Croat 61123*, Suriname, LT995080, LT996365, LT996547; ***Philodendron megalophyllum***, ARA245, DB 29803, (B 10 0746889), *N. Köster 2867*, -, -, -; ***Philodendron melanochrysum***, ARA030, DB 29588, (B 10 0746922), *s.n.*, Cultivated in Botanical Garden of Berlin, LT994987, LT996272, LT996454; ***Philodendron melanoneuron***, ARA169, DB 29727, (MO-1211671, MO-1211672), *T.B. Croat 93354*, Ecuador, LT995068, LT996353, LT996535; ***Philodendron melinonii***, ARA225, DB 29783, (B 10 0746847), *N. Köster 2893*, French Guiana, LT995108, LT996393, LT996575; ***Philodendron microstictum***, ARA093, DB 29651, (B 10 0746912), *Cl. Horich, s.n.*, Costa Rica, LT995014, LT996299, LT996481; ***Philodendron moonenii***, ARA171, DB 29729, (MO-2330190, MO-2330191), *T.B. Croat 103359*, French Guiana, LT995069, LT996354, LT996536; ***Philodendron nangaritense sp. nov. ined.***, ARA173, DB 29731, (MO-2295373), *T.B. Croat 98757*, Ecuador, LT995071, LT996356, LT996538; ***Philodendron ninoanum***, ARA287, DB 29845, (UNO), *M. Celis DC 524*, Colombia, -, -, -; ***Philodendron oligospermum***, ARA354, DB 29912, (MO-), *T.B. Croat 106686*, -, -, -, -; ***Philodendron ornatum***, ARA110, DB 29668, (B 10 0746855), *J.*

Plummer 214, Brazil: Espirito Santo, LT995025, LT996310, LT996492; ***Philodendron ornatum***, ARA288, DB 29846, (UNO), *M. Celis DC 734*, Colombia, -, -, -; ***Philodendron pastazanum***, ARA076, DB 29634, (B 10 0543096, B 10 0543097), *Cubr (Köster) 49812*, Cultivated in Botanical Garden of Berlin, LT995006, LT996291, LT996473; ***Philodendron patriciae***, ARA289, DB 29847, (UNO), *M. Celis DC 566*, Colombia, -, -, -; ***Philodendron pedatum***, ARA115, DB 29673, (B 10 0746853), *s.n.*, Peru, LT995029, LT996314, LT996496; ***Philodendron pierrelianum***, ARA358, DB 29916, (B 10 0605630), *Cubr (Köster) 50300*, Peru, -, -, -; ***Philodendron pinnatifidum***, ARA228, DB 29786, (B 10 0746972), *N. Köster 2906*, French Guiana, LT995110, LT996395, LT996577; ***Philodendron pinnatifidum***, ARA372, DB 29930, (B 10 0746870) , -, -, -; ***Philodendron platypetiolatum***, ARA290, DB 29848, (UNO), *M. Celis DC 472*, Colombia, -, -, -; ***Philodendron platypetiolatum***, ARA291, DB 29849, (UNO), *M. Celis DC 550*, Colombia, -, -, -; ***Philodendron pseudauriculatum***, ARA179, DB 29737, (MO-1072916, MO-1072917, MO-1072918, MO-1072919), *T.B. Croat 33526*, Panama, LT995076, LT996361, LT996543; ***Philodendron purulhense***, ARA019, DB 29577, (B 10 0746961), *A. Rieger 22*, Guatemala, LT994981, LT996266, LT996448; ***Philodendron radiatum***, ARA364, DB 29922, (B 10 0030787, B 10 0030788, B 10 0030789), -, -, -, -, -; ***Philodendron renauxii***, ARA012, DB 29570, (B 10 0746992, B 10 0746993, B 10 0746994), *s.n.*, Cultivated in Botanical Garden of Berlin, LT994975, LT996260, LT996442; ***Philodendron roseocataphyllum***, ARA296, DB 29854, (UNO), *M. Celis DC 558*, Colombia, -, -, -; ***Philodendron rugosum***, ARA028, DB 29586, (B 10 0746924, B 10 0746925), *J. Brenner s.n.*, Ecuador, LT994986, LT996271, LT996453; ***Philodendron sagittifolium***, ARA006, DB 29564, (B 10 0746979, B 10 0746980, B 10 0746981, B 10 0746974), *Cl. Horich, s.n.*, Costa Rica, LT994970, LT996255, LT996437; ***Philodendron sagittifolium***, ARA036, DB 29594, (B 10 0746975, B 10 0171515), *Cl. Horich, s.n.*, Costa Rica, LT994990, LT996275, LT996457; ***Philodendron sagittifolium***, ARA156, DB 29714, (MO-1072462, MO-1072463), *T.B. Croat 67111*, Panama, LT995056, LT996341, LT996523; ***Philodendron sagittifolium***, ARA297, DB 29855, (UNO), *M. Celis DC 499*, Colombia, -, -, -; ***Philodendron scherberichii***, ARA032, DB 29590, (B 10 0746889), -, -, -, -, -; ***Philodendron schmidtiae***, ARA117, DB 29675, (B 10 0746851), *Hodgson s.n.*, Ecuador, LT995031, LT996316, LT996498; ***Philodendron scottmorianum***, ARA185, DB 29743, (MO-993600), *T.B. Croat 33531*, French Guiana, LT995078, LT996363, LT996545; (MO-993603); ***Philodendron scottmorianum***, ARA340, DB 29898, (B 10), *N. Köster 2884*, -, -, -, -; ***Philodendron simsii***, ARA094, DB 29652, (B 10 0746910, B 10 0746911), *Cubr (Köster) 50971*, Trinidad and Tobago, LT995015, LT996300, LT996482; ***Philodendron smithii***, ARA203, DB 29761, (MO-440740, MO-440741, MO-440764), *T.B. Croat 40079*, Mexico, LT995090, LT996375, LT996557; ***Philodendron sodiroi***, ARA201, DB 29759, (MO-KBCC.7234), *s.n.*, Cultivated in Missouri Botanical Garden, LT995089, LT996374, LT996556; ***Philodendron* sp.**, ARA126, DB 29684, (MO-2295368), *T.B. Croat 90166*, Unknown, LT995039, LT996324, LT996506; ***Philodendron* sp.**, ARA127, DB 29685, (MO-2119513, MO-2119514), *T.B. Croat 69765*, Venezuela, LT995040, LT996325, LT996507; ***Philodendron* sp.**, ARA153, DB 29711, (MO-1243265), *T.B. Croat 81921*, Peru, LT995053, LT996338, LT996520; ***Philodendron* sp.**, ARA159, DB 29717, (MO-1255444, MO-1255445, MO-2500795), *T.B. Croat 71917*, Brazil: Rio de Janeiro, LT995059, LT996344, LT996526; ***Philodendron* sp.**, ARA189, DB 29747, (MO-2295375), *T.B. Croat 101529*, Cultivated in Missouri Botanical Garden, LT995082, LT996367, LT996549; ***Philodendron* sp.**, ARA299, DB 29857, (UNO), *M. Celis DC 647*, Colombia, -, -, -; ***Philodendron sp.***, ARA337, DB 29895, (B 10), *N. Köster 2911*, -, -, -, -; ***Philodendron* sp.**, ARA348, DB 29906, (MO-), *T.B. Croat 106675*, -, -, -, -; ***Philodendron* sp.**, ARA350, DB 29908, (MO-), *T.B. Croat 106677*, -, -, -, -;

Philodendron* sp.**, ARA351, DB 29909, (MO-), *T.B. Croat 106678*, -, -, -, -; ***Philodendron* sp. nov. aff. *renauxii, ARA122, DB 29680, (B 10 0746960, K001239981, K001239982), *S.J. Mayo, A.K. Mayo, H.C. de Lima & P.R. Reitz 578*, Brazil: Santa Catarina, LT995035, LT996320, LT996502; ***Philodendron sparreorum***, ARA305, DB 29863, (UNO), *M. Celis DC 706*, Colombia, LT995124, LT996409, LT996591; ***Philodendron squamicaule***, ARA321, DB 29879, (UNO), *M. Celis DC 560*, Colombia, -, -, -; ***Philodendron squamicaule***, ARA322, DB 29880, (UNO), *M. Celis DC 678*, Colombia, -, -, -; ***Philodendron squamiferum***, ARA202, DB 29760, (MO-2330215), *T.B. Croat 103381*, -, -, -, -; ***Philodendron squamiferum***, ARA341, DB 29899, (B 10), *N. Köster 2876*, -, -, -, -; ***Philodendron squamipetiolatum***, ARA323, DB 29881, (UNO), *M. Celis DC 431*, Colombia, -, -, -; ***Philodendron subhastatum***, ARA045, DB 29603, (B 10 0746983, B 10 0746989, B 10 0746988, B 10 0746991, B 10 0746990), *s.n.*, Cultivated in Botanical Garden of Berlin, LT994993, LT996278, LT996460; ***Philodendron subincisum***, ARA191, DB 29749, (MO-2295363), *T.B. Croat 107788*, Cultivated in Missouri Botanical Garden, LT995084, LT996369, LT996551; ***Philodendron sulcicaule***, ARA325, DB 29883, (UNO), *M. Celis DC 491*, Colombia, -, -, -; ***Philodendron tenue***, ARA158, DB 29716, (MO-1073657), *T.B. Croat 38039*, Panama, LT995058, LT996343, LT996525; ***Philodendron tenue***, ARA303, DB 29861, (UNO), *M. Celis DC 563*, Colombia, -, -, -; ***Philodendron tenue***, ARA304, DB 29862, (UNO), *M. Celis DC 676*, Colombia, -, -, -; ***Philodendron tortum***, ARA013, DB 29571, (B 10 0746948, B 10 0746949), *s.n.*, Cultivated in Botanical Garden of Berlin, LT994976, LT996261, LT996443; ***Philodendron tripartitum***, ARA020, DB 29578, (B 10 0746965, B 10 0746966, B 10 0746967), *s.n.*, Cultivated in Botanical Garden of Berlin, LT994982, LT996267, LT996449; ***Philodendron tripartitum***, ARA118, DB 29676, (B 10 0746899), *S.J. Mayo 26*, Mexico: Chiapas, LT995032, LT996317, LT996499; ***Philodendron tripartitum***, ARA328, DB 29886, (UNO), *M. Celis DC 420*, Colombia, -, -, -; ***Philodendron uleanum***, ARA106, DB 29664, (B 10 0746895), *Hodgson 51*, Ecuador, LT995022, LT996307, LT996489; ***Philodendron ushanum***, ARA207, DB 29765, (MO-2119961), *T.B. Croat 102968*, French Guiana, LT995093, LT996378, LT996560; ***Philodendron venulosum***, ARA329, DB 29887, (UNO), *M. Celis DC 618*, Colombia, -, -, -; ***Philodendron verrucosum***, ARA092, DB 29650, (B 10 0746913), *R. Mangelsdorff RMP 265*, Panama, LT995013, LT996298, LT996480; ***Philodendron verrucosum***, ARA330, DB 29888, (UNO), *M. Celis DC 672*, Colombia, -, -, -; ***Philodendron werkhoveniae***, ARA196, DB 29754, (MO-1295132), *T.B. Croat 79413*, Suriname, LT995085, LT996370, LT996552; ***Philodendron wilburii* var. *longipedunculatum***, ARA197, DB 29755, (MO-1043267), *T.B. Croat 77083*, Panama, LT995086, LT996371, LT996553; ***Philodendron wittianum***, ARA331, DB 29889, (UNO), *M. Celis DC 723*, Colombia, -, -, -; ***Philodendron* subgenus *Pteromischum***: ***Philodendron* cf. *guttiferum***, ARA080, DB 29638, (B 10 0715002, B 10 0715003), *M. Schwerdtfeger s.n.*, Ecuador, LT995008, LT996293, LT996475; ***Philodendron divaricatum***, ARA257, DB 29815, (UNO), *M. Celis DC 709*, Colombia, LT995117, LT996402, LT996584; ***Philodendron gonzalezii***, ARA010, DB 29568, (B 10 0413590, B 10 0413591, B 10 0029000, B 10 0028999), *Lohse 96-G-107*, Venezuela, LT994973, LT996258, LT996440; ***Philodendron ichthyoderma***, ARA274, DB 29832, (UNO), *M. Celis DC 559*, Colombia, LT995122, LT996407, LT996589; ***Philodendron palaciosii***, ARA174, DB 29732, (MO-1691144), *L. Hannon 96-108*, Ecuador, LT995072, LT996357, LT996539; ***Philodendron pierrelianum***, ARA358, DB 29916, (B 10 0605630), *Cubr (Köster) 50300*, Peru, -, -, -; ***Philodendron pteropus***, ARA293, DB 29851, (UNO), *M. Celis DC 725*, Colombia, -, -, -; ***Philodendron sonderianum***, ARA121, DB 29679, (K001183368), *G. Hatschbach 46079*, Brazil: Parana, LT995034, LT996319, LT996501; ***Philodendron* sp. (subgen. *Pteromischum*)**, ARA209, DB 29767, (B 10 0746968), *N. Köster 2872*, French Guiana, LT995094,

LT996379, LT996561; ***Philodendron* sp. (subgen. *Pteromischum*)**, ARA210, DB 29768, (B 10 0746969), *N. Köster 2873*, French Guiana, LT995095, LT996380, LT996562; ***Philodendron* sp. (subgen. *Pteromischum*)**, ARA307, DB 29865, (UNO), *M. Celis DC 450*, Colombia, -, -, -; ***Philodendron* sp. (subgen. *Pteromischum*)**, ARA308, DB 29866, (UNO), *M. Celis DC 462*, Colombia, -, -, -; ***Philodendron* sp. (subgen. *Pteromischum*)**, ARA309, DB 29867, (UNO), *M. Celis DC 463*, Colombia, -, -, -; ***Philodendron* sp. (subgen. *Pteromischum*)**, ARA310, DB 29868, (UNO), *M. Celis DC 556*, Colombia, -, -, -; ***Philodendron* sp. (subgen. *Pteromischum*)**, ARA313, DB 29871, (UNO), *M. Celis DC 617*, Colombia, -, -, -; ***Philodendron* sp. (subgen. *Pteromischum*)**, ARA314, DB 29872, (UNO), *M. Celis DC 623*, Colombia, -, -, -; ***Philodendron* sp. (subgen. *Pteromischum*)**, ARA315, DB 29873, (UNO), *M. Celis DC 645*, Colombia, -, -, -; ***Philodendron* sp. (subgen. *Pteromischum*)**, ARA318, DB 29876, (UNO), *M. Celis DC 708*, Colombia, -, -, -; ***Philodendron* sp. (subgen. *Pteromischum*)**, ARA319, DB 29877, (UNO), *M. Celis DC 715*, Colombia, -, -, -; ***Philodendron* sp. (subgen. *Pteromischum*)**, ARA320, DB 29878, (UNO), *M. Celis DC 737*, Colombia, -, -, -; ***Philodendron* sp. (subgen. *Pteromischum*)**, ARA333, DB 29891, (B 10), *N. Köster 2902*, -, -, -, -; ***Philodendron* sp. (subgen. *Pteromischum*)**, ARA356, DB 29914, (CUVC), *A. Zuluaga 1751*, Colombia, -, -, -; ***Philodendron surinamense***, ARA342, DB 29900, (B 10), *N. Köster 2878*, -, -, -, .

Appendix B2. Maximum clade credibility tree obtained in BEAST based on three plastid regions (*petD, rpl16* and *trnK/matK*) with age estimates with three secondary calibration constraints. Time intervals in million years ago (mya) are indicated by black circles. Geological time scale is indicated by the orange gradient band. Light violet stars correspond to the secondary calibration points referred in the text. Clades 1-12 correspond to subgenus *Philodendron.*

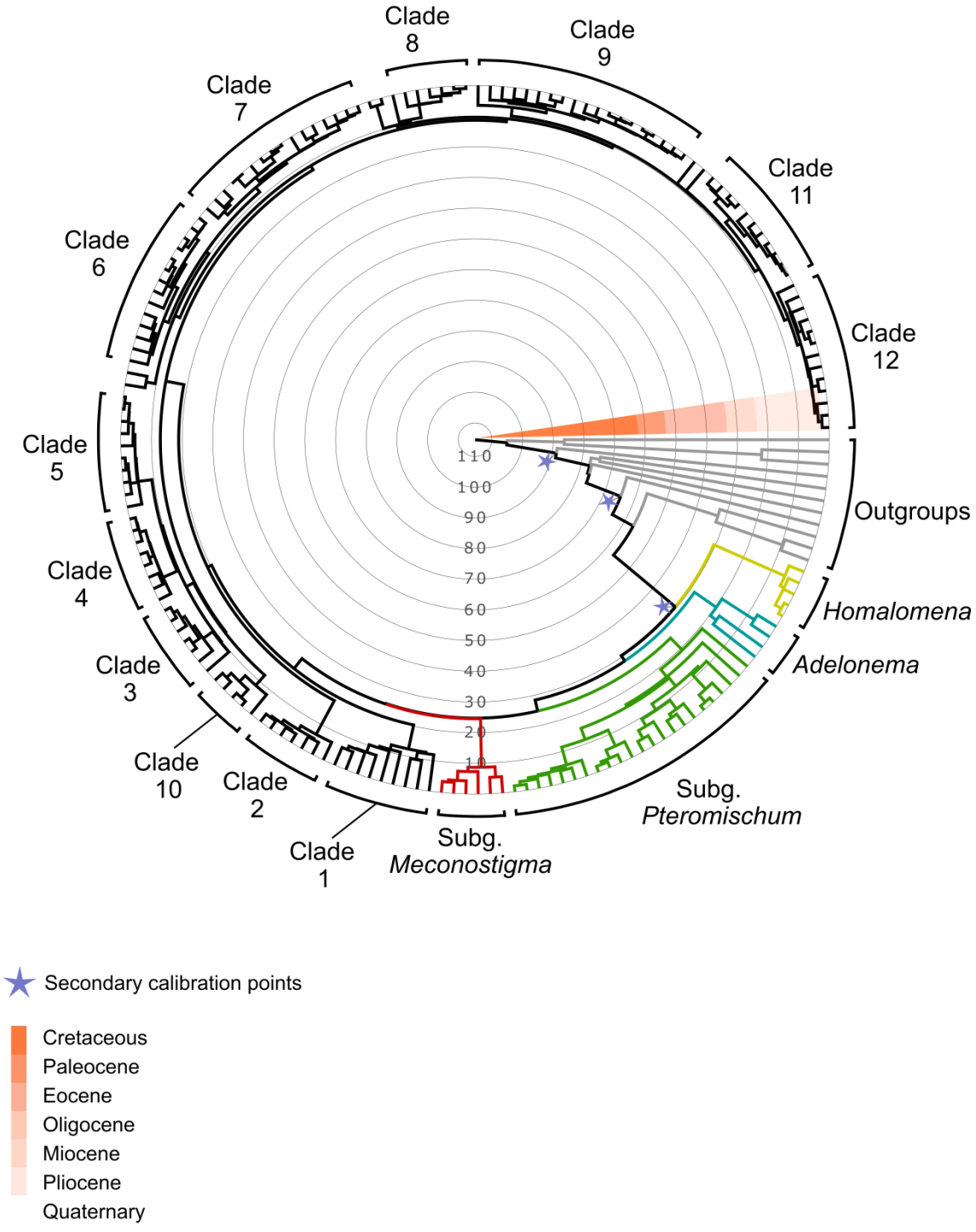

Appendix B3. Null distribution of dAIC obtained from randomly shuffled geographic distribution data of *Philodendron*.

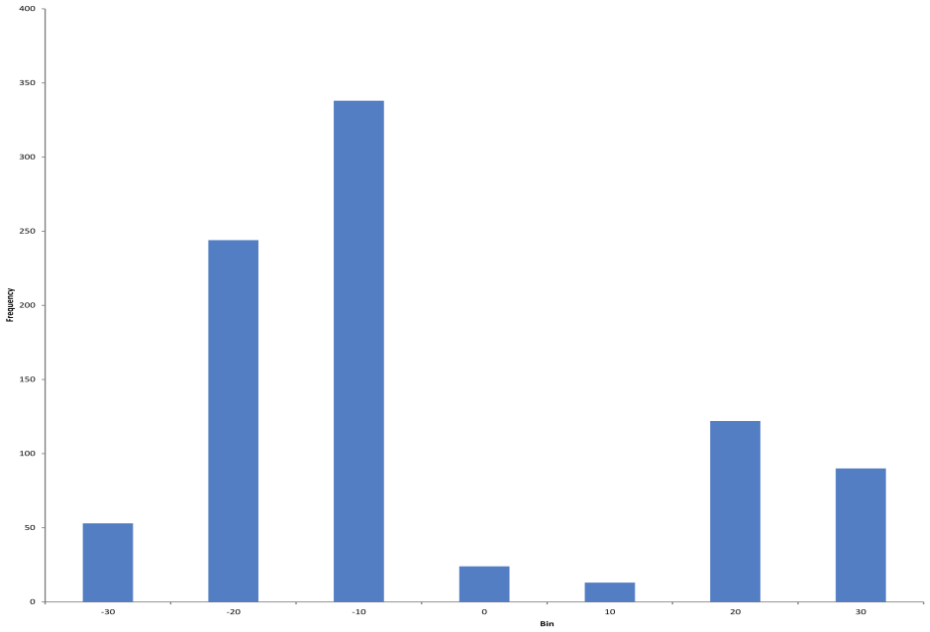

Appendix B4. Summary of character statistics, evolutionary models and trees statistics for each dataset under maximum likelihood (ML), maximum parsimony (MP) and Bayesian inference (BI). [a] The number of accessions included for each data matrix was *N*=154. [b] Including the corresponding indel coded matrix. [c] L: length of the most parsimonious tree; CI: consistency index; RI: retention index. [d] The number of moderate to strong supported nodes by ≥75 maximum parsimony - MP (Jack-knife), ≥75 maximum likelihood - ML (Bootstrap) and ≥0.95 Bayesian inference - BI (Posterior probability). [1] Combined matrix of *petD, rpl16* and *trnK/matK*. [2] Models of sequence evolution obtained for each partition were maintained as described in the row Substitution model (BI analyses).

	petD	***rpl16***	***trnK/matK***	**Combined plastid DNA[1]**
Aligned length[a]	1140	1277	2962	5379
No. variable sites[b]	303	538	921	1763
MP analyses				
No. parsimony-informative sites[b]	161	234	441	875
No. MP trees	1791	1814	1918	19927
L[c]	478	837	1620	3037
CI[c]	0.728	0.744	0.653	0.668
RI[c]	0.872	0.878	0.830	0.834
No. supp. nodes[d]	22	33	61	88
ML analyses				
Substitution model	GTR + Γ	GTR + Γ	GTR + Γ	GTR + Γ
No. supp. nodes[d]	35	38	61	100
BI analyses				
Partition	*petB* Spacer	*rpl16* intron	*matK*	8
	petD 5' exon		*trnK* 3' exon	
	petD intron		*trnK* 3' intron	
			trnK 5' intron	
Substitution model	TVM + Γ	TIM2 + Γ	TVMef + Γ + I	Partitioned[2]
	JC		K80	
	TPM1uf + Γ		TVM + Γ	
			TPM1uf + Γ	
No. supp. nodes[c]	37	48	93	133

Appendix B5. (a-c) Bayesian 50% majority-rule consensus tree of *Philodendron* with three plastid markers (*petD*, *rpl16*, and *trnK/matK*). Values above branches indicate posterior probability (bold, left) and bootstrap (right) supports, and values below branches indicate Jack-knife support. Values in square brackets indicate conflicting topologies between Bayesian inference and maximum likelihood (above branches) and maximum parsimony (below branches) detected in TreeGraph. Node tips are DNA number and species names. Star = genus *Philodendron*.

(a)

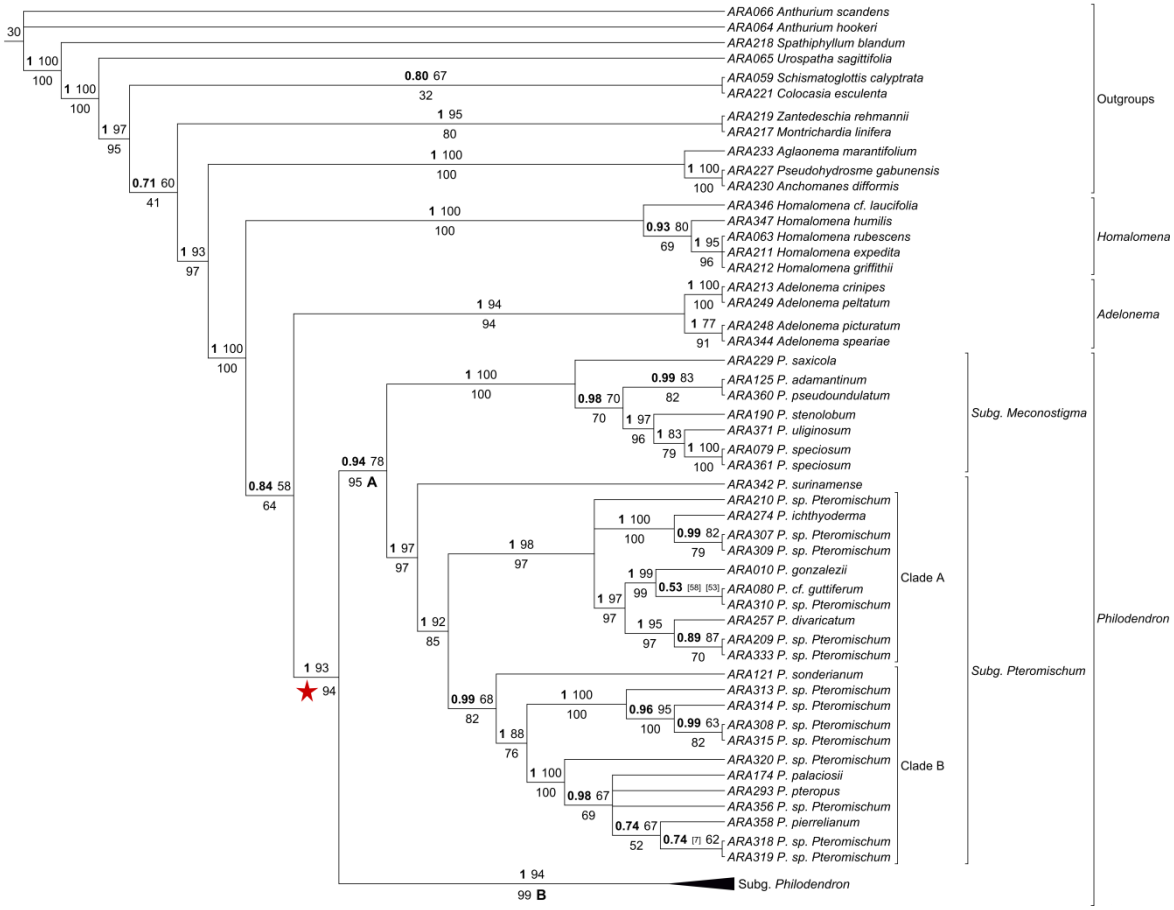

Appendix B5. (b, continued)

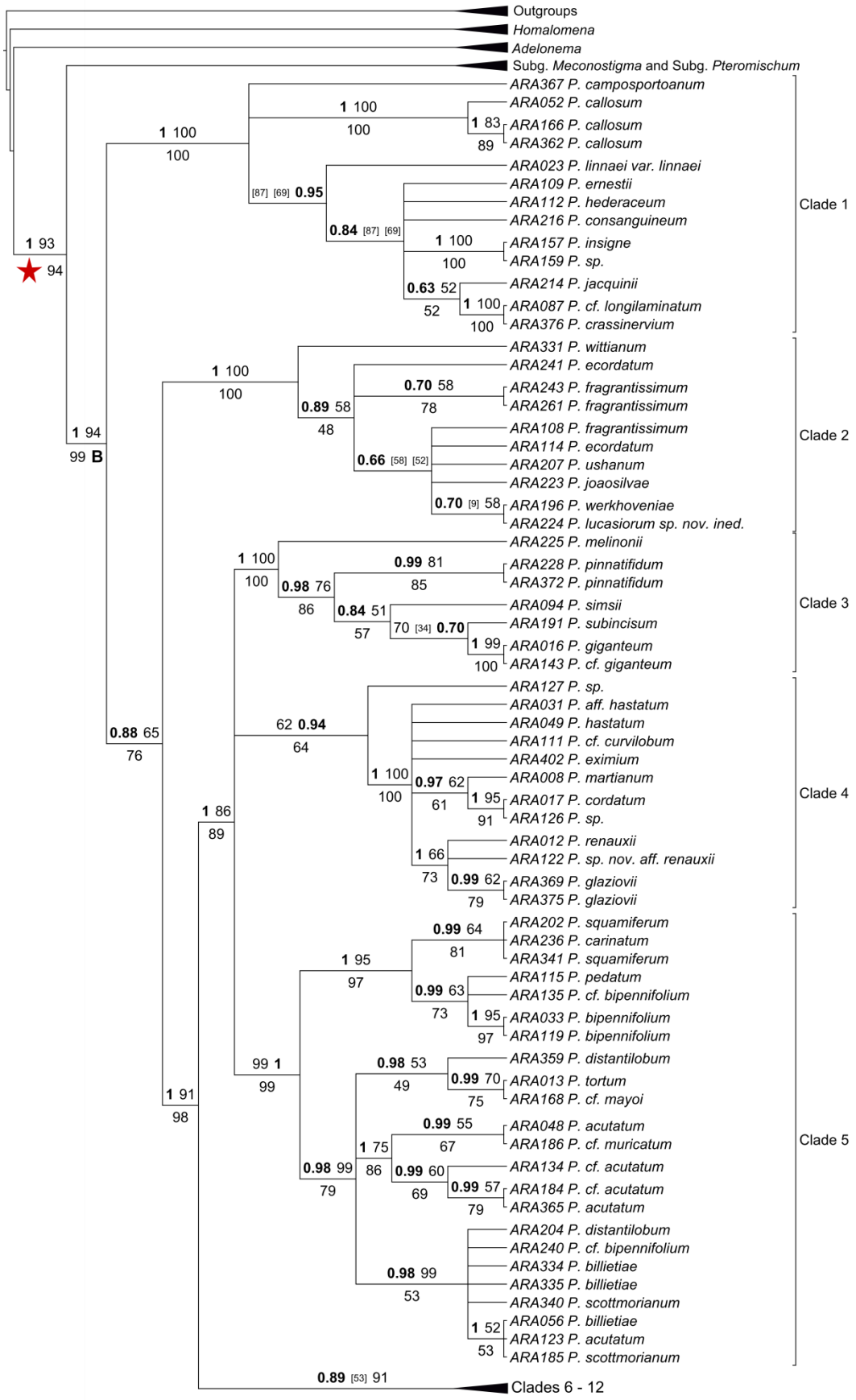

Appendix B5. (c, continued)

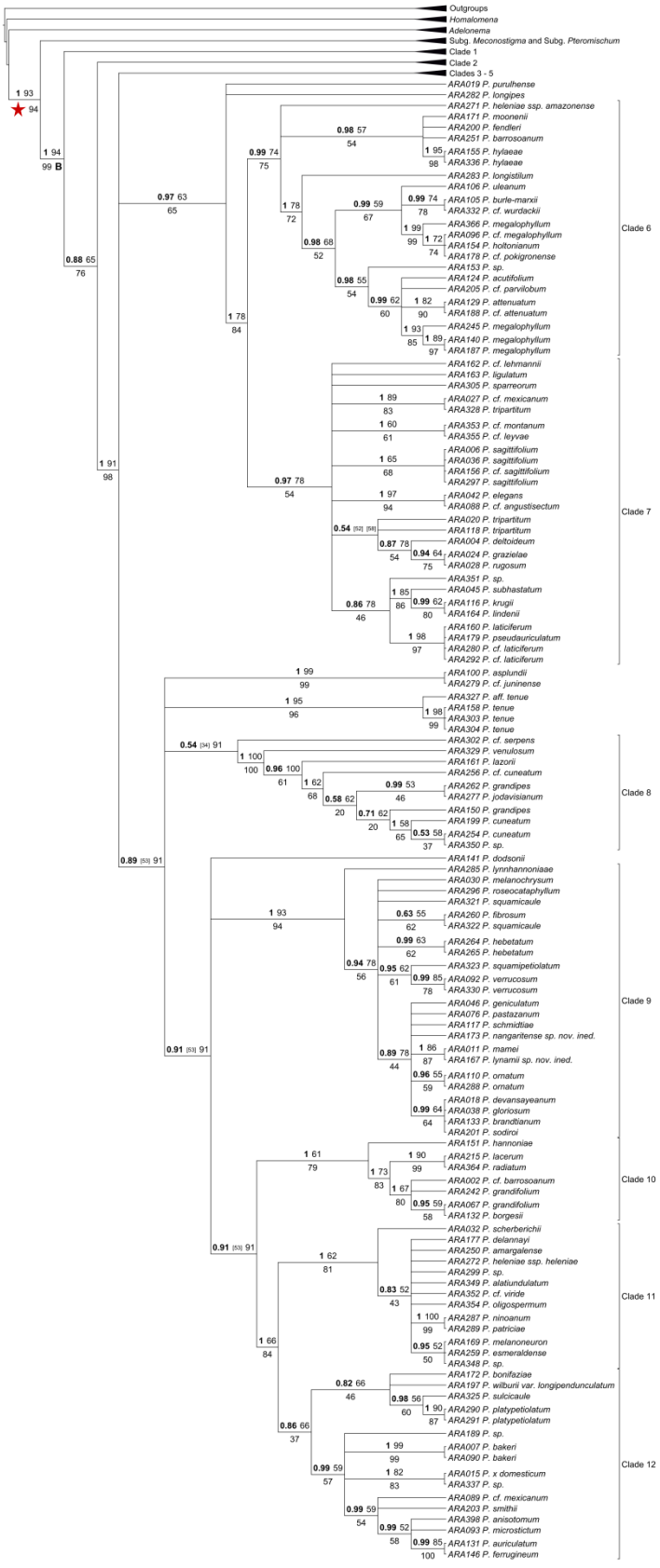

Appendix B6. The p-value of the LRT (Likelihood Ratio Test) used to compare the likelihood of the model with the parameter +J and the model nested (without +J parameter). Alt, alternative model; Null, null model; LnL, Log-likelihood; DF, degrees of freedom; P-val, P values; AIC, Akaike Information Criterion; AICwt, AIC weight.

Alt	Null	LnLAlt	LnLNull	DFAlt	DFNull	DF	Dstatistic	P val	AIC1	AIC2	AICwt1	AICwt2	AIC Weight ratio model1	AIC Weight ratio model2
DEC+J	DEC	-285.6	-291.4	3	2	1	11.48	0.0007	577.3	586.7	0.99	0.0087	114.2	0.0088
DIVALIKE+J	DIVALIKE	-290.7	-294.7	3	2	1	7.87	0.0050	587.5	593.3	0.95	0.050	18.82	0.053
BAYAREALIKE+J	BAYAREALIKE	-297.4	-319.4	3	2	1	44.06	3.2e-11	600.8	642.9	1.00	7.4e-10	1.36e+09	7.4e-10

Appendix C. Supplementary material for Chapter 4

Appendix C1. Matrix of five morphological characters used in the ancestral character-state inferences of *Philodendron* using BayesTraits version 2.0. Growth form in adult plant: C, climbing; R, rosulate; T, terrestrial. Persistence of cataphylls: A, absent; D, deciduous; Pf, persistent as fibers; Pi, persistent intact; Ps, shortly persistent. Overall blade outline: Co, cordate; Na, narrow; Mu, multiply incised; Tr, tripartite. Locules/Ovary: F, few; M, many. Ovules/Locule: F, few; M, many; S, solitary. C, crown node; S, stem node; PP, Bayesian posterior probability; PC, Primary characters; SC, Secondary characters; Hyphen, unknown.

#	Taxon	Growth form	Persistence of cataphylls	Overall blade outline	Locules/Ovary PC		Locules/Ovary SC	Ovules/locule PC		Ovules/locule SC
1	*ARA213 Adelonema crinipes*	T	A	C	5	5	F	10	20	M
2	*ARA249 Adelonema peltatum*	T	A	C	4	5	F	10	20	M
3	*ARA344 Adelonema speariae*	T	A	E	2	2	F	10	20	M
4	*ARA248 Adelonema picturatum*	T	A	C	3	4	F	10	20	M
5	*ARA229 Philodendron saxicola*	T	D	P	6	11	M	2	4	F
6	*ARA125 Philodendron adamantinum*	T	D	P	4	8	M	3	7	F
7	*ARA360 Philodendron pseudoundulatum*	T	D	C	8	10	M	-	-	-
8	*ARA190 Philodendron stenolobum*	T	D	C	7	8	M	2	3	F
9	*ARA079 Philodendron speciosum*	T	D	C	9	11	M	2	4	F
10	*ARA371 Philodendron uliginosum*	T	D	C	3	6	F	1	5	F
11	*ARA342 Philodendron surinamense*	C	A	E	3	5	F	20	30	M
12	*ARA121 Philodendron sonderianum*	C	A	E	3	4	F	33	51	M
13	*ARA210 Philodendron* sp. (Pteromischum)	C	A	E	4	4	F	20	30	M
14	*ARA274 Philodendron ichthyoderma*	C	A	E	4	4	F	20	30	M
15	*ARA307 Philodendron* sp. (Pteromischum)	C	A	E	4	4	F	20	30	M
16	*ARA309 Philodendron* sp. (Pteromischum)	C	A	E	4	4	F	20	30	M
17	*ARA310 Philodendron* sp. (Pteromischum)	C	A	E	4	4	F	20	30	M
18	*ARA010 Philodendron gonzalezii*	C	A	E	2	3	F	20	30	M

#	Taxon	Growth form	Persistence of cataphylls	Overall blade outline	Locules/Ovary PC		Locules/Ovary SC	Ovules/locule PC		Ovules/locule SC
19	*ARA080 Philodendron* cf. *guttiferum*	C	A	E	4	4	F	20	30	M
20	*ARA257 Philodendron divaricatum*	C	A	E	4	4	F	20	30	M
21	*ARA209 Philodendron* sp. (Pteromischum)	C	A	E	4	4	F	20	30	M
22	*ARA333 Philodendron* sp. (Pteromischum)	C	A	E	4	4	F	20	30	M
23	*ARA313 Philodendron* sp. (Pteromischum)	C	A	E	4	4	F	20	30	M
24	*ARA314 Philodendron* sp. (Pteromischum)	C	A	E	4	4	F	20	30	M
25	*ARA308 Philodendron* sp. (Pteromischum)	C	A	E	4	4	F	20	30	M
26	*ARA315 Philodendron* sp. (Pteromischum)	C	A	E	4	4	F	20	30	M
27	*ARA320 Philodendron* sp. (Pteromischum)	C	A	E	4	4	F	20	30	M
28	*ARA293 Philodendron pteropus*	C	A	E	4	4	F	20	30	M
29	*ARA356 Philodendron* sp. (Pteromischum)	C	A	E	4	4	F	20	30	M
30	*ARA174 Philodendron palaciosii*	C	A	E	4	4	F	20	30	M
31	*ARA358 Philodendron pierrelianum*	C	A	E	4	4	F	20	30	M
32	*ARA318 Philodendron* sp. (Pteromischum)	C	A	E	4	4	F	20	30	M
33	*ARA319 Philodendron* sp. (Pteromischum)	C	A	E	4	4	F	20	30	M
34	*ARA367 Philodendron camposportoanum*	C	D	T	4	4	F	10	20	M
35	*ARA112 Philodendron hederaceum*	C	D	C	4	7	M	20	25	M
36	*ARA214 Philodendron jacquinii*	C	D	C	4	4	F	2	2	F
37	*ARA109 Philodendron ernestii*	C	D	C	5	6	F	10	20	M
38	*ARA376 Philodendron crassinervium*	C	Pi	E	4	6	F	10	20	M
39	*ARA023 Philodendron linnaei* var. *linnaei*	R	Pi	E	6	12	M	2	2	F
40	*ARA216 Philodendron consanguineum*	C	D	C	3	4	F	10	20	M
41	*ARA157 Philodendron insigne*	R	P	E	4	5	F	4	6	F
42	*ARA362 Philodendron callosum*	C	Pi	E	2	2	F	1	5	F
43	*ARA331 Philodendron wittianum*	R	Pi	E	?	?	?	1	4	F
44	*ARA243 Philodendron fragrantissimum*	R	Pf	C	6	10	M	24	36	M
45	*ARA114 Philodendron ecordatum*	C	Pi	C	-	-	-	10	20	M

#	Taxon	Growth form	Persistence of cataphylls	Overall blade outline	Locules/Ovary PC		Locules/Ovary SC	Ovules/locule PC		Ovules/locule SC
46	*ARA207 Philodendron ushanum*	C	Pi	E/(C)	5	6	F	3	4	F
47	*ARA223 Philodendron joaosilvae*	T	Pi	C	5	5	F	10	12	F
48	*ARA196 Philodendron werkhoveniae*	T	Pi	T	4	6	F	15	20	M
49	*ARA224 Philodendron lucasiorum* sp. nov. ined.	R	Pf	E	-	-	-	-	-	-
50	*ARA151 Philodendron hannoniae*	C	Ps	E	-	-	-	1	1	A
51	*ARA067 Philodendron grandifolium*	C	Ps	C	10	12	M	15	15	M
52	*ARA132 Philodendron borgesii*	C	Ps	C	6	9	M	3	5	F
53	*ARA215 Philodendron lacerum*	C	D	P	6	9	M	3	4	F
54	*ARA364 Philodendron radiatum*	C	Ps	P	7	8	M	8	8	F
55	*ARA225 Philodendron melinonii*	R	Pf	E	3	5	F	10	10	F
56	*ARA228 Philodendron pinnatifidum*	R	Pf	P	4	6	F	4	6	F
57	*ARA372 Philodendron pinnatifidum*	R	Pf	P	4	6	F	4	6	F
58	*ARA094 Philodendron simsii*	R	Pf	C	5	6	F	2	5	F
59	*ARA016 Philodendron giganteum*	C	Pf	C	4	6	F	2	2	F
60	*ARA191 Philodendron subincisum*	C	Pf	C	6	12	M	1	5	F
61	*ARA127 Philodendron* sp.	-	-	-	-	-	-	-	-	-
62	*ARA049 Philodendron hastatum*	C	D	C	5	6	F	2	5	F
63	*ARA111 Philodendron* cf. *curvilobum*	C	D	C	7	12	M	3	4	F
64	*ARA402 Philodendron eximium*	C	D	C	6	10	M	2	4	F
65	*ARA008 Philodendron martianum*	R	D	E	7	8	M	4	4	F
66	*ARA017 Philodendron cordatum*	C	D	C	9	13	M	3	6	F
67	*ARA012 Philodendron renauxii*	T	D	E	8	11	M	5	10	F
68	*ARA122 Philodendron* sp. nov. aff. *renauxii*	T	D	C	-	-	-	-	-	-
69	*ARA375 Philodendron glaziovii*	C	D	E	6	8	M	5	7	F
70	*ARA033 Philodendron bipennifolium*	C	D	P	6	7	M	10	20	M
71	*ARA115 Philodendron pedatum*	C	D	P	7	9	M	3	4	F
72	*ARA202 Philodendron squamiferum*	C	D	P	6	9	M	2	3	F

#	Taxon	Growth form	Persistence of cataphylls	Overall blade outline	Locules/Ovary PC		Locules/Ovary SC	Ovules/locule PC		Ovules/locule SC
73	*ARA236 Philodendron carinatum*	R	D	E	6	8	M	2	4	F
74	*ARA204 Philodendron distantilobum*	C	D	P	4	8	M	10	20	M
75	*ARA013 Philodendron tortum*	C	D	P	6	7	M	3	3	F
76	*ARA048 Philodendron acutatum*	C	D	C	6	10	M	2	9	F
77	*ARA186 Philodendron* cf. *muricatum*	C	D	C	4	4	F	2	3	F
78	*ARA056 Philodendron billietiae*	C	D	C	6	11	M	10	20	M
79	*ARA185 Philodendron scottmorianum*	C	D	C	8	9	M	10	12	F
80	*ARA019 Philodendron purulhense*	C	D	C	6	7	M	13	20	M
81	*ARA282 Philodendron longipes*	R	Pi	E	4	4	F	1	1	F
82	*ARA271 Philodendron heleniae* ssp. *amazonense*	C	D	E	5	9	M	1	4	F
83	*ARA155 Philodendron hylaeae*	C	D	T	5	11	M	1	2	F
84	*ARA171 Philodendron moonenii*	C	D	E	6	12	M	1	5	F
85	*ARA200 Philodendron fendleri*	C	D	P	8	10	M	3	4	F
86	*ARA251 Philodendron barrosoanum*	C	D	T	8	11	M	4	6	F
87	*ARA283 Philodendron longistilum*	C	D	E	4	6	F	1	1	A
88	*ARA106 Philodendron uleanum*	C	D	E	6	7	M	1	1	A
89	*ARA154 Philodendron holtonianum*	C	D	T	5	5	F	1	1	A
90	*ARA105 Philodendron burle-marxii*	C	D	E	5	5	F	1	1	A
91	*ARA332 Philodendron* cf. *wurdackii*	C	D	E	6	6	M	1	1	A
92	*ARA205 Philodendron* cf. *parvilobum*	C	D	E	4	5	F	1	1	A
93	*ARA245 Philodendron megalophyllum*	C	D	C	3	5	F	1	1	A
94	*ARA124 Philodendron acutifolium*	R	D	E	5	6	F	1	1	A
95	*ARA129 Philodendron attenuatum*	C	D	C	5	5	F	1	1	A
96	*ARA004 Philodendron deltoideum*	C	D	C	4	5	F	1	1	A
97	*ARA024 Philodendron grazielae*	C	D	C	5	5	F	1	1	A
98	*ARA028 Philodendron rugosum*	C	D	C	6	6	M	1	1	A
99	*ARA305 Philodendron sparreorum*	C	D	C	8	9	M	1	1	A

#	Taxon	Growth form	Persistence of cataphylls	Overall blade outline	Locules/Ovary PC		Locules/Ovary SC	Ovules/locule PC		Ovules/locule SC
100	*ARA042 Philodendron elegans*	C	D	P	5	6	M	2	2	F
101	*ARA101 Philodendron* sp.	-	-	-	-	-	-	-	-	-
102	*ARA353 Philodendron montanum*	C	D	C	6	7	M	4	5	F
103	*ARA355 Philodendron leyvae*	C	D	C/P	-	-	-	-	-	-
104	*ARA006 Philodendron sagittifolium*	C	D	C	6	9	M	2	4	F
105	*ARA163 Philodendron ligulatum*	C	D	E	6	8	M	1	1	A
106	*ARA328 Philodendron tripartitum*	C	D	T	6	10	M	1	2	F
107	*ARA351 Philodendron* sp.	C	D	E	-	-	-	-	-	-
108	*ARA160 Philodendron laticiferum*	C	D	E	6	6	M	1	1	A
109	*ARA179 Philodendron pseudauriculatum*	C	D	E	5	9	M	1	4	F
110	*ARA045 Philodendron subhastatum*	C	D	C	4	6	F	1	1	A
111	*ARA116 Philodendron krugii*	C	D	C	6	12	M	1	5	F
112	*ARA164 Philodendron lindenii*	C	D	C	8	8	M	1	1	A
113	*ARA100 Philodendron asplundii*	C	Pf	C/E	4	6	F	4	7	F
114	*ARA279 Philodendron juninense*	C	Pf	E	3	3	F	10	20	M
115	*ARA302 Philodendron* cf. *nanegalense*	C	Pf	C	-	-	-	-	-	-
116	*ARA329 Philodendron venulosum*	C	Pf	C	5	6	F	20	20	M
117	*ARA161 Philodendron lazorii*	C	Pf	C	4	6	F	10	18	M
118	*ARA262 Philodendron grandipes*	T	Pf	C	4	6	F	7	22	M
119	*ARA277 Philodendron jodavisianum*	C	Pf	C	4	7	M	18	28	M
120	*ARA199 Philodendron cuneatum*	R	Pf	E	5	6	M	10	20	M
121	*ARA350 Philodendron* sp.	R	Pf	E	-	-	-	-	-	-
122	*ARA141 Philodendron dodsonii*	C	Pf	C	4	5	F	20	20	M
123	*ARA303 Philodendron tenue*	C	Pf	C	4	5	F	12	14	M
124	*ARA285 Philodendron lynnhannoniaae*	C	Pf	C	6	8	M	20	25	M
125	*ARA030 Philodendron melanochrysum*	C	Pf	C	4	6	F	10	20	M
126	*ARA260 Philodendron fibrosum*	C	Pf	C	5	10	M	9	10	F

#	Taxon	Growth form	Persistence of cataphylls	Overall blade outline	Locules/Ovary PC		Locules/Ovary SC	Ovules/locule PC		Ovules/locule SC
127	*ARA264 Philodendron hebetatum*	C	Pi	C	4	8	M	(4–)20	24	M
128	*ARA296 Philodendron roseocataphyllum*	C	Pf	C	5	10	M	-	-	-
129	*ARA321 Philodendron squamicaule*	C	Pf	C	3	5	F	20	28	M
130	*ARA322 Philodendron squamicaule*	C	Pf	C	3	5	F	20	28	M
131	*ARA092 Philodendron verrucosum*	C	Pf	C	4	5	F	20	34	M
132	*ARA323 Philodendron squamipetiolatum*	C	Pf	C	5	6	F	20	30	M
133	*ARA046 Philodendron geniculatum*	T	Pf	E	3	4	F	20	30	M
134	*ARA076 Philodendron pastazanum*	T	Pf	C	5	6	F	20	30	M
135	*ARA110 Philodendron ornatum*	R	Pf	C	4	6	F	20	25	M
136	*ARA117 Philodendron schmidtiae*	R	Pf	C	5	6	F	20	20	M
137	*ARA173 Philodendron nangaritense* sp. nov. ined.	T	Pf	C	-	-	-	-	-	-
138	*ARA011 Philodendron mamei*	T	Pi/Pf	C	4	5	F	20	20	M
139	*ARA167 Philodendron lynamii* sp. nov. ined.	T	Pi/Pf	C	-	-	-	-	-	-
140	*ARA133 Philodendron brandtianum*	C	D	C	-	-	-	-	-	-
141	*ARA038 Philodendron gloriosum*	T	Pi	C	?	?	?	?	?	?
142	*ARA201 Philodendron sodiroi*	C	Pf	C	-	-	-	-	-	-
143	*ARA032 Philodendron scherberichii*	C	Ps/Pi	E	4	6	F	3	5	F
144	*ARA177 Philodendron delannayi*	C	Ps	C	4	5	F	2	3	F
145	*ARA250 Philodendron amargalense*	C	Ps/Pi/Pf	C	-	-	-	-	-	-
146	*ARA272 Philodendron heleniae* ssp. *heleniae*	C	D	E	5	9	M	1	4	F
147	*ARA299 Philodendron* sp.	C	Ps	C	-	-	-	-	-	-
148	*ARA349 Philodendron alatiundulatum*	C	D	C	4	6	F	1	1	A
149	*ARA352 Philodendron viride*	C	Ps	C	4	5	F	1	2	F
150	*ARA354 Philodendron oligospermum*	C	D	E/C	4	5	F	1	1	A
151	*ARA287 Philodendron ninoanum*	C	Ps	C	4	6	F	1	2	F
152	*ARA289 Philodendron patriciae*	C	Ps	E	7	7	M	10	12	F
153	*ARA169 Philodendron melanoneuron*	C	Ps	C	5	6	F	4	5	F

#	Taxon	Growth form	Persistence of cataphylls	Overall blade outline	Locules/Ovary PC		Locules/Ovary SC	Ovules/locule PC		Ovules/locule SC
154	*ARA259 Philodendron esmeraldense*	C	Ps	C	5	6	F	6	10	F
155	*ARA348 Philodendron melanoneuron*	C	Ps	C	5	6	F	4	5	F
156	*ARA172 Philodendron bonifaziae*	C	D	E	8	9	M	2	2	F
157	*ARA197 Philodendron wilburii* var. *longipendunculatum*	C	D	C	5	8	M	1	2	F
158	*ARA291 Philodendron platypetiolatum*	C	D	C	6	8	M	3	3	F
159	*ARA325 Philodendron sulcicaule*	C	D	C	4	5	F	1	1	A
160	*ARA007 Philodendron bakeri*	C	D	E	5	10	M	1	2	F
161	*ARA089 Philodendron* cf. *mexicanum*	C	D	C	-	-	-	-	-	-
162	*ARA203 Philodendron smithii*	C	D	C	6	8	M	1	1	A
163	*ARA093 Philodendron microstictum*	C	D	C	6	7	M	1	1	A
164	*ARA398 Philodendron anisotomum*	C	D	T	6	8	M	3	3	F
165	*ARA131 Philodendron auriculatum*	R	D	E	5	9	M	3	4	F
166	*ARA146 Philodendron ferrugineum*	C	D	C	8	10	M	4	7	F